FIELDIANA

Zoology

NEW SERIES, NO. 100

Osteology of the Extant North American Fishes of the Genus *Hiodon* Lesueur, 1818 (Teleostei: Osteoglossomorpha: Hiodontiformes)

Eric J. Hilton

December 31, 2002
Publication 1520

PUBLISHED BY FIELD MUSEUM OF NATURAL HISTORY

Information for Contributors to Fieldiana

General: *Fieldiana* is primarily a journal for Field Museum staff members and research associates, although manuscripts from nonaffiliated authors may be considered as space permits.

The Journal carries a page charge of $65.00 per printed page or fraction thereof. Payment of at least 50% of page charges qualifies a paper for expedited processing, which reduces the publication time. Contributions from staff, research associates, and invited authors will be considered for publication regardless of ability to pay page charges, however, the full charge is mandatory for nonaffiliated authors of unsolicited manuscripts. Three complete copies of the text (including title page and abstract) and of the illustrations should be submitted (one original copy plus two review copies which may be machine copies). No manuscripts will be considered for publication or submitted to reviewers before all materials are complete and in the hands of the Scientific Editor.

Manuscripts should be submitted to Scientific Editor, *Fieldiana*, Field Museum of Natural History, Chicago, Illinois 60605-2496, U.S.A.

Text: Manuscripts must be typewritten double-spaced on standard-weight, 8½- by 11-inch paper with wide margins on all four sides. If typed on an IBM-compatible computer using MS-DOS, also submit text on 5¼-inch diskette (WordPerfect 4.1, 4.2, or 5.0, MultiMate, Displaywrite 2, 3 & 4, Wang PC, Samna, Microsoft Word, Volkswriter, or WordStar programs or ASCII).

For papers over 100 manuscript pages, authors are requested to submit a "Table of Contents," a "List of Illustrations," and a "List of Tables" immediately following title page. In most cases, the text should be preceded by an "Abstract" and should conclude with "Acknowledgments" (if any) and "Literature Cited."

All measurements should be in the metric system (periods are not used after abbreviated measurements). The format and style of headings should follow that of recent issues of *Fieldiana*.

For more detailed style information, see *The Chicago Manual of Style* (13th ed.), published by The University of Chicago Press, and also recent issues of *Fieldiana*.

References: In "Literature Cited," book and journal titles should be given in full. Where abbreviations are desirable (e.g., in citation of synonymies), authors *consistently* should follow *Botanico-Periodicum-Huntianum* and *TL-2 Taxonomic Literature* by F. A. Stafleu & R. S. Cowan (1976 *et seq.*) (botanical papers) or *Serial Sources for the Biosis Data Base* (1983) published by the BioSciences Information Service. Names of botanical authors should follow the "Draft Index of Author Abbreviations, Royal Botanic Gardens, Kew," 1984 edition, or *TL-2*.

References should be typed in the following form:

CROAT, T. B. 1978. Flora of Barro Colorado Island. Stanford University Press, Stanford, Calif., 943 pp.

GRUBB, P. J., J. R. LLOYD, AND T. D. PENNINGTON. 1963. A comparison of montane and lowland rain forest in Ecuador. I. The forest structure, physiognomy, and floristics. Journal of Ecology, **51:** 567–601.

LANGDON, E. J. M. 1979. Yagé among the Siona: Cultural patterns in visions, pp. 63–80. In Browman, D. L., and R. A. Schwarz, eds., Spirits, Shamans, and Stars. Mouton Publishers, The Hague, Netherlands.

MURRA, J. 1946. The historic tribes of Ecuador, pp. 785–821. In Steward, J. H., ed., Handbook of South American Indians. Vol. 2, The Andean Civilizations. Bulletin 143, Bureau of American Ethnology, Smithsonian Institution, Washington, D.C.

STOLZE, R. G. 1981. Ferns and fern allies of Guatemala. Part II. Polypodiaceae. Fieldiana: Botany, n.s., **6:** 1–522.

Illustrations: Illustrations are referred to as "figures" in the text (not as "plates"). Figures must be accompanied by some indication of scale, normally a reference bar. Statements in figure captions alone, such as "×0.8," are not acceptable. Captions should be typed double-spaced and consecutively. See recent issues of *Fieldiana* for details of style.

All illustrations should be marked on the reverse with author's name, figure number(s), and "top."

Figures as submitted should, whenever practicable, be 8½ by 11 inches (22 × 28 cm) and may not exceed 11½ by 16½ inches (30 × 42 cm). Illustrations should be mounted on boards in the arrangement to be obtained in the printed work. This original set should be suitable for transmission to the printer as follows: Pen and ink drawings may be originals (preferred) or photostats; shaded drawings must be originals, but within the size limitation; and photostats must be high-quality, glossy, black and white prints. Original illustrations will be returned to the corresponding author upon publication unless otherwise specified.

Authors who wish to publish figures that require costly special paper or color reproduction must make prior arrangements with the Scientific Editor.

Page Proofs: *Fieldiana* employs a two-step correction system. The corresponding author will normally receive a copy of the edited manuscript on which deletions, additions, and changes can be made and queries answered. Only one set of page proofs will be sent. All desired corrections of type must be made on the single set of page proofs. Changes in page proofs (as opposed to corrections) are very expensive. Author-generated changes in page proofs can only be made if the author agrees in advance to pay for them.

♾ **This paper meets the requirements of ANSI/NISO Z39.48-1992 (Permanence of Paper).**

FIELDIANA

Zoology
NEW SERIES, NO. 100

Osteology of the Extant North American Fishes of the Genus *Hiodon* Lesueur, 1818 (Teleostei: Osteoglossomorpha: Hiodontiformes)

Eric J. Hilton

Department of Geology
Field Museum of Natural History
1400 South Lake Shore Drive
Chicago, Illinois 60605-2496
U.S.A.

Accepted January 10, 2002
Published December 31, 2002
Publication 1520

PUBLISHED BY FIELD MUSEUM OF NATURAL HISTORY

ISSN 0015-0754
PRINTED IN THE UNITED STATES OF AMERICA

Table of Contents

List of Illustrations

List of Tables

Osteology of the Extant North American Fishes of the Genus *Hiodon* Lesueur, 1818 (Teleostei: Osteoglossomorpha: Hiodontiformes)

Eric J. Hilton

Abstract

Despite the widespread use of *Hiodon* as a "representative" osteoglossomorph in systematic analyses of basal teleostean fishes, no previous study has thoroughly examined the skeletal anatomy of this genus as has been done recently for other groups of fishes. The goal of this study is to describe and illustrate the osteology of *Hiodon,* using a detailed postlarval growth series of both extant species. Large series of specimens allow the best opportunity to detect and understand potential sources of morphological variation (phylogenetic, ontogenetic, sexually dimorphic, and individual). Many aspects of the osteology of *Hiodon* are clarified by this study (e.g., there are only seven hypurals at all stages of development) or recorded here for the first time (e.g., sclerotic ossifications are present in specimens greater than 100 mm SL). The postlarval development of the entire skeleton is described and illustrated for the first time. For example, the vomer, which is typically a single median element in the adult of *Hiodon,* begins development as two distinct ossification centers. Comparable ontogenetic data such as these are lacking for many basal teleostean taxa (e.g., other osteoglossomorphs and elopomorphs).

I conclude by commenting on some issues of general significance to the broader study of comparative osteology. The contribution of ontogenetic data to studies of comparative anatomy and systematics can be critical in the processes of character conceptualization and character state definition, and therefore influence ideas of homology. Similarly, hypotheses of phylogenetic fusion between skeletal elements can influence the assessment of primary homology. Phylogenetic fusion of skeletal elements is an unobservable process that can only be hypothesized following an analysis of relationships, although it is often an assumption made in character state definition. If undetected, individual morphological variation, also discussed in the conclusions, may compromise the unambiguous description of characters and must be a component of future morphological analyses.

Introduction

. . . all life is a great chain, the nature of which is known whenever we are shown a single link of it. Like all other arts, the Science of Deduction and Analysis is one which can only be acquired by long and patient study. . . . Before turning to those moral and mental aspects of the matter which present the greatest difficulties, let the inquirer begin by mastering more elementary problems.

—Arthur Conan Doyle (1887)

Hypotheses of relationships within Teleostei—and actinopterygian fishes in general—have changed continuously since Müller first named the group in 1844 (see also Müller, 1846). Within the past 35 years, considerable attention has been paid to the systematics of various subgroups of teleosts (e.g., see papers in Greenwood et al., 1973; Stiassny et al., 1996; Kocher & Stepien, 1997) resulting from the adoption of cladistic methodology (e.g., Hennig, 1966; Wiley, 1981; Kitching et al., 1998) as the basis for phylogenetic recon-

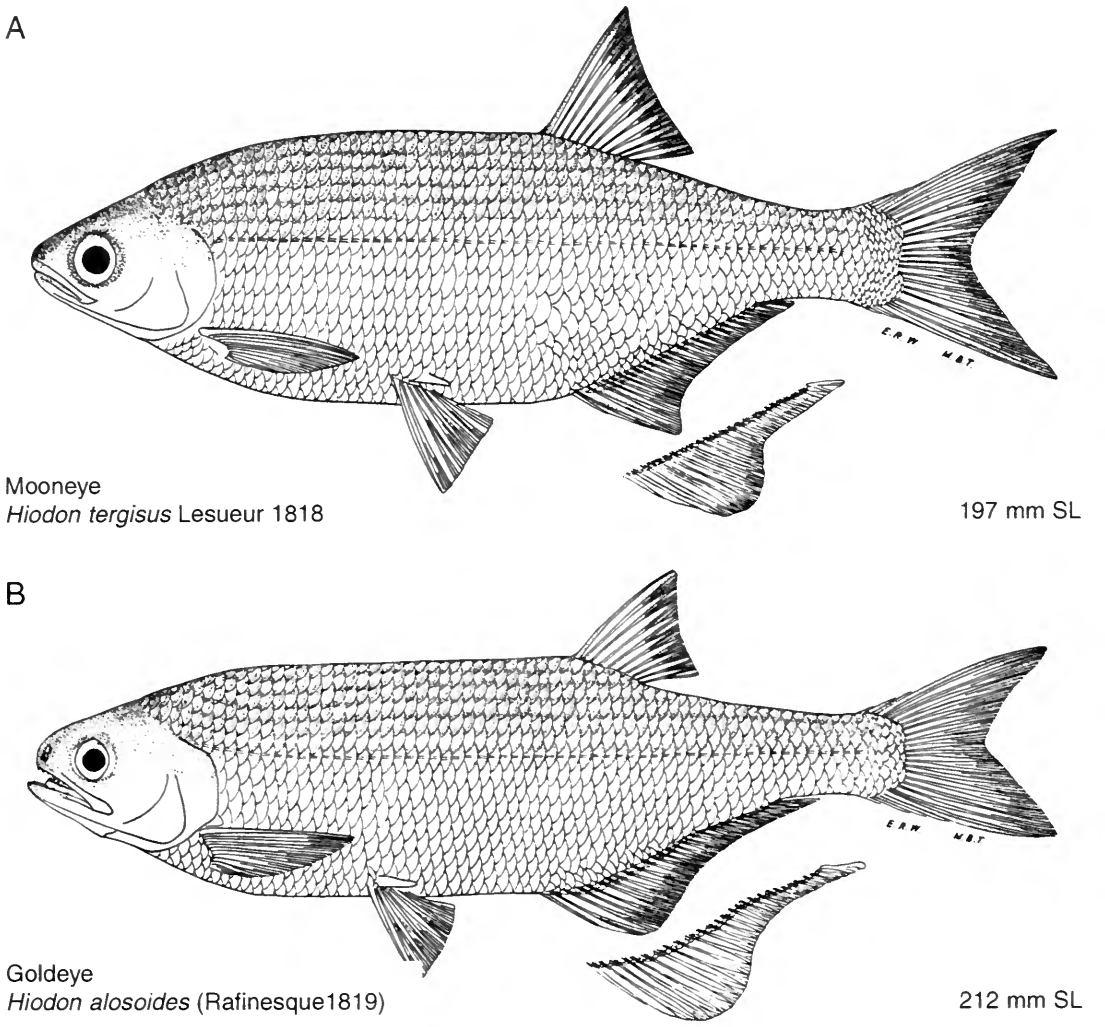

FIG. 1. The two living species of *Hiodon*. **A**. The mooneye, *H. tergisus*. **B**. The goldeye, *H. alosoides* (both from Trautman, 1957). These specimens are immature, and this is reflected in the shape of the anal fin, which resembles the anal fin in adult females. Insets below each figure show the morphology of the anal fin of a mature male.

struction. The continual change in ideas regarding the systematics of teleostean fishes is demonstrated by the many changes in the classifications presented in the various editions of J. S. Nelson's *Fishes of the World* (1976, 1984, 1994; see also Eschmeyer, 1998). Integrated analysis of fossil and living actinopterygians has become common (e.g., Wiley, 1976; Patterson & Rosen, 1977; Lauder & Liem, 1981; Grande & Bemis, 1991, 1998; Arratia, 1997, 1999), yet the detailed anatomical knowledge of living taxa needed for interpretation of fossils is lacking for many groups, including some that are commonly included in broad phylogenetic studies. As clearly articulated by Rieppel and Zaher (2000: 510), "A high degree of character congruence in itself says nothing about the quality of a phylogenetic hypothesis if it is based on . . . questionable statements of primary homology" (also see Patterson & Johnson, 1997a,b). Sound statements of (morphological) primary homology can only result from rigorous analysis of morphology. Comparative morphology, often regarded as an outdated science (see, however, Janvier, 1998), is enjoying a renaissance and has become increasingly vital for modern morphological phylogenetic analyses.

In this paper, I describe the osteology of the two living species of the genus *Hiodon* (Fig. 1).

Hiodontiformes (*sensu* Li & Wilson, 1999) contains four genera: †*Plesiolycoptera* Chang and Chou, 1976 (Middle Cretaceous, Asia), †*Yanbiania* Li, 1987 (Early Cretaceous, Asia), †*Eohiodon* Cavender, 1966 (1966a; Eocene, western North America), and *Hiodon* Lesueur, 1818 (Eocene to present, North America). Fossil fishes of the family †Lycopteriformes (Cretaceous, Asia) often are allied to Hiodontiformes, an interpretation stemming mainly from the work of Greenwood (1970). However, the †lycopterids have most recently been considered the sister-group to all other osteoglossomorphs (Li & Wilson, 1996a, 1999). The genus *Hiodon* is known only from North America (Fig. 2). The genus contains two living species (Fig. 1): the mooneye, *H. tergisus* Lesueur, 1818, and the goldeye, *H. alosoides* (Rafinesque, 1819). A single valid fossil species, †*H. consteniorum* Li and Wilson, 1994, is known from two specimens from the Eocene of Montana (Fig. 3A–E). Fragmentary material (i.e., pieces of lower jaws and vertebrae) referred to *Hiodon* has been recovered from the Pliocene and Pleistocene of Nebraska (e.g., Fig. 3F, G; G. R. Smith & Lundberg, 1972; Bennett, 1979; G. R. Smith, 1981). The genus †*Eohiodon* Cavender, 1966 (1966a), includes three described species from the Eocene of western North America (see Li, Wilson, & Grande, 1997). A new study of the anatomy of this fossil genus is currently in progress (Hilton & Grande, in prep.).

Species of *Hiodon* are used often as representative osteoglossomorphs in analyses of basal teleostean relationships. Despite this, no study has thoroughly and critically examined and illustrated their skeleton, as has been done recently for groups of sarcopterygians (e.g., Actinistia—Forey, 1998), nonteleostean actinopterygians (e.g., Polyodontidae—Grande & Bemis, 1991; Lepisosteidae—Wiley, 1976; Amiidae—Grande & Bemis, 1998), and certain groups of teleosts (e.g., Characidae—Weitzman, 1962; Elopiformes—Forey, 1973; Clupeomorpha—Grande, 1985; Salmonidae—Sanford, 2000). Various portions of the skeleton of *Hiodon* have been described in a scattered literature (e.g., Ridewood, 1904; Boulenger, 1922; Gregory, 1933; Gosline, 1960; G. J. Nelson, 1968a, 1969a,b; Greenwood, 1970, 1973; Schultze & Arratia, 1988; Arratia & Schultze, 1991; Li & Wilson, 1994), and it was not until Taverne (1977, 1978, 1979) published a series of monographs concerning osteoglossomorph osteology and relationships that the entire skeleton of *Hiodon* was described and illustrated. These papers became important contributions to the morphology of osteoglossomorphs, and of basal teleosts in general. However, only few and relatively small individuals were examined in Taverne's studies (four specimens of *H. alosoides* and three of *H. tergisus*), and only a single specimen served as the basis for most of his figures. This sort of description and illustration cannot control for individual variation, which has proved to be important in understanding the comparative osteology of actinopterygians (e.g., Arratia, 1983; Grande & Bemis, 1991, 1998; Arratia & Cloutier, 1996; Cloutier, 1997; Hilton & Bemis, 1999; Poyato-Ariza, 1999; Davis & Martill, 1999). Also, it is difficult, if not impossible, to understand ontogenetic variation when specimens of a single or even a few life history stages (e.g., juvenile or adult) are studied.

Methods

Specimen Preparation

The skeletal materials studied consisted of both dried and cleared and stained specimens. All newly prepared dry skeletons were made from fresh (i.e., not preserved) specimens using dermestid beetles or water maceration. After a series of standard body measurements was taken (see Counts and Measurements; Fig. 4A), specimens were dissected to confirm or determine, if possible, the sex of the individual (see Anal Fin). The branchial arches and the ventral portions of the hyoid arch were removed as a single unit. Specimens to be prepared by beetles (Dermestidae) were air-dried in a fume hood and placed in a dermestarium. After beetle preparation, any remaining tissue was removed by hand. Some dry skeletons were prepared by water maceration and stored as disarticulated elements. Clearing and staining for study of bone (stained with alizarin red S) and cartilage (stained with alcian blue 8GX) was based on the protocol of Dingerkus and Uhler (1977) as modified by Hanken and Wassersug (1981; see also Hildebrand, 1968; Wassersug, 1976).

Two specimens of *Hiodon alosoides* were prepared as histological sections. I used the low-viscosity nitrocellulose (LVN; Nikolas Co., Bellwood, Ill.) embedding method for preparing thick histological sections, as described by Thomas (1983). Most sections were cut at 30 μm using a sledge microtome, and approximately every 10th

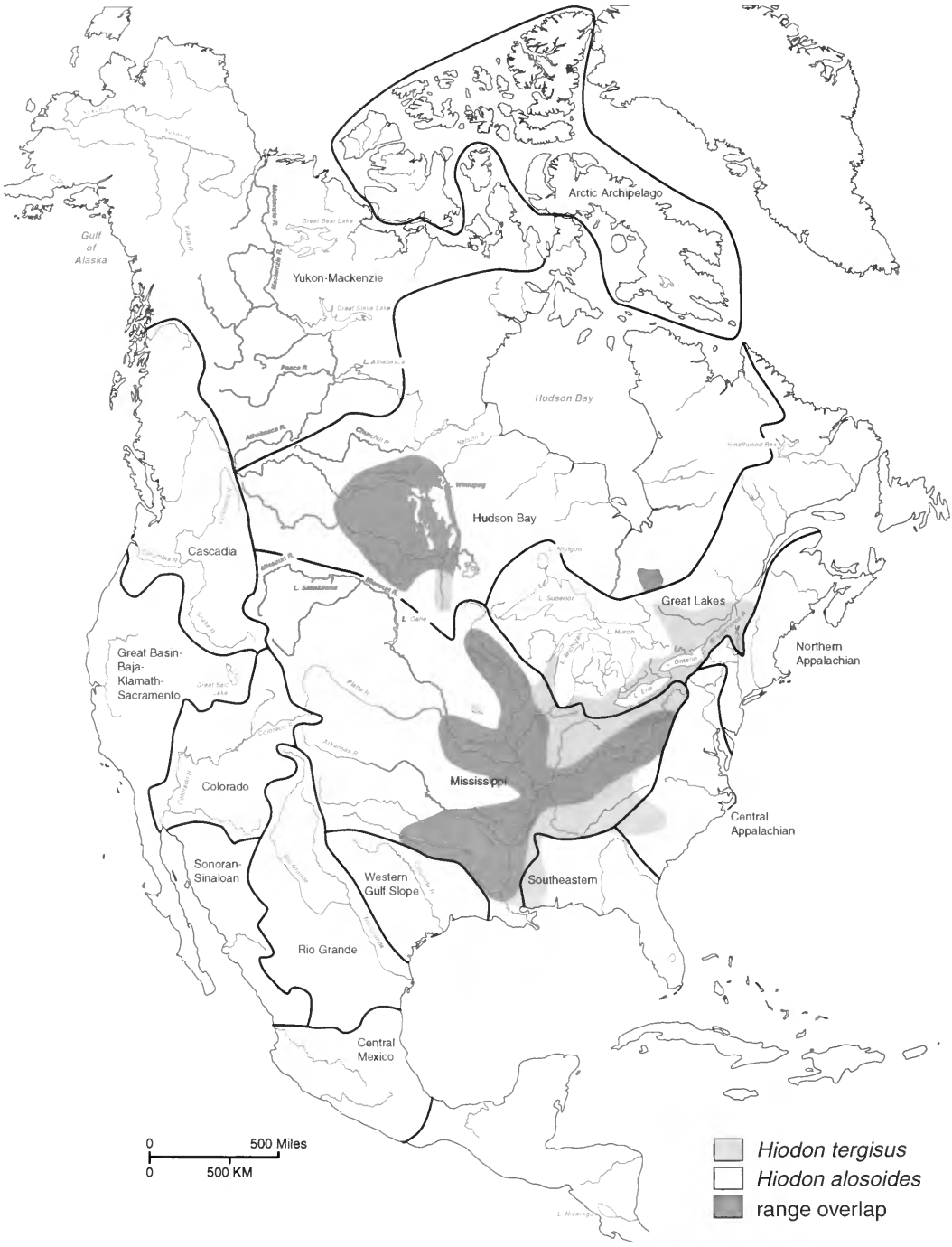

FIG. 2. Ranges of the two living species of *Hiodon* (the mooneye, *H. tergisus*, in blue; the goldeye, *H. alosoides*, in green; overlap between the two in gray). Ranges adapted from Page and Burr (1991); biogeographic provinces based on Burr and Mayden (1992; see also Hocutt & Wiley, 1986, and papers therein). Base map adapted from MapArt Geopolitical Deluxe v2.0 software (© 1998 Cartesia Software).

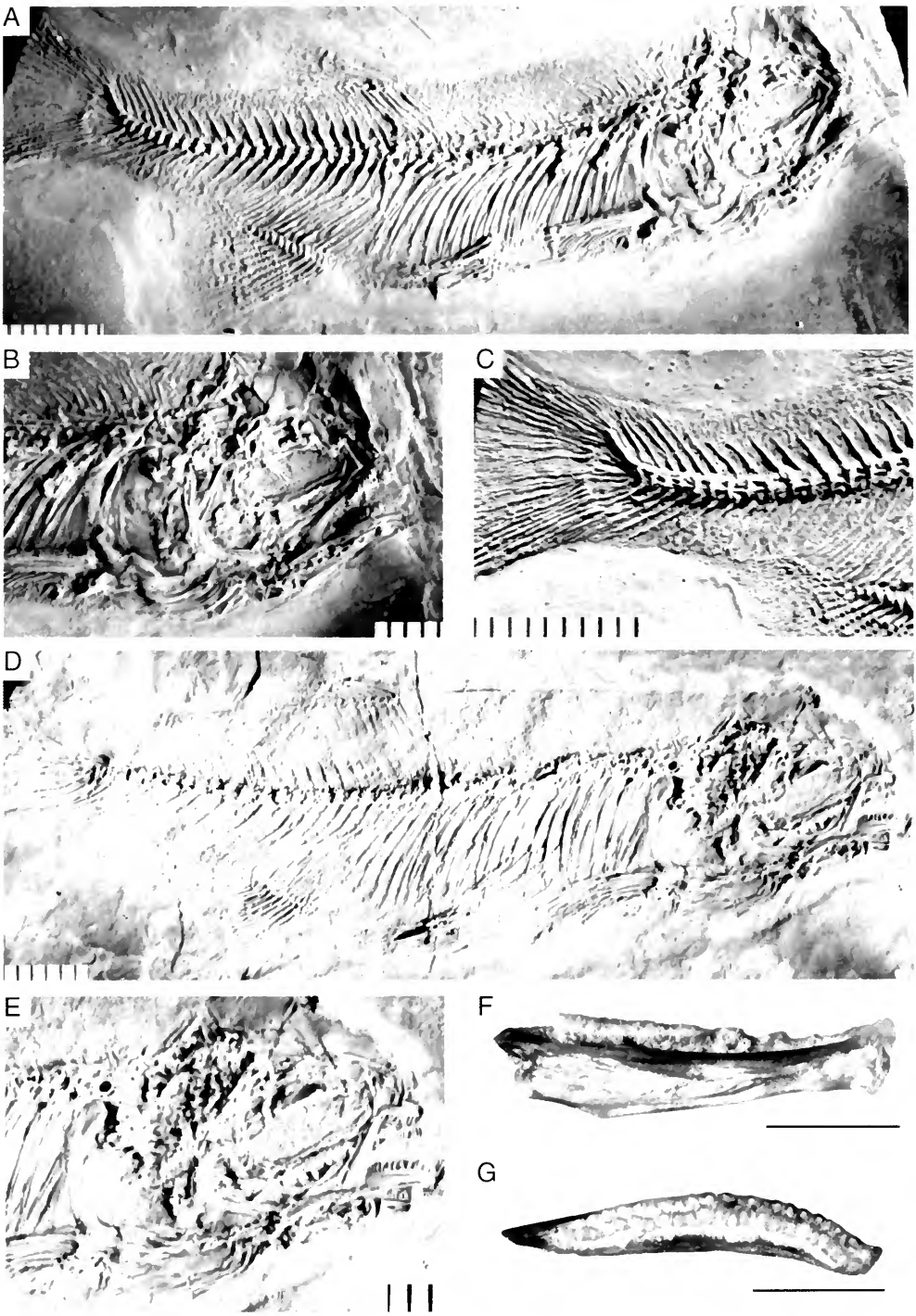

FIG. 3. Nominal fossil *Hiodon*. **A–E**, †*H. consteniorum* Li and Wilson, 1994, from the Eocene of Montana (**A–C**, UALVP 38875, holotype; **D** and **E**, UALVP 24200, paratype and only other known specimen). **F** and **G**, †*H. lirellus* Bennett, 1979, from the Pleistocene of Nebraska; this taxon is considered here a nomen dubium. †*Hiodon lirellus* is known only from isolated angulars and dentaries (specimen shown here is a dentary in **F**, medial and **G**, dorsal views; KUVP 31139). **A–E**, scale bars in millimeters; **F** and **G**, scale bars = 2 mm. Anterior facing right in all.

section was stained with Ehrlich hematoxylin and counterstained with picric-ponceau (Humason, 1979) and mounted on glass microscope slides using Eukitt mounting reagent (Calibrated Instruments, Inc., Hawthorne, N.Y.). Slides were examined and photographed under a Zeiss Axioskop compound microscope. The head and pectoral girdle of one specimen (UAMZ 4041A, 63 mm SL) were sectioned in the transverse plane. For the second specimen (UMA F10595, 55 mm SL), the head and pectoral girdle were cut in frontal sections and the abdominal cavity was cut in sagittal sections.

Study, Photography, and Illustration

In general, names of bones and cartilages follow those of Grande and Bemis (1998) where applicable; exceptions are noted in the text. Terminology for portions of the scales follows Lagler (1947). Terminology for skeletal tissues and systems follows the outline of Hilton and Bemis (1999: table 1), which is based on Patterson (1977a), M. M. Smith and Hall (1990, 1993), and Grande and Bemis (1998). Although a description of the soft tissue anatomy (e.g., muscles, nerves, and blood vessels) is beyond the scope of this study, specimens stored in alcohol were dissected to examine soft tissue anatomy in relationship to the skeleton (e.g., points of muscle attachment or determination of foramina). However, many details of the nervous system in particular remain unclear, and future confirmation must be derived from the focused study of these soft tissue systems. Names of muscles follow Winterbottom (1974).

Skeletons were examined under a Wild M5 dissecting microscope equipped with fiber-optic lights. Specimens were photographed using either 9 × 16 cm black-and-white Polaroid Type 55 positive-negative film or 35 mm color slide film. Small specimens were photographed using a Wild M8 monocular microscope with substage illumination, fiber-optic lights, and a camera attachment. Cleared and stained specimens were photographed in an 4:1 solution of glycerin:water. Scales stored in alcohol were submerged and photographed under water. Photographs and slides were scanned and illustrations were created electronically using Adobe Illustrator software. Some images were digitally captured using a Nikon Cool-Pix 990 digital camera attached to a Nikon or Wild dissecting microscope.

Meristic Data, Measurements, and Skeletal Landmarks

All specimens were visually examined, and a sample of ten specimens of each species was selected for counts and measurements. This sample represents the ontogenetic range of specimens examined in this study. I used staining of elements to recognize the presence of particular elements in small specimens; this method, however, has inherent problems (e.g., bones may not stain owing to decalcification during fixation, preservation, or preparation). Most cranial elements found in adult specimens were found to be present in the smallest individuals studied (21 mm SL for *H. tergisus* and 24 mm SL for *H. alosoides*); any that were found to develop later are noted in the text. Interspecific differences in the earliest appearance of ossification in an element were noted between small individuals of equal sizes. Given the small number of specimens of these early stages, and the fact that they were all museum specimens of wild-caught individuals (subject to different temperatures, feeding regimes, etc.), it is unclear whether these differences are phylogenetic or due to extrinsic factors (see discussion under Future Study of Hiodontid Osteology). Where such differences were detected, I have so noted in the text.

BODY MEASUREMENTS—Figures 4 and 5 show the measurements recorded and summarized in 20 tables for ten specimens of each species. In general, these measurements are adapted from Hubbs and Lagler (1958) and Grande and Bemis (1998). All whole-body measurements were recorded to the nearest millimeter except for specimens that were less than 35 mm standard length (SL), which were measured using digital calipers and were recorded to the nearest 0.1 mm. Any sort of preparation may influence the overall size of a specimen, and because many of the specimens prepared during the course of this study were acquired from museum collections (i.e., already preserved), it was impossible to determine actual lengths; no calculations were made to determine "live" lengths of the specimens (e.g., Mabee et al., 1998). All body measurements were made on fresh or fixed specimens before preparation by either clearing and staining or by dermestid beetles; skeletal structures were measured after preparation.

MERISTIC DATA—All meristic data (i.e., counts of serial structures) were collected with the aid of a dissecting microscope. In general, serial structures are numbered anterior to posterior or medial

to lateral; exceptions (e.g., preural vertebrae) are indicated below and in the text.

TEETH—Following Grande and Bemis (1998), counts of teeth (Fig. 4B) include all teeth associated with the margin of the jaw (even if only connected to a socket by soft tissue, as in young individuals or replacement teeth) as well as empty sockets from which teeth had fallen out (e.g., in dry skeletons). This method allows reasonable comparisons to be made with fossil material, from which teeth often are missing.

POSTCRANIAL AXIAL SKELETON—The axial skeleton is divided into an abdominal region and a caudal region. The first caudal vertebra is the anteriormost vertebra to possess a complete haemal arch. Posterior abdominal vertebrae, in which the left and right haemal arches are not fused, are termed transitional vertebrae. Preural caudal vertebrae (e.g., Fig. 5A) are numbered posterior to anterior (e.g., preural 1 is the first vertebra anterior to the ural caudal region). The parhypural is the posteriormost element that surrounds the dorsal aorta. Ural centra are defined as those that support hypurals.

MEDIAN FINS AND PTERYGIOPHORES—A pterygiophore consists of a single series of radials (i.e., proximal, middle, and distal, if present; Grande & Bemis, 1998); sequential pterygiophores are numbered anterior to posterior. I distinguish between segmented and rudimentary fin rays (Fig. 5B, C; note that this distinction applies to all fin rays of all fins, not just those of the median fins). Segmented rays are defined as all fin rays that are divided into two or more lepidotrichia, whereas rudimentary rays are defined as all unsegmented rays (Grande & Bemis, 1998) and are typically restricted to the leading edge of the fin. Patterson (1992: 147) defined supernumerary fin rays as those which "lie in front of the ray serially associated with the first radial." Rudimentary rays, as defined above, compose a subset of the supernumerary fin rays of a fin (i.e., all rudimentary rays are supernumerary, but not all supernumerary rays are rudimentary). I further distinguish between branched and unbranched fin rays (Fig. 5). This scheme of fin ray classification differs from the recognition of "principal fin rays" (e.g., Hubbs & Lagler, 1958). Because I found that the last two fin rays of the dorsal and anal fins were separate in small specimens, the last "double fin ray" characteristic of adults was counted as two fin rays, also differing from the convention of Hubbs and Lagler (1958: fig. 3).

CAUDAL FIN AND SUPPORTS—The lengths of the upper and lower lobes of the caudal fin were measured as the length of the longest fin ray (Fig. 5A). Hypurals are defined as cartilaginous or ossified elements supported by a ural centrum or the notochord posterior to the centrum that supports the parhypural (pu1; see above). By convention, hypurals are numbered from anterior to posterior. The condition of the neural spine of pu1 was examined and recorded as rudimentary (less than half the length of the next-anterior neural spine, i.e., nspu2), moderately developed (more than half the length but not the full length of nspu2) or well-developed (equivalent in length to nspu2).

SCALE MORPHOLOGY AND COUNTS—Scales were sampled from six locations on the body (see Scales). Scales were removed from the dermis with forceps, rinsed clean under warm water, and placed into 70% ethanol. Scales were lightly stained by placing a drop of alizarin red S dissolved in 0.05% potassium hydroxide into the alcohol. Once stained, the scales were returned to clean 70% ethanol. Scale counts (Fig. 4A) follow those of Hubbs and Lagler (1958) and Grande and Bemis (1998). All scale counts reported in the tables were made on whole specimens stored in alcohol and not prepared as skeletons. Counts of scale rows above and below the lateral line do not include the lateral line, and the counts of those above the lateral line include the single median scale row along the dorsal margin of the body. The scales of *Hiodon* are deciduous, and a few scales are likely to have fallen out of preserved specimens, particularly older material that was not well fixed at the time of collection. However, a missing scale could be counted by probing the scale pocket to confirm the presence of a pocket as well as by correlation with adjacent scale rows. If such "presence" of a missing scale could not be justified, the specimen was not included in the tables of scale counts.

Materials Examined

Thirty-nine skeletal specimens of *Hiodon tergisus* and 81 skeletal specimens of *H. alosoides* were examined during the course of this study. My descriptions and illustrations are based primarily on *H. alosoides*, although postlarval growth series of both species were examined and compared. Ossification was well under way in the smallest of my specimens (21 mm SL for *H. tergisus*; 24 mm SL for *H. alosoides*), so I can com-

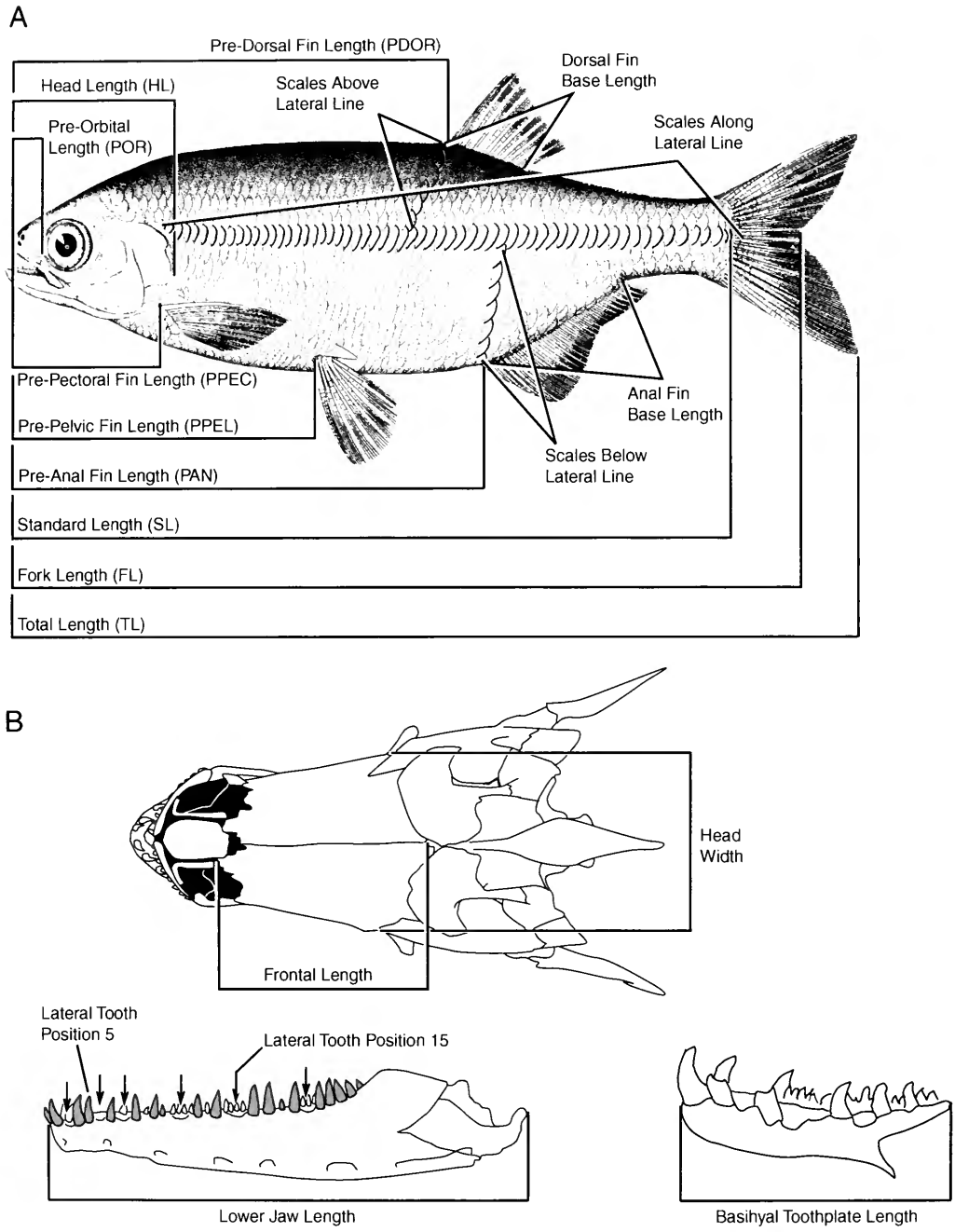

FIG. 4. Illustrations showing how some of the counts and measurements were taken. **A**, Body measurements. Drawing of *H. tergisus* (modified from Goode, 1884). **B**, Cranial measurements and meristic counts. Lateral dentary teeth are highlighted in blue; arrows point to empty tooth sockets.

ment only on the sequence of later ossifications. More specimens and a more complete growth series were available for *H. alosoides* than for *H. tergisus*, although earlier developmental stages were available for *H. tergisus* than for *H. alosoides*. Differences I discovered between the two species are described and illustrated.

Following is a list of the specimens of Hiodon-

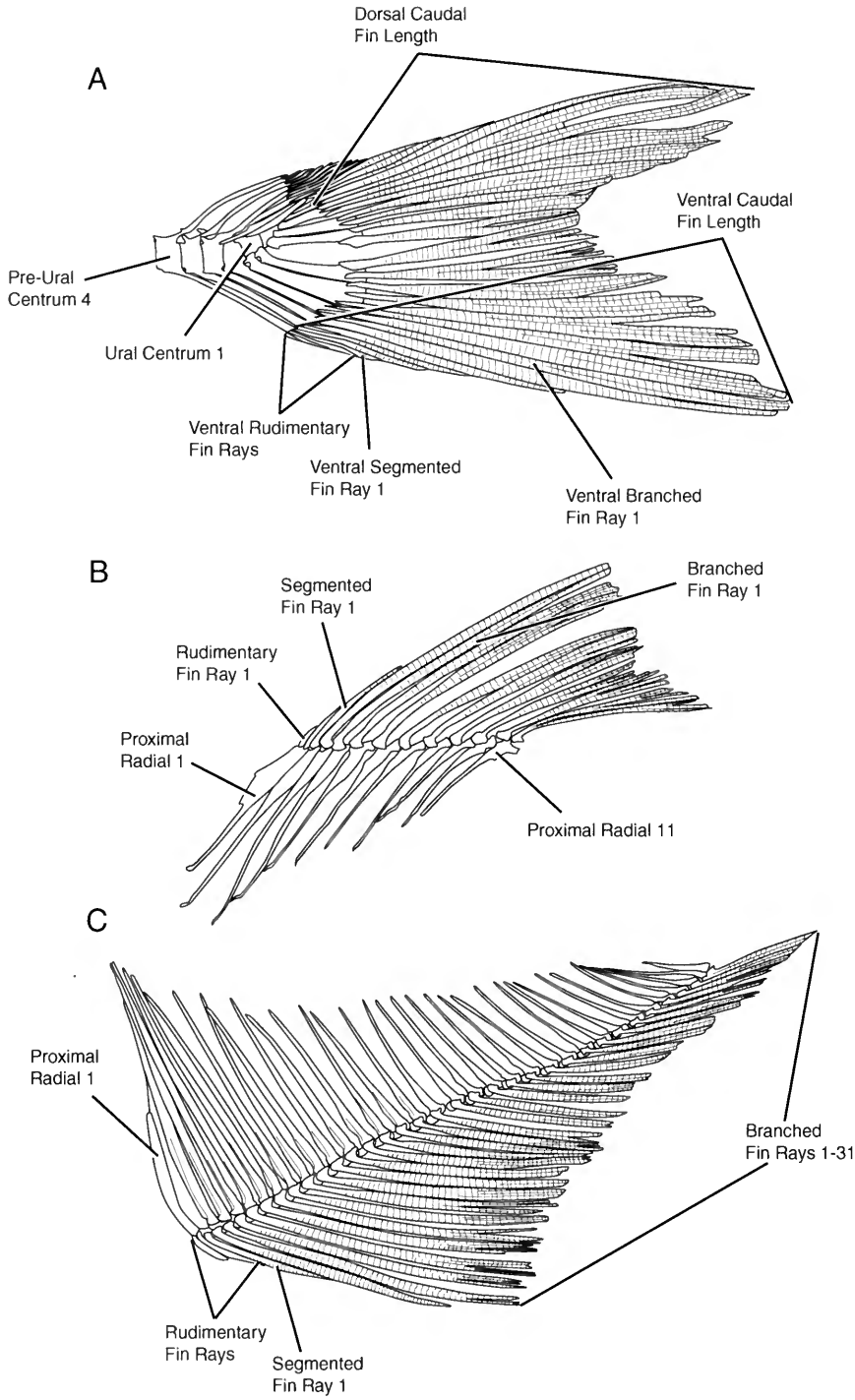

FIG. 5. Illustrations showing how some of the postcranial measurements and meristic counts were taken. **A**, Caudal fin and skeleton. **B**, Dorsal fin and skeleton. **C**, Anal fin and skeleton.

tidae (*Hiodon* and †*Eohiodon*) that I prepared and/or examined during the course of this study. Specimens are described as stored in alcohol (a), serially sectioned (sec), cleared and double stained (c&s), or dry skeleton (ds). Specimens of nonhiodontid taxa that were used during this study are referred to in the text where relevant. All taxa known exclusively as fossils are preceded by a dagger (†). All fossils listed below are complete specimens unless otherwise noted.

Hiodon tergisus: 66 specimens total; 21 mm to 230 mm SL, including: ANSP 108903 (1 a), ANSP 114175 (1 a), ANSP 169010 (1 a), FMNH 100590 (1 c&s), FMNH 109186 (1 ds), FMNH 109187 (1 ds), JFBM 22746 (1 c&s), JFBM 22748 (3 c&s), JFBM 22747 (3 c&s), JFBM 24760 (3 c&s), JFBM 27508 (1 a), JFBM 11262 (1 a), MCZ 40888 (1 a), MCZ 17906 (2 a), MCZ 17694 (1 a), MCZ 23824–23829 (6 a), MCZ 17714–17716 (3 a), TU 16811 (4 a, 6 c&s), TU 108145 (1 a), TU 108166 (5 c&s), UAIC 10473.02 (1 c&s), UF 31651 (1 ds), UF 78537 (1 a), UF 78879 (1 c&s), UMA F10379 (1 a), UMA F10599 (1 a), UMA F10607–F10613 (4 ds, 3 c&s), UMA F10635–F10640 (4 ds, 2 c&s).

Hiodon alosoides: 104 specimens total; 24 mm to 294 mm SL, including: ANSP 149441 (2 a, 1 c&s), ANSP 159095 (1 ds), AUM 5169 (1 a, 2 c&s), FMNH 109173–109185 (12 ds, 1 c&s), MCZ 17908 (3 a), MCZ 54926 (1 c&s), MCZ 157462 (1 a), NMC 75-1553 (1 a, 1 c&s), TU 108118 (5 c&s), TU 113117 (5 c&s), TU 113236 (3 c&s), UAIC 10473.01 (5 a, 2 c&s), UAMZ 4041 (5 c&s), UAMZ 4043 (2 c&s, 1 sec), UF 65838 (1 a), UMA F10149 (2 a), UMA F10150 (1 ds), UMA F10380 (1 a), UMA F10580–F10598, UMA F10600–F10606 (19 ds, 5 c&s, 1 a, 1 sec), UMA F10634 (1 ds), UMA F10641–F10653 (11 ds, 2 c&s), UMA F11259 (1 ds); USNM 007529 (3 a).

†*Hiodon lirellus:* KU 31134–31140 (isolated partial dentaries), KU 31155 (isolated articular), KU 31156 (isolated articular), KU 31158 (isolated articular).

†*Hiodon consteniorum:* UALVP 38875 (holotype), UALVP 24200 (paratype, only other known specimen).

†*Eohiodon falcatus:* FMNH PF9878, FMNH PF9880, FMNH PF9881, FMNH PF10424 (holotype), FMNH PF 10630, FMNH PF10637, FMNH PF12516, FMNH PF 13065a & b, FMNH PF15167, FMNH PF15174, FMNH PF15175; UMA F10614, UMA F10650, UMA F10651.

†*Eohiodon woodruffi:* FMNH PF12996 (partial specimen), FMNH PF14331; UALVP 13227 (holotype), UALVP 41213, UALVP 22905a & b.

†*Eohiodon rosei:* AMNH 8059 (paratype), AMNH 8059a (paratype, head only), AMNH 8060 (paratype, partial specimen); FMNH PF12991 (partial specimen), FMNH PF12995.

List of Abbreviations

Anatomical

abbtp, anterior basibranchial toothplate (= basibranchial 1–3 toothplate, G. J. Nelson, 1968a; Taverne, 1977); **ac/pm**, posterior opening of aortal canal and posterior myodome; **af**, auditory fenestra; **afd**, anterior field of scale (Lagler, 1947); **afon**, anterior fontanelle; **ag**, aortal groove on ventral surface of basioccipital (Allis, 1919); **ahh**, anterior head of hyomandibula; **ama**, ampullae of anterior duct of membranous labyrinth; **ame**, ampullae of external (= horizontal) duct of membranous labyrinth; **amp**, ampullae of posterior duct of membranous labyrinth; **ang-rar**, anguloretroarticular; **ao**, antorbital; **aon**, aortic notch of the parasphenoid; **aor**, aorta; **ap**, pars autopalatina, cartilage of palatoquadrate that ossifies as autopalatine bone in other teleosts (Arratia & Schultze, 1991); **apr**, anterior process of parasphenoid; **ar**, articular (= endosteal articular; Ridewood, 1904); **arp**, ascending ramus of parasphenoid; **as**, pelvic axillary scale; **asd**, anterior duct of membranous labyrinth (= anterior vertical canal); **asmxp**, articulating surface on premaxilla for anterior process of maxilla; **bb**, basibranchial; **bfr**, branched fin ray; **bhtp**, basihyal toothplate; **bo**, basioccipital; **br**, branchiostegal; **bsp**, basisphenoid; **bspt**, basipterygium of pelvic girdle; **c**, vertebral centrum; **cama**, chamber for ampulla of anterior duct of membranous labyrinth; **cb**, ceratobranchial; **cc**, caudal vertebral centrum; **cesd**, chamber for anterior bend of external (= horizontal) semicircular duct; **cf**, caudal fin; **cfpm**, cartilaginous floor of posterior myodome; **cg**, longitudinal groove on ventral surface of abdominal vertebral centra; **cha**, anterior ceratohyal; **chp**, posterior ceratohyal; **cl**, cleithrum; **clf**, foramen on dorsolateral sur-

face of horizontal arm of cleithrum (function unknown); **cl-cofn**, fenestra formed between ventromedial edge of cleithrum and dorsal edge of coracoid; **cm**, coronomeckelian (= sesamoid articular, Ridewood, 1904); **co**, coracoid; **cof**, small vascular foramen in posterior portion of coracoid; **clot**, chamber in basioccipital for lagenar otolith; **cpl**, cheek pit line (G. J. Nelson, 1972b); **cpsd**, chamber for ventral bend of posterior semicircular duct; **crc**, crus commune of membranous labyrinth; **csoc**, supraoccipital crest, bony extension of supraoccipital that forms in vertical epaxial septum; **csp**, process on anteroventral part of preural haemal arches and hypurals of caudal skeleton; **cut**, chamber in prootic for utricule; **d**, dentary; **dpl**, dermopalatine; **dr**, distal radial of dorsal and anal fin pterygiophores; **dsp**, dermosphenotic (= posteriormost infraorbital bone); **eb**, epibranchial; **ecp**, ectopterygoid; **ecs**, extracranial space dorsal to spinal cord; **enp**, endopterygoid (= entopterygoid, Arratia & Schultze, 1991); **ep**, epural; **epl**, ethmoidal pit line (G. J. Nelson, 1972b); **epn**, epineural; **epo**, epioccipital (following rationale of Patterson, 1975: 425; = epiotic, Ridewood, 1904; Taverne, 1977; Li & Wilson, 1994); **es**, extrascapular (= scale bone, Ridewood, 1904; = supratemporal); **esd**, external duct of membranous labyrinth (= horizontal canal); **etc**, triangular portion of ethmoid cartilage exposed between supraethmoid and frontals; **exo**, exoccipital; **facv**, foramen for anterior cephalic vein; **fepa**, foramen for efferent pseudobranchial artery (Taverne, 1977); **fht**, foramen for anteroventral lateral line nerve; **fic**, foramen for internal carotid artery (Taverne, 1977); **fjc**, common foramen for jugular canal and trigeminal and facial nerves; **fm**, foramen magnum; **fo**, focus of scale; **for**, foramen for the otic lateral line nerve (Northcutt & Bemis, 1993); **fpsd**, foramen for posterior duct of membranous labyrinth; **fr**, frontal (= parietals of Jollie, 1962); **fson**, foramen for a spinooccipital nerve; **fII**; foramen for optic nerve; **fIII**, foramen for oculomotor nerve; **fV+VII**, foramen for trigeminal and facial nerves; **fV+VII(op)**, foramen for ophthalmic portions of the anterodorsal lateral line nerve; **fVI**, foramen for abducent nerve; **fIX+X**, foramen for glossopharyngeal and vagal nerves; **gr**, gill rakers; **h**, hyomandibula; **ha**, haemal arch; **hb**, hypobranchial; **hcl**, haemal canal; **hhd**, dorsal hypohyal; **hhv**, ventral hypohyal; **hmf**, foramen for compound facial and anteroventral lateral line nerves (Northcutt & Bemis, 1993); **hp**, opercular head of hyomandibula; **hs**, haemal spine; **hy**, hypural; **hyfa**, anterior fossa for dorsal head of hyomandibula; **hyfp**, posterior fossa for dorsal head of hyomandibula; **ic**, intercalar; **ihy**, interhyal (cartilaginous); **io**, infraorbital; **iocn**, infraorbital sensory canal; **iop**, interopercle; **iph**, infrapharyngobranchial (G. J. Nelson, 1968a, following rationale of G. J. Nelson, 1968b); **jf**, opening of jugular canal; **le**, lateral ethmoid; **lem**, membranous lateral extension from lateral ethmoid (= antorbital, Patterson, 1977a; Taverne, 1977; Li & Wilson, 1994); **lexo**, membrane bone wall of exoccipital lateral to spinal cord; **lfd**, lateral field of scale (Lagler, 1947); **lig**, ligament connecting dorsal limb of posttemporal to epioccipital; **llcn**, lateral line sensory canal (= trunk canal, Liem et al., 2001); **lot**, lagenar otolith (Nolf, 1985; = asterisk); **lptp**, lower (ventral) pharyngeal toothplates; **ls**, ligamentous sheath separating the intra- and extracranial spaces dorsal to spinal cord; **maf**, membrane closing auditory fenestra; **mc**, Meckel's cartilage; **mcn**, mandibular sensory canal; **mco**, mesocoracoid; **mcp**, mandibular canal pore; **mf**, meckelian fossa; **met**, mesethmoid; **mpl**, middle pit line (G. J. Nelson, 1972b; Northcutt, 1989); **mpt**, metapterygoid; **mx**, maxilla; **mxp**, anterior process of maxilla; **n**, nasal; **na**, neural arch; **nacn**, nasal sensory canal; **ncap**, nasal capsule; **ncf**, notochord foramen; **ncn**, neural canal; **ncp**, concavity on posterior face of basioccipital that marks anterior extent of notochord; **nf**, facets on dorsal surface of centra for articulation of neural arches; **not**, notochord; **ns**, neural spine; **nspu1**, neural spine of preural vertebrae 1; **occ**, cartilage of occipital region extending posteriorly over foramen magnum; **op**, opercle; **ops**, posterodorsal spine of opercle; **ors**, orbitosphenoid; **otcn**, otic sensory canal; **pa**, parietal (= postparietal of Jollie, 1962); **parp**, postarticular process (G. J. Nelson, 1973a,b; = retroarticular process); **pap**, pectoral axillary process (Arratia, 1997); **pas**, parasphenoid; **pb**, pelvic bone (Grande & Bemis, 1998; = ossified portion of basipterygium of Sewertzoff, 1934) (note that Grande and Bemis (1998) use basipterygium to include both the cartilage and its ossification, which together form most of the pelvic girdle); **pbbtp**, posterior basibranchial toothplates (= basibranchial 4 toothplates, G. J. Nelson, 1968a); **pcf**, pectoral fin rays; **pcl**, postcleithrum; **pf**, prootic foramen allowing contact between utricule and perilymphatic sac (= foramen utriculo-vésiculaire du prootique of Taverne, 1977); **pfd**, posterior field of scale (Lagler, 1947); **pfon**, posterior fontanelle; **pg**, groove in ethmoid cartilage for the anterior process of parasphenoid; **phh**, posterior

head of hyomandibula; **phy**, parhypural; **pla**, anterior pit line (G. J. Nelson, 1972b; Northcutt, 1989); **plf**, pelvic fin rays; **plm**, middle pit line (G. J. Nelson, 1972b; Northcutt, 1989); **pm**, posterior myodome; **pmcn**, preoperculomandibular sensory canal; **pmo**, posterior opening of posterior myodome; **pmx**, premaxilla; **pop**, preopercle; **popc**, opening of preopercular sensory canal; **popcn**, preopercular sensory canal; **pp**, parapophysis (= ossification of basiventral portion of abdominal vertebrae); **ppb**, postpelvic bone; **pr**, proximal radial; **pro**, prootic; **pt**, posttemporal; **ptcn**, posttemporal sensory canal; **pt(d)**, dorsal arm of posttemporal; **pt(l)**, ventrolateral arm of posttemporal; **pt(m)**, ventromedial arm of posttemporal; **pto**, pterotic (Patterson, 1973; = fused dermopterotic and autopterotic); **pts**, pterosphenoid; **ps**, pelvic splint (Gosline, 1961); **pu**, preural centrum; **q**, quadrate; **qg**, groove where quadrate rests against preopercle; **r**, rib; **ra**, radial; **rad**, radii of scale (Lagler, 1947); **rar**, retroarticular (= ectosteal articular of Ridewood, 1904); **rfr**, rudimentary (= unsegmented) fin rays of dorsal and anal fins; **ri**, ridges (= circuli) of scale (Lagler, 1947); **sac**, saccule; **sc**, scapula (= hypercleithrum of Taverne, 1977); **sca**, anterior supracarinalis muscle; **scf**, scapular foramen; **scl**, supracleithrum; **set**, supraethmoid; **sfr**, segmented fin rays (as opposed to rudimentary fin rays); **slc**, supradorsal ligament canal; **sn**, supraneural; **soc**, supraoccipital; **socn**, supraorbital sensory canal; **sop**, subopercle; **sot**, saccular otolith (Nolf, 1985); **spc**, spinal cord; **spo**, sphenotic; **sr**, sclerotic ring; **stcn**, supratemporal sensory canal; **swb**, cranial diverticula of swim bladder; **sym**, symplectic; **tf**, temporal fossa; **tp**, transverse process of an abdominal centrum; **tv**, transitional vertebrae; **u**, ural centrum; **uh**, urohyal; **un**, uroneural (= urodermal of Monod, 1968); **uos**, unossified posterior portion of posterior field of a scale; **uot**, utricular otolith (Nolf, 1985; = lapillus); **uptp**, upper (= dorsal) pharyngeal toothplate; **vppb**, process on ventral surface of the pelvic bone; **vrfr**, ventral rudimentary fin rays of caudal fin; **X**, tenth (= vagal) cranial nerve.

Measurements and Meristic Data

D, dorsal; **FL**, fork length; **L**, left side; **PAN**, preanal fin length; **PDOR**, pre-dorsal fin length; **POR**, pre-orbital length; **PPEC**, pre-pectoral fin length; **PPEL**, pre-pelvic fin length; **R**, right side; **SL**, standard length; **TL**, total length; **V**, ventral.

Institutional

AMNH, American Museum of Natural History (New York, N.Y.); ANSP, Academy of Natural Sciences of Philadelphia (Philadelphia, Penn.); AUM, Auburn University Museum Fish Collection (Auburn, Ala.); BMNH, The Natural History Museum (London); FMNH, Field Museum of Natural History (Chicago, Ill.); JFBM, James Ford Bell Museum of Natural History, University of Minnesota (St. Paul, Minn.); KU, University of Kansas Museum of Natural History (Lawrence, Kan.); MCZ, Museum of Comparative Zoology, Harvard University (Cambridge, Mass.); MNHN, Muséum National d'Histoire Naturelle (Paris, France); NMC, Canadian Museum of Nature (Ottawa, Canada); TU, Tulane University Museum of Natural History (Belle Chasse, La.); UAIC, University of Alabama Ichthyology Collection (Tuscaloosa, Ala.); UAMZ, Museum of Zoology, University of Alberta (Edmonton, Canada); UALVP, Laboratory for Vertebrate Paleontology, University of Alberta (Edmonton, Canada); UF, Florida Museum of Natural History, University of Florida (Gainesville, Fla.); UMA, University of Massachusetts Museum of Natural History (Amherst, Mass.); USNM, Smithsonian Institution, National Museum of Natural History (Washington, D.C.).

Systematic Description of *Hiodon*

Teleostei Müller, 1844
Osteoglossomorpha Greenwood et al., 1966
Hiodontiformes Taverne, 1979
Hiodontidae Cuvier and Valenciennes, 1846
***Hiodon* Lesueur, 1818**

REJECTED SYNONYMS—*Glossodon* (Rafinesque, 1818), *Amphiodon* (Rafinesque, 1819), *Clodalus* (Rafinesque, 1820), *Elattonistius* (Gill & Jordan, in Jordan & Bean, 1877).

TYPE SPECIES—*Hiodon tergisus* Lesueur, 1818. Type by subsequent designation (Eschmeyer, 1998).

SPECIES INCLUDED AS VALID—*Hiodon tergisus* Lesueur, 1818; *Hiodon alosoides* (Rafinesque, 1819); †*Hiodon consteniorum* Li and Wilson, 1994.

DISTRIBUTION—Fossil and living species of *Hiodon* are known only from North America, and as a genus, *Hiodon* is found throughout much of the continent, from the northernmost portion of

continental Canada to the northern coast of the Gulf of Mexico (Fig. 2). The single valid fossil species, †*H. consteniorum,* is known from two specimens collected in the Eocene-Oligocene Kishenehn Formation of Montana. Other fossil material referred to *Hiodon* is known from the Miocene, Pliocene, and Early Pleistocene of Nebraska (G. R. Smith & Lundberg, 1972; Bennett, 1979; G. R. Smith, 1981). Discussions of fossil hiodontids and their allies can be found in Cavender (1966a, 1986), Greenwood (1970), Chang and Chou (1976), Chang (1999), Wilson (1977, 1978, 1980), Grande (1979), Ma (1980, 1987), Patterson (1981b), Li (1987, 1994), Shen (1989, 1996), Su (1991), Jin (1991), Wilson and Williams (1993), Jin, Zhang, and Zhou (1995), Li, Wilson, and Grande (1997), and Li and Wilson (1999).

EMENDED GENERIC DIAGNOSIS—*Hiodon* differs from all other teleostean fishes by possessing a postpelvic bone.

REMARKS—An additional fossil species, †*Hiodon lirellus* Bennett, 1979, was described based on isolated and fragmentary lower jaws from the Pliocene of Nebraska. The characters used by Bennett (1979) to distinguish this material from other *Hiodon* were found in one or both of the living species. Given also the fragmentary nature of these specimens, this taxon is here considered *Hiodon lirellus* Bennett, 1979, nomen dubium.

Other characteristics of the genus *Hiodon* include 6–10 branchiostegals (usually 8); 11–13 branched pectoral fin rays (usually 12); 7 pelvic fin rays (rarely, 6 or 8); 16 (8 dorsal and 8 ventral) branched (rarely, 15) caudal fin rays.

In Jordan and Bean (1877: 67), D. S. Jordan wrote, "Prof. Gill and myself, therefore, propose the new subgeneric term *Elattonistius* . . . ." This term, intended to include only *Hiodon chrysopsis* (a synonym of *H. alosoides,* see below) was subsequently raised to generic status (e.g., Jordan & Thompson, 1910) and given the authorship "Gill and Jordan, 1877." Jordan (1923) commented that Rafinesque used *Amphiodon* because the word *Hiodon* sounded too much like *Diodon,* a genus of Tetraodontiformes (Rafinesque, 1820: 41). *Hyodon* is commonly seen as the spelling of the genus in older literature and is considered invalid, although perhaps more proper etymologically. Jordan and Evermann (1896: 412) noted, "It is not certain which of these two names, *Hiodon* and *Glossodon,* has precedence of date. *Hiodon* is in common use and was accompanied by a much better description than Rafinesque usually furnished. We therefore retain it."

Members of the genus *Hiodon* in general are referred to as "mooneyes" (*Hiodon tergisus*) or "goldeyes" (*Hiodon alosoides*; Jordan & Evermann, 1896; Scott & Crossman, 1973). Another vernacular name for members of the genus collectively is "false herring" (Rafinesque, 1820).

The living species of *Hiodon* are sometimes considered (informally, at least) living fossils, although this term is often used ambiguously and nonchalantly (Patterson, 1984). True enough, *Hiodon* is a member of a largely fossil group of fishes (Hiodontiformes) that is believed to have separated from other teleosts at least by the Early Cretaceous (based on the oldest putative members of this clade), and portions of its anatomy closely resemble those of other early groups of teleosts (i.e., it possesses many plesiomorphies) that are known only as fossils. However, one meaning of the term living fossil is that the taxon is experiencing a state of arrested evolution (Eldredge & Stanley, 1984: 1). This is certainly not true for *Hiodon,* as members of the genus possess many derived features (i.e., autapomorphies) as well; merely because a taxon is plesiomorphic does not necessarily make it a living fossil. As Eldredge and Stanley (1984: 3) observed, taxa "cannot qualify [as living fossils] simply because they are primitive—by such a yardstick, virtually everything is a living fossil."

Forey (1998) posed four questions in considering whether or not the coelacanth, *Latimeria chalumnae,* is a living fossil (a question that he ultimately answered negatively): (1) Is it a "missing link"? (2) Is it anatomically close to the earliest members of its group? (3) Does it signify a long unrepresented fossil record? (4) Does it have a very restricted range? Although *Hiodon* possesses many plesiomorphic features, it is not a "missing link" at any level of comparison (e.g., within neopterygians, teleosts, or osteoglossomorphs). *Hiodon* does closely resemble the earliest members of its group (e.g., †*Eohiodon* and †*Yanbiania*). The fossil record of hiodontiform fishes is relatively continuous from the Early Cretaceous. The description of the range of *Hiodon* as "relictual" (Li & Wilson, 1999: 371) is somewhat misleading, as there is no evidence to suggest that the present range of *Hiodon* is restricted relative to a more widespread ancestral taxon (i.e., †*Eohiodon* and other fossil hiodontids do not have a wider range that encompasses that of living *Hio-*

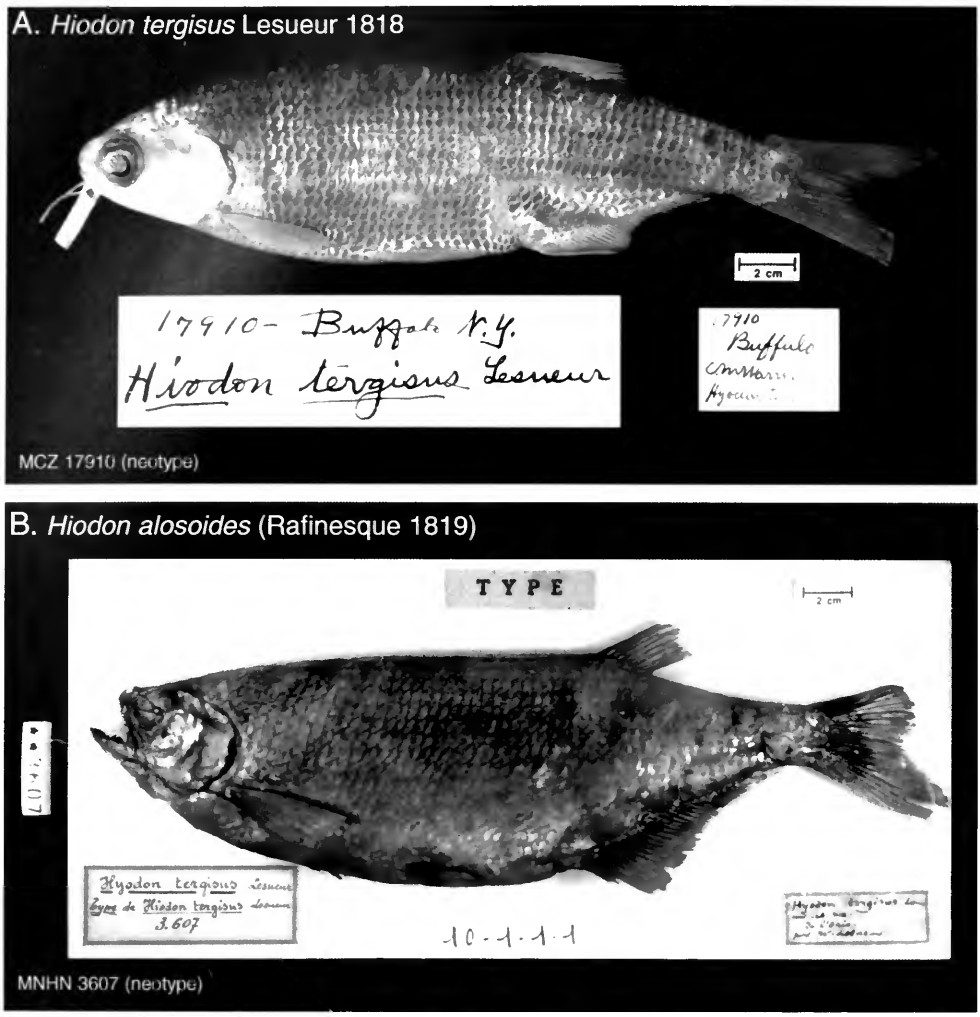

FIG. 6. Neotype specimens of **A**, *H. tergisus* (MCZ 17910), and **B**, *H. alosoides* (MHNH 3607). Body measurements of these specimens are given in Table 1. (See also Note Added in Proof, p. 134.)

don). By these criteria, therefore, *Hiodon* is only weakly, if at all, supported as a living fossil.

ETYMOLOGY—*Hyoeides* (Greek), shaped like the letter upsilon (Υ, υ), referring to the hyoid arch; *odontos* (Greek), tooth, referring to the large teeth on elements of the gill arches (Jordan & Evermann, 1896).

Hiodon tergisus Lesueur, 1818

1818 *Hiodon tergisus* Lesueur: 366
1818 *Hiodon clodalus* Lesueur: 367, pl. XIV: figs. 1–3
1818 *Glossodon harengoides* Rafinesque: 354
1818 *Glossodon heterurus* Rafinesque: 354
1820 *Hyodon vernalis* Rafinesque: 43
1820 *Hyodon* (*Clodalus*) *Clodalus* Rafinesque: 43
1823 *Hiodon clodalis* Richardson: 716
1836 *Cyprinus* (*Abramis*?) *smithii* Richardson: 110 ("fig. faulty," Günther, 1868: 376)
1836 *Hiodon chrysopsis* Richardson: 232
1846 *Hyodon claudalus* Cuvier and Valenciennes: 313
1847 *Hiodon tergissus* Kirtland: 338–339, pl. 28, figs. 1 and 2 (a misspelling of *H. tergisus*)
1868 *Hyodon tergisus* Günther: 375
1877 *Hiodon selenops* Jordan and Bean: 67

HOLOTYPE—No holotype exists for *Hiodon ter-*

TABLE 1. Body measurements for neotypes of *Hiodon tergisus* (MCZ 17910) and *H. alosoides* (MNHN 3607).*

Specimen (TL)	Sex	SL (%TL)	FL (%TL)	PPEC (%TL)	PPEL (%TL)	PDOR (%TL)	PAN (%TL)
Hiodon tergisus MCZ 17910 (290 mm TL)	Male	243 mm (83.8%)	270 mm (93.1%)	45 mm (15.5%)	103 mm (35.5%)	145 mm (50.0%)	155 mm (53.4%)
Hiodon alosoides MNHN 3607 (est. 356 mm TL)	Female	302 mm (est. 84.9%)	327 mm (est. 92.0%)	48 mm (est. 13.5%)	123 mm (est. 34.6%)	203 mm (est. 57.0%)	196 mm (est. 55.1%)

* See also Note Added in Proof, p. 134.

gisus (Eschmeyer, 1998). I designate MCZ 17910 as a neotype. This specimen (Fig. 6A, Table 1) is an alcohol-stored specimen collected by C. M. Warren in Buffalo, New York, probably in Lake Erie. This specimen was received by the MCZ in 1854. (See also Note Added in Proof, p. 134.)

TYPE LOCALITY AND DISTRIBUTION—Lake Erie at Buffalo, New York, U.S.A. (Lesueur, 1818). *Hiodon tergisus* is found in eastern and central North America in five of Burr and Mayden's (1992) faunal provinces (Hudson Bay, Great Lakes, Mississippi, Central Appalachian, and Southeastern; see Fig. 2).

DIAGNOSIS—Differs from other members of the genus by possessing irregular pattern of scale rows above insertion of anal fin; fleshy keel present from pelvic fin to anus only; a groove on anterodorsal portion of orbitosphenoid; smaller oral teeth; basihyal toothplate more than 65% of mandibular length (>35 mm SL); 53–57 preural vertebrae; 13–16 branched dorsal fin rays; 24–27 branched anal fin rays.

NATURAL HISTORY—Relatively less is known about the natural history of *H. tergisus* than of *H. alosoides* (see below), and much of what is known was summarized by Scott and Crossman (1973). Glenn and Williams (1976) studied a population of *H. tergisus* in Manitoba, Canada, and concluded that individuals began to mature in the fourth year of life, and that all individuals over the age of 6 years in their sample were mature. However, age at maturity is likely to vary across the range of the species (Scott & Crossman, 1973), and males generally mature 1 year before females (Glenn & Williams, 1976). *Hiodon tergisus* migrates upstream in spring (April–June) to spawn in fast waters of large clear rivers. The buoyant eggs of *H. tergisus* presumably are carried downstream from the spawning site by the current (Scott & Crossman, 1973). Glenn and Williams (1976) estimated the relative fecundity of *H. tergisus* as 2,000–4,000 ova per 100 g of body weight (5,000–9,000 ova per female in their study), and concluded that there was a steady increase in fecundity over the life of the fish until the age of 8 years, when fecundity began to decrease. Glenn and Williams (1976) further concluded that males have a shorter life span (8 years) than females (10 years).

Scott and Crossman (1973) listed the food of *H. tergisus* as aquatic and terrestrial invertebrates (primarily insects, but also including crayfish and mollusks) and small fishes. Boesel (1938; cited in Wallus 1990: 165) found that "Summer stomach

contents of 16 mooneye, 25–133 mm, were insects and crustaceans; some *Cladocera* in 106–146 mm specimens, but terrestrial insects were the most abundant food." Glenn (1975) found similar gut contents in his sample, and that corixids were the major component of the diet. Glenn (1975) also found that there were vernal and autumnal peaks in feeding in a population of *H. tergisus* in Manitoba, Canada.

Trautman (1957) concluded that *H. tergisus* is found only in the clearest and largest waters within Ohio. Trautman (1957) also stated that Ohio riverine populations of *H. tergisus* have declined since the mid-1800s because of an increase in the turbidity of the waters in which it lives (see also Scott & Crossman, 1973). This statement was based primarily on catch records and general early accounts. Roberts (1989: 140), however, found *H. tergisus* to be abundant in turbid water systems in Alberta, Canada, and suggested that "an increase in turbidity is probably the most visible, but not the only change that occurred in Ohio."

Hiodon tergisus is rare or extirpated in many areas of its range (e.g., New York: Smith, 1985, http://www.dec.state.ny.us/website/dfwmr/wildlife/endspec/etsclist.html [visited September 2000]; Pennsylvania: Cooper, 1983; Michigan: http://www.dnr.state.mi.us./pdfs/wildlife [visited September 2000]; Missouri: Pflieger, 1997; North Carolina: Rhode et al., 1994, 1998), although in other areas it is stable or common (e.g., Tennessee: Etnier & Starnes, 1993; Alabama: Mettee, O'Neil, & Pierson, 1996).

ETYMOLOGY—*Tergisus* (Greek), polished, referring to its silver color (Scott & Crossman, 1973).

REMARKS—Other characteristics of *H. tergisus* include 11–25 premaxillary tooth positions; 8–17 maxillary tooth positions; 19–40 dentary tooth positions; 55–59 scales along lateral line; and insertion of dorsal fin anterior to that of anal fin (plesiomorphic: also present in †*H. consteniorum*, †*Eohiodon*, and †*Yanbiania*). General morphometric and meristic measures of a sample of ten specimens from a growth series of *H. tergisus* are presented in Tables 2, 4, 6, 9, 11, 13, 15, 17, 19, and 21 (see p. 19 *ff.*).

When Lesueur (1818: 367–368) described *H. tergisus*, he also described the species *H. clodalus*, but suggested that this might be the other sex of *H. tergisus*, a hypothesis he "had not the opportunity of settling by an examination of the sexual organs, as [his] stay at the places where they are found was very short, and [he] was enabled to procure but two solitary individuals." *Hiodon clodalus* was formally recognized as the female of *H. tergisus* by Kirtland (1847: 339), who gave full credit to Lesueur: "but it is due to him [Lesueur] to say that he suggested that such might be the fact" (see also Storer, 1846).

Vernacular names of *H. tergisus* include "mooneye" (this is the most common), "toothed herring," "larger herring," "toothed herring of the lakes," "summer false herring," "spring false herring," "May false herring," "lake false herring," "river whitefish," "notch-fin Hiodon," "fresh water herring," and "laquaiche argentée" (Rafinesque, 1820; Kirtland, 1847; Jordan & Evermann, 1896; Scott & Crossman, 1973).

REFERENCES ON ANATOMY OF SOFT TISSUES—Allis, 1919 (eye muscles, swim bladder, cranial nerves, and cranial blood vessels); Moore, 1944; Moore and McDougal, 1949 (retinae); Haedrich, Winterberg, and Nelson, 1973 (optic septum); H.-J. Wagner and Ali, 1978 (retinae); Zyznar, Gross, and Nicol, 1978 (retinae).

REFERENCES ON EARLY ONTOGENY—Snyder and Douglas (1978); Wallus (1986); Wallus and Buchanan (1989); Wallus (1990).

Hiodon alosoides (Rafinesque, 1819)

1818 *Clupea alosoides* Rafinesque: 354 ("Appeared first as name only ["*Cl- alosoides* R."; Rafinesque, 1818: 354] and not available . . ."; Eschmeyer, 1998: 76)
1819 *Amphiodon alveoides* Rafinesque: 421 (*alveoides* is regarded as a misspelling of *alosoides*)
1820 *Hyodon amphiodon* Rafinesque: 42
1820 *Hyodon heterurus* Rafinesque: 42
1836 *Cyprinus* (*Abramis*?) *smithii* Richardson: 110 ("fig. faulty," Günther, 1868: 376)
1836 *Hiodon chrysopsis* Richardson: 232, 311, pl. 94, fig. 3
1842 *Glossodon smithii* Heckel: 1033
1877 *Elattonistius chrysopsis* Gill and Jordan, in Jordan and Bean: 67
1883 *Hyodon alosoides* Jordan and Gilbert: 259

HOLOTYPE—No type specimen exists for *Hiodon alosoides* (Eschmeyer, 1998). I designate MNHN 3.607 as a neotype. This specimen (Fig. 6B, Table 1) is a dried specimen collected by Lesueur in 1828 from the Ohio River at Cincinatti, Ohio. This specimen was referred to as a "nontype Lesueur specimen" of *H. tergisus* by Eschmeyer (1998: 1664); however, this specimen is *H.*

alosoides (Fig. 6B). (See Note Added in Proof, p. 134.)

TYPE LOCALITY AND DISTRIBUTION—Lee et al. (1980) reported the type locality of *H. alosoides* as the Ohio River, U.S.A., probably at Louisville, Kentucky. Although *H. alosoides* is found in only three of Burr and Mayden's (1992) faunal provinces (Yukon-Makenzie, Hudson Bay, and Mississippi; see Fig. 2), it has a much broader range across North America than does *H. tergisus*, which is found in five provinces. Of all North American freshwater fishes, *H. alosoides* has one of the widest latitudinal ranges, rivaled only by few other species (e.g., *Aplodinotus grunniens*, Page & Burr, 1991). *Hiodon alosoides* is known from the Early Pleistocene of Nebraska (G. R. Smith & Lundberg, 1972).

DIAGNOSIS—Differs from other members of genus by having dorsal fin insertion above or posterior to anal fin insertion; a fleshy keel from pectoral girdle to anus; no groove on anterodorsal portion of orbitosphenoid (unknown in †*H. consteniorum*); larger oral teeth; basihyal toothplate more than 55%–60% of mandibular length (>35 mm SL); 56–61 vertebrae; 9–10 branched dorsal fin rays; 30–31 branched anal fin rays.

NATURAL HISTORY—Scott and Crossman (1973: 329) stated that *H. alosoides* is typically found in "quiet, turbid waters of large rivers, the small lakes, ponds, and marshes connected to them, and the muddy shallows of larger lakes." In the Scioto River in Ohio, Trautman (1957) found that *H. alosoides* was most abundant in deep pools with a swift current. Hendrickson and Power (1999: 414) found that *H. alosoides* "followed the general pattern of increases in abundance, followed by declines and stabilized abundances" after creation in 1953 of Lake Sakakawea, a reservoir in northwestern North Dakota. These authors further noted that favored conditions for *H. alosoides* "were prevalent during the early years of impoundment, and the increase in goldeye between 1990 and 1994 was attributable to good recruitment caused by very turbid conditions in the upper portion of the reservoir during the recent drought" (Hendrickson & Power, 1999: 414).

Based on studies by Kennedy and Sprules (1967) and others, Scott and Crossman (1973) list as the food of *H. alosoides* aquatic and terrestrial invertebrates (primarily insects, but also including crayfish and mollusks), small fishes, and other vertebrates, including green frogs, shrews, and mice. *Hiodon alosoides* appears to be an opportunistic feeder, with prey reflecting local, seasonal, and annual changes in availability (Donald & Kooyman, 1977a). Moon, Fisher, and Krentz (1998) found that Corixidae, Coleoptera, Copepoda, and Cladocera form the bulk of the diet during peak abundance of *H. alosoides* in two backwaters of the Missouri River in North Dakota, and that larval fishes are not an important part of their diet.

Donald and Kooyman (1977b) studied the migration patterns of immature and adult *H. alosoides* in the Peace River system in northern Alberta, Canada. They found that adults migrated from the Peace River into the Peace–Athabasca Delta following ice breakup in late April, although individuals were caught near the delta in early March. Spawning took place in mid-May and hatching occurred in early June. Both juveniles and adults were caught in the delta through August, although they found that the migration back to the Peace River peaked during the last week of July and the first week of August, and that juveniles tended to remain in the delta longer. The migration of the young of the year did not begin until mid-July and lasted until November, with no consistent peak during the study (3 years). In this study, some animals were estimated to migrate up to 800 km between wintering and spawning habitat. Moon et al. (1998) found *H. alosoides* in peak abundance in backwaters of the Missouri River in North Dakota during July.

Hiodon alosoides seems to be faring better than *H. tergisus* (e.g., Pflieger, 1997; Etnier & Starnes, 1993; Robinson & Buchanan, 1988), although it has declined at the margins of its range (e.g., Alabama: Mettee et al., 1996; Pennsylvania: Cooper, 1983).

ETYMOLOGY—*Alosa* (Classical Latin), a shad; *-oides* (New Latin), denoting likeness of form (Jaeger, 1978), referring to the superficial resemblance to members of the clupeid genus *Alosa*.

REMARKS—Other characteristics of *H. alosoides* include 11–17 premaxillary tooth positions; 15–30 maxillary tooth positions; 22–30 dentary tooth positions; 58–63 scales along the lateral line. General morphometric and meristic measures of a sample of ten specimens from a growth series of *H. alosoides* are presented in Tables 3, 5, 7, 10, 12, 14, 16, 18, 20, and 22.

The misspelling of the species name (*alveoides*) by Rafinesque (1819) is considered a misprint (Jordan & Evermann, 1896), although, as Scott and Crossman (1973: 332) remark, "There seems little reason for this decision of later authors." However, it seems clear, both etymologically and

based on the name *alosoides* given in Rafinesque (1818), that *alosoides* was Rafinesque's (1819) intent. Vernacular names of *H. alosoides* include "goldeye" (this is the most common), "toothed false herring," "la Quesche," "naccaysh," "yellow herring," "shad mooneye," "weepicheesis," and "laquaiche aux yeux d'or" (Rafinesque, 1820; Jordan & Evermann, 1896; Scott & Crossman, 1973).

References on Anatomy of Soft Tissues—Moore and McDougal, 1949 (retinae); Greenwood, 1971 (ventral gill arch and hyoid musculature); G. J. Nelson, 1972a (stomach and intestine); Haedrich et al., 1973 (optic septum); H.-J. Wagner and Ali, 1978 (retinae); Zyznar et al., 1978 (retinae); Best and Nicol, 1979 (eye); Braekevelt, 1982a,b, 1985 (retinae); Hilton, 2001 (ventral gill arch and hyoid musculature).

References on Early Ontogeny—Battle and Sprules (1960), Pankhurst (1985), Pankhurst, Stacey, and Van Der Kraak (1986), Wallus (1986, 1990).

Osteological Descriptions

Skull Roof and Dorsal and Lateral Ethmoid Region

Ten paired dermal bones, including extrascapulars, parietals, frontals, pterotics, and nasals, and the median supraethmoid form the skull roof of *Hiodon*. The median chondral supraoccipital also comprises a significant part of the posterior skull (discussed under Posterior and Ventral Portions of the Braincase and Ventral Ethmoid Region). The dorsal and lateral ethmoid region is comprised of four bones: the median supraethmoid (dermal) and mesethmoid (chondral), and the paired lateral ethmoid (chondral with a large membrane-bone flange, see below). All of the skull bones in *Hiodon* are smooth, unornamented, and, with the exception of the extrascapulars, lie mostly below a thick layer of dermis and adipose tissue. The skull roof and ethmoid region are illustrated in Figures 7 to 14, 16, 28, and 29. Details of the posterior skull roof and braincase in fossil hiodontids are not well known, in part because of the large, superficial extrascapulars, which often are preserved covering the deeper elements.

The thin, concave extrascapulars (es, Fig. 8) lie above the epaxial musculature that inserts on the temporal and occipital regions of the skull. These elements are the most superficial bones of the skull roof and develop initially as simple tubular ossifications of the supratemporal sensory canal (Fig. 14), but become roughly triangular in the adult (e.g., Fig. 28) and cover much of the dorsal surface of the parietals and the supraoccipital, as well as the portions of the epioccipitals and pterotics that border the temporal fossae. In some specimens, the extrascapulars may extend forward to contact the frontals. Contrary to Taverne (1977), the left and right extrascapulars do not meet in the midline, even in the largest individuals examined. Thin, expanded extrascapulars are found in several basal teleost taxa, both within (e.g., *Petrocephalus*, †*Palaeonotopterus*, and *Mormyrops*, Cavin & Forey, 2001: fig. 10) and outside (e.g., *Megalops*, Forey, 1973: fig. 26) of Osteoglossomorpha.

The parietals (pa, Figs. 7 and 9) occupy the central portion of the skull roof and form the anterior borders of the temporal fossae (see discussion under Temporal Fossae). These bones lie dorsal to the posterior fontanelles and the portion of the neurocranial cartilage that carries the anterior semicircular canals. Anteriorly, there is a tight suture between the parietals and frontals. Often the left and right parietals share a tight suture for a small length in the midline of the skull, although the degree of this contact is variable (compare the specimens illustrated in Figs. 7 and 9). The parietals overlap the dorsal surface of the supraoccipital posterodorsally and the pterotics laterally. An elongate posterior process of the parietal contacts the epioccipital and forms a "bridge" over the ventral margin of the supraoccipital (here termed the "parietal bridge"). A similar-shaped parietal is present in †*Eohiodon rosei* (AMNH 8059). The parietals variably support a small segment of the supraorbital canal that runs toward the posterior midline of the skull (Figs. 14, 15D, E, and 16; see discussion under Sensory Canals). This is in contradiction to Li and Wilson (1999, character 12; also Li, Grande, & Wilson, 1997), who coded *Hiodon* as having the supraorbital canal ending in the frontal bone (versus ending in the parietal).

The frontals (fr, Figs. 7–9) lie anterior to the parietals and are the largest elements of the dermal skull roof. These elements form early as simple ossifications surrounding the supraorbital sensory canal (already present in the smallest available specimens of both species; Fig. 14), but become roughly trapezoidal by 39 mm SL (e.g., UAMZ 4041B; see also Fig. 16); the posterior mar-

TABLE 2. Sex and body measurements for a growth series of *Hiodon tergisus*.

Specimen (TL)	Sex*	SL (%TL)	FL (%TL)	PPEC (%TL)	PPEL (%TL)	PDOR (%TL)	PAN (%TL)	POR (%TL)
JFBM 22748	?	21.0 mm	25.0 mm	6.0 mm	10.0 mm	13.0 mm	14.0 mm	2.0 mm
(26.0 mm)		(80.8%)	(96.2%)	(23.1%)	(38.5%)	(50.0%)	(53.8%)	(7.7%)
JFBM 22747C	?	24.0 mm	26.0 mm	7.0 mm	11.0 mm	14.0 mm	15.0 mm	2.0 mm
(28.0 mm)		(85.7%)	(92.9%)	(25.0%)	(39.3%)	(50.0%)	(53.6%)	(7.1%)
TU 108166E	?	34 mm	38 mm	8.0 mm	15.0 mm	19.0 mm	20.0 mm	1.7 mm
(40 mm)		(85.0%)	(95.0%)	(20.0%)	(37.5%)	(47.5%)	(50.0%)	(4.3%)
TU 108166D	?	49 mm	55 mm	11.0 mm	21.0 mm	28.0 mm	29. mm	2.6 mm
(58 mm)		(84.5%)	(94.8%)	(19.0%)	(36.2%)	(48.2%)	(50.0%)	(4.5%)
UMA F10608	?	57 mm	62 mm	13.0 mm	24.0 mm	31 mm	33 mm	3.1 mm
(66 mm)		(86.4%)	(93.9%)	(19.7%)	(36.4%)	(47.0%)	(50.0%)	(4.7%)
UMA F10609	F	160 mm	174 mm	33 mm	65 mm	93 mm	100 mm	7.0 mm
(194 mm)		(82.5%)	(89.7%)	(17.0%)	(33.5%)	(47.9%)	(51.5%)	(3.6%)
UMA F10610	M	183 mm	200 mm	39 mm	77 mm	107 mm	117 mm	9.0 mm
(222 mm)		(82.4%)	(90.1%)	(17.6%)	(34.7%)	(48.2%)	(52.7%)	(4.1%)
UMA F10611	M	210 mm	229 mm	45 mm	85 mm	121 mm	134 mm	8.0 mm
(246 mm)		(85.4%)	(93.1%)	(18.3%)	(34.6%)	(49.2%)	(54.5%)	(3.3%)
UMA F10612	M	215 mm	235 mm	41 mm	89 mm	126 mm	137 mm	9.0 mm
(263 mm)		(81.7%)	(89.4%)	(15.6%)	(33.8%)	(47.9%)	(52.1%)	(3.4%)
UMA F10613	F	230 mm	256 mm	44 mm	98 mm	130 mm	144 mm	10.0 mm
(280 mm)		(82.1%)	(91.4%)	(15.7%)	(35.0%)	(46.4%)	(51.4%)	(3.6%)

* M, male; F, Female.

TABLE 3. Sex and body measurements for a growth series of *Hiodon alosoides*.

Specimen (TL)	Sex*	SL (%TL)	FL (%TL)	PPEC (%TL)	PPEL (%TL)	PDOR (%TL)	PAN (%TL)	POR (%TL)
TU 113117E	?	24.3 mm	27.5 mm	6.4 mm	10.9 mm	16.0 mm	13.8 mm	1.5 mm
(29.3 mm)		(82.9%)	(93.9%)	(21.8%)	(37.2%)	(54.6%)	(47.1%)	(5.1%)
TU 108118A	?	30.0 mm	35 mm	7.0 mm	14.0 mm	20.0 mm	19.0 mm	1.3 mm
(37 mm)		(81.1%)	(95.6%)	(18.9%)	(37.8%)	(54.1%)	(51.4%)	(3.5%)
UAMZ 4041B	?	38 mm	40 mm	9.0 mm	17.0 mm	26.0 mm	24.0 mm	2.0 mm
(47 mm)		(83.0%)	(91.5%)	(19.1%)	(36.2%)	(55.3%)	(51.1%)	(4.3%)
UMA F10600	?	52 mm	57 mm	12 mm	21.0 mm	31 mm	29.0 mm	2.5 mm
(61 mm)		(85.2%)	(93.4%)	(19.7%)	(34.4%)	(50.8%)	(47.5%)	(4.1%)
UMA F10601	?	107 mm	122 mm	23 mm	43 mm	71 mm	63 mm	4.0 mm
(122 mm)		(81.1%)	(92.4%)	(17.4%)	(32.6%)	(53.8%)	(47.7%)	(3.0%)
UMA F10604	F	184 mm	207 mm	36 mm	76 mm	122 mm	113 mm	6.0 mm
(225 mm)		(81.8%)	(92.0%)	(16.0%)	(33.8%)	(54.2%)	(50.2%)	(2.7%)
UMA F10588	M	252 mm	274 mm	47 mm	104 mm	164 mm	154 mm	6.0 mm
(305 mm)		(82.6%)	(89.8%)	(15.4%)	(34.1%)	(53.8%)	(50.5%)	(2.0%)
UMA F10606	M	254 mm	282 mm	50 mm	112 mm	169 mm	165 mm	7.0 mm
(308 mm)		(82.5%)	(91.6%)	(16.2%)	(37.7%)	(54.9%)	(53.6%)	(2.3%)
UMA F10605	F	279 mm	309 mm	50 mm	116 mm	189 mm	180 mm	7.0 mm
(335 mm)		(82.3%)	(92.2%)	(14.9%)	(34.6%)	(59.1%)	(53.7%)	(2.1%)
UMA F10634	F	300 mm	330 mm	46 mm	120 mm	195 mm	190 mm	7.0 mm
(360 mm)		(83.3%)	(91.7%)	(12.8%)	(33.3%)	(54.2%)	(52.8%)	(1.9%)

* M, male; F, Female.

TABLE 4. Head measurements and meristic data for a growth series of *Hiodon tergisus*.

Specimen (SL)	Head length (%SL)	Head width (%SL)	Frontal length (%SL)	Lower jaw length (%SL)	L, R mandibular sensory canal openings (in dentary)
JFBM 22748 (21.0 mm)	6.0 mm (28.6%)	2.5 mm (11.9%)	Not fully ossified	3.3 mm (15.7%)	5, 4
JFBM 22747C (24.0 mm)	7.0 mm (29.2%)	2.3 mm (9.6%)	2.1 mm (8.8%)	3.6 mm (15.0%)	5, 5
TU 108166E (34 mm)	8.0 mm (23.5%)	3.3 mm (9.7%)	2.8 mm (8.2%)	5.4 mm (15.9%)	5, 5
TU 108166D (49 mm)	12.0 mm (24.5%)	4.4 mm (9.0%)	4.1 mm (8.4%)	7.0 mm (14.3%)	5, 5
UMA F10608 (57 mm)	14.0 mm (24.6%)	4.6 mm (8.1%)	4.4 mm (7.7%)	7.5 mm (13.2%)	5, 6
UMA F10609 (160 mm)	32 mm (20.0%)	11.6 mm (7.3%)	11.0 mm (6.9%)	19.5 mm (12.2%)	5, 6
UMA F10610 (183 mm)	40 mm (21.9%)	13.6 mm (7.4%)	16.3 mm (8.9%)	21.0 mm (11.5%)	5, 6
UMA F10611 (210 mm)	46 mm (21.9%)	14.4 mm (6.9%)	17.9 mm (8.5%)	23.6 mm (11.2%)	4, 5
UMA F10612 (215 mm)	47 mm (21.4%)	14.8 mm (6.9%)	17.6 mm (8.2%)	25.0 mm (11.6%)	5, 5
UMA F10613 (230 mm)	49 mm (21.3%)	13.9 mm (6.0%)	18.4 mm (8.0%)	26.4 mm (11.5%)	7, 7

TABLE 5. Head measurements and meristic data for a growth series of *Hiodon alosoides*.

Specimen (SL)	Head length (%SL)	Head width (%SL)	Frontal length (%SL)	Lower jaw length (%SL)	L, R mandibular sensory canal openings (in dentary)
TU 113117E (24.3 mm)	5.7 mm (23.5%)	2.7 mm (11.1%)	2.2 mm (9.1%)	3.8 mm (15.6%)	6, 6?
TU 108118A (30.0 mm)	7.0 mm (23.3%)	3.1 mm (10.3%)	2.7 mm (9.0%)	5.4 mm (14.6%)	7, 6
UAMZ 4041B (39 mm)	9.0 mm (23.1%)	3.8 mm (9.7%)	2.9 mm (7.4%)	5.5 mm (14.1%)	6, 6
UMA F10600 (52 mm)	13.0 mm (25.0%)	4.7 mm (9.4%)	3.6 mm (6.9%)	6.7 mm (12.9%)	6, 6
UMA F10601 (107 mm)	23.0 mm (21.5%)	7.7 mm (21.5%)	7.8 mm (7.3%)	14.3 mm (13.4%)	7, 6
UMA F10604 (184 mm)	36 mm (19.6%)	11.4 mm (6.2%)	11.2 mm (6.1%)	21.7 mm (11.8%)	8, 6
UMA F10588 (252 mm)	48 mm (19.0%)	16.3 mm (6.5%)	14.6 mm (5.8%)	28.7 mm (11.4%)	7, 8
UMA F10606 (254 mm)	51 mm (20.1%)	16.5 mm (6.5%)	17.8 mm (7.0%)	30.7 mm (12.1%)	7, 8
UMA F10605 (279 mm)	55 mm (19.7%)	17.9 mm (6.4%)	17.5 mm (5.2%)	31.9 mm (11.4%)	7, 7
UMA F10634 (300 mm)	52 mm (17.3%)	17.2 mm (5.7%)	18.3 mm (6.1%)	31.7 mm (10.6%)	7, 7

TABLE 6. Meristic data and measurements for the head region of a growth series of *Hiodon tergisus*.

Specimen (SL)	L, R dentary tooth positions	L, R premaxillary tooth positions	L, R maxillary tooth positions	L, R branchio-stegals	Basihyal toothplate length (%SL)	Basihyal toothplate length as a % of lower jaw length
JFBM 22748 (21 mm)	19, 20	14, 11	9, 8	8, 8	2.0 mm (9.5%)	60.6%
JFBM 22747C (24 mm)	21, 17	14, 14	8, 9	9, 8	2.1 mm (8.8%)	58.3%
TU 108166E (34 mm)	31, 31	16, 15	11, 11	8, 7	3.4 mm (10.0%)	63.0%
TU 108166D (49 mm)	30, 31	19, 19	13, 12	8, 8	4.8 mm (9.8%)	68.6%
UMA F10608 (57 mm)	36, 29	21, 20	16, 17	8, 8	5.4 mm (9.5%)	72.0%
UMA F10609 (160 mm)	32, 37	23, 19	15, 16	7, 8	14.1 mm (8.8%)	72.3%
UMA F10610 (183 mm)	35, 32	?*, 24	16, 14	8, 8	15.5 mm (8.5%)	73.8%
UMA F10611 (210 mm)	36, 35	25, 22	12, 11	8, 7	17.3 mm (8.2%)	73.3%
UMA F10612 (215 mm)	39, 40	22, 22	14, 13	8, 8	17.7 mm (6.7%)	70.8%
UMA F10613 (230 mm)	36, 36	25, 22	11, 13	8, 8	18.0 mm (7.8%)	68.2%

* The left premaxilla of this specimen was broken, and the anterior piece is missing.

TABLE 7. Meristic data and measurements for the head region of a growth series of *Hiodon alosoides*.

Specimen (SL)	L, R dentary tooth positions	L, R premaxillary tooth positions	L, R maxillary tooth positions	L, R branchio-stegals	Basihyal toothplate length (%SL)	Basihyal toothplate length as a % of lower jaw length
TU 113117E (24.3 mm)	23, 23	12, 14	18, 17	8, 8	2.5 mm (10.3%)	65.8%
TU 108118A (30.0 mm)	30, 28	15, 15	24, 20	9, 9	2.8 mm (9.3%)	51.8%
UAMZ 4041B (39 mm)	30, 28	17, 13	15, 14	8, 8	3.1 mm (7.9%)	56.4%
UMA F10600 (52 mm)	30, 26	14, 12	21, 21	8, 8	4.2 mm (8.1%)	62.7%
UMA F10601 (107 mm)	22, 24	11, 13	18, 22	9, 8	8.2 mm (7.7%)	57.3%
UMA F10604 (184 mm)	27, 29	13, 13	27, 30	8, 8	12.1 mm (6.6%)	58.5%
UMA F10588 (252 mm)	27, 30	14, 13	27, 30	8, 8	15.9 mm (6.3%)	55.4%
UMA F10606 (254 mm)	27, 28	13, 14	27, 27	8, 7	16.3 mm (6.4%)	53.1%
UMA F10605 (279 mm)	25, 27	11, 10	30, 28	8, 8	17.5 mm (6.3%)	54.5%
UMA F10634 (300 mm)	25, 27	14, 13	26, 25	9, 8	18.8 mm (6.3%)	59.3%

TABLE 8. Average basihyal toothplate length of hiodontid fishes reported as a percentage of lower jaw length.

Taxa (n)	Basihyal toothplate length (as % of lower jaw length)
†*Eohiodon* FMNH PF10637, UMA F10614 (2)	49%
Hiodon tergisus (10)	70%
†*Hiodon consteniorum* UALVP 38875 (1)	60%
Hiodon alosoides (10)	53%

Note: Adult specimens of *Hiodon tergisus* and *Hiodon alosoides* other than those recorded in Tables 6 and 7 were used for calculating means; n is the number of specimens used to retrieve the average.

TABLE 9. Meristic data of vertebrae and centra for a growth series of *Hiodon tergisus*.

Specimen (SL)	Total centra	Total preural centra	Total abdominal centra	Transitional vertebrae	Total preural caudal centra
JFBM 22748 (21.0 mm)	*1*	*0*	*0*	*0*	*0*
JFBM 22747C (24.0 mm)	*3**	*2*	*0*	*0*	*0*
TU 108166E (34 mm)	57	55	30	1	25
TU 108166D (49 mm)	57	55	31	1	24
UMA F10608 (57 mm)	56	54	30	0	24
UMA F10609 (160 mm)	57	55	31	1	24
UMA F10610 (183 mm)	56	54	30	1	24
UMA F10611 (210 mm)	54	54	30	1	24
UMA F10612 (215 mm)	57	55	30	1	25
UMA F10613 (230 mm)	52†	53†	29†	1	24

Note: Numbers in italics indicate lower than typical counts because of early stage of development.

* c1, c2, and u2 are the only centra that have completely formed (i.e., completely surrounded the notochord). Other centra have started to form, although most are only a spot of bone in the ventral midline and thus are not included in this count.

† These counts are lower than average because of the pathological fusion of the first five centra (c1–5). This is counted as a single centrum because it occupies the space of a single centrum, although it is recognized as a fusion because the associated five neural arches are not fused to one another (i.e., they are distinguishable). The neural arches are fused to this pathological centrum.

TABLE 10. Meristic data of vertebrae and centra for a growth series of *Hiodon alosoides*.

Specimen (SL)	Total centra	Total preural centra	Total abdominal centra	Transitional vertebrae	Total preural caudal centra
TU 113117E (24.3 mm)	59*	57	32	1†	25
TU 108118A (30.0 mm)	60	58	31	1	27
UAMZ 4041B (39 mm)	60	58	33	1	25
UMA F10600 (52 mm)	59*	57	32	1	25
UMA F10601 (107 mm)	59	57	32	1	25
UMA F10604 (184 mm)	59	57	32	1	25
UMA F10588 (252 mm)	59	57	32	1	25
UMA F10606 (254 mm)	59	57	33	2	24
UMA F10605 (279 mm)	58	56	31	0	25
UMA F10634 (300 mm)	60	58	33	1	25

* Some centra are not complete rings.

† The left and right portions of the anterior haemal arches of this specimen may not be fused to one another to form a haemal spine because of the early stage of development, but do curve toward one another to approximate the adult condition. The left and right sides of the haemal arch of the transitional vertebra do not show this morphology.

TABLE 11. Meristic data of vertebral elements for a growth series of *Hiodon tergisus*.

Specimen (SL)	Total preural neural arches (excluding pu1)	Autogenous neural arches	Supraneurals	L, R epineural bones
JFBM 22748 (21.0 mm)	54 (None ossified)	Centra not formed	24 (None ossified)	None ossified
JFBM 22747C (24.0 mm)	55	Centra not formed	24	*10, 10*
TU 108166E (34 mm)	54	*55*	24	26, 25
TU 108166D (49 mm)	54	31	25	27, 28
UMA F10608 (57 mm)	53	31	25	27, 27
UMA F10609 (160 mm)	54	31	25	28, 27
UMA F10610 (183 mm)	53	29	24	27, 26
UMA F10611 (210 mm)	53	27	?	25, 27
UMA F10612 (215 mm)	54	29	26	27, 27
UMA F10613 (230 mm)	53	24	26	27, 27

Note: Numbers in italics indicate higher or lower than typical counts because of early stage of development.

TABLE 12. Meristic data of vertebral elements for a growth series of *Hiodon alosoides*.

Specimen (SL)	Total preural neural arches (excluding pu1)	Autogenous neural arches	Supraneurals	L, R epineural bones
TU 113117E (234.3 mm)	56	*31?*	27*	30, 30
TU 108118A (30.0 mm)	58	*58*	31	29, 29
UAMZ 4041B (39 mm)	57	57	31	31, 31
UMA F10600 (52 mm)	56	?	30	29, 30
UMA F10601 (107 mm)	56	31	30	30, 31
UMA F10604 (184 mm)	56	31	31	30, 30
UMA F10588 (252 mm)	57	31	30	29, 29
UMA F10606 (254 mm)	56	31	?	30, 30
UMA F10605 (279 mm)	56	31	30	30, 29
UMA F10634 (300 mm)	57	32	30	30, 31

Note: Numbers in italics indicate higher or lower than typical counts because of early stage of development.
* Only the anterior 17 supraneurals of this specimen stained with alcian. The remaining are assumed to be precartilaginous.

TABLE 13. Fin measurements and ratios for a growth series of *Hiodon tergisus*.

Specimen (SL)	Dorsal fin base (%SL)	Anal fin base (%SL)	Dorsal to anal fin base ratio	Dorsal lobe caudal fin (%SL)	Ventral lobe caudal fin (%SL)
JFBM 22748 (21.0 mm)	3.2 mm (15.2%)	5.5 mm (26.2%)	1 : 1.7	4.8 mm (22.9%)	5.2 mm (24.8%)
JFBM 22747C (24.0 mm)	3.2 mm (13.3%)	5.6 mm (23.2%)	1 : 1.8	4.8 mm (20.0%)	5.3 mm (22.1%)
TU 108166E (34 mm)	3.8 mm (11.1%)	7.5 mm (22.1%)	1 : 2.0	7.2 mm (21.2%)	8.0 mm (23.5%)
TU 108166D (49 mm)	6.1 mm (12.4%)	11.0 mm (22.4%)	1 : 1.8	11.1 mm (22.7%)	12.5 mm (25.5%)
UMA F10608 (57 mm)	7.1 mm (12.4%)	13.3 mm (23.3%)	1 : 1.9	13.5 mm (23.7%)	14.3 mm (25.1%)
UMA F10609 (160 mm)	20.3 mm (12.7%)	37 mm (23.2%)	1 : 1.8	47 mm (26.2%)	44 mm (27.2%)
UMA F10610 (183 mm)	22.9 mm (12.5%)	43 mm (23.3%)	1 : 1.9	50 mm (27.3%)	52 mm (28.4%)
UMA F10611 (210 mm)	21.4 mm (10.2%)	39 mm (18.4%)	1 : 1.8	56 mm (26.9%)	60 mm (28.5%)
UMA F10612 (215 mm)	24.0 mm (11.2%)	42 mm (19.1%)	1 : 1.7	56 mm (25.9%)	60 mm (27.9%)
UMA F10613 (230 mm)	25.5 mm (11.1%)	46 mm (19.9%)	1 : 1.8	63 mm (27.2%)	62 mm (27.0%)

TABLE 14. Fin measurements and ratios for a growth series of *Hiodon alosoides*.

Specimen (SL)	Dorsal fin base (%SL)	Anal fin base (%SL)	Dorsal to anal fin base ratio	Dorsal lobe caudal fin (%SL)	Ventral lobe caudal fin (%SL)
TU 113117E	2.3 mm	7.4 mm	1 : 3.2	5.4 mm	6.8 mm
(24.3 mm)	(9.5%)	(30.5%)		(22.2%)	(28.0%)
TU 108118A	2.9 mm	8.2 mm	1 : 2.8	6.8 mm	7.1 mm
(30.0 mm)	(9.7%)	(22.2%)		(22.7%)	(23.7%)
UAMZ 4041B	4.1 mm	10.4 mm	1 : 2.5	7.0 mm	7.7 mm
(39 mm)	(10.5%)	(26.7%)		(17.9%)	(19.7%)
UMA F10600	5.0 mm	14.8 mm	1 : 3.0	11.6 mm	13.0 mm
(52 mm)	(9.6%)	(28.5%)		(22.3%)	(25.0%)
UMA F10601	10.7 mm	30 mm	1 : 2.8	?*	31 mm
(107 mm)	(10.0%)	(28.1%)		(?)	(28.7%)
UMA F10604	16.7 mm	51 mm	1 : 3.0	43 mm	46 mm
(184 mm)	(9.1%)	(27.4%)		(23.5%)	(25.2%)
UMA F10588	22.2 mm	70 mm	1 : 3.2	50 mm	55 mm
(252 mm)	(8.8%)	(27.9%)		(19.9%)	(21.9%)
UMA F10606	19.8 mm	68 mm	1 : 3.4	57 mm†	62 mm†
(254 mm)	(7.8%)	(26.8%)		(22.4%)	(24.2%)
UMA F10605	24.9 mm	69 mm	1 : 2.8	62 mm	69 mm
(279 mm)	(8.9%)	(24.6%)		(22.4%)	(24.7%)
UMA F10634‡	26.5 mm	72 mm	1 : 2.7	66 mm	71 mm
(300 mm)	(8.8%)	(24%)		(22.0%)	(23.7%)

* All fin rays of the dorsal lobe of the caudal fin are damaged on this specimen; no estimate was possible.
† Estimated measurement because the distal tip of the leading fin ray is broken.
‡ Estimated measurements because the median fins and their pterygiophores, although complete, are disarticulated.

TABLE 15. Meristic data of the caudal fin and skeleton of *Hiodon tergisus*.

Specimen (SL)	Hypurals (no. ossified)	Epurals	Dorsal (ventral) segmented caudal rays	Dorsal (ventral) branched caudal rays	Condition of nspu1	Neural arches on u1	L, R uroneurals
JFBM 22748	7	1	viii, 9	(5)	Rudimentary	Centrum not	3, 4
(21.0 mm)	(7)		(v, 10)	(5)		ossified	
JFBM 22747C	7	1	vi, 12	8	Rudimentary	3	3, 4
(24.0 mm)	(7)		(vi, 12)	(7)			
TU 108166E	7	1	vii, 13	8	Rudimentary	1	3, 2
(34 mm)	(7)		(v, 14)	(8)			
TU 108166D	7	1	vi, 14	8	Rudimentary	2	3, 2
(49 mm)	(7)		(v, 15)	(8)			
UMA F10608	7	1	vii, 14	8	Rudimentary	3	3, 3
(57 mm)	(7)		(vi, 14)	(8)			
UMA F10609	7	1	iv, 16	8	Rudimentary	2	3, 3
(160 mm)	(7)		(i, 17)	(8)			
UMA F10610	7	1	ii, 17	8	Rudimentary	2	3, 2
(183 mm)	(7)		(i, 18)	(8)			
UMA F10611	7	1	iv, 15	8	Rudimentary	2	4, 3
(210 mm)	(7)		(ii, 16)	(8)			
UMA F10612	7	1	ii, 16	8	Rudimentary	2	2, 2
(215 mm)	(7)		(iv, 15)	(8)			
UMA F10613	7	1	iii, 16	8	Rudimentary	2	3, 3
(230 mm)	(7)		(ii, 16)	(8)			

Note: Lowercase Roman numerals indicate the number of unsegmented fin rays. Numbers in italics indicate lower than typical counts because of early stage of development.

TABLE 16. Meristic data of the caudal fin and skeleton of *Hiodon alosoides*.

Specimen (SL)	Hypurals (no. ossified)	Epurals	Dorsal (ventral) segmented caudal rays	Dorsal (ventral) branched caudal rays	Condition of nspu1	Neural arches on u1	L, R uroneurals
TU 113117E (24.3 mm)	7 (7)	1	viii, 12 (vii, 12)	8 (8)	Rudimentary	1	3, 3
TU 108118A (30.0 mm)	7 (7)	1	ix, 12 (vii, 12)	8 (8)	Rudimentary	2	3, 3
UAMZ 4041B (39 mm)	7 (7)	1	viii, 12 (v, 13)	8 (8)	Full	2	3, 4
UMA F10600 (52 mm)	7 (7)	1	viii, 12 (vi, 13)	8 (8)	Rudimentary	3	2, 3
UMA F10601 (107 mm)	7 (7)	1	viii, 13 (iv, 14)	? (8)	Rudimentary	2	3, 2
UMA F10604 (184 mm)	7 (7)	1	vi, 13 (ii, 14)	8 (8)	Moderate	2	3, 3
UMA F10588 (252 mm)	7 (7)	1	vii, 13 (iii, 14)	8 (8)	Rudimentary	2	2, 3
UMA F10606 (254 mm)	7 (7)	1	v, 14 (iv, 15)	8 (8)	Rudimentary	2	2, 3
UMA F10605 (279 mm)	7 (7)	1	vi, 13 (i, 14)	8 (8)	Rudimentary	1*	3, 2
UMA F10634 (300 mm)	7 (7)	1	iv, 15 (iii, 14)	8 (8)	Rudimentary	2	2, 3

Note: Lowercase Roman numerals indicate the number of unsegmented fin rays.
* A second, more posterior neural arch may be fused to the first uroneural.

TABLE 17. Meristic data of dorsal and anal fin rays and pterygiophores for *Hiodon tergisus*.

Specimen (SL)	Dorsal fin rays	Branched dorsal rays	Dorsal proximal radials	Anal fin rays	Branched anal rays	Anal proximal radials
JFBM 22748 (21.0 mm)	iii, 14 (none ossified)	Distal lepidotrichi are poorly developed	15 (none ossified)	iii, 28	Distal lepidotrichia are poorly developed	29
JFBM 22747C (24.0 mm)	iii, 14	Distal lepidotrichia are poorly developed	14 (none ossified)	iii, 29	Distal lepidotrichia are poorly developed	29
TU 108166E (34 mm)	iii, 13	9	15	iv, 31	27	30
TU 108166D (49 mm)	iii, 15	11	14	ii, 31	27	29
UMA F10608 (57 mm)	iii, 15	11	15	ii, 31	26	29
UMA F10609 (160 mm)	i, 16	11	14	i, 31	26	28
UMA F10610 (183 mm)	ii, 15	11	14	i, 32	26	28
UMA F10611 (210 mm)	iii, 14	12	14	i, 30	24	28
UMA F10612 (215 mm)	iii, 13	11	14	o, 32	27	30
UMA F10613 (230 mm)	ii, 13	11	13	ii, 29	25	28

Note: Lowercase Roman numerals indicate the number of unsegmented fin rays. Numbers in italics indicate lower than typical counts because of early stage of development.

TABLE 18. Meristic data of dorsal and anal fin and supports for *Hiodon alosoides*.

Specimen (SL)	Dorsal fin rays	Branched dorsal rays	Dorsal proximal radials	Anal fin rays	Branched anal rays	Anal proximal radials
TU 113117E (24.3 mm)	ii, 12	Distal lepidotrichia are poorly developed	12 (none ossified)	iii, 35	Distal lepidotrichia are poorly developed	35 (none ossified)
TU 108118A (30.0 mm)	iii, 12	9	12	iii, 35	31	36
UAMZ 4041B (39 mm)	ii, 13	9	12	iii, 34	30	35
UMA F10600 (52 mm)	ii, 13	10	12	iii, 35	31	34
UMA F10601 (107 mm)	i, 12	10	13	i, 37	31	36†
UMA F10604 (184 mm)	ii, ?*	?*	11	ii, 34	31	34
UMA F10588 (252 mm)	ii, 11	9	12	v, 33	31	35
UMA F10606 (254 mm)	ii, 12	9	11	iii, 34	31	35
UMA F10605 (279 mm)	ii, 12	10	12	iii, 33	31	33
UMA F10634 (300 mm)	iii, 11	9	11	iii, 32	30	32

Note: Lowercase Roman numerals indicate the number of unsegmented fin rays.
* Posteriormost dorsal fin rays are missing from this specimen.
† The first and second proximal radials of anal fin (pr1 and pr2) are fused in this specimen.

TABLE 19. Meristic data of paired fins for a growth series of *Hiodon tergisus*.

Specimen (SL)	L, R pectoral fin rays (no. branched)	L, R pectoral radials (no. ossified)	L, R pelvic fin rays
JFBM 22748 (21.0 mm)	13, 13 Distal lepidotrichia are poorly developed	4, 4 *(0, 0)*	6, 6
JFBM 22747C (24.0 mm)	14, 11 Distal lepidotrichia are poorly developed	4, 4 (4, 4)	7, 7
TU 108166E (34 mm)	13, 12 (12, 11)	4, 4 (4, 4)	7, 7
TU 108166D (49 mm)	12, 13 (11, 12)	4, 4 (4, 4)	7, 7
UMA F10608 (57 mm)	13, 13 (12, 12)	4, 4 (4, 4)	7, 7
UMA F10609 (160 mm)	14, 13 (13, 12)	4, 4 (4, 4)	7, 7
UMA F10610 (183 mm)	13, 13 (12, 12)	4, 4 (4, 4)	7, 7
UMA F10611 (210 mm)	12, 13 (11, 12)	4, 4 (4, 4)	7, 7
UMA F10612 (215 mm)	13, 13 (12, 12)	4, 4 (4, 4)	7, 7
UMA F10613 (230 mm)	14, 14 (13, 13)	4, 4 (4, 4)	7, 7

Note: Numbers in italics indicate lower than typical counts because of early stage of development.

TABLE 20. Meristic data of paired fins for a growth series of *Hiodon alosoides*.

Specimen (SL)	L, R pectoral fin rays (no. branched)	L, R pectoral radials (no. ossified)	L, R pelvic fin rays
TU 113117E (24.3 mm)	12, 12 (11, 11)	4, 4 (4, 4)	7, 7
TU 108118A (30.0 mm)	11, 11 (10, 10)	4, 4 (4, 4)	7, 7
UAMZ 4041B (39 mm)	12, 12 (11, 11)	4, 4 (4, 4)	7, 8
UMA F10600 (52 mm)	12, 12 (11, 11)	4, 4 (4, 4)	7, 7
UMA F10601 (107 mm)	12, 12 (11, 11)	4, 4 (4, 4)	7, 7
UMA F10604 (184 mm)	11, 12 (10, 11)	4, 4 (4, 4)	7, 7
UMA F10588 (252 mm)	11, 12 (10, 11)	4, 4 (4, 4)	7, 7
UMA F10606 (254 mm)	11, 11 (10, 10)	4, 4 (4, 4)	7, 7
UMA F10605 (279 mm)	12, 12 (11, 11)	4, 4 (4, 4)	7, 7
UMA F10634 (300 mm)	12, 12 (11, 11)	4, 4 (4, 4)	7, 7

TABLE 21. Meristic data of scales for a growth series of *Hiodon tergisus*.

Specimen (SL)	Scales along the lateral line	Scale rows above the lateral line	Scale rows below the lateral line
TU 108145 (39 mm)	55	*6*	9
ANSP 114175 (55 mm)	56	7	9
TU 16811 (104 mm)	56	7	9
ANSP 169010 (125 mm)	53	7	9
UMA F10379 (138 mm)	58	6	9
MCZ 23825 (175 mm)	57	7	10
MCZ 23827 (230 mm)	57	7	9
JFBM 27508 (270 mm)	56	7	9
JFBM 11262* (275 mm)	57	7	10
MCZ 17906 (295 mm)	59	6	9

Note: "Rows above the lateral lines" includes the single dorsal median row. Numbers in italics indicate lower than typical counts because of early stage of development.

* Scale counts were made on the right side of this specimen.

TABLE 22. Meristic data of scales for a growth series of *Hiodon alosoides*.

Specimen (SL)	Scales along the lateral line	Scale rows above the lateral line	Scale rows below the lateral line
NMC 75-1553 (34 mm)	58	*3*	*6*
ANSP 149441 (45 mm)	59	6	9
UAIC 10473.01 (53 mm)	58	7	9
UMA F10602 (92 mm)	62	7	11
UF 65838 (98 mm)	62	7	11
UMA F10603 (114 mm)	60	7	11
MCZ 17908 (215 mm)	59	6	9
UMA F10149 (280 mm)	63	6	9
UMA F10380 (285 mm)	60	7	11
MCZ 157462* (340 mm)	62	8	11

Note: "Rows above the lateral lines" includes the single dorsal median row. Numbers in italics indicate lower than typical counts because of early stage of development.

* Scale counts were made on the right side of the specimen.

gin is always wider than the anterior. The left and right frontals meet each other along the midline but are never tightly sutured together, and there is a slight ridge in the midline of the anterior portion of the neurocranium formed by the suture between the two frontals. The shallow concavity on either side of the midline, formed as a result of this ridge, is filled with adipose tissue. The anterior edges of the frontals are irregular, but there is always a roughly triangular portion of the ethmoid cartilage exposed between the frontals and supraethmoid (etc., Figs. 7–9). Outside of *Hiodon*, this pattern of supraethmoid-frontal contact is seen only in †*Eohiodon* and possibly †*Lycoptera* (see Gaudant, 1968: fig. 5B), although more detailed study of †*Lycoptera* is needed to confirm the arrangement of the anterior dermal skull bones. The lateral edge of the frontal is strongly arched and forms the dorsal roof of the orbit (Fig. 13). The frontals entirely cover the paired anterior fontanelles (afon, Figs. 17 and 18; see discussion under Posterior and Ventral Portions of the Braincase and Ventral Ethmoid Region), which are large openings in the dorsal surface of the neurocranial cartilage separated from each other by a strut of cartilage in the dorsal midline of the neurocrania. Thin laminae of bone extend from the ventral surface of the frontals and follow the lateral margin of the fontanelles.

As in †leptolepids and most living teleosts (Patterson, 1975, 1977a), the pterotics of *Hiodon* (pto, Figs. 7, 9 and 13) are compound bones formed by a dermal ossification surrounding the otic sensory canal (= dermopterotic portion) and a chondral element roofing the dorsal bend of the external (= horizontal) semicircular duct (= autopterotic portion). Even in the very smallest individuals of *Hiodon* examined, the two components were not independent ossifications, although this bone was fairly well-developed in these specimens (Fig. 14; note that only the dermal portion of the pterotic is drawn in this figure). Patterson (1977a) discussed several teleostean taxa in which fusion of the dermal and chondral components of the pterotic is known to be ontogenetic (e.g., *Salmo:* de Beer, 1937; certain cyprinoids: Lekander, 1949; and certain siluroids: Bamford, 1948), as well as some in which it is thought to be phylogenetic (e.g., *Esox:* Jollie, 1975; *Leuciscus:* Lekander, 1949; and *Ictalurus:* Kindred, 1919). The hypothesis that the pterotic represents phylogenetic fusion of originally separate bones in *Hiodon* and other teleostean fishes is supported by the presence of ontogenetic fusion in some taxa (but see Remarks on Phylogenetic Fusion). In *Hiodon*, the dermal portion of the pterotic contacts the parietal anteriorly and the intercalar posteriorly and forms much of the posterolateral margin of the skull roof. The chondral portion of the pterotic is bordered by the epioccipital and intercalar posteriorly and ventrally, and by the sphenotic and prootic anteriorly. A ventrally directed lamella is involved in the posterior hyomandibular fossae (hyfp, Figs. 18–22). A more anterior ventral lamella forms the wall of a fossa for the dilatator operculi muscle. In a specimen of †*Eohiodon falcatus* (FMNH PF9881), the pterotic is well-preserved in ventral view, and has a morphology exactly like that of *Hiodon*.

There is no supraorbital bone in *Hiodon*. Absence of a supraorbital was found to be a synapomorphy of Osteoglossomorpha by Li and Wilson (1996a, 1999). Ma (1987, fig. 1) figured †*Lycoptera* with a single supraorbital; more recent interpretations contend that the supraorbital is absent in this taxon as well (e.g., Jin et al., 1995). Li and Wilson (1999) described the fossil genera †*Kuyangichthys* and †*Jiuquanichthys* as the only osteoglossomorphs with a supraorbital, and they (along with †*Tongxinichthys*) were found to be the sister-group to all remaining osteoglossomorphs. Therefore, loss of the supraorbital should be viewed not as a synapomorphy of Osteoglossomorpha but as a synapomorphy of a less inclusive subgroup of osteoglossomorphs.

The ethmoid region of *Hiodon* is largely cartilaginous. The ossifications of the dorsal and lateral ethmoid region include the mesethmoid, the supraethmoid, and the lateral ethmoid (Figs. 16–18). The perichondral mesethmoid and dermal supraethmoid are the last of the bones of the ethmoid region to ossify, and they fuse to one another in the adult to form a compound bone (Fig. 28). The smallest specimen examined with these bones is a 38 mm SL specimen of *H. alosoides* (TU 113117B). The smallest specimen examined of *H. tergisus* with these bones is a 45 mm SL specimen (TU 108166B), although a slightly larger specimen of *H. tergisus* (UF 78879, 50 mm SL) has only the supraethmoid. These two bones are still separate in a cross-section of a 63 mm SL specimen of *H. alosoides* (UAMZ 4043A, Fig. 23A). In this specimen, the mesethmoid is shown to ossify perichondrally on the lateral surfaces of the cartilage between the left and right nasal capsules. The supraethmoid is well separate from the mesethmoid ossification, but it does lie on the dorsal surface of the ethmoid cartilage, below a

layer of adipose tissue. The margin of the supraethmoid grows posteriorly and contacts the frontals along their anterolateral corners. The bone labeled by Li and Wilson (1994: fig. 2) as "mesethmoid" in †*H. consteniorum* is the supraethmoid, which has been preserved in dorsal view.

Immediately anterior to the orbit lies a bone that forms in the posterolateral wall of the nasal capsule, which I interpret as the lateral ethmoid (let, Figs. 14 and 18–22) with a large, lateral membrane-bone flange (lem, Figs. 13, 18, 20, and 21). Gosline (1961: 29) remarked that this flange makes the lateral ethmoid "look like a circumorbital" in lateral view, although he was not suggesting homology of the flange with a bone of the infraorbital series. The lateral ethmoid has been interpreted as a fused element (e.g., Patterson, 1977a; Taverne, 1977; Li & Wilson, 1994), composed of the lateral ethmoid (chondral component) and antorbital (membrane-bone component), although, as noted by Patterson (1977a: 97), its ontogeny has never been studied. I never observed this bone to be two separate ossifications; thus, there is no direct evidence that it is a fused lateral ethmoid and antorbital (see Remarks on Phylogenetic Fusion). The lateral ethmoid is the first of the ethmoid bones to develop (light chondral mineralization was observed in a 22 mm SL specimen of *H. tergisus*, JFBM 22747B). Early ossification is confined to the lateral margin of the cartilaginous wall between the nasal capsule and the orbit, and from this splint of bone, the circular chondral component grows medially and the membrane-bone flange grows anteriorly along the lateral surface of the ethmoid cartilage (Fig. 14). The posterior margin of the flange develops a troughlike appearance along its posterior margin early in its development, but does not assume its adult shape until relatively late in ontogeny (e.g., a 38 mm SL specimen of *H. alosoides* TU 113117B). In the adult, the lateral flange is triangular and contacts the frontals dorsally. The condition of the "antorbital" in †*H. consteniorum* was described as similar to that in living *Hiodon* (Li & Wilson, 1994: 157). However, the "antorbital" of Li and Wilson (1994: fig. 2) is the lateral ethmoid (a circular bone lying on the posterolateral portion of the nasal capsule). The holotype (UALVP 38875) appears to lack the lateral flange, whereas there is an element that may correspond to the lateral flange in the paratype (UALVP 24200).

The nasals of *Hiodon* (n, Figs. 7–11) are simple tubular ossifications of the anteriormost portion of the supraorbital sensory canal (= nasal sensory canal; nacn, Fig. 15) that form early in ontogeny (Fig. 14). These bones bend sharply ventrolaterally around the anterior margin of the cartilage of the nasal sac. A curved, tubular nasal was identified as a synapomorphy of *Hiodon* by Li and Wilson (1994, 1996a, 1999), although a similarly shaped nasal is found in †*Eohiodon* (e.g., UMA F11249).

Sensory Canals

The cephalic sensory canal system of *Hiodon* was previously described or illustrated by G. J. Nelson (1972b), Taverne (1977), Arratia (1997), and Cavin and Forey (2001). Four pit lines (rows of free neuromast organs) are present in *Hiodon* (Fig. 15B, C; also see G. J. Nelson, 1972b: fig. 13B), but none makes any indentation or scarring in the bone, as they do in *Amia calva* (Grande & Bemis, 1998). Nelson (1972b) observed that the pit lines of *Hiodon* are reduced. Two pit lines (anterior and middle pit lines; pla and plm, respectively, Fig. 15) lie on the dorsal surface of the head posterior to the orbit. The extremely short ethmoidal pit line (epl, Fig. 15) crosses the anterior tip of the snout. The cheek pit line (cpl, Fig. 15) is very faint, and was not clearly visible in any of my specimens.

The lateral sensory canal (llcn, Fig. 15) of *Hiodon* is single and runs the entire length of the body, but does not extend onto the caudal fin; a lateral line scale is shown in Figure 92E. The canal opens to the surface through a single pore per scale. Trautman (1957: figs. 16 and 17; reproduced here as Fig. 1A, B, respectively) incorrectly figured the posteriormost scales of the lateral line as lacking the sensory canal.

The cephalic sensory canals open to the environment through pores that are well separated from the bone-enclosed sensory canal by a long tube in soft tissue (e.g., Fig. 15). The lateral sensory canal pierces both the supracleithrum and posttemporal, becoming the posttemporal sensory canal (ptcn, Figs. 14 and 15). The posttemporal canal forks, with one branch entering the extrascapular and running medially as the supratemporal sensory canal (stcn, Fig. 15C–E); the left and right supratemporal canals do not connect in bone. The other branch continues anteriorly to become the otic sensory canal (see below).

A ventral branch from the posttemporal sensory canal is the preoperculomandibular sensory canal

(pmcn, Fig. 15B, E, F). This canal can be divided into two components: the preopercular sensory canal (popcn) and the mandibular sensory canal (mcn). The preopercular sensory canal closely follows the anterior edge of the preopercle. It continues as the mandibular sensory canal, which enters the angular bone along its posterolateral margin, runs obliquely and ventrally, and continues into the dentary, where it terminates near the mandibular symphysis.

The posttemporal sensory canal continues anteriorly, becoming the otic sensory canal (otcn, Fig. 15B–E). The otic sensory canal runs almost entirely through the pterotic before entering the dermosphenotic, where it becomes the infraorbital sensory canal (iocn, Fig. 15B, E). The infraorbital sensory canal runs along the orbital margin of the infraorbital bones and terminates near the end of the nasal sensory canal; the two canals remain separate. A short segment runs anteriorly in the dermosphenotic but ends before joining the supraorbital canal (Fig. 15E).

There is no connection between the infraorbital sensory canal and the supraorbital sensory canal (socn, Fig. 15B, E). There is a short posterior portion of the supraorbital canal in the parietal, although this condition is variable in *Hiodon* (cf. Figs. 14–16; Li & Wilson, 1994; Cavin & Forey, 2001: fig. 8A). From the parietal, this canal runs the length of the frontal bone before leading into the nasal sensory canal (nacn, Figs. 15B–E and 23A). Li and Wilson (1999: character 12, state 1, fig. 3) found the posterior termination of the supraorbital sensory canal in the frontal was derived independently in three different groups of osteoglossomorphs: once in †*Eohiodon* + *Hiodon*, once in Osteoglossoidei minus (†*Paralycoptera* + †*Tanolepis*), and once in Notopteroidei minus †*Thaumaturus*. Because I found that the supraorbital canal does enter the parietal in some specimens of *Hiodon*, reexamination of this character is necessary, particularly in †*Eohiodon*.

Posterior and Ventral Portions of the Braincase and Ventral Ethmoid Region

Posterior to the orbit, the neurocranium of *Hiodon* is well-ossified and forms a nearly complete bony box surrounding part of the brain; anteriorly the neurocranium is predominantly cartilaginous, particularly dorsally (Figs. 17 and 18). On the dorsal surface of the neurocranium there are two paired fontanelles. The anterior fontanelles (afon, Fig. 17) are the smaller of the two pairs and are covered entirely by the frontals. The posterior fontanelles (pfon, Fig. 17) are large openings that are covered by portions of the frontals, parietals, and the dermal portion of the pterotics. In front of the anterior fontanelles, the dorsal surface of the neurocranium is marked by a pair of grooves, roughly marking the path of the supraorbital canal through the frontal bones. These grooves are perhaps for the superficial ophthalmic rami of the anterodorsal lateral line nerves. In *Hiodon*, as in most teleosts, the chondral autopterotic (part of the posterior portion of the braincase) is fused to the dermal dermopterotic (part of the dermal skull roof) to form a single pterotic bone, and was discussed earlier (see Skull Roof and Dorsal and Lateral Ethmoid Region).

In *Hiodon*, the paired exoccipitals (exo, Figs. 10, 30, and 31) are the only ossifications to immediately surround the foramen magnum (fm, Fig. 12). The left and right exoccipitals are separated dorsomedially by a thin area of cartilage associated with the supraoccipital (not shown in Fig. 12). The exoccipitals contact the supraoccipital and epioccipitals dorsally, the intercalars laterally, and the basioccipital ventrally. Anteriorly, the exoccipitals meet the prootics and together define the dorsal and anterior limits of the auditory fenestrae (af, Fig. 18). A large membrane-bone wall (lexo, Figs. 18, 20, and 21) lies lateral to the spinal cord as it exits the foramen magnum, and two spino-occipital nerves pass though foramina in the exoccipitals at the base of these walls (not shown). Allis (1919) found that in his sectioned specimen of *H. tergisus*, only the dorsal roots of the spino-occipital nerves passed through the anterior of these foramina; the ventral root disappeared before exiting the skull. The posterior faces of the exoccipitals and epioccipitals form the paired posttemporal fossae, which serve as attachment sites for epaxial musculature. The paired, common foramina for the vagus and glossopharyngeal nerves (fIX–X, Fig. 22) are entirely within the exoccipitals and are found on their ventral surface, dorsal to the diverticula of the swim bladder. Anteroventrally, the exoccipitals form the roof to the recess for the lagenar otolith in the basioccipital (clot, Figs. 26 and 30); in turn, they also form the floor of the posterior part of the braincase.

The basioccipital (bo, Figs. 20 and 21) contacts the exoccipital dorsally and the prootics anteriorly and forms the ventral portion of the articulation between the braincase and the first vertebral cen-

trum (Fig. 12C, D). There is a pronounced aortal groove (ag, Fig. 22) along the ventral surface of the basioccipital that is continuous anteriorly with the posterior myodome. Allis (1919: 211) provided the following description of this aortal groove:

> [T]he groove on the ventral surface of the basioccipital of my 51-mm. specimen lodges the anterior portion of the median dorsal aorta. When, proceeding anteriorly, the aorta begins to widen, preparatory to separating into a lateral dorsal aorta on either side, it recedes from the groove and is replaced by the hind ends of the musculi recti externi; these muscles soon occupying the entire groove, the aorta lying ventral to them and outside the groove. The lateral edges of the groove give insertion to the tunica externa of the air-bladder, the tissues of the tunica forming, in the posterior, but not the anterior portion of the groove, an arched bridge beneath the aorta and so enclosing it in a canal: this being as described by Bridge ('99) in *Notopterus*. The notochord, enclosed in the basioccipital, lies directly above the bottom of the groove, separated from it by only a thin layer of bone of perichordal origin.

As observed by Allis (1919: 216), the only skeletal distinction between the posterior myodome and the aortal groove is that the posterior myodome is "closed ventrally by the parasphenoid and that it lies in the prootic region." Two cartilages (cfpm, Figs. 18 and 19) are continuous anteriorly with the ventrolateral ridges (= the "lateral edges" described by Allis, 1919: 211) demarcating the aortal groove of the basioccipital. These cartilages lie against the medial surfaces of the ascending processes of the parasphenoid (arp, Fig. 30) and meet ventrally to form the floor of the posterior myodome. The dorsal surface of the basioccipital forms the floor and walls of the paired chambers for the lagenar otoliths (clot, Figs. 26 and 30), which are separated from each other by a medial lamella of bone.

In *Hiodon*, the median basioccipital and paired exoccipitals together form a tripartite occiput ("the boundary between the skull and vertebral column"; Bemis & Forey, 2001: 359; Fig. 12). No vertebral centra are incorporated into the occipital region of *Hiodon*, either ontogenetically or phylogenetically. Bemis and Forey (2001: fig. 20.4) found that incorporation of at least three neural arches and centra into the occipital region of the skull "characterized" Chondrostei + Neopterygii. However, as these authors note (Bemis & Forey, 2001: 373), there is much variation of the condition within teleosts, and in teleosts, "up to and including osteoglossomorphs . . . both centra and neural arches are included in the skull (although by no means all members of the various clades may show such incorporation)."

The intercalars (ic, Figs. 8 and 9) form the posterolateral corners of the neurocranium and contribute to the fossae for the posterior heads of the hyomandibulae (hyfp, Fig. 22). This condition is found also in notopteroids (Greenwood, 1973) and most members of †Icthyodectiformes (Patterson & Rosen, 1977). The intercalar is a winglike element with a strong ventrolateral concavity that contacts the exoccipital medially, the epioccipital dorsally, and the pterotic anteriorly. The intercalar develops lateral to the vagal nerve foramen in the exoccipital but does not contribute to the formation of this foramen. Patterson (1973, 1975) commented extensively on the comparative anatomy of this bone within actinopterygians, and particularly within teleosts. Patterson (1973) concluded that the condition found in teleosts, in which the intercalar is entirely a membrane bone (i.e., the endochondral component found in †caturids, †pholidophorids, and basal †leptolepids has been lost), is a derived condition that is a "consequence of closure of the cranial fissure" (Patterson, 1973: 254). This condition was derived independently in *Amia* (Grande & Bemis, 1998: 61–62).

The paired epioccipital bones (epo, Figs. 9, 10, and 12) of *Hiodon* lie on the posterolateral corners of the braincase and, along with the supraoccipital, enclose the dorsal portion of the posterior semicircular duct (fpsd, Fig. 29). Ventrally, this canal widens into a chamber that contains the ampullae of the posterior semicircular ducts (cpsd, Fig. 29). The center of ossification is along the posterolateral edge of this element, which begins to develop in *H. tergisus* at about 22 mm SL (JFBM 22747B), but was not observed in *H. alosoides* until 31 mm SL (UAMZ 4041C, Fig. 14C, D). In the adult, these bones contact the supraoccipital medially, the exoccipitals ventrally, and the intercalars and pterotics laterally. The posterior arm of the parietal, which forms the parietal bridge, overlaps the epioccipital dorsally but does not actually suture into the posterior neurocranium. The sutures between the epioccipitals and all adjacent bones are smooth or cartilage-filled. An anterior extension of the epioccipital overlaps the dorsal surface of the pterotic (Figs. 17 and 24). The slightly concave anterior face of the epioccipital forms the posterior limits of the temporal fossae (see discussion under Temporal Fossae). The concave posterior face of the epioccipital contributes to the dorsal portion of the posttemporal fossae (Fig. 12). The posterior apex of the epioccipital

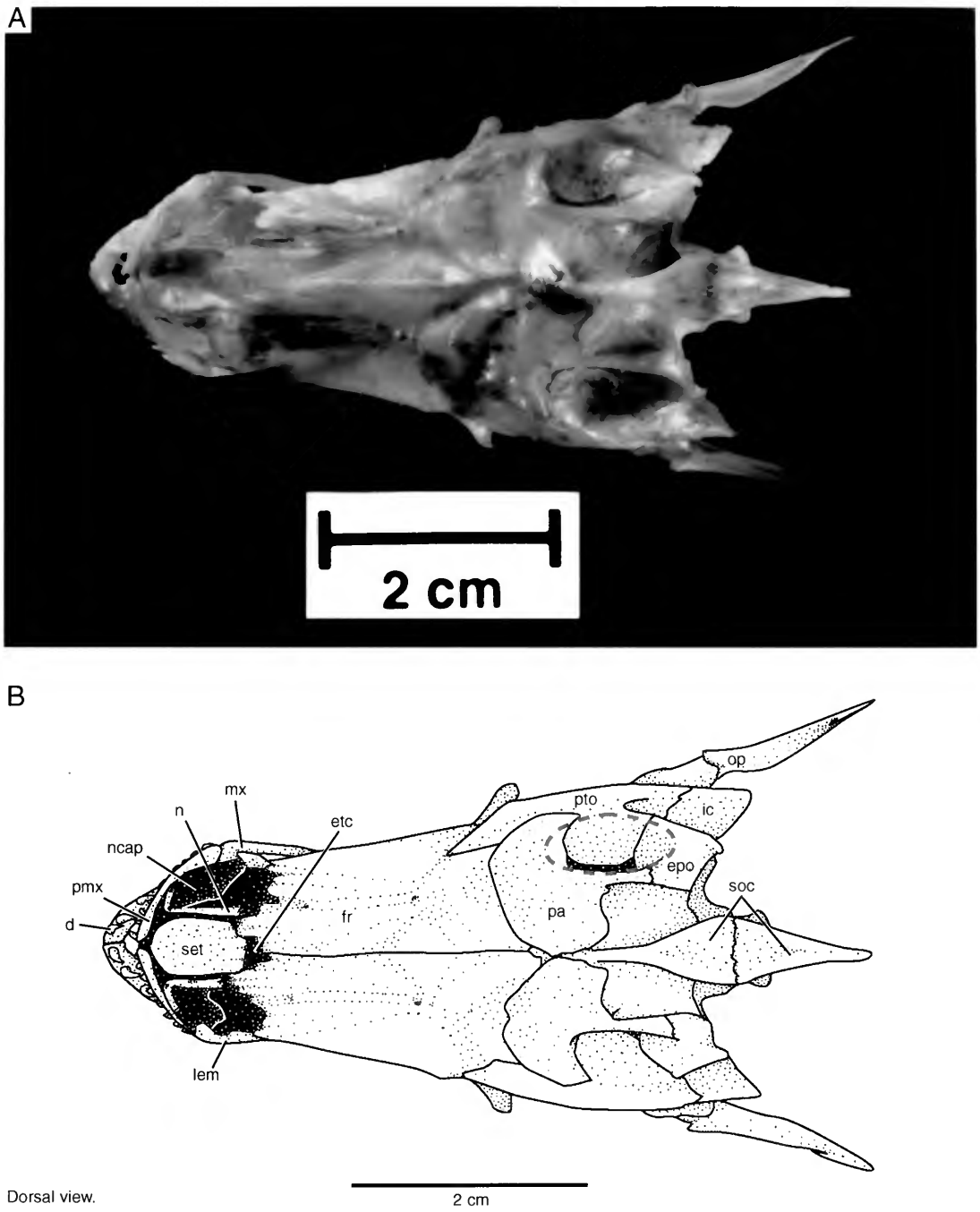

FIG. 7. *Hiodon alosoides*. **A**, Photograph, and **B**, Line drawing of skull in dorsal view of an adult (UMA F10580, 270 mm SL, female). Right temporal fossa is outlined in red. Infraorbitals were removed. Anterior faces left.

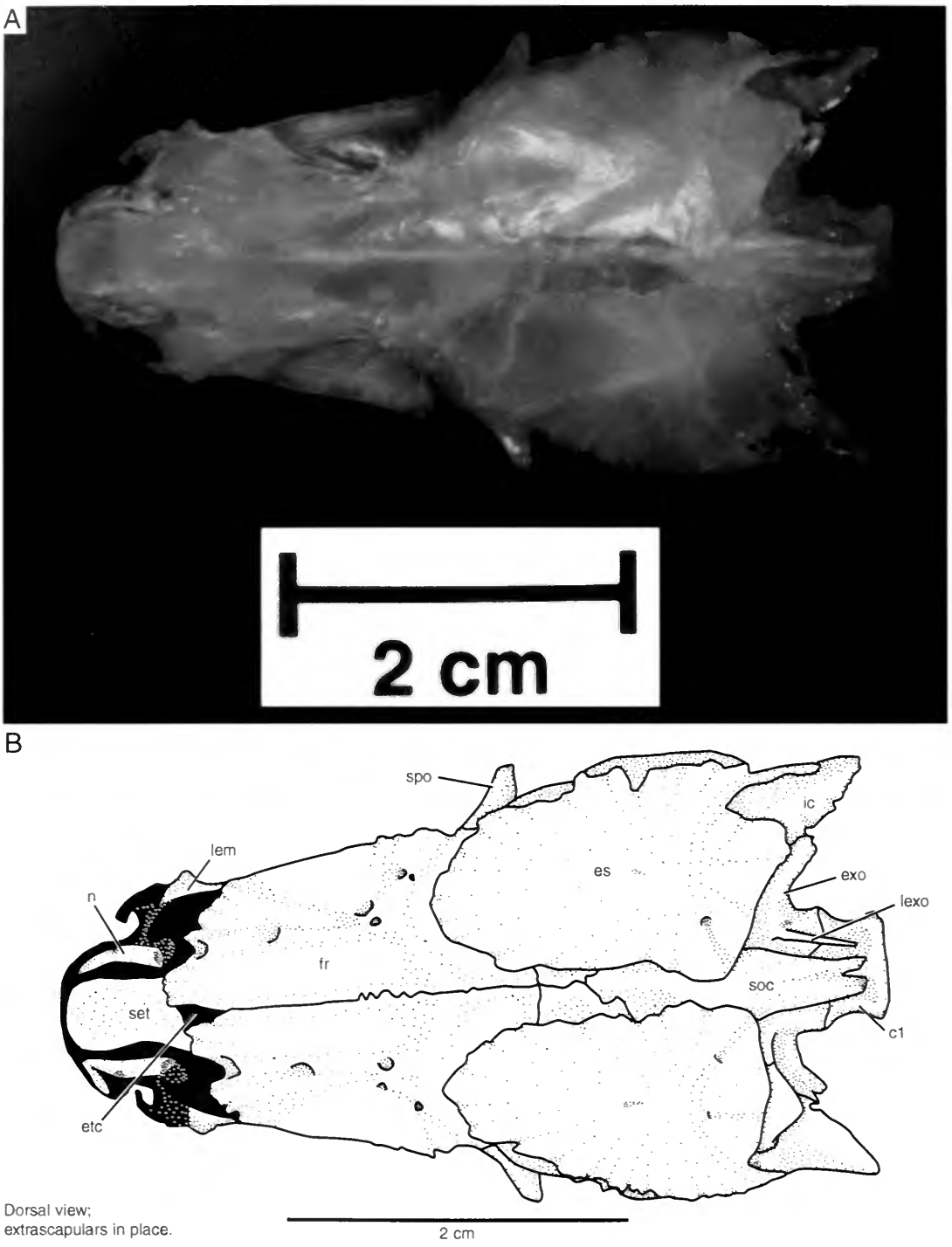

FIG. 8. *Hiodon alosoides*. **A**, Photograph, and **B**, line drawing of neurocranium and associated dermal bones of an adult (UMA F10581, 315 mm SL, female) in dorsal view.

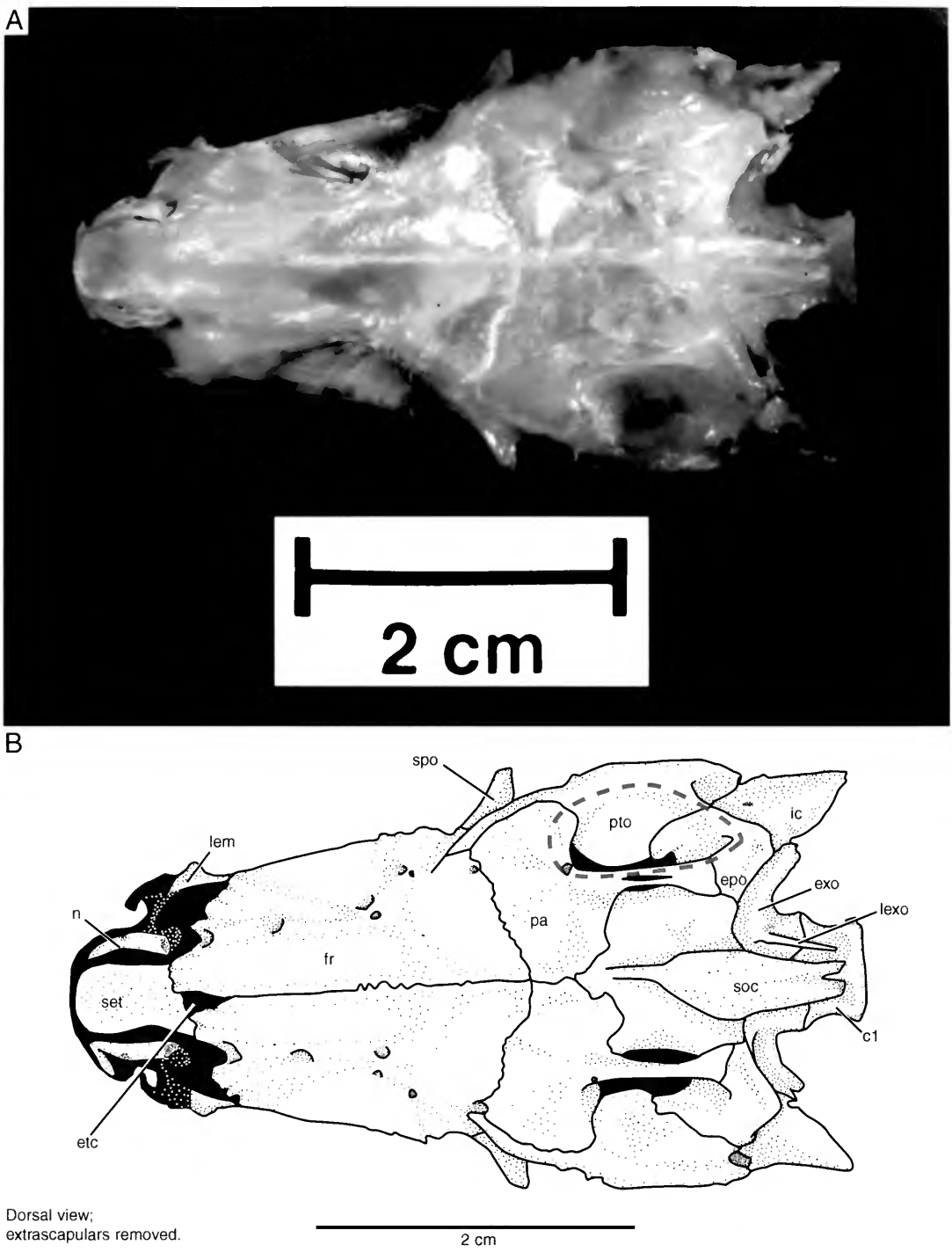

FIG. 9. *Hiodon alosoides*. **A**, Photograph, and **B**, line drawing of neurocranium and associated dermal bones of an adult (UMA F10581, 315 mm SL, female) in dorsal view with extrascapulars removed. Right temporal fossa is outlined in red. Anterior faces left.

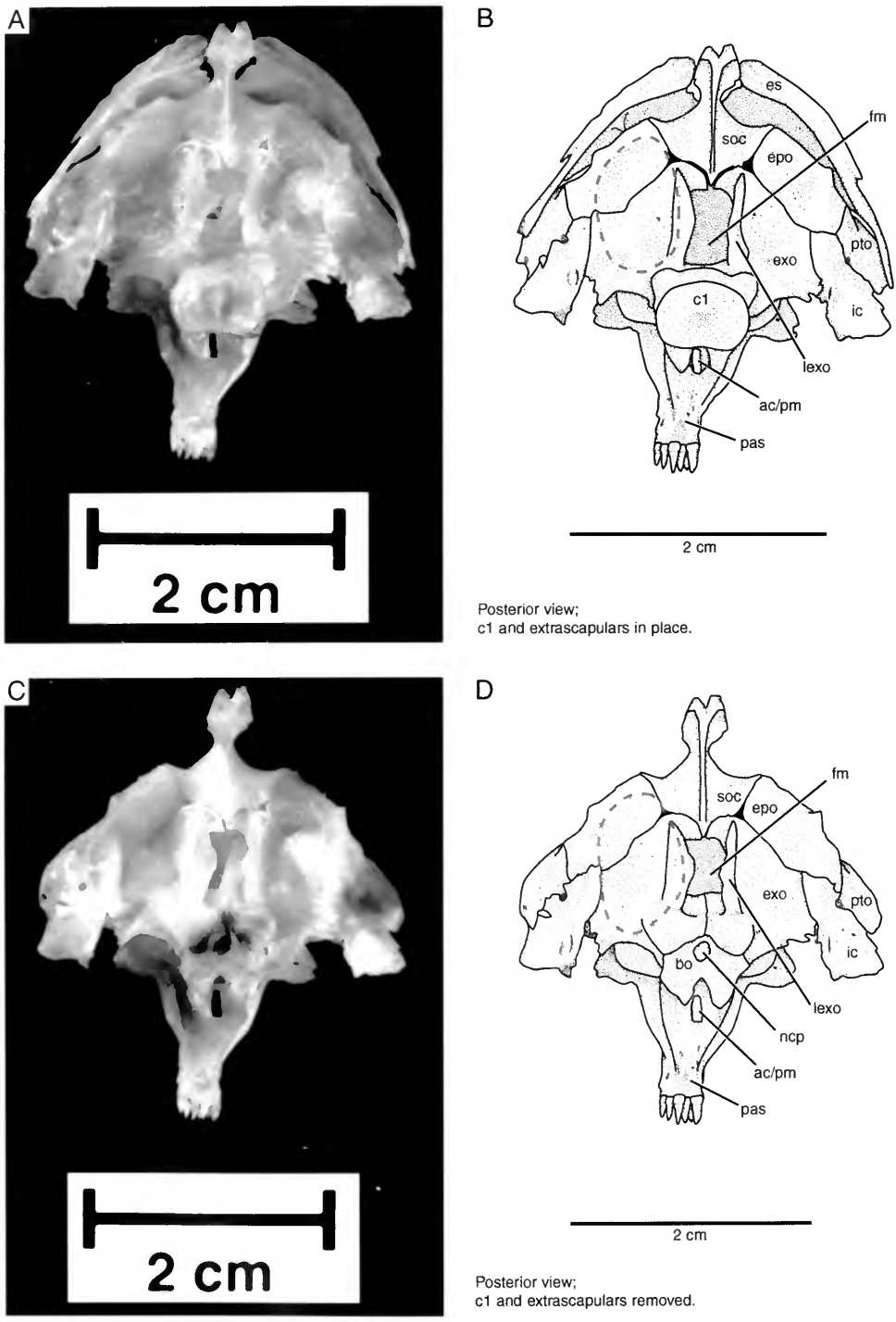

FIG. 12. *Hiodon alosoides*. **A** and **C**, Photograph, and **B** and **D**, line drawing of neurocranium and associated dermal bones of an adult (UMA F10581, 315 mm SL, female) in posterior view. In C and D, the extrascapulars (es) and first centrum (c1) were removed. Left posttemporal fossa is outlined in red.

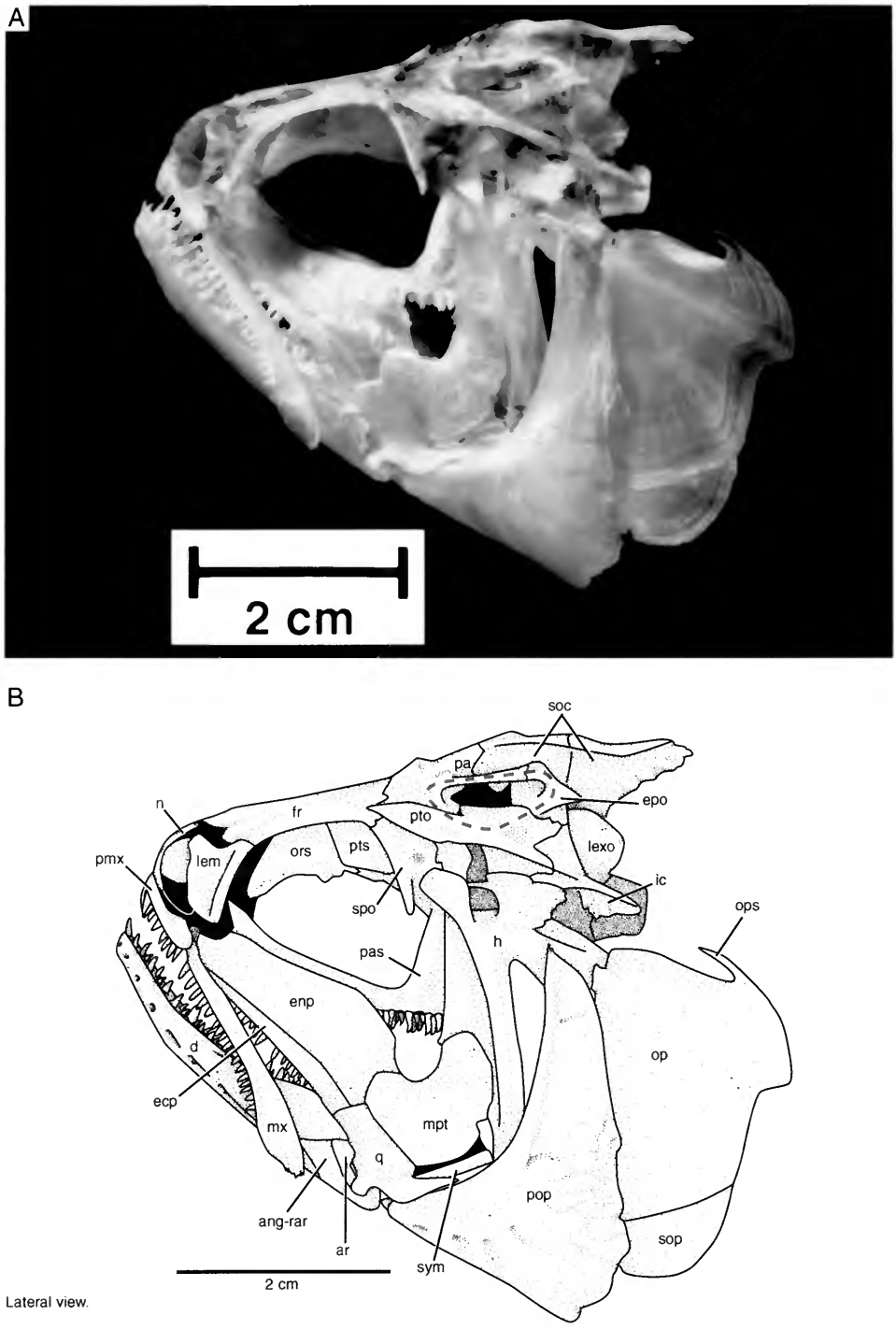

FIG. 13. *Hiodon alosoides*. **A**, Photograph, and **B**, line drawing of skull in lateral view of an adult (UMA F10580, 270 mm SL, female). Left temporal fossa is outlined in red. Infraorbitals and extrascapulars were removed. Anterior faces left.

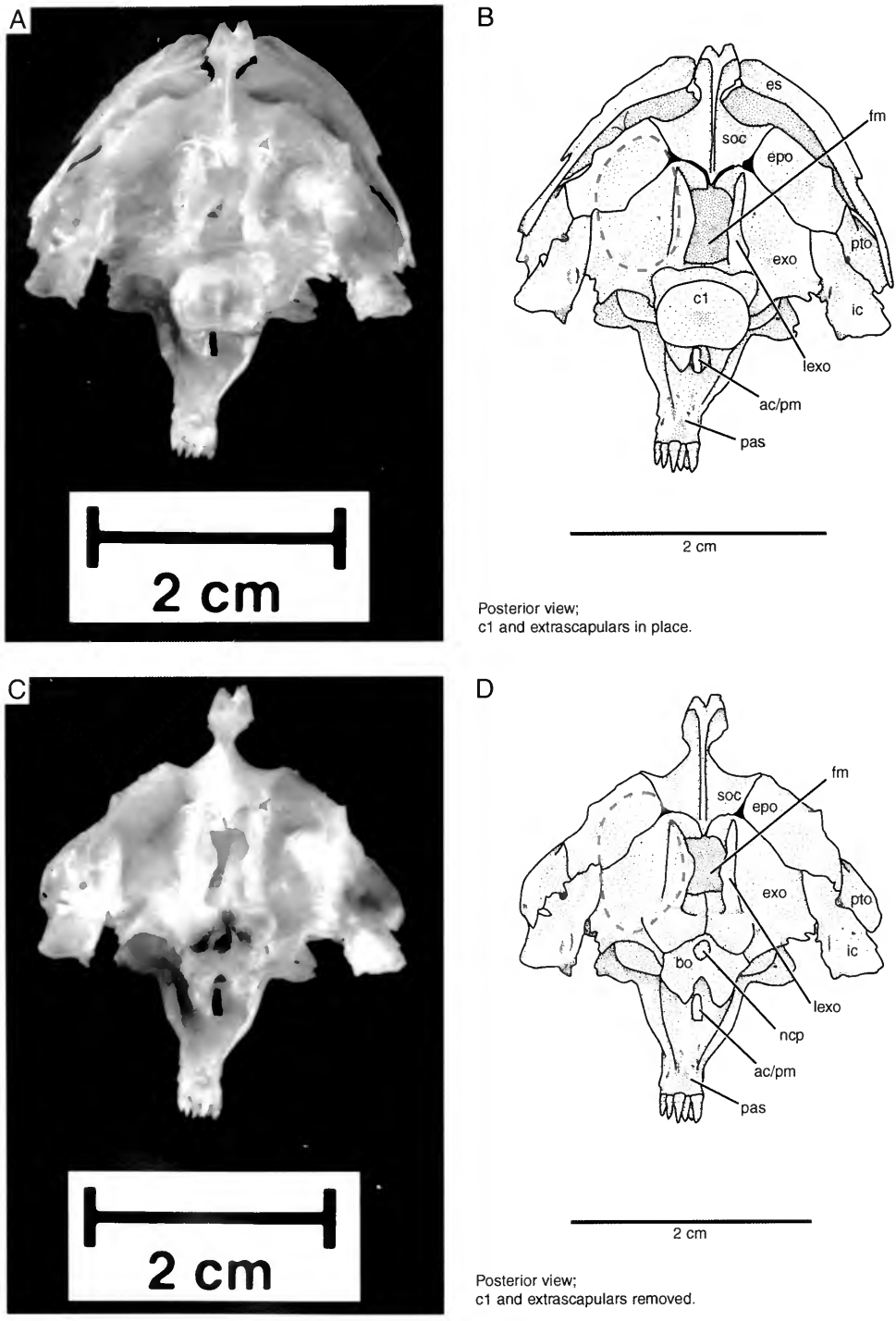

FIG. 12. *Hiodon alosoides*. **A** and **C**, Photograph, and **B** and **D**, line drawing of neurocranium and associated dermal bones of an adult (UMA F10581, 315 mm SL, female) in posterior view. In C and D, the extrascapulars (es) and first centrum (c1) were removed. Left posttemporal fossa is outlined in red.

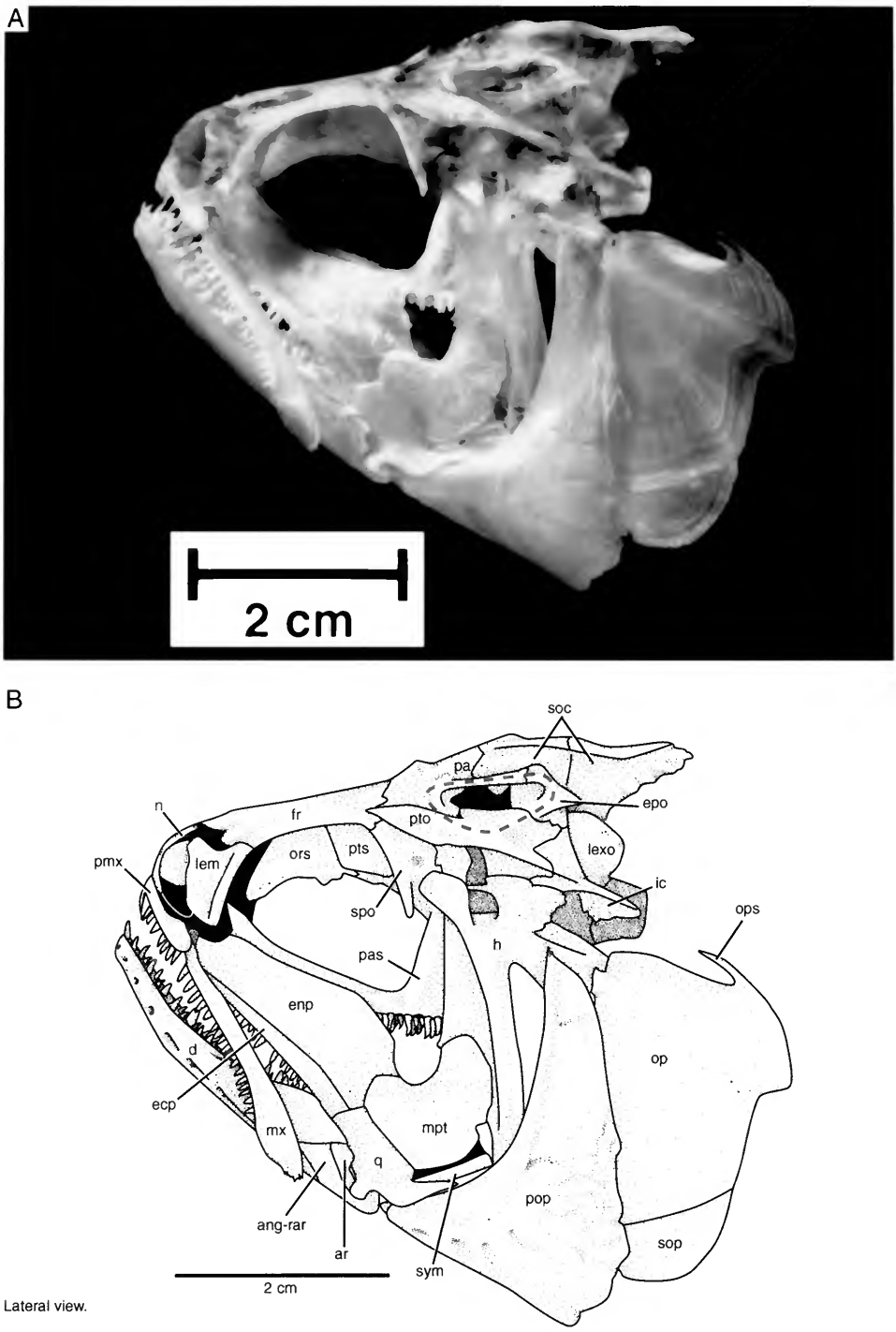

FIG. 13. *Hiodon alosoides*. **A**, Photograph, and **B**, line drawing of skull in lateral view of an adult (UMA F10580, 270 mm SL, female). Left temporal fossa is outlined in red. Infraorbitals and extrascapulars were removed. Anterior faces left.

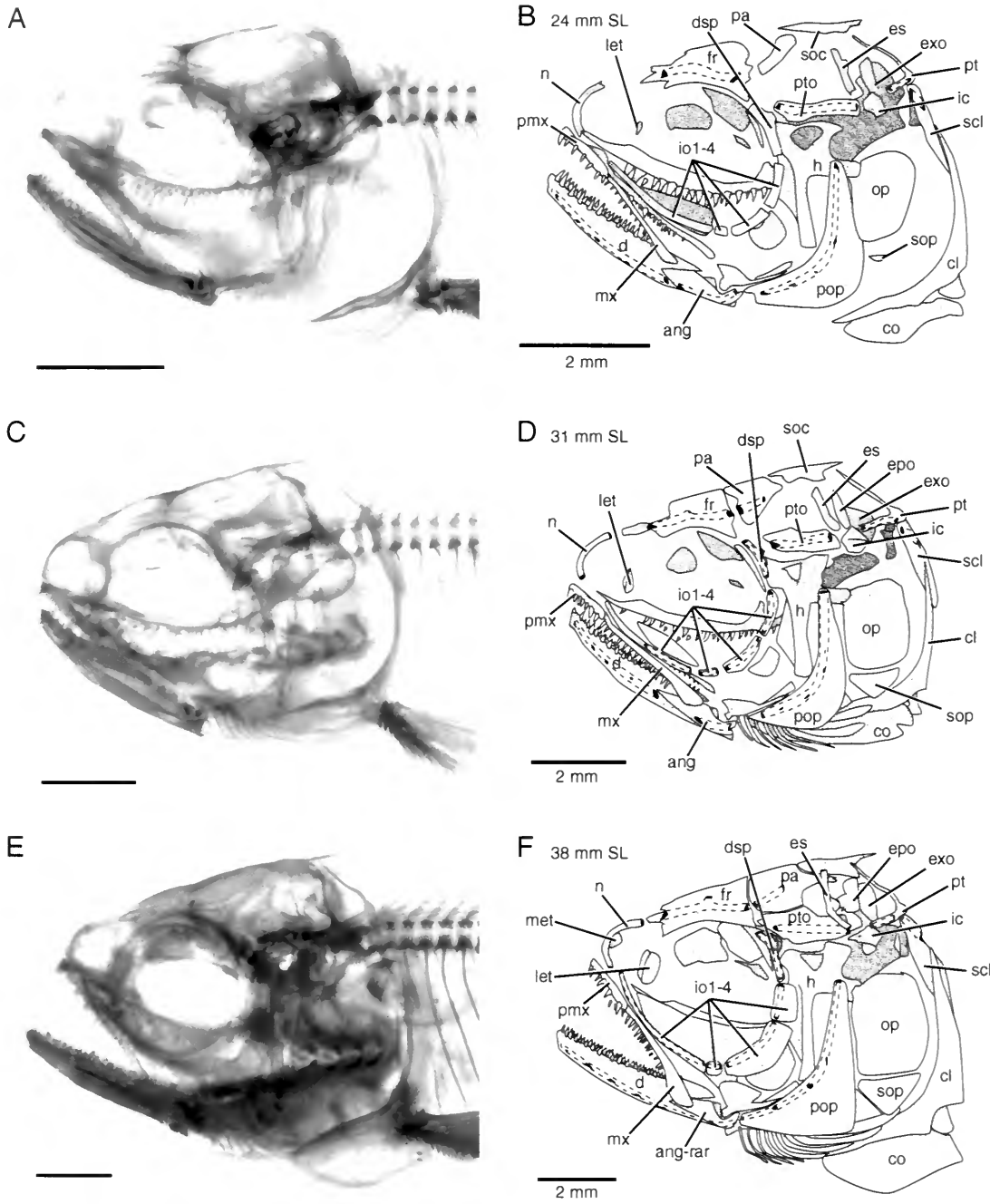

FIG. 14. *Hiodon alosoides*. **A**, **C**, and **E**, Photographs; **B**, **D**, and **F**, line drawings of cleared and stained skulls and pectoral girdles from a growth series in lateral view showing the development of some skull bones. A and B, TU 113117E (24 mm SL). C and D, UAMZ 4041C (31 mm SL). E and F, TU 113117B (38 mm SL). Dashed lines indicate position of sensory canals enclosed in bone. Ventral portions of the hyoid arch and all of the branchial arches were removed in the specimen illustrated in A and B. Anterior faces left.

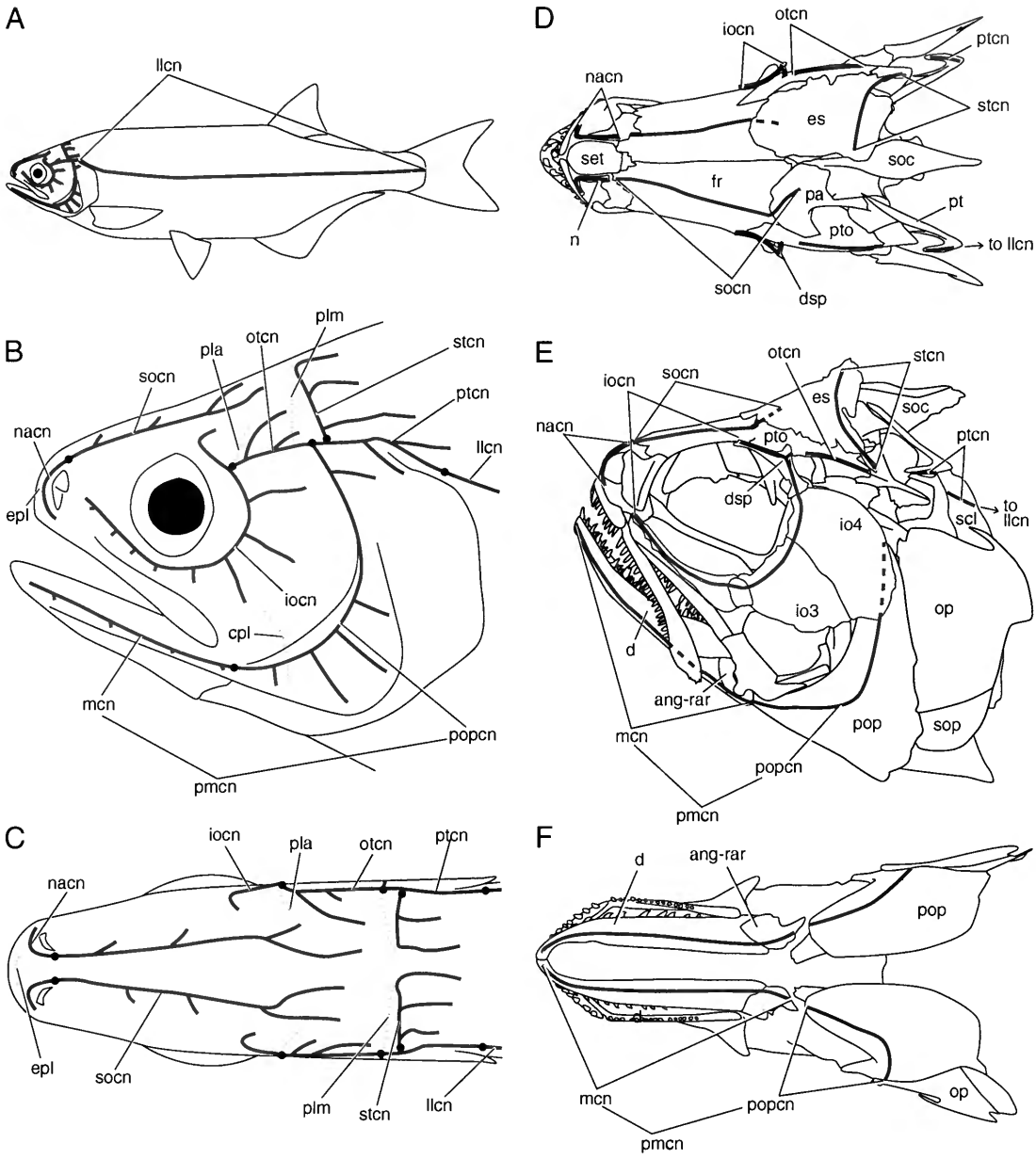

FIG. 15. *Hiodon,* sensory canals. **A**, Outline of an entire fish, showing the cephalic sensory and lateral sensory canal system. **B** and **C**, Close-up view of the cephalic sensory canal system in lateral (B) and dorsal (C) views. Sensory canals and tubes are drawn based largely on *H. tergisus* (UMA F10599, 235 mm SL, male). This alcohol specimen was patted dry and the air-filled sensory canals and tubes (blue lines) and pit lines (blue dots) became clearly visible through the dermis. Position of pit lines after Nelson, 1972b, and specimens. Black dots indicate boundaries between regions of continuous, yet distinctly defined, sensory canals. **D–F**, Line drawings of the skull and pectoral girdle showing the position of the cephalic sensory canals in dorsal (D), lateral (E), and ventral (F) views. Note that only the portions of the canals enclosed in bone are illustrated in D, E, and F. Dashed lines indicate portions of canals covered by more superficial dermal bones.

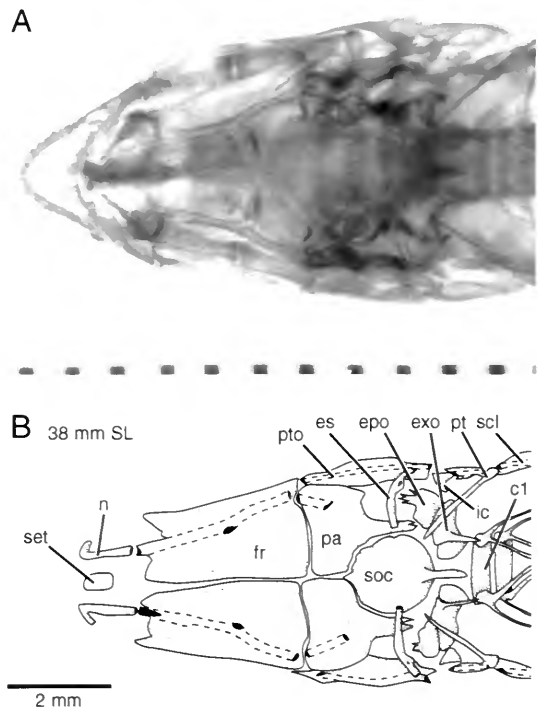

FIG. 16. *Hiodon alosoides*. **A**. Photograph, and **B**. line drawing of skull roof and other skull elements of a small juvenile (TU 113117B, 38 mm SL) in dorsal view. Dashed lines indicate position of sensory canals enclosed in bone. Note that the cartilages and many of the bones visible in the photograph have been omitted from the line drawing (e.g., oral jaw elements). Anterior faces left. Scale in A in millimeters.

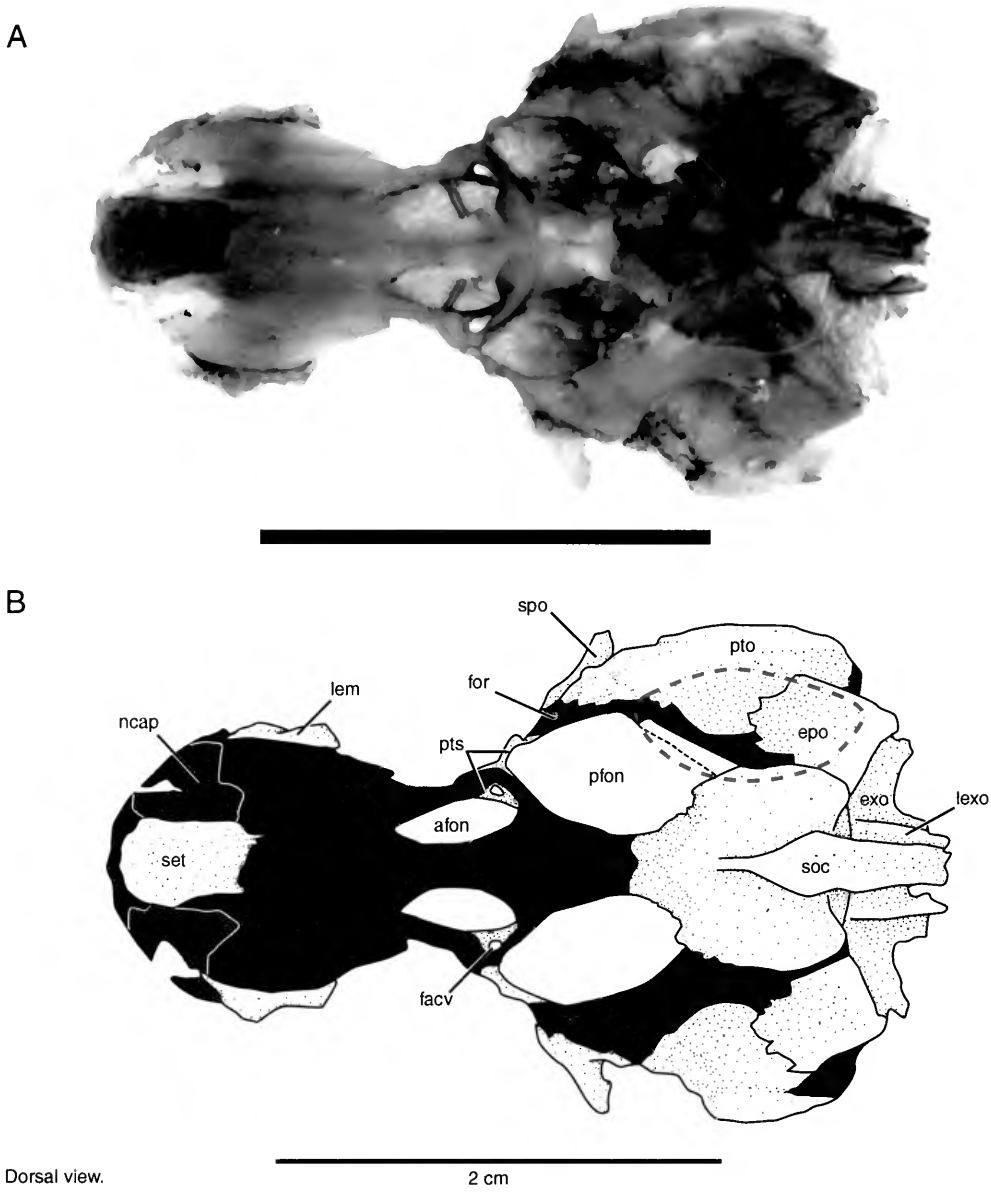

FIG. 17. *Hiodon alosoides*. **A**, Photograph, and **B**, line drawing of neurocranium of an adult (UMA F10582, 275 mm SL, male) in dorsal view. Most of the dermal bones and the anterior dermal portion of the pterotic (= dermopterotic) bones have been removed from the left side to show underlying cartilaginous portions of neurocranium. The neurocranium of this specimen was prepared following the method of Hilton and Bemis (1999). Briefly, after soaking in hot water to remove dermal bones and soft tissue, the neurocranium was placed in 70% ethanol and all remaining soft tissue was removed by hand under a dissecting microscope. The specimen was then transferred to a 0.5% potassium hydroxide (KOH) solution to which a few drops of alizarin red S was added. After the bones were stained, the neurocranium was returned to clean 70% ethanol. In the photograph, bones appear as dark structures, and cartilage is white. Scale bar = 2 cm. In the line drawing, cartilage is shown as black with a white stipple. Dashed line indicates a portion of cartilage that was broken during preparation. Right temporal fossa is outlined in red. Anterior faces left.

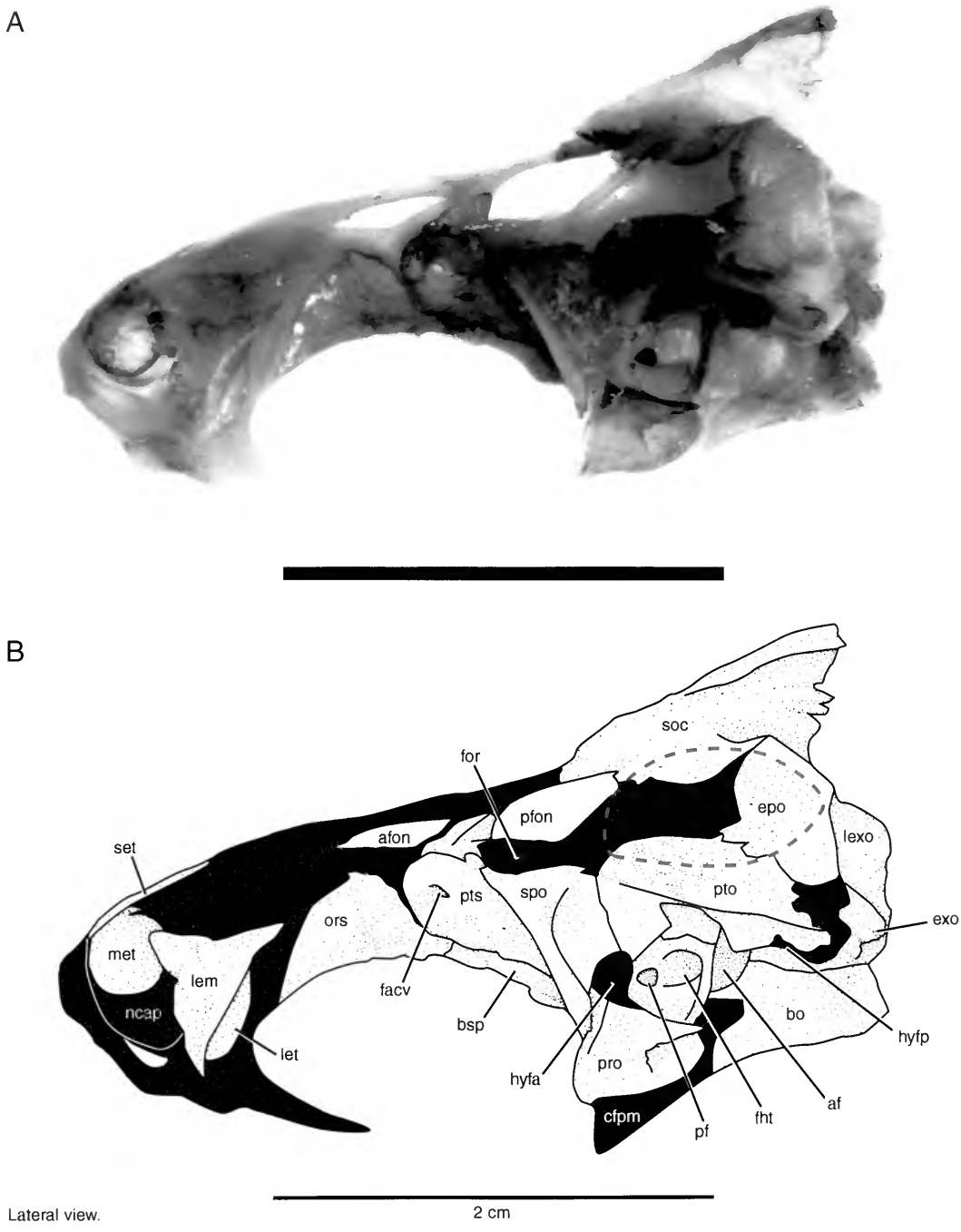

FIG. 18. *Hiodon alosoides*. **A**, Photograph, and **B**, line drawing of neurocranium of an adult (UMA F10582, 275 mm, SL male) in lateral view. Most of the dermal bones and the anterior membrane bone portion of the pterotic (= dermopterotic) have been removed to show the underlying cartilaginous portions of the neurocranium. In the photograph, bones appear as dark structures, and cartilage is white. Scale bar = 2 cm. In the line drawing, cartilage is shown as black with a white stipple. Left temporal fossa is outlined in red. Anterior faces left.

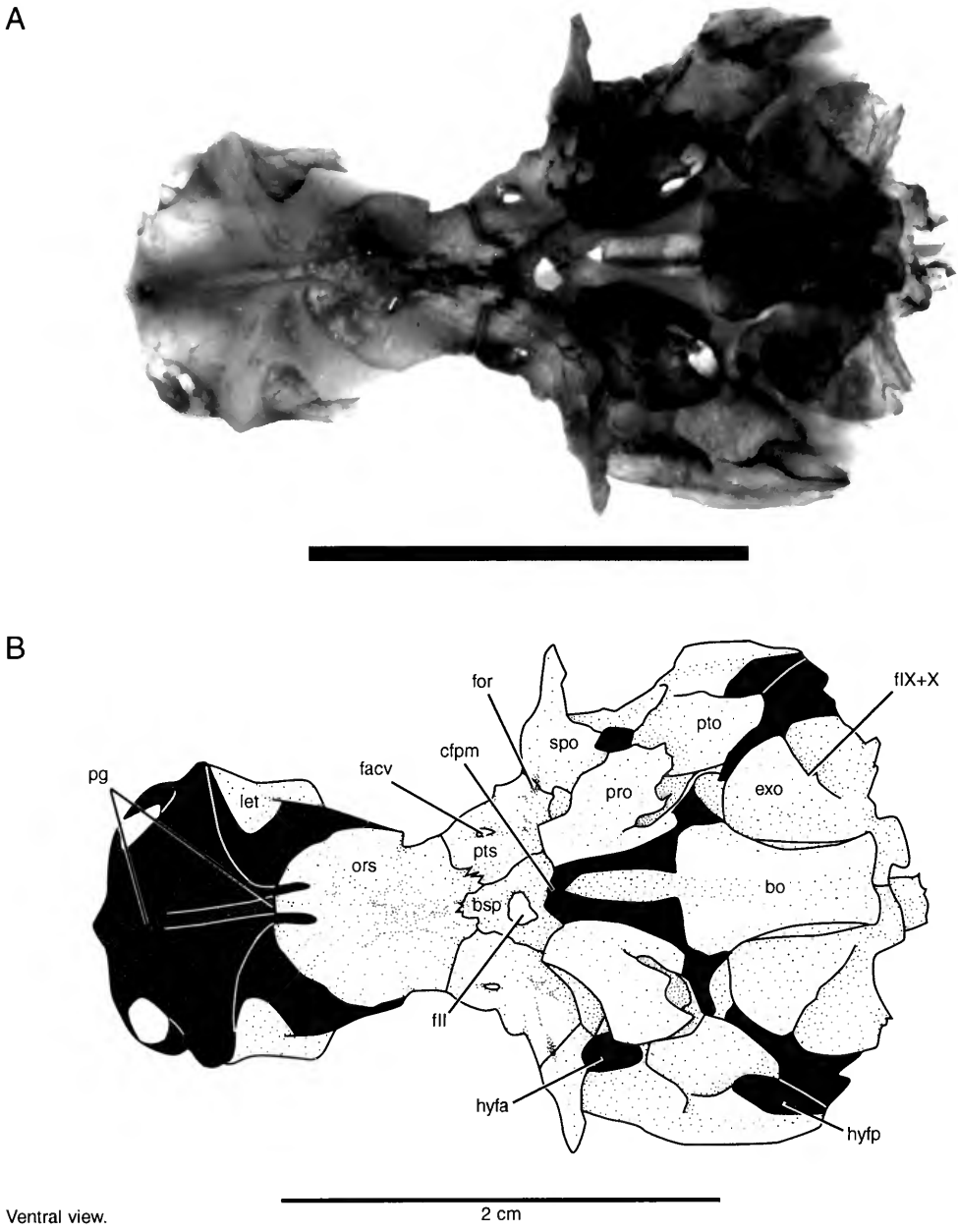

FIG. 19. *Hiodon alosoides*. **A**, Photograph, and **B**, line drawing of neurocranium of an adult (UMA F10582, 275 mm SL, male) in ventral view. Most of the dermal bones and the anterior membrane bone portion of the pterotic (= dermopterotic) have been removed to show the underlying cartilaginous portions of the neurocranium. In the photograph, bones appear as dark structures, and the cartilage is white. Scale bar = 2 cm. In the line drawing, cartilage is shown as black with a white stipple. Anterior faces left.

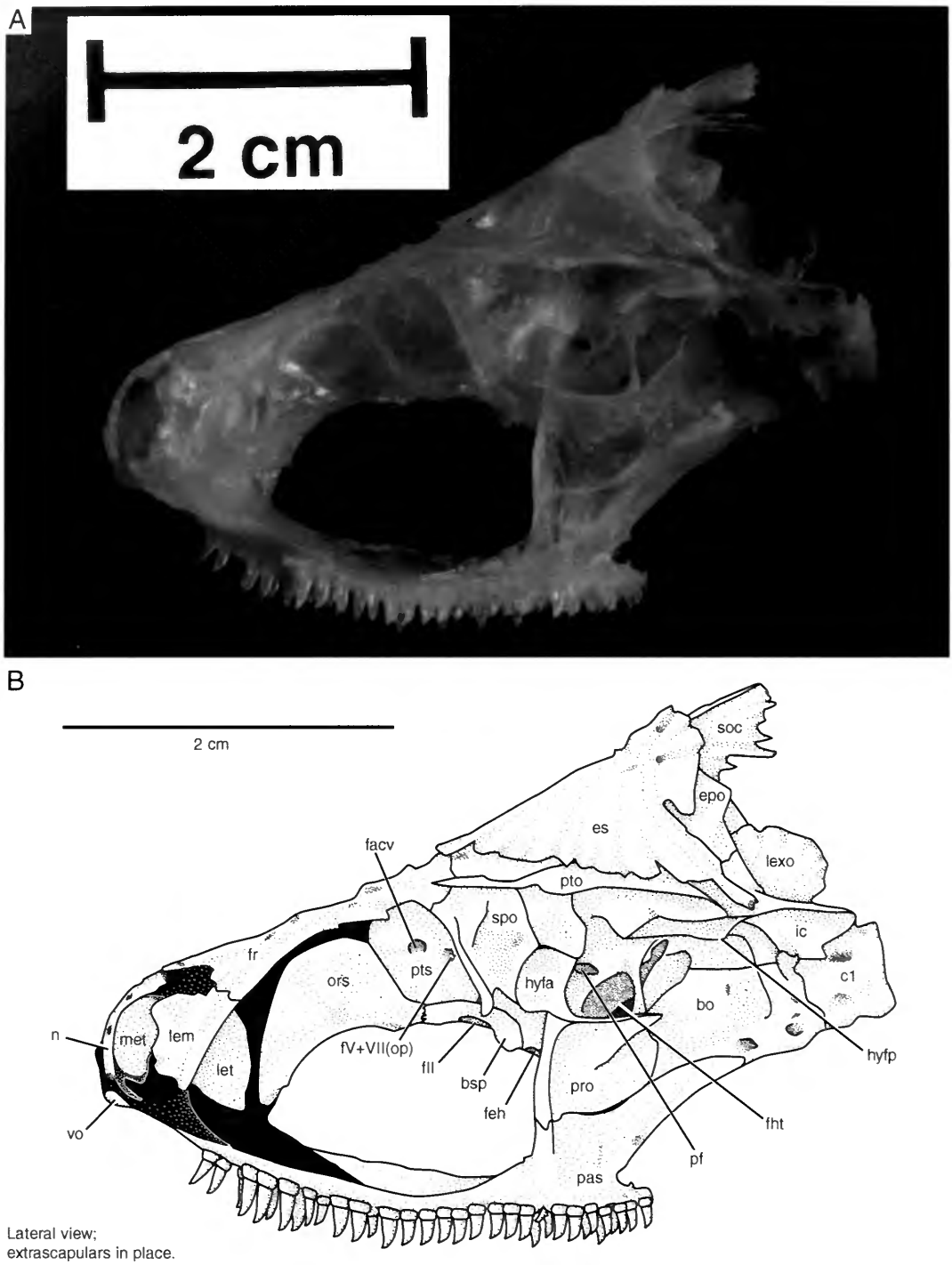

FIG. 20. *Hiodon alosoides*. **A**, Photograph, and **B**, line drawing of neurocranium and associated dermal bones of an adult (UMA F10581, 315 mm SL, female) in lateral view. Anterior faces left.

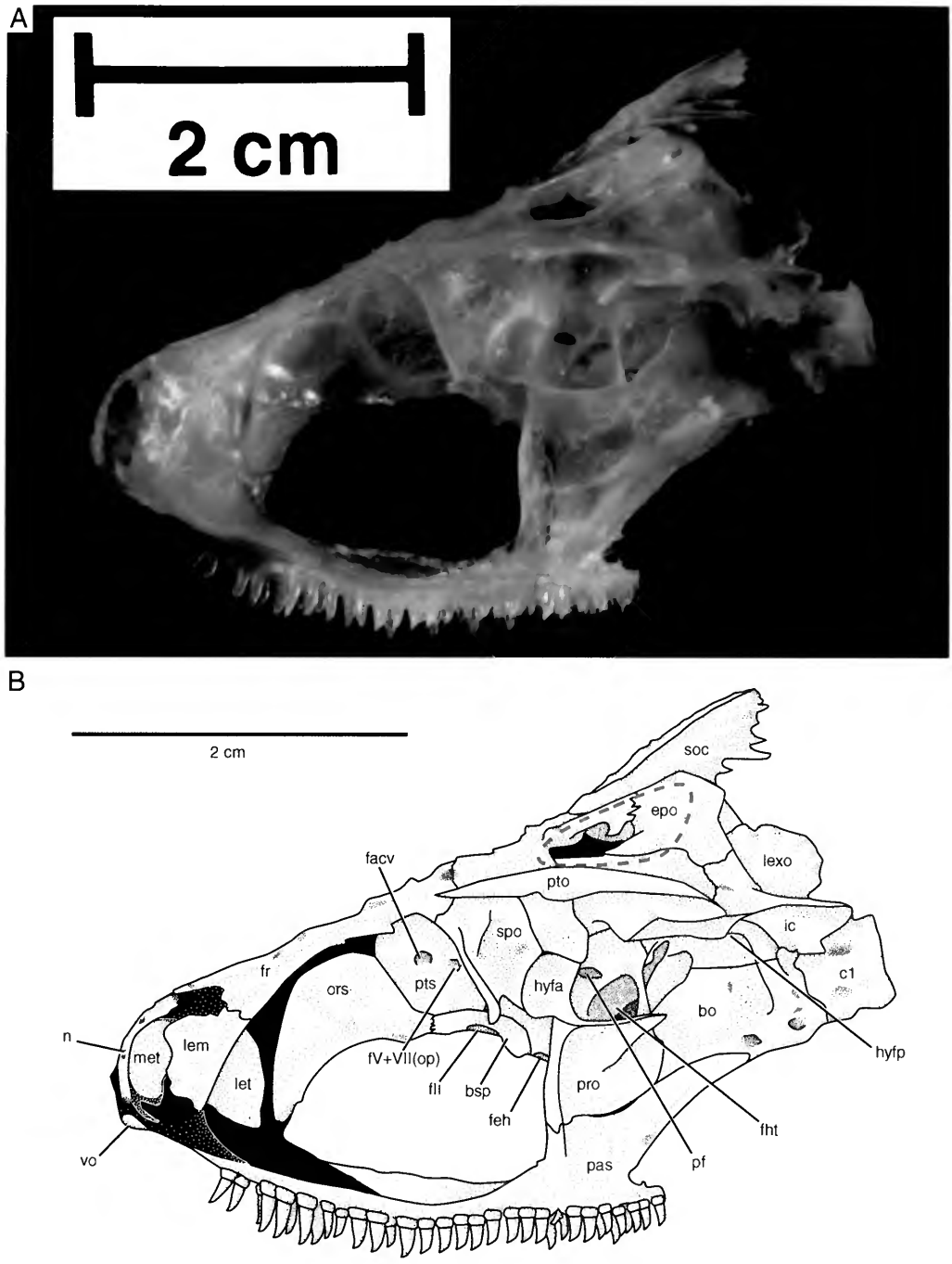

Lateral view;
extrascapulars removed.

FIG. 21. *Hiodon alosoides*. **A**, Photograph, and **B**, line drawing of neurocranium and associated dermal bones of an adult (UMA F10581, 315 mm SL, female) in lateral view with extrascapulars removed and left temporal fossa outlined in red. Anterior faces left.

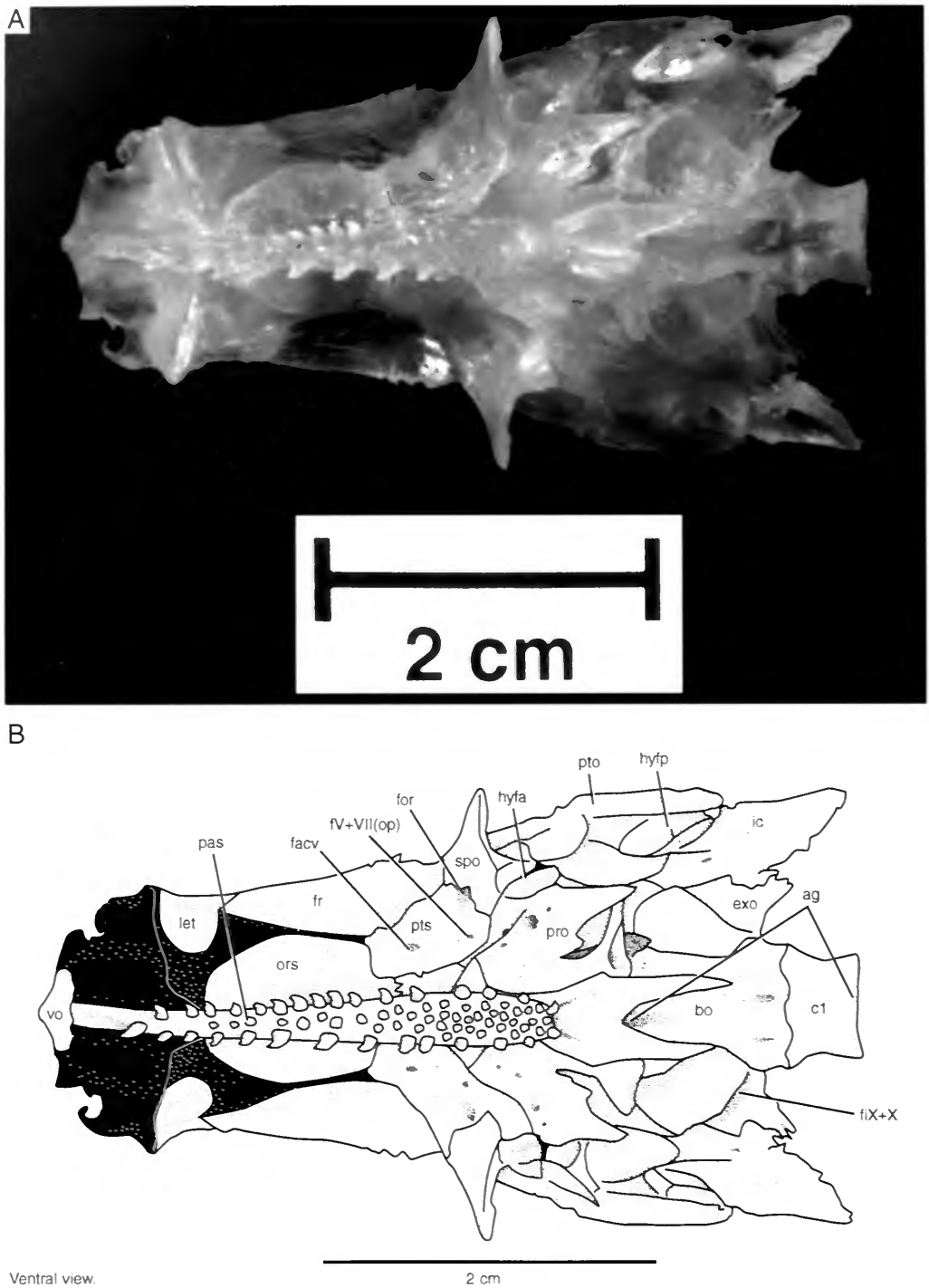

FIG. 22. *Hiodon alosoides*. **A.** Photograph, and **B.** line drawing of neurocranium and associated dermal bones of an adult (UMA F10581, 315 mm SL, female) in ventral view. Anterior faces left.

serves as the attachment site of a strong ligament that connects the dorsal arm of the posttemporal to the skull (lig, Fig. 24).

In *Hiodon*, a single median supraoccipital (soc, Figs. 8, 9, and 17) contacts the parietals anteriorly, epioccipitals posterolaterally, and exoccipitals posteroventrally. The supraoccipital borders the dorsal portion of the cartilage of the temporal fossae, ventral to the parietal bridge. The supraoccipital initially develops perichondrally and then ossifies endochondrally. This bone grows posteriorly and ventrally but is excluded from the foramen magnum by a thin ridge of cartilage that extends posteriorly as a rod of cartilage from the occipital cartilage to the first neural arch (occ, Figs. 24, 25A–C) and serves as a site of attachment for the anterior supracarinalis muscle (Fig. 25C). The ventral surface of the supraoccipital is strongly concave (Fig. 29). The posterior semicircular duct passes through the posterolateral border of the supraoccipital (fpsd, Fig. 29). The condition of having the posterior duct completely surrounded by bone of the supraoccipital was noted for several osteoglossomorphs by Cavin and Forey (2001). Maisey (1999: 34) also noted this condition for osteoglossomorphs (*Arapaima*), a chanid (†*Tharrhias*), and elopomorphs (†*Notelops* and †*Rhacolepis*), and suggested that the "bone gradually encloses the canal during ontogeny," citing Taverne's (1977) observation that the supraoccipital did not surround the posterior sensory duct in a small specimen of *Arapaima*. This interpretation is also supported by some of my specimens of *Hiodon* in which the posterior sensory duct on one side is fully surrounded by bone, whereas on the other it is not (e.g., Fig. 29).

The posterior part of the supraoccipital is a membrane-bone crest (csoc, Fig. 25A) that is T- or Y-shaped in cross-section and that extends posteriorly, in continuity with the membranous connective tissue of the median vertical septum. In one individual (UMA F10580, 270 mm SL, Figs. 7 and 13), the posterior portion of the supraoccipital crest is formed by a separate ossification, a condition that is clearly anomalous. As discussed by Patterson (1977a), the teleostean supraoccipital has been incorrectly interpreted to result from the phylogenetic fusion of a chondral supraoccipital bone and a dermal "dermosupraoccipital" (i.e., the supraoccipital crest, here). I also found no support for this hypothesis. For instance, in a 23 mm SL specimen of *H. tergisus* (JFBM 22746), I found a chondral supraoccipital already continuous with a rudimentary supraoccipital crest formed in the ligamentous tissue of the median vertical septum that separates the left and right components of the epaxial musculature.

The complexly shaped prootic (pro, Figs. 18–22) of *Hiodon* contacts the parasphenoid ventrally, the basioccipital and exoccipital posteriorly, the pterotic and sphenotic dorsally, and the pterosphenoid and basisphenoid anteriorly. Two chambers associated with the inner ear are formed by the prootic. Dorsally, the bony portion of the chamber that houses the utricule of the membranous labyrinth (cut, Figs. 26A, B, and 30) is entirely made up by the prootic. In the floor of the utricular chamber is the prootic foramen (pf, Figs. 20, 21, 26B, and 30), which allows contact between the utricule and the perilymphatic vesicle, which lies ventral to this foramen (Greenwood, 1973). The ill-defined sacular chamber, which encloses the sacular otolith, is ventromedial to the prootic foramen and continuous with the space occupied by the perilymphatic vesicle. A large foramen (fht, Figs. 20 and 21), entirely within the prootic anterior to a vertical bar of bone, serves as the exit of the anteroventral lateral line nerve. A lateral lamellar "prootic wing" (Greenwood, 1973: 323) extends laterally and posteriorly at the ventral opening of this foramen (Figs. 20 and 21) and contacts a shelf on the medial surface of the hyomandibula (see below). The jugular vein and the trigeminal and facial nerves exit through a common canal on the anterior face of the prootic, although within this canal there can be two distinct foramina (fV+VII, jf, Fig. 34); in some specimens, these two foramina are nearly distinct (e.g., Taverne, 1977: fig. 10), whereas in others the nerve and vessel exit the prootic together. A foramen from which the oculomotor nerve exits lies medial to the jugular canal (fIII, Fig. 34C, D). Medially, the prootic meets its antimere to form the roof of the posterior myodome and floor of the braincase. The foramen for the abducent nerve exits the braincase in the anterodorsal portion of the posterior myodome (fVI, Fig. 34). Deeper inside the roof of the posterior myodome is a foramen (not shown) for the palatine ramus of the facial nerve, which runs ventrally along the anterior opening of the myodome and then anteriorly immediately adjacent to the parasphenoid. Along with the sphenotic and pterotic, the prootic forms the facet for the anterior head of the hyomandibula (hyfa, Figs. 18–22). Laterally, the prootic and parasphenoid form a fossa for the origin of the levator arcus palatini muscle.

The paired sphenotics (spo, Figs. 18–22) meet

the pterosphenoids and frontals anteriorly, the prootics ventrally, and the pterotics posteriorly. The inner surface is strongly concave and forms a chamber for the ampullae of the anterior semicircular duct (cama, Fig. 29). A large lateral wing of the sphenotic forms the posterior border of the orbit. Along with the prootic and pterotic, the sphenotic forms the fossa for the anterior head of the hyomandibula. The dilatator operculi and levator arcus palatini muscles originate from a deep lateral fossa formed by the posterodorsal portion of the sphenotic and the anterior ventral lamella of the pterotic; this fossa lies dorsal to the facet for the anterior head of the hyomandibula. These muscles are completely separated from one another by a thick band of connective tissue, and the dilatator operculi inserts onto a small process on the lateral edge of the opercular facet via a thick tendon.

The orbital region of the braincase, just anterior to the prootic and sphenotic bones, is comprised primarily of four chondral elements: the median basisphenoid and orbitosphenoid and the paired pterosphenoids. The basisphenoid is a small, roughly rectangular element that completely surrounds the optic nerve (fII, Fig. 34C, D). The basisphenoid and prootic bones together form the hypophyseal fenestra (feh, Figs. 20, 21, and 34C, D).

The paired pterosphenoids and median orbitosphenoid form most of the medial wall of the orbits. The pterosphenoids (pts, Figs. 18, 20, and 21) contact the sphenotics and prootics posteriorly, the basisphenoid ventrally, and the orbitosphenoids anteriorly (Figs. 18 and 19) and possess a pronounced extension medially (Fig. 30). Near the junction of the pterosphenoid, sphenotic, and prootic is a relatively large foramen (fV+VII(op), Figs. 20–22 and 30). Taverne (1977: fig. 10) illustrated this foramen as three independent foramina, one each for two rami of the anterodorsal lateral line nerve (labeled as trigeminal and facial nerves by Taverne) and one for a posterior cephalic vein. I observed only a single foramen in my specimens and could not confirm the exit of a blood vessel through this foramen. A nerve, likely the anterodorsal lateral line nerve, quickly divides, and the superficial ophthalmic ramus runs anteriorly. A ramule from this nerve (*rami ophtalmici* [sic] of Taverne, 1977) splits off and runs posterodorsally through a foramen that straddles the suture between the pterosphenoid and sphenotic (for, Figs. 22 and 34C, D). This nerve exits dorsally through the cartilage lateral to the posterior fontanelle (Figs. 17 and 18), presumably to innervate the otic sensory canal (otic lateral line nerve of Northcutt & Bemis, 1993; again, identification of nerves discussed here must be viewed as tentative). The superficial ophthalmic ramus runs obliquely against the medial surface of the orbit and enters a canal on the anterodorsal cartilage of the neurocranium dorsal to the orbitosphenoid (see below). A small foramen for the trochlear nerve lies roughly in the center of the pterosphenoid (not shown). The largest and most anterior foramen in the pterosphenoid carries the anterior cephalic vein (facv, Figs. 17–19). This vessel exits the braincase dorsally in the angle of the medial ledge of the pterosphenoid (Fig. 17).

Anterior to the pterosphenoid is the median orbitosphenoid (ors, Figs. 18–22), which is the most anterior bone on the surface of the ventral neurocranium (the ethmoid bones are more anterior, but do not form on the ventral surface of the neurocranium). The orbitosphenoid is tightly joined to the basisphenoid by a jagged suture, and its anterior and dorsal margins are continuous with a cartilaginous portion of the neurocranium (Fig. 18). In *H. tergisus*, a deep groove on the dorsolateral edge of the orbitosphenoid marks where the superficial ophthalmic nerve exits the orbit; this groove was not found in my specimens of *H. alosoides* (Fig. 33), and its presence is considered diagnostic for *H. tergisus* (its presence could not be determined in †*H. consteniorum* owing to preservation). In large specimens of both species, I found irregular ventral lamellae of bone on either side of the midline that are likely continuous with the membranous optic septum.

The ventral portion of the dermatocranium in *Hiodon* is comprised of two single median elements, the parasphenoid and vomer. The parasphenoid (pas, Figs. 20–22) of *Hiodon* runs almost the entire length of the neurocranium, and is well-toothed with caniniform, slightly recurved teeth (Figs. 20 and 21). The presence of parasphenoid teeth is plesiomorphic for teleosts (Patterson, 1975), and their enlargement is characteristic of osteoglossomorphs (although not uniquely) and is a component of the so-called "parasphenoid–tongue bite apparatus" (Hilton, 2001). Several osteoglossomorphs have secondarily reduced (e.g., *Chitala*, UMA F10349) or lost (e.g., *Heterotis*, MCZ 50959) parasphenoid dentition. In *Hiodon*, the lateral rows of parasphenoid teeth are larger than those in the center of the parasphenoid, which are scattered along the midline. This arrangement of parasphenoid teeth is also found

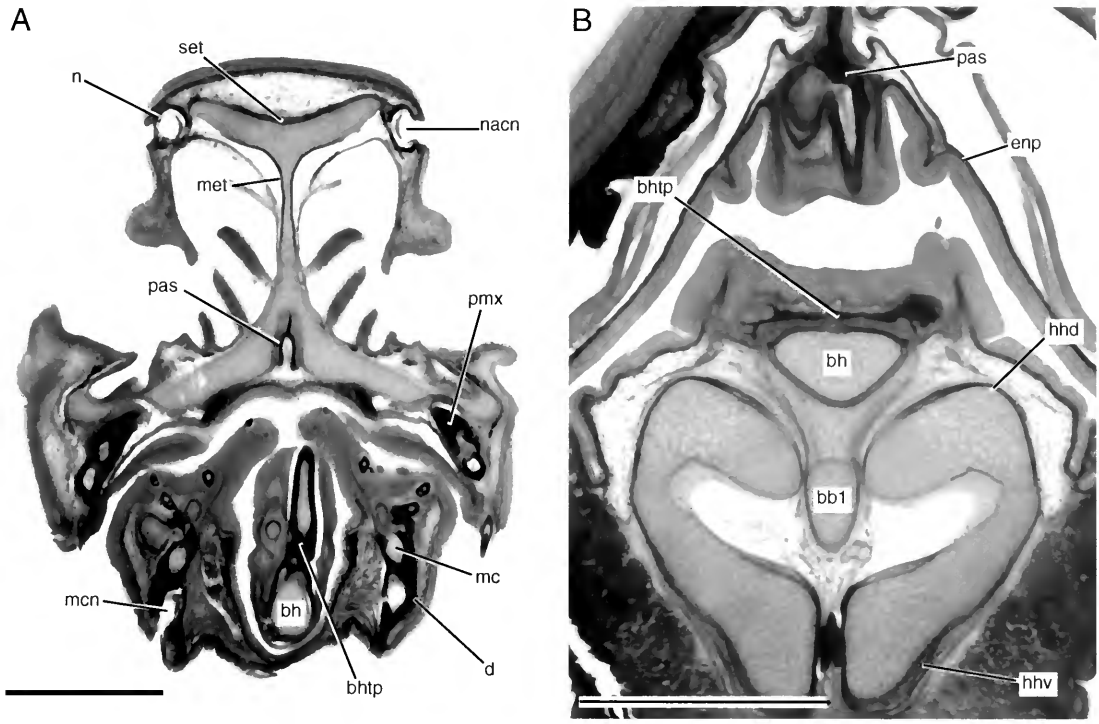

FIG. 23. *Hiodon alosoides.* Transverse histological sections through the skull of a juvenile (UAMZ 4043A, 63 mm SL). **A**, Section through nasal capsule and ethmoid region. **B**, Section through hypohyals. Scale bars = 1 mm.

in †*Eohiodon* (e.g., FMNH PF10638) and †*Lycoptera* (e.g., UMA F10652). A specimen of †*Joffrichthys* (FMNH PF12171a) clearly shows an arrangement of parasphenoid teeth similar to that of *Hiodon*. In *Hiodon,* two posterior basioccipital processes (bop, Figs. 30 and 31) overlap the anteroventral half of the basioccipital and define the aortic notch of the parasphenoid (aon). The low ascending processes (arp, Figs. 30 and 31) are nearly continuous with the basioccipital processes and contact the prootic. Together, the parasphenoid and prootic form the posterior myodome (pm, Figs. 25 and 34). Anteriorly, the parasphenoid ends in a sharp point (the anterior process of the parasphenoid; apr, Figs. 30 and 31) that lies in a groove in the cartilage of the ventral surface of the ethmoid region (pg, Fig. 19). A thin, median lamella of bone on the dorsal midline of the parasphenoid (Figs. 20, 21, and 23A) is continuous with the membranous tissue of the optic septum. A similar lamella is preserved in †*Eohiodon* (e.g., FMNH PF10638) and possibly †*Lycoptera* (e.g., UMA F10652). Two foramina, which carry the internal carotid artery and the efferent pseudobranchial artery (Taverne, 1977), pierce either side of the parasphenoid ventral to the ascending processes (fic, fepa, Fig. 34A, B). However, in many specimens these foramina are confluent, so that there is only a single foramen on each side of the parasphenoid, as was described by Greenwood (1970: fig. 5) and Patterson (1975). Allis (1919: 224) described his specimen of *H. tergisus* as having a common foramen for these two vessels on one side of the parasphenoid and two foramina separated by a "narrow column of bone" on the other. Patterson (1975: 532) wrote that "a foramen for the efferent pseudobranchial artery is less frequent [than a foramen for the internal carotid] in teleosts, but it is always present . . . where a well developed basipterygoid process persists . . . and occurs sporadically amongst teleosts in which the basipterygoid process is lost" and considered that "it is reasonable to interpret absence of an efferent pseudobranchial foramen in the parasphenoid of teleosts as a secondary condition, following loss of the basipterygoid process, reduction in breadth of the parasphenoid, or coalescence of the foramen with that of the internal carotid."

Anterior to the parasphenoid is a small vomer

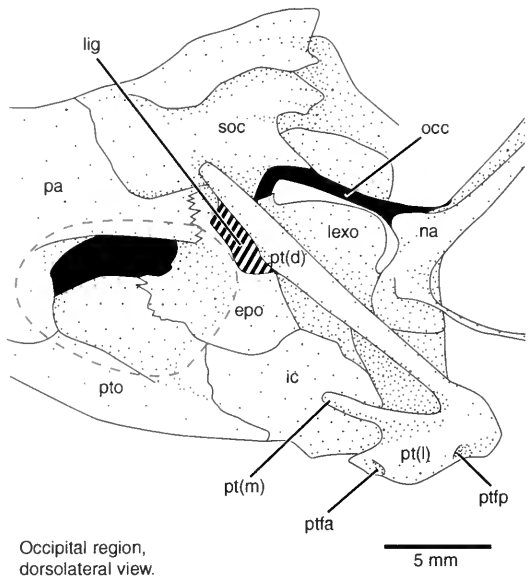

FIG. 24. *Hiodon alosoides,* drawing of occipital region of an adult (UMA F10583, 272 mm SL, female) in an oblique dorsal view showing the cartilaginous connection between the supraoccipital cartilage and the first neural arch. This dry skull was prepared by dermestid beetles, but preparation was stopped before the cartilage was consumed. Skull was rinsed clean and soaked in a 0.5% solution of potassium hydroxide (KOH) to allow cartilages to swell before the drawing was made (specimen is now stored dry). Left temporal fossa is outlined in red. Anterior faces left.

(vo, Figs. 20–22). *Hiodon* and *Heterotis* are the only living osteoglossomorphs in which the vomer is edentulous (pers. obs.; Taverne, 1977, e.g., fig. 96). Daget (1964), however, commented on the plasticity of vomerine dentition in teleostean fishes. In the adult of *Hiodon,* a slight groove on the dorsal surface of the vomer marks the contact point with the parasphenoid (Fig. 30). The vomer ossifies relatively late (first observed in *H. alosoides* at 30 mm SL), and forms as paired ossifications ventral and lateral to the anterior process of the parasphenoid (Fig. 32A, B). These two ossifications grow medially, and by 42 mm SL (in *H. alosoides*) they have fused into a single element (Fig. 32C, and D). Patterson (1975: 513) found the vomer to be paired in three specimens of *H. alosoides* that he studied (different specimens than examined here) and unpaired in one specimen of *H. tergisus,* and suggested that "the paired condition might be primitive," because †pholidophoroids, †leptolepids, and more derived teleosts (except *Osmerus,* see Starks, 1926: fig. 4) have a median vomer. I found a paired vomer in only three of my adult specimens of *H. alosoides,* suggesting that a single element is the "typical" condition. The ontogeny of this element is unknown for many groups. In small (e.g., 30 mm SL, UMA F11258) specimens of *Elops saurus,* the vomer is a single median element. Jollie (1975: 76) found that the vomer of *Esox* develops from paired "anlagen," which he first discovered in 15 mm specimens, and were fused by 18 mm. He considered this "a more-or-less direct development toward the adult condition [a single median element]." It is also interesting to note that Sewertzoff (1925: 124) stated in a footnote that "[t]he unpaired vomer of the Teleosts arises as a paired ossification," although he gave no reference for this observation or stated to which teleosts he was referring. Daget and d'Aubenton (1957) made no mention of the vomer in *Heterotis* smaller than 33 mm TL, at which point it is a single element (there was, however, a large gap in their series—the next smallest specimen was 14 mm TL). The ontogeny of the vomer warrants further study in a broader taxonomic survey of teleostean fishes.

Temporal Fossae

One region of the skull of *Hiodon* that has received a moderate amount of study is the temporal

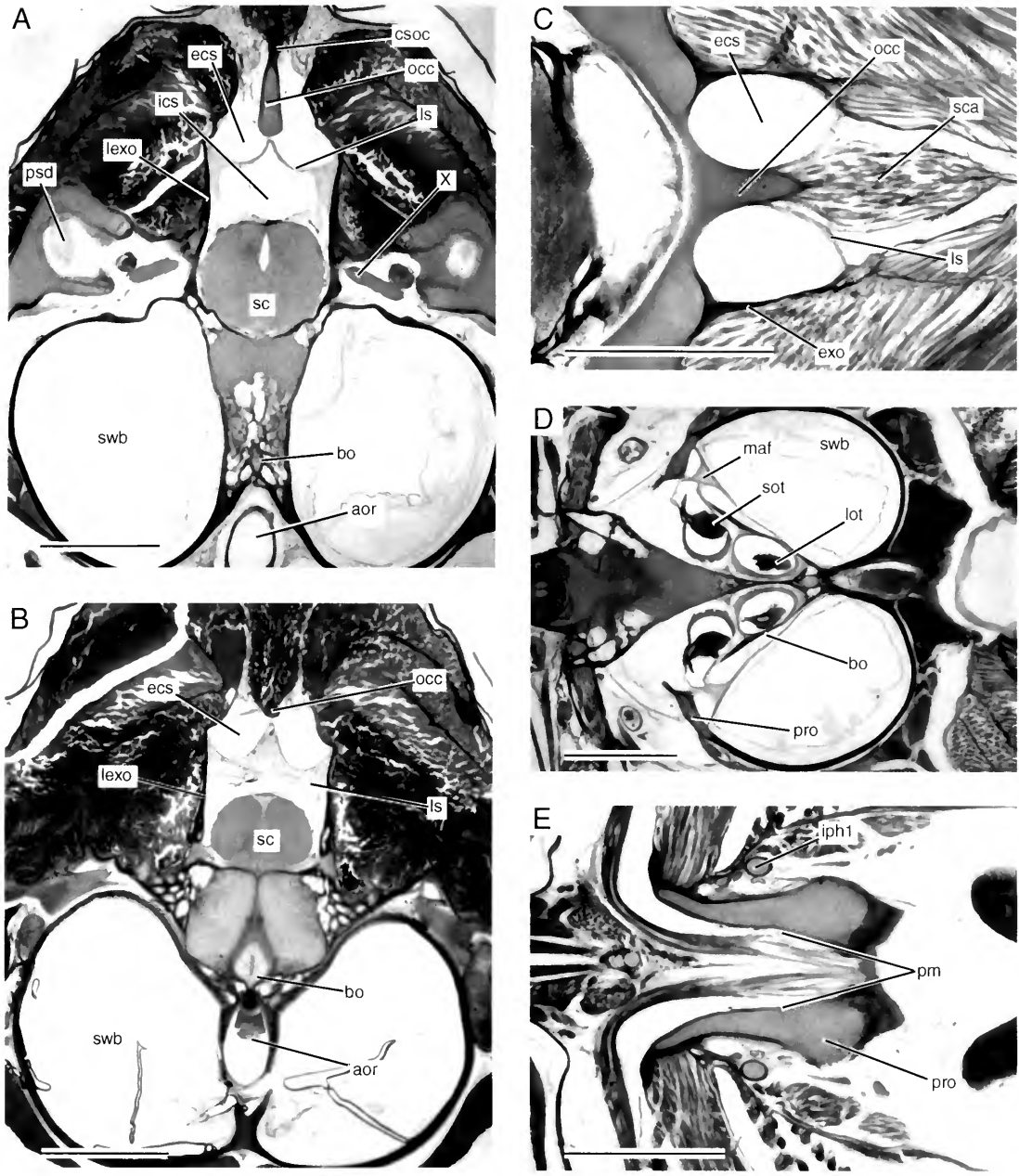

FIG. 25. *Hiodon alosoides*, histological sections through skull and pectoral girdle of juveniles. **A**, Transverse section through occipital region. **B**, Transverse section through occipital region, slightly posterior to that shown in A. **C**, Frontal section just dorsal to foramen magnum. **D**, Frontal section through ventral portion of inner ear showing auditory fenestra. **E**, Frontal section through posterior myodome. A and B: UAMZ 4043A (63 mm SL); C–E: UMA F10595 (55 mm SL). Frontal sections with anterior facing left. Scale bars = 1 mm.

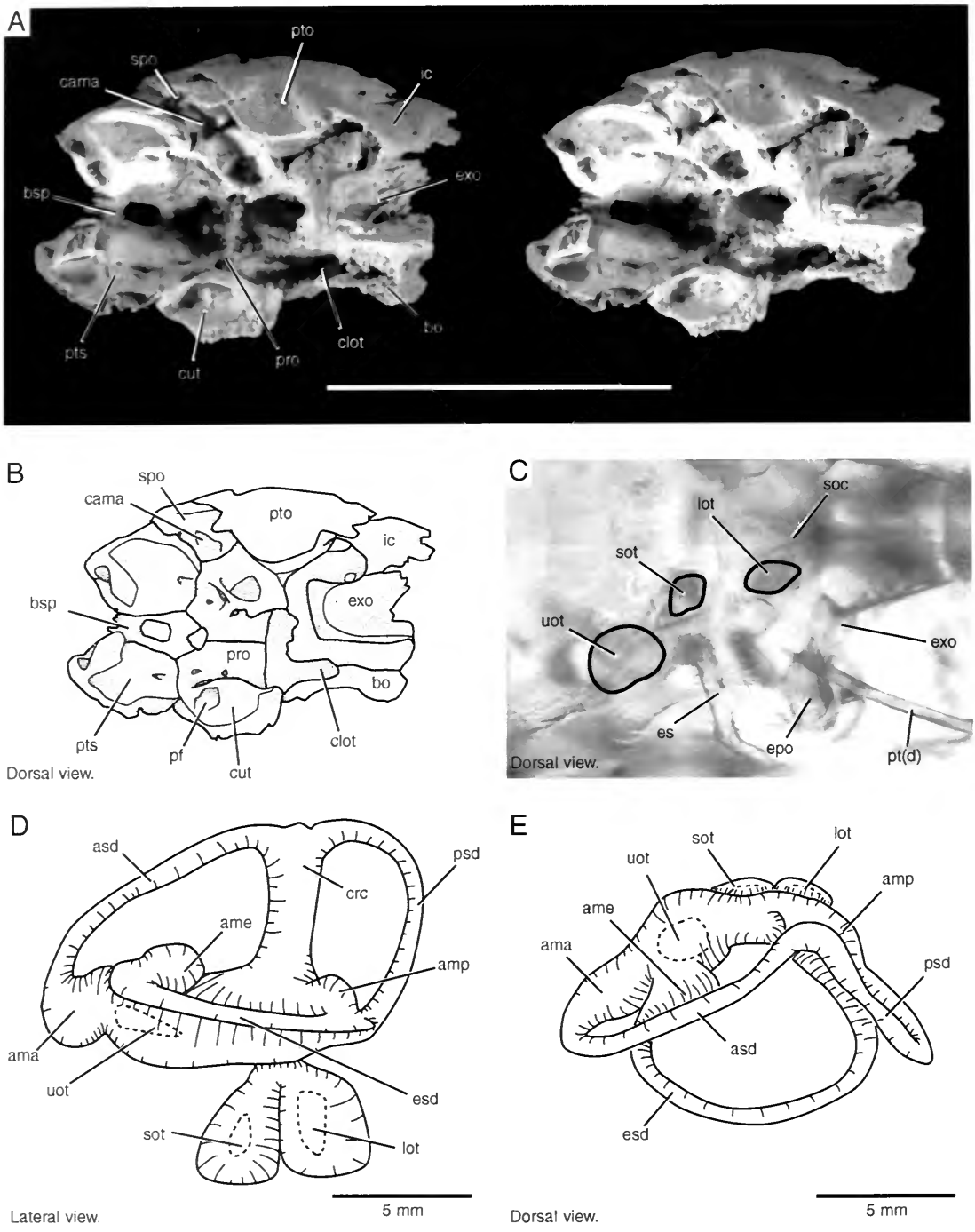

FIG. 26. *Hiodon alosoides*, posteroventral portion of neurocrania of an adult (UMA F10584, 250 mm SL, female) in dorsal view. **A**. Stereopair. **B**. Line drawing (for orientation). Dermal roofing bones, supraoccipital, left and right epioccipitals, left pterotic and left sphenotic have been removed. Specimen was dusted with ammonium chloride smoke before being photographed. Scale bar in A equals 2 cm. **C**. Cleared and stained specimen with otoliths outlined in situ. Dorsal view. **D**. Lateral and **E**. dorsal view of left membranous labyrinth. Composite illustrations based on multiple specimens. Dashed lines indicate approximate position of the otoliths. Anterior faces left.

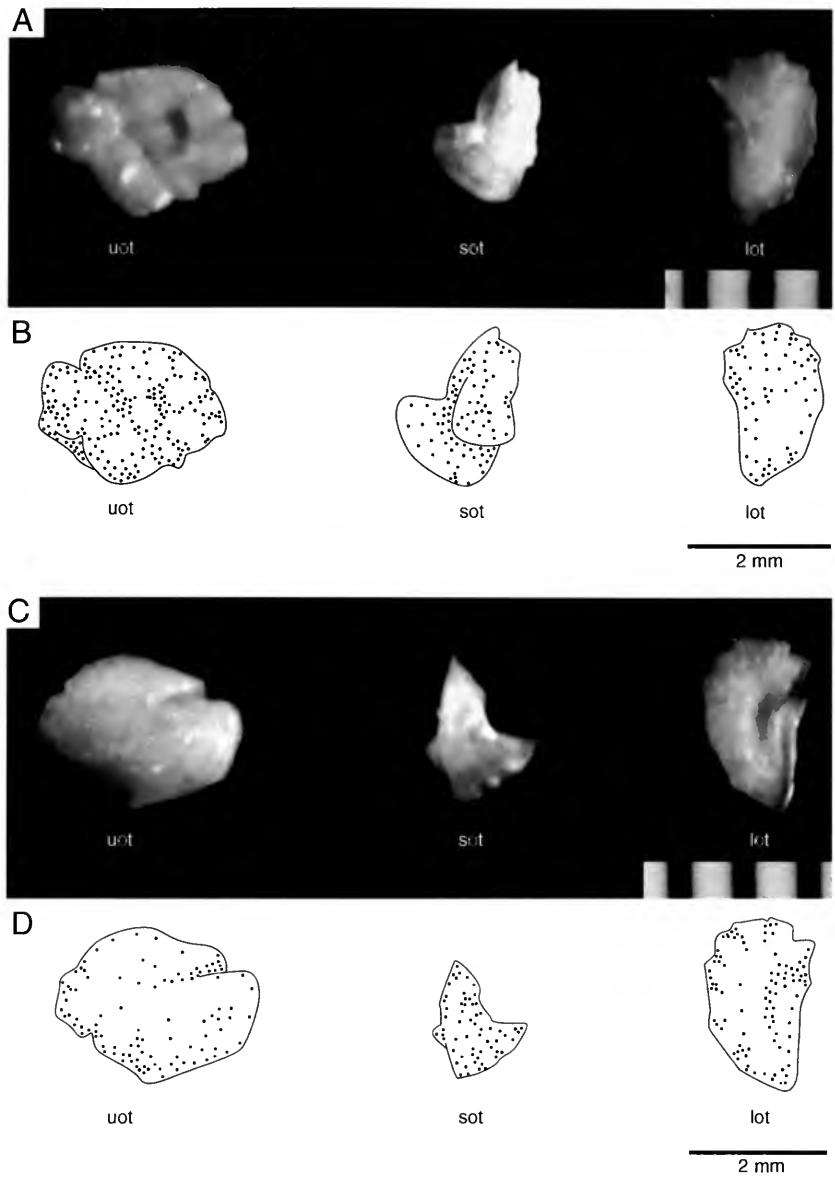

FIG. 27. *Hiodon alosoides*. **A** and **C**, Photographs, and **B** and **D**, line drawings of otoliths from left side of an adult (UMA F10585, 255 mm SL, female). Utricular otolith in dorsal (A and B) and ventral (C and D) views; other otoliths in lateral (A and B) and medial (C and D) views. Anterior faces left in A and B; anterior faces right in C and D. Scale bars in A and C in millimeters.

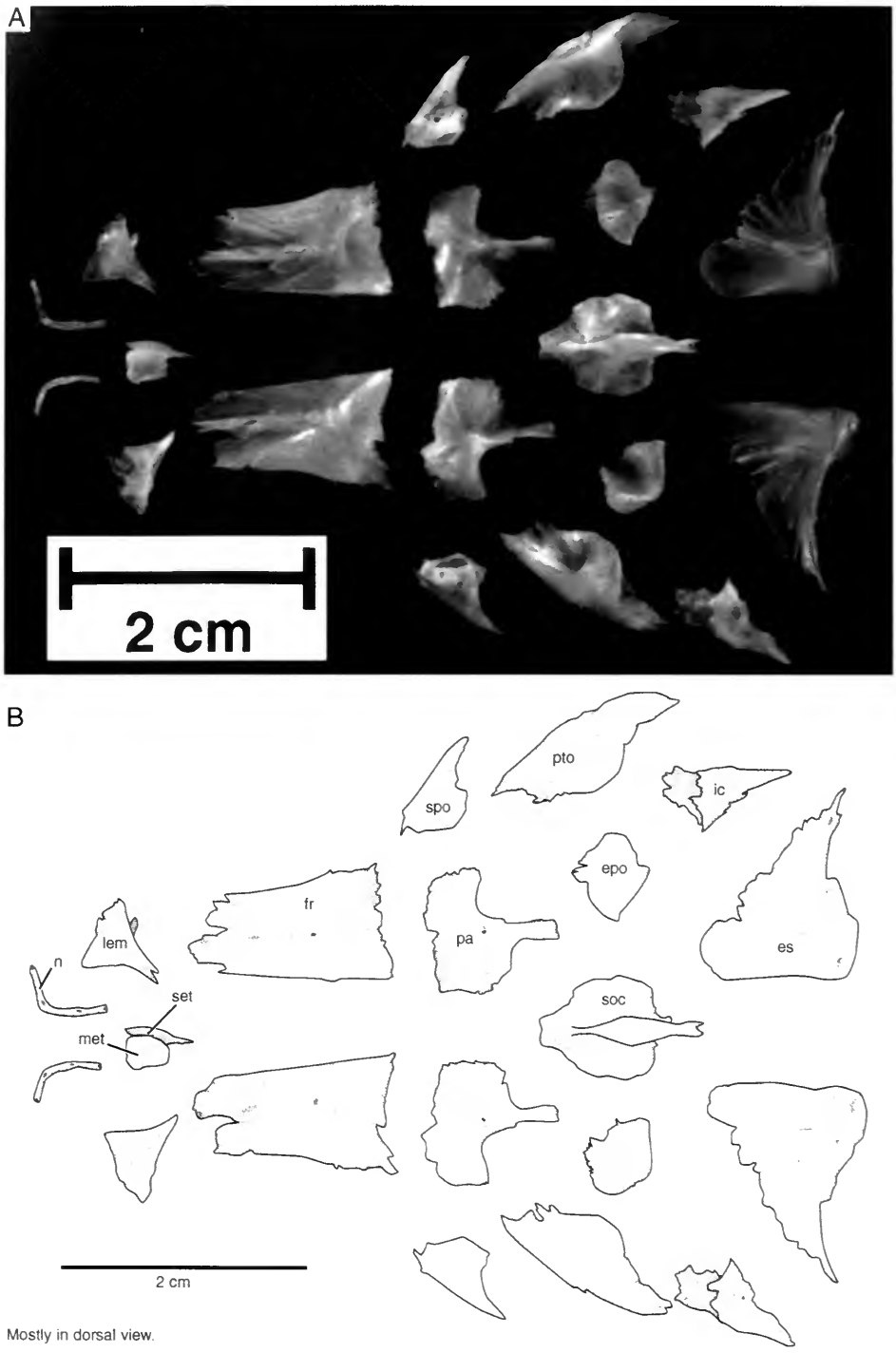

FIG. 28. *Hiodon alosoides*. **A**, Photograph, and **B**, line drawing of disarticulated skull roof of an adult (UMA F10586, 273 mm SL, female) in dorsal view. Sphenotic (spo) bones in anterior view; mesethmoid (met), lateral ethmoid membrane bone extension (lem), and supraethmoid (set) in lateral view. Anterior faces left.

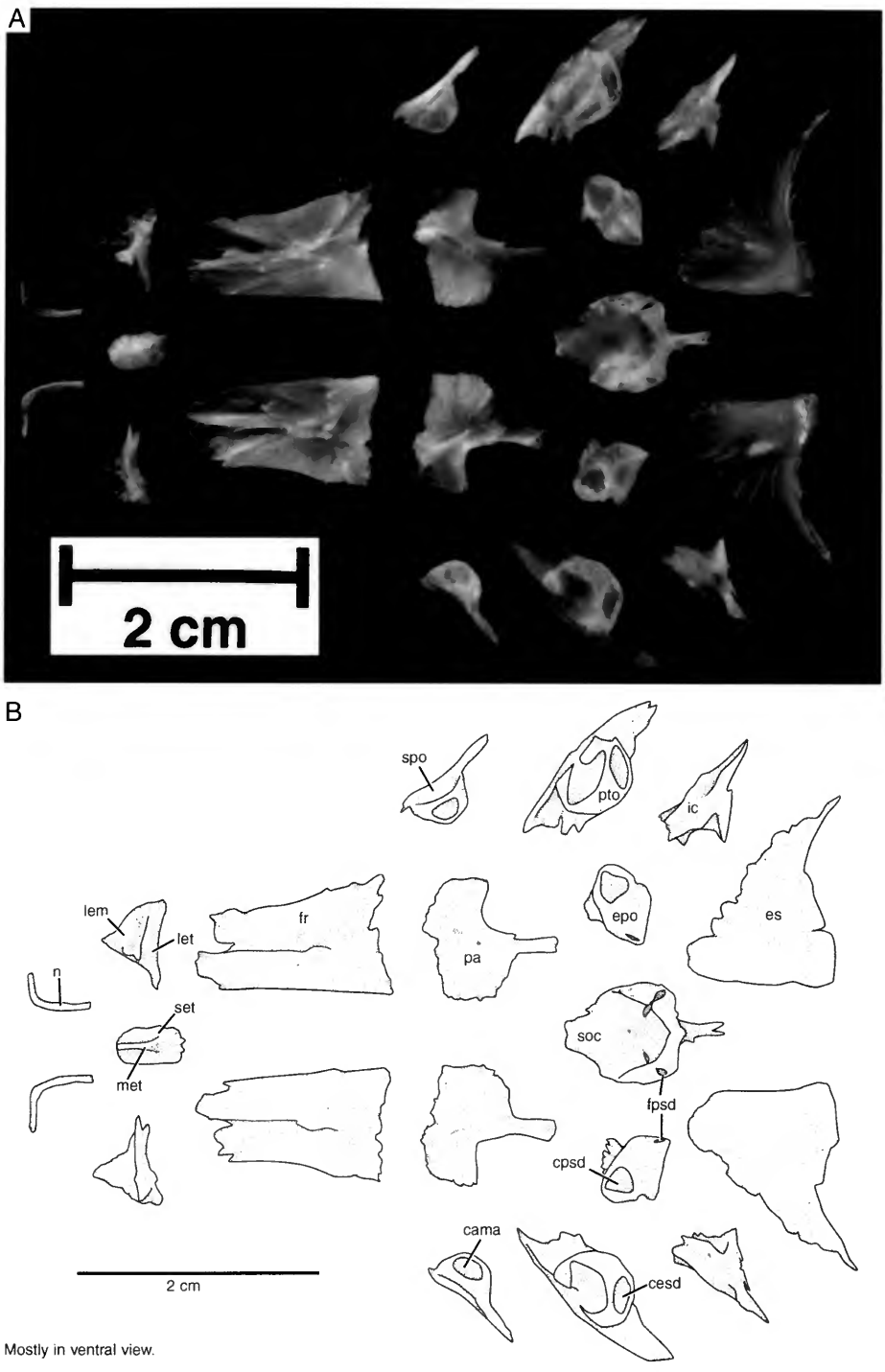

FIG. 29. *Hiodon alosoides*. **A**, Photograph, and **B**, line drawing of disarticulated skull roof of an adult (UMA F10586, 273 mm SL, female) in ventral view. Sphenotic (spo) bones in posterior view; lateral ethmoid (let) and lateral ethmoid membrane bone extension (lem) in medial view. Anterior faces left.

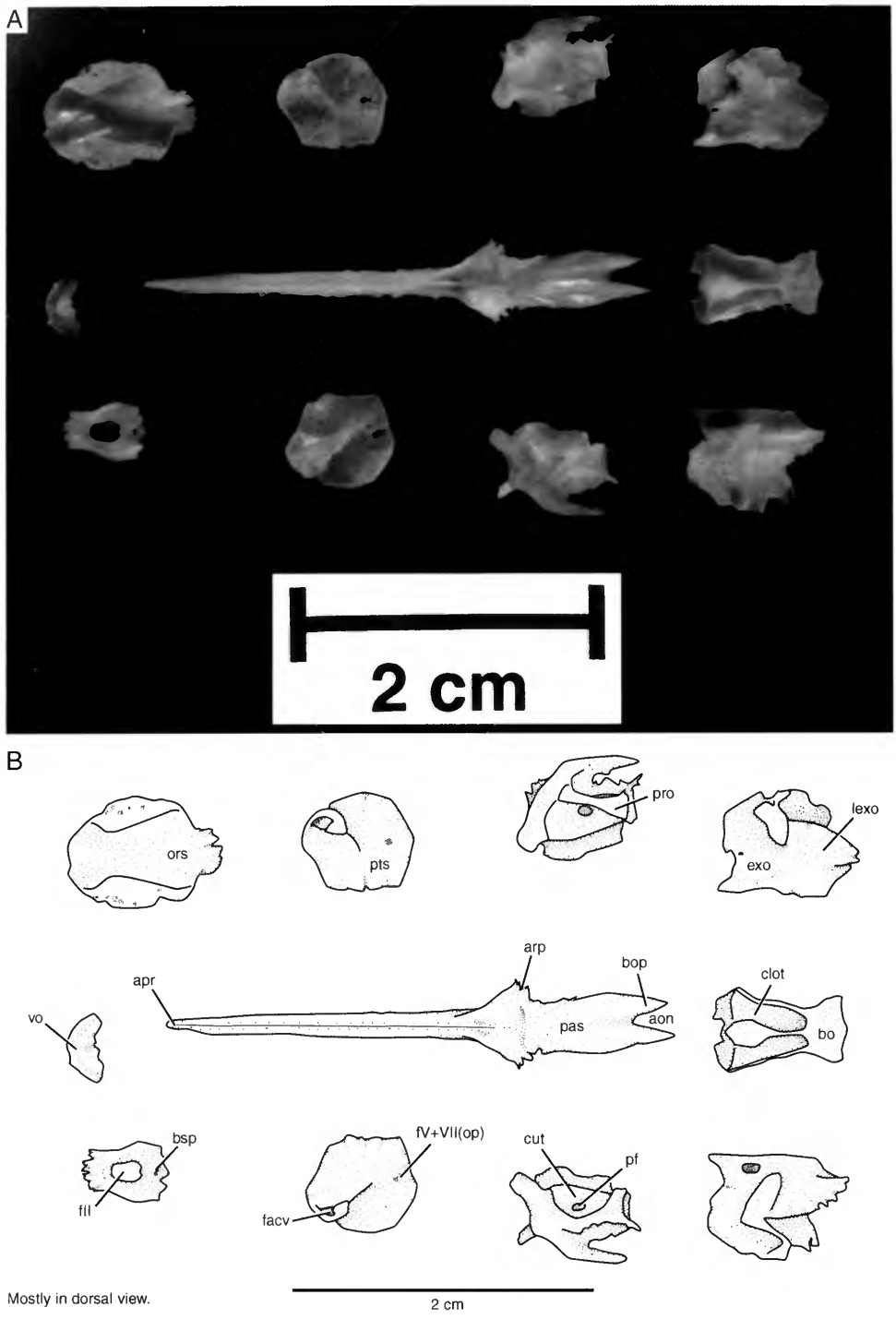

FIG. 30. *Hiodon alosoides*. **A**, Photograph, and **B**, line drawing of disarticulated neurocranium and ventral dermal skull bones of an adult (UMA F10586, 273 mm SL, female) in dorsal view. Anterior faces left.

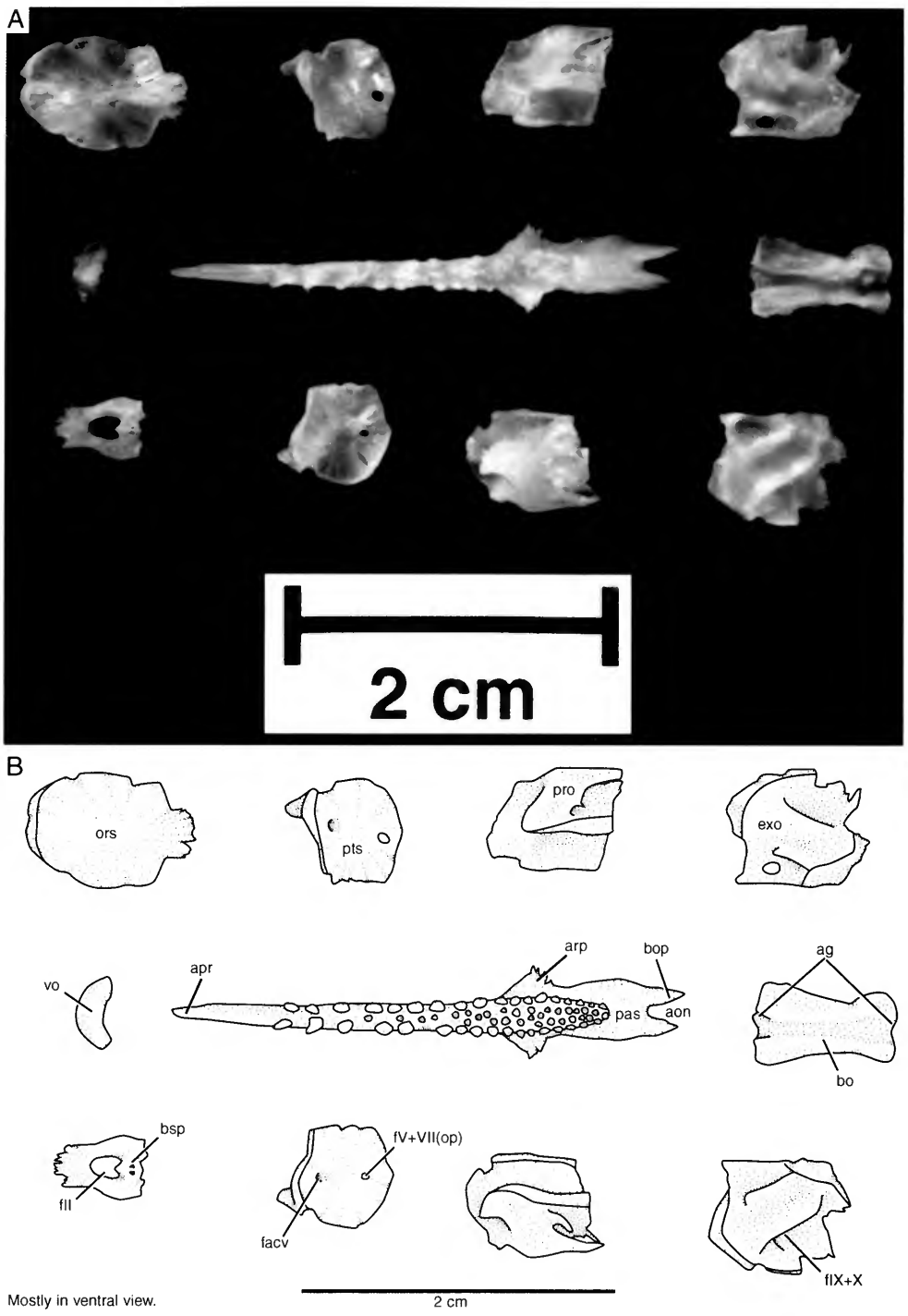

FIG. 31. *Hiodon alosoides*. **A**, Photograph, and **B**, line drawing of disarticulated neurocranium and ventral dermal skull bones of an adult (UMA F10586, 273 mm SL, female) in ventral view. Anterior faces left.

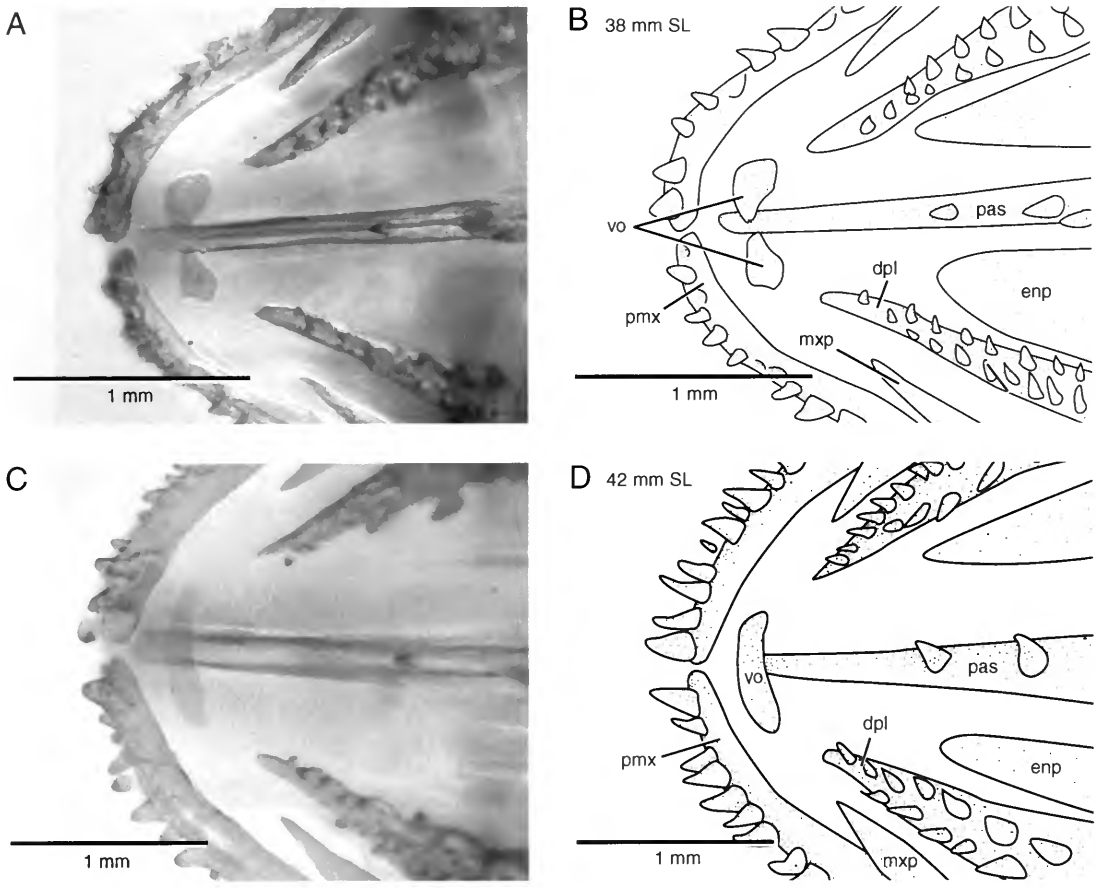

FIG. 32. *Hiodon alosoides*. **A** and **C**, Photographs, and **B** and **D**, line drawings of cleared and stained specimens illustrating ventral surface of ethmoid region showing development of the single median vomer from a paired element. A and B, TU 113117B, 38 mm SL. B and C, UAIC 10473.01B, 42 mm SL. Anterior faces left.

region, specifically with regard to the presence of the temporal "fenestra" (more appropriately termed a "fossa" because it is fully floored). This structure in *Hiodon* is a depression in the lateral surface of the posterior skull roof, and serves as an attachment site for epaxial musculature. The parietal, pterotic, and epioccipital bones border this depression (Figs. 9 and 13). The bones grow toward the center of the fossa but do not meet, leaving a remnant of cartilage in the center of the fossa. A similarly bounded fossa has been described for †*H. consteniorum* (Li & Wilson, 1994: fig. 2) and †*Eohiodon* (Li, Wilson, & Grande, 1997: 1113), although this region of the skull is often not preserved well in these taxa, and details are often obscured by the overlying extrascapulars. The temporal region in †*Lycoptera* also has been reconstructed as similar to that of *Hiodon* (e.g., Gaudant, 1968), and was used, in part, by Greenwood (1970) to link the †lycopterids with the hiodontids. The outline of the temporal fossae in †*Lycoptera* was faint in specimens examined by Greenwood (1970: 264), and again, this region of the skull is typically crushed and is poorly known in both †Lycopteriformes and fossil Hiodontiformes (pers. obs.); interpretation must await study based on better preserved specimens. A condition similar to that found in *Hiodon* is also present in Salmoniformes (e.g., *Coregonus*, FMNH 94848; Li & Wilson, 1996a; = posttemporal fenestra of Sanford, 2000). Li and Wilson (1996a) followed Ridewood (1904) in postulating that the temporal fossa of hiodontids (and †lycopterids) is homologous to the pre-epioccipital fossa of clupeomorphs (= pre-epiotic fossa of other authors; e.g., Grande, 1985) and concluded, therefore, that

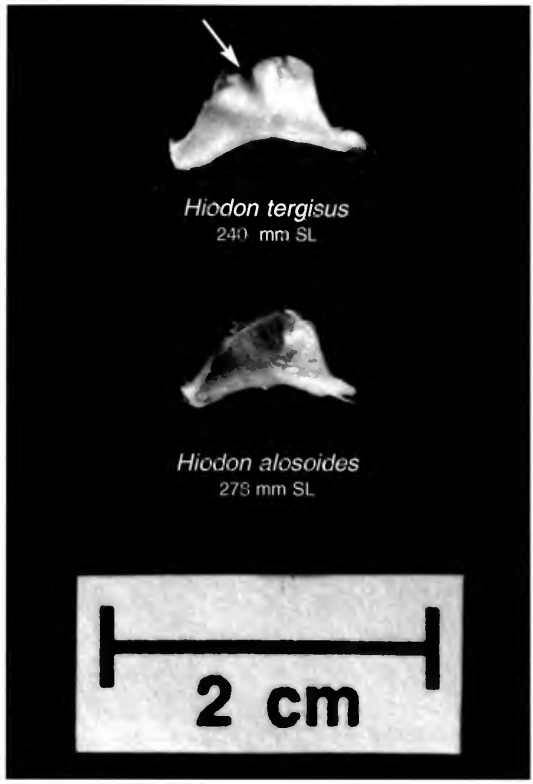

FIG. 33. Orbitosphenoid of *Hiodon tergisus* (UF 31651, 240 mm SL, female) compared with that of *H. alosoides* (UMA F10586, 273 mm SL, female), showing the pronounced anterodorsal groove in *H. tergisus* (marked with arrow) in lateral view. Anterior faces left.

the shared presence of a temporal fossa in hiodontids and †lycopterids is not a synapomorphy of these two groups.

Other osteoglossomorphs also possess structures that have been considered homologous with the temporal fossa of *Hiodon,* and this was reviewed by Cavin and Forey (2001). The same bones as in *Hiodon* border a similar, although smaller, depression in †*Ostariostoma* (Grande & Cavender, 1991: fig. 2). The arrangement of bones is also similar in *Pantodon,* with the exception that the sphenotic enters into the anterior margin of the fossa (Taverne, 1978: fig. 31). In notopteroids and mormyroids the temporal fossa is bordered by the epioccipital, pterotic, and exoccipital (Cavin & Forey, 2001). Ridewood (1904: 206–207), who was the first to study this character in osteoglossomorphs, was careful to distinguish the temporal fossa of *Hiodon* from the "lateral foramen [temporal fossa]" found in these taxa, but did propose that "there is some degree of morphological relationship existing between the two." In notopterids and mormyrids, the fossa is a large opening in the side of the cranium that is closed over by membrane, greatly differing from the "oval tract of cartilage" found in *Hiodon.* Osteoglossiformes (*sensu* Li & Wilson, 1996a) possess posttemporal fossae (except *Pantodon*; see above) that are roofed by arches of bone formed by the parietal and pterotic bones where they meet to form the skull roof. Cavin and Forey (2001) suggested that the temporal fossae are homologous among the various groups at the level of Osteoglossomorpha, and differ only in the details of their bordering bones. Cavin and Forey (2001) also discussed the possibility that the roofed posttemporal fossa of Osteoglossiformes (except *Pantodon*), bordered by the parietal, epioccipital and pterotic, is a roofed temporal fossa. The true homology (i.e., features shared due to common ancestry) of the pre-epioccipital fossae and temporal fossae, both within osteoglossomorphs and among basal teleosts, remains an open question.

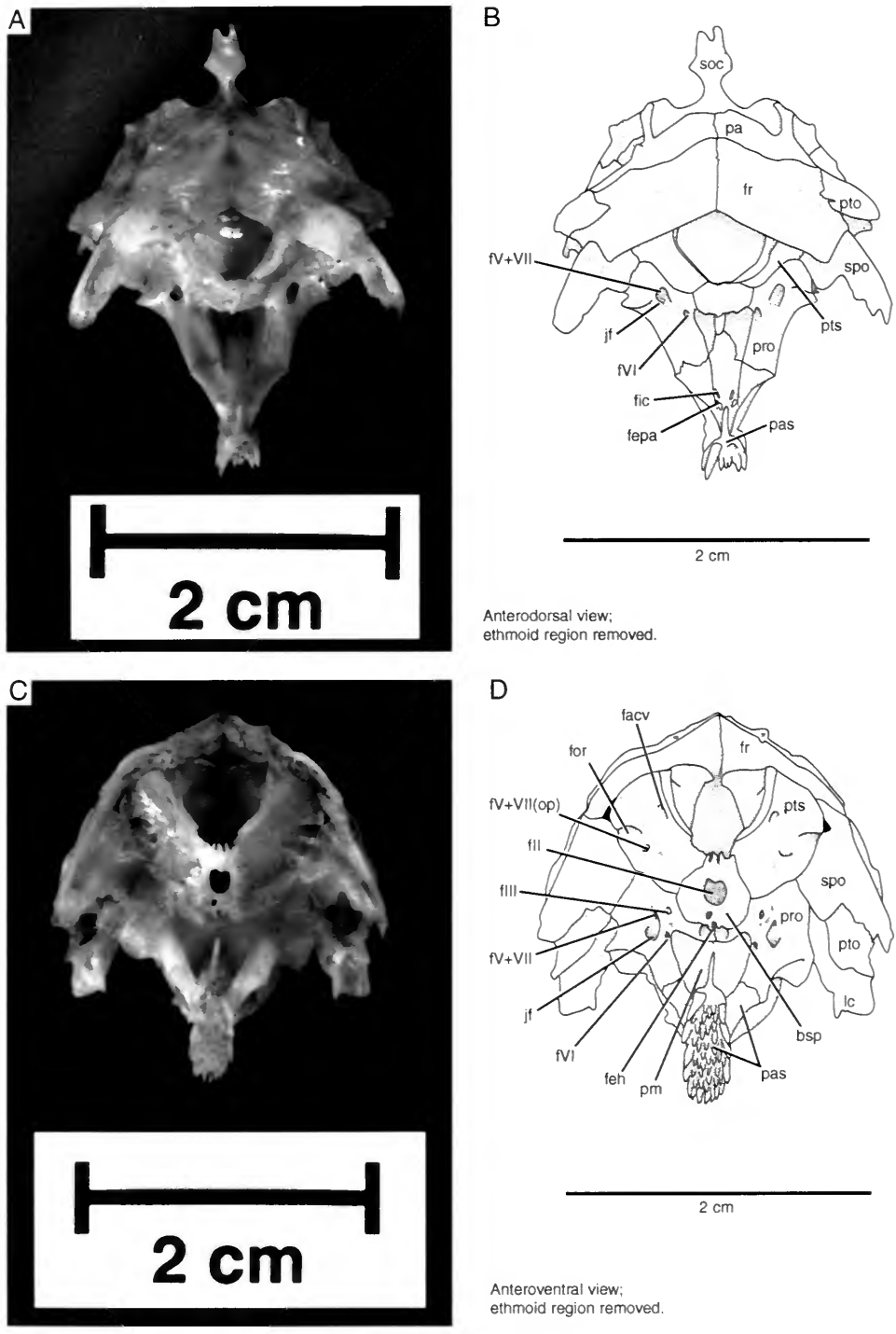

FIG. 34. *Hiodon alosoides*. **A** and **C**, Photographs, and **B** and **D**, line drawings of posterior portion of neurocranium and skull roof of an adult (UMA F10589, 275 mm SL, female) in anterodorsal (A and B) and anteroventral (C and D) views showing portions of the trigemino-facialis chamber.

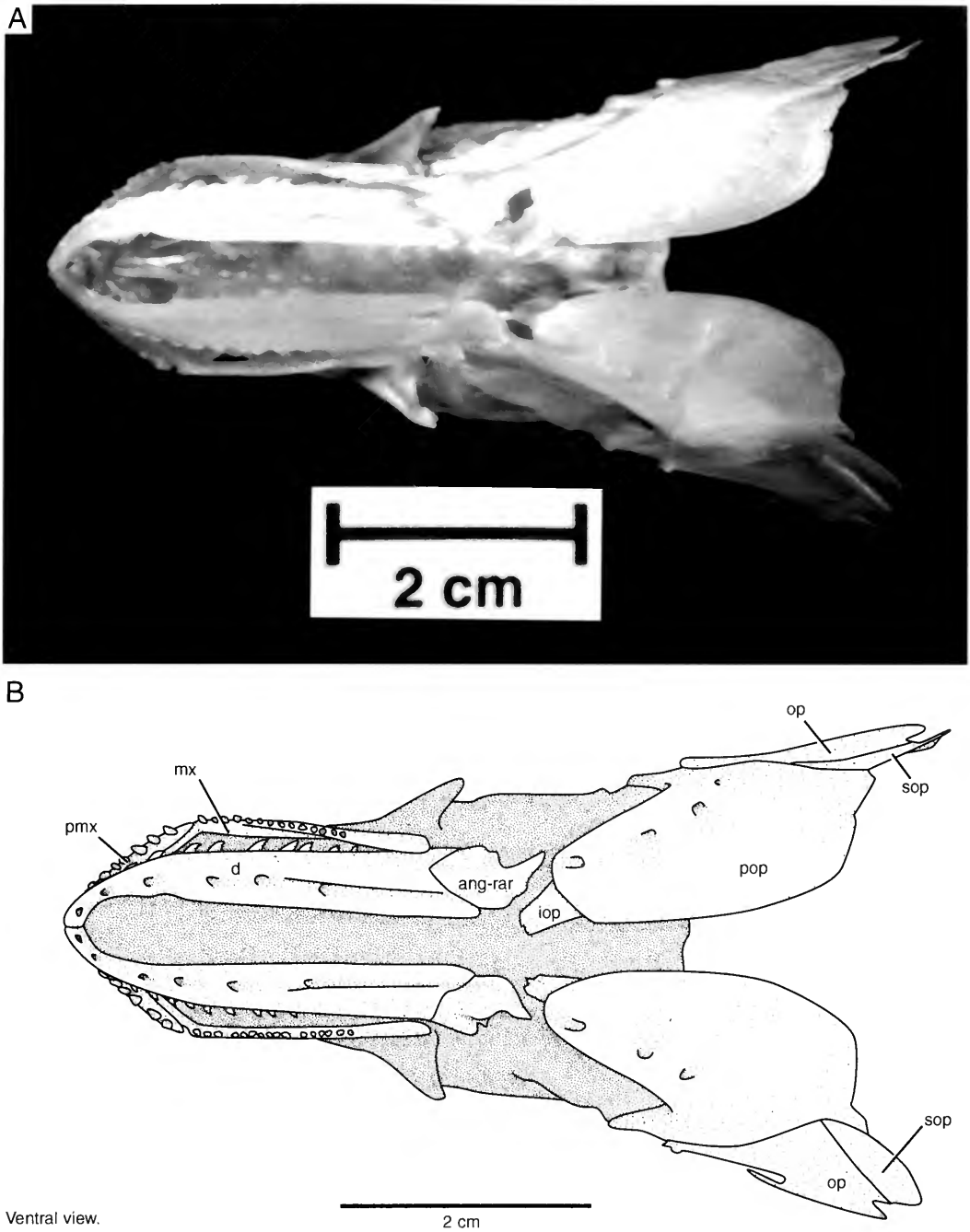

FIG. 35. *Hiodon alosoides*. **A**, Photograph, and **B**, line drawing of skull in ventral view from an adult (UMA F10580, 270 mm SL, female). Infraorbitals have been removed. Anterior faces left.

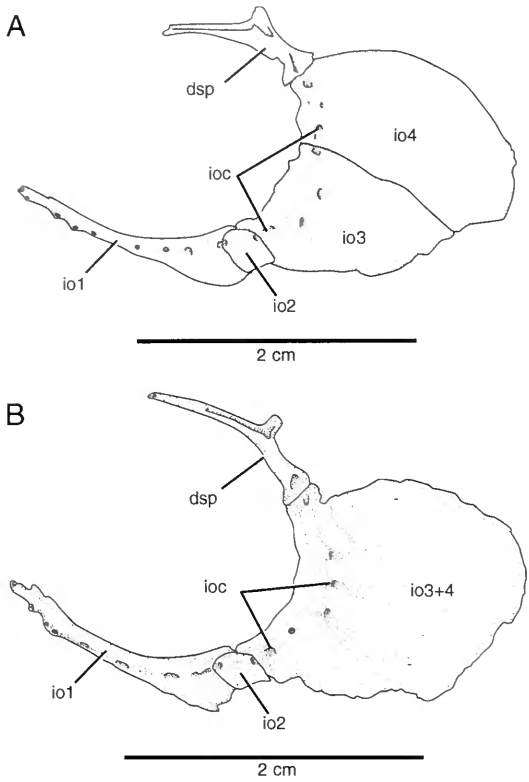

FIG. 36. *Hiodon alosoides,* adult infraorbital bones. **A**, Typical arrangement of bones (UMA F10150, 293 mm SL, female). **B**, A variation (UMA F10587, 272 mm SL, male). Anterior faces left.

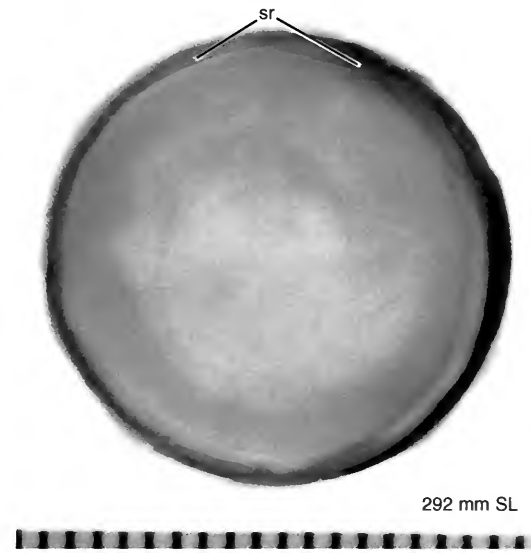

FIG. 37. *Hiodon alosoides,* cleared and stained left eye ball from an adult (UMA F10592, 292 mm SL, female) in lateral view showing sclerotic ring. Scale bar in millimeters. Anterior faces left.

Membranous Labyrinth, Otoliths, and Auditory Fenestrae

The inner ear of *Hiodon* has been described and illustrated by Greenwood (1963, 1973: fig. 6) and Taverne (1977). The anterior semicircular ducts of the membranous labyrinth (asd, Fig. 26D, E) pass obliquely from the crus commune through grooves in the cartilage of the neurocranium. These grooves follow the posterolateral edge of the posterior fontanelles and open ventrally into chambers in the sphenotic (cama, Figs. 26A, B, and 29), which partially house the ampullae of the anterior semicircular duct (ama, Fig. 26D, E). The sphenotic chamber is nearly continuous with the prootic chamber, which encloses the utricule (cut, Fig. 26A, B). Posteriorly, the anterior semicircular duct joins the crus commune (crc, Fig. 26D, E) ventral to the supraoccipital.

The posterior semicircular duct runs posteriorly from the dorsal part of the crus commune along the ventral surface of the supraoccipital and passes through a foramen in the lateral margin of the supraoccipital (fpsd, Fig. 29). This foramen may not be completely enclosed by bone (e.g., right side of the specimen in Fig. 29), although the ventral sides of the foramen frequently at least contact each other. The posterior semicircular duct enters the epioccipital and runs laterally and ventrally along its posterior margin. As the posterior semicircular duct curves medially, it opens into a chamber within the epioccipital (cpsd, Fig. 29). Both the posterior and external semicircular ducts are housed in this chamber, which is formed by the exoccipital ventrally, the epioccipital dorsally, and the pterotic laterally.

The external semicircular duct of the membranous labyrinth (esd, Fig. 26D, E) runs laterally from the posterior extent of the utricule and enters the pterotic bone, which completely encloses it. This semicircular duct exits the pterotic into a wide chamber in the anterior part of this bone (cesd, Fig. 29). A large, bulbous ampulla (ame, Fig. 26D, E), partially housed by this chamber, lies at the point where the external semicircular duct meets the utricule.

The utricule is elongate and contains the utricular otolith in its anterior end (Fig. 26D, E). The utricular otolith (uot, Figs. 26C and 27) is scallop-shaped. The saccule and lagena are ventral to the

rest of the membranous labyrinth (Fig. 26D, E). These portions of the inner ear share a common branch from the posterior portion of the utricule which passes medially around the prootic shelf, but very quickly divides into discrete compartments. The saccule and saccular otolith are enclosed in a poorly defined chamber within the prootic, medial to the perilymphatic vesicle. The saccular otolith (sot, Figs. 26C and 27) is oriented vertically and is oddly shaped, in that it bears a vertical groove (= sulcus of Taverne, 1977) along its lateral surface (noticeable in frontal section; Fig. 25D). This is the smallest of the three otoliths, as was noted by Taverne (1977). The lagena and the lagenar otolith (lot, Figs. 26C and 27) are enclosed in a chamber in the dorsal surface of the basioccipital (clot, Figs. 26 and 30), which is roofed over by the exoccipital. This chamber is separated from the auditory fenestrae by a thin membrane, although the diverticulum of the swimbladder does contact the membrane of the auditory fenestrae (maf, Fig. 25D; see below), as was noted by Greenwood (1973). The lagenar otolith is positioned vertically and bears a sulcus along its lateral surface.

The utricular otolith is the largest of the three otoliths of *Hiodon,* although the lagenar otolith is not much smaller (Fig. 27). In most teleosts, the saccular otolith is the largest of the three (Ostariophysi, in which the lagenar otolith is enlarged, is a notable exception; see Popper & Coombs, 1982; Maisey, 1999). In discussion of relative otolith size in neopterygians, Maisey (1999), following Rosen and Greenwood (1970), suggested that enlargement of the lagenar otolith in ostariophysans and others may be functionally related to the otophysic connection of these fishes. However, several taxa have enlarged lagenar otoliths yet lack an otophysic connection (e.g., *Polypterus,* amiids; Maisey, 1999), or have an otophysic connection but lack enlarged lagenar otoliths (e.g., *Hiodon*).

In *Hiodon,* a membrane-closed auditory fenestra bordered by the basioccipital, prootic, and exoccipital allows for indirect communication between the swimbladder and the inner ear (maf, Fig. 25D; af, Fig. 18). In particular, it is the saccule that is opposed through membrane by the swimbladder (swb, Fig. 25A, B, D). The paired cranial diverticula of the swimbladder are enclosed by cranial extensions of the peritoneal covering of the swimbladder (Greenwood, 1973, misidentified as the tunica externa in Greenwood, 1963). This thickened tissue is tightly connected to the prootic and exoccipital, and less tightly to the basioccipital. Greenwood (1973: 324) described the swimbladder-ear connection of *Hiodon* and clupeomorphs and concluded that the otophysic connection may indicate relationship between the two groups. He cautioned, however, that "Similarities between the ear-swimbladder connection in the two groups are, it must be admitted, restricted to the basic 'bauplan', but they do involve homologous elements and are of a kind not found elsewhere among teleosts."

Infraorbital Bones and Sclerotic Ring

The infraorbital bones of *Hiodon* consist of five thin, dermal ossifications (i.e., infraorbitals 1–4 [io1–4] and the dermosphenotic [dsp], Fig. 36) that first develop as tubular ossifications surrounding the infraorbital sensory canal (Figs. 14 and 15). The Y-shaped (= triradiate, Li & Wilson, 1994) dermosphenotic bone is considered a synapomorphy of Hiodontiformes (Li & Wilson, 1996a, 1999). I regard the presence of three elements between io1 and the dermosphenotic to be the "typical" condition in *Hiodon* (Fig. 36A). One specimen of *H. alosoides* (UMA F10587) had a single element between io2 and the dermosphenotic (Fig. 36B) on one side. Taverne (1977: fig. 9) figured the infraorbitals of a small *H. tergisus* that had six elements, on which he commented (Taverne, 1977: 30):

> Sur l'un des spécimens de *Hiodon tergisus* et d'un seul côté du crâne seulement, on observe la présence de six os circumorbitaires au lieu de cinq. Un os supplémentaire s'intercalle entre les troisième et quatrième circumorbitaires traditionnels, qui voient tous deux leur taille réduite. Il n'est pas possible de dire si cet os supplémentaire s'est individualisé à partir du troisième ou du quatrième circumorbitaire puisque la position de cet os empiète à la fois sur celle occupée primitivement pars les troisième et quatrième circumorbitaires.

Clearly, however, the infraorbitals of *Hiodon* are very conservative in their pattern. The infraorbital series of teleostean fishes primitively consists of seven discrete bones, including the antorbital and dermosphenotic. The infraorbital series of all osteoglossomorphs (except putatively †Lycopteriformes, Jin et al., 1995), comprises only four elements between the antorbital (if present) and the dermosphenotic, and therefore is considered derived within teleosts (G. J. Nelson, 1969a); reduction in the number of infraorbitals is found

in many groups of teleosts (e.g., G. D. Johnson & Patterson, 1996: 265). As noted by Nelson (1969a: 11), the infraorbitals of *Hiodon*, "despite their reduced number, are highly peculiar and do not resemble those of any other Recent osteoglossomorph, or apparently of any other Recent teleost."

Two possibilities exist for the observed reduction: the loss of an element or the fusion of two elements into a single bone. Loss of an infraorbital in osteoglossomorphs has never been hypothesized. Based on correlation with the number of neuromasts associated with particular infraorbital bones in basal teleosts, Nelson (1969a) suggested that io3 and io4 of other teleosts have become phylogenetically fused in osteoglossomorphs. Li and Wilson (1996a: character 11), however, suggested that it was io4 and io5 that have fused in osteoglossomorphs (also Li & Wilson, 1999: fig. 5B; Arratia, 1999: character 34), because the element adjacent to the dermosphenotic in osteoglossomorphs is positionally similar to that of a combined io4 and io5 of other teleosts. In a single individual examined here (UAMZ 4043C, 71 mm SL), the bone posterior of io2 (on both sides) shows a deep furrow in its middle, suggesting that io3 and io4 have fused. However, other individuals at earlier stages of development (i.e., smaller) possess a single element in this position. Early ontogenetic studies of osteoglossomorphs, including earlier stages in *Hiodon* than were available to me, may help to address this question. Currently, however, the presence of a single element ("io3–4" of Nelson or "io4–5" of Li & Wilson) in the smallest individuals studied here suggests that if a fusion has occurred, it was phylogenetic rather than ontogenetic (see subsequent discussion under Remarks on Phylogenetic Fusion). I therefore have chosen to label the infraorbitals in sequence from anterior to posterior and not to make any statement of primary homology between individual bones of the infraorbital series of *Hiodon* with those of other teleosts.

An antorbital bone is absent in *Hiodon* (see earlier discussion of the lateral ethmoid under Skull Roof and Dorsal and Lateral Ethmoid Region).

Contrary to Taverne (1977) and others, I have found ossified sclerotic bones in *Hiodon* (sr, Fig. 37). These elements do not begin to form until relatively late in ontogeny and were found only in specimens 100 mm SL and larger (e.g., UMA F10598). The sclerotic ring comprises a pair of slender, anterior and posterior elements circling the lateral border of the eyeball. These elements are perichondral in origin, as in other extant teleosts that have sclerotic elements, although this could not be confirmed with my histological sections because the sclerotic bones had not yet formed in these specimens (i.e., they were too small). Patterson (1975) provided a brief overview of sclerotic bones in basal teleosts and other neopterygians and concluded that the primitive condition is to possess four elements, two of dermal origin and two of perichondral origin, as seen in †*Pholidophorus* and †*Australosomus*. In some taxa, such as †*Caturus*, †*Lepidotes*, †*Pholidophorus*, and several †Ichthyodectiformes, there is an additional perichondral basal sclerotic bone (Patterson, 1975: fig. 94), and its distribution suggests that the presence of this basal element is primitive for neopterygians, although it is poorly known from fossil taxa (Patterson, 1975). Patterson (1977a: 104) further discussed the possibility of variable histogenesis of sclerotic bones in osteichthyans, but concluded that "the dermal sclerotics of tetrapods and sturgeons and the endoskeletal sclerotics of teleosts are not examples of variable histogenesis, but of differential loss, the dermal sclerotics having been lost in teleosts."

Oral Jaws and Suspensorium

The upper jaw of *Hiodon* consists of paired premaxillae (pmx, Figs. 38 and 39) and maxillae (mx, Figs. 38 and 39). As in most other osteoglossomorphs (all except †*Tongxinichthys*, †*Kuangichthys*, †*Lycoptera*, †*Tanolepis*, and †*Paralycoptera*; Gaudant, 1968; Li & Wilson, 1999), supramaxillae are absent. The premaxilla is a stout element that is closely associated with the cartilage of the ethmoid region, resulting in a firm (i.e., nonmobile) attachment. Both the premaxilla and maxilla bear strong conical teeth. *Hiodon tergisus* has a greater number of premaxillary teeth than does *H. alosoides* (Tables 6 and 7), and also may have more than one row of teeth anteriorly, whereas only a single row of premaxillary teeth was found in all examined specimens of *H. alosoides*. I counted 12 premaxillary tooth positions in both specimens of †*H. consteniorum*, which is closer to the condition found in *H. alosoides* (Table 7) and †*Eohiodon* (pers. obs.). Characters describing the shape of the premaxillae were used as synapomorphies of *Hiodon* by Li and Wilson (1994: characters 17 and 18; also see Li, Wilson, & Grande, 1997). The premaxillae of the extant *Hiodon* are similar in shape, and do

bear a wide depression on their dorsal surfaces (= mid-dorsal concavity of Li & Wilson, 1994). The premaxillae of †*H. consteniorum* is a shorter and deeper element, and there is considerable variation between the two known specimens, which may be due to preservation (pers. obs.).

The maxilla articulates with the premaxilla along an elongate process (mxp, Figs. 38 and 39) that is bent sharply medially, as also seen in †*Eohiodon* and †*Lycoptera* (pers. obs.). Posteriorly, the maxilla is flat and thin and bears a single row of teeth along its ventral margin. In *H. alosoides,* the teeth are present along much of the length of the maxilla, whereas in *H. tergisus* the teeth, which are fewer in number, are more restricted to the middle of the bone (Fig. 40, Tables 6 and 7). There are at least 14 teeth on the maxilla of the holotype of †*H. consteniorum* (UALVP 38875), although the full series could not be counted.

Mature teeth of *Hiodon* have the dentine of the tooth associated firmly with the bone of attachment (Type 1 of Fink, 1981). This form of tooth attachment was considered to be plesiomorphic for actinopterygians by Fink (1981), who noted that, of the osteoglossomorphs he surveyed, only *Papyrocranus* possessed a different mode of tooth attachment (= his Type 2, in which a ring of collagen separates the dentine and the bone of attachment), and in this taxon, this was only found in the pharyngeal dentition. Type 2 dentition was considered to be a synapomorphy of all teleosts except Osteoglossomorpha (i.e., Elopomorphs and all other teleosts; Fink, 1981: table 1), although there are some taxa within this group that show reversals to the plesiomorphic condition (e.g., some clupeomorphs) or possess another derived condition (e.g., Types 3 and 4, the "hinged" teeth).

In *Hiodon,* each side of the lower jaw comprises five bones, two of which are fused. The largest bone of the lower jaw is the dentary (d, Figs. 38, 39, 41, and 42) and this is the only one to bear teeth, which are firmly attached to it along most of its dorsal margin. The posterior margin of the dentary is notched in lateral view (Figs. 41 and 42), and its posterior portion is laterally flattened or only slightly concave where it comes in close contact with the articular, coronomeckelian, and angulo-retroarticular. The mandibular sensory canal opens through four to eight pores along the ventrolateral margin of the dentary (Tables 4 and 5). There is no medial wall of the meckelian fossa in *Hiodon* (Fig. 38C, D), which is also lacking among osteoglossomorphs (of those studied here) only in †*Eohiodon* and possibly †*Lycoptera* (e.g., BMNH P28847). Outside Osteoglossomorpha, clupeomorphs also lack this structure (G. J. Nelson, 1973a; pers. obs.), as do the †ichthyodectiform genera †*Saurodon* (e.g., FMNH PF27413) and †*Prosaurodon* (e.g., Stewart, 1999: figs. 2 and 9). The distribution of this character warrants future study.

No living teleost has an autogenous series of coronoid bones (G. J. Nelson, 1973a), which are the other typical toothbearing bones of neopterygians, although Nelson (1973a) suggested that the inner tooth row at the anterior end of the jaw of *Scleropages* and *Osteoglossum* might represent the coronoid series. A similar argument could be made for the medial rows of teeth on the dentary of *Hiodon,* which, positionally at least, resemble coronoid teeth. These teeth, however, are firmly associated with the dentary bone, even in small specimens, suggesting that they are not remnants of an independent series of coronoid bones. The lateral teeth are generally the largest, although the anteriormost medial teeth can be equal in size. All teeth of the dentary are slightly medially curved, and those of the lingual rows are angled very medially (Fig. 39). The arrangement of teeth of the lower jaw is noticeably different in *H. tergisus* and *H. alosoides,* in that the patch of teeth on the dentary of *H. tergisus* is wider and forms a medial (= labial) shelf, whereas in *H. alosoides* the teeth are more or less restricted to two or three rows along the dorsal margin of the dentary (Fig. 43). The dentary teeth are smaller and more numerous (Tables 6 and 7) in *H. tergisus* than in *H. alosoides* (Fig. 43). Scott and Crossman (1973: 327) reported that in *H. alosoides,* the teeth are "stronger" in males than in females; this correlation was not observed here.

In *Hiodon,* three bones form in the posterior part of Meckel's cartilage, although a large portion remains cartilaginous in the adult (mc, Fig. 38C, D). The coronomeckelian (cm, Figs. 38, 39, 41, and 42) is a small, roughly triangular chondral bone that forms as a thin splint of bone in the dorsal surface of Meckel's cartilage and in the adult comes in contact with the articular and the medial surface of the dentary (Fig. 38C, D). In other teleostean fishes examined here (e.g., *Elops saurus,* UMA F10255), the coronomeckelian lies along the floor of the meckelian fossa.

In *Hiodon* the chondral articular (ar, Figs. 38, 39, 41, and 42) forms in the posterior portion of Meckel's cartilage, although there is a sharp an-

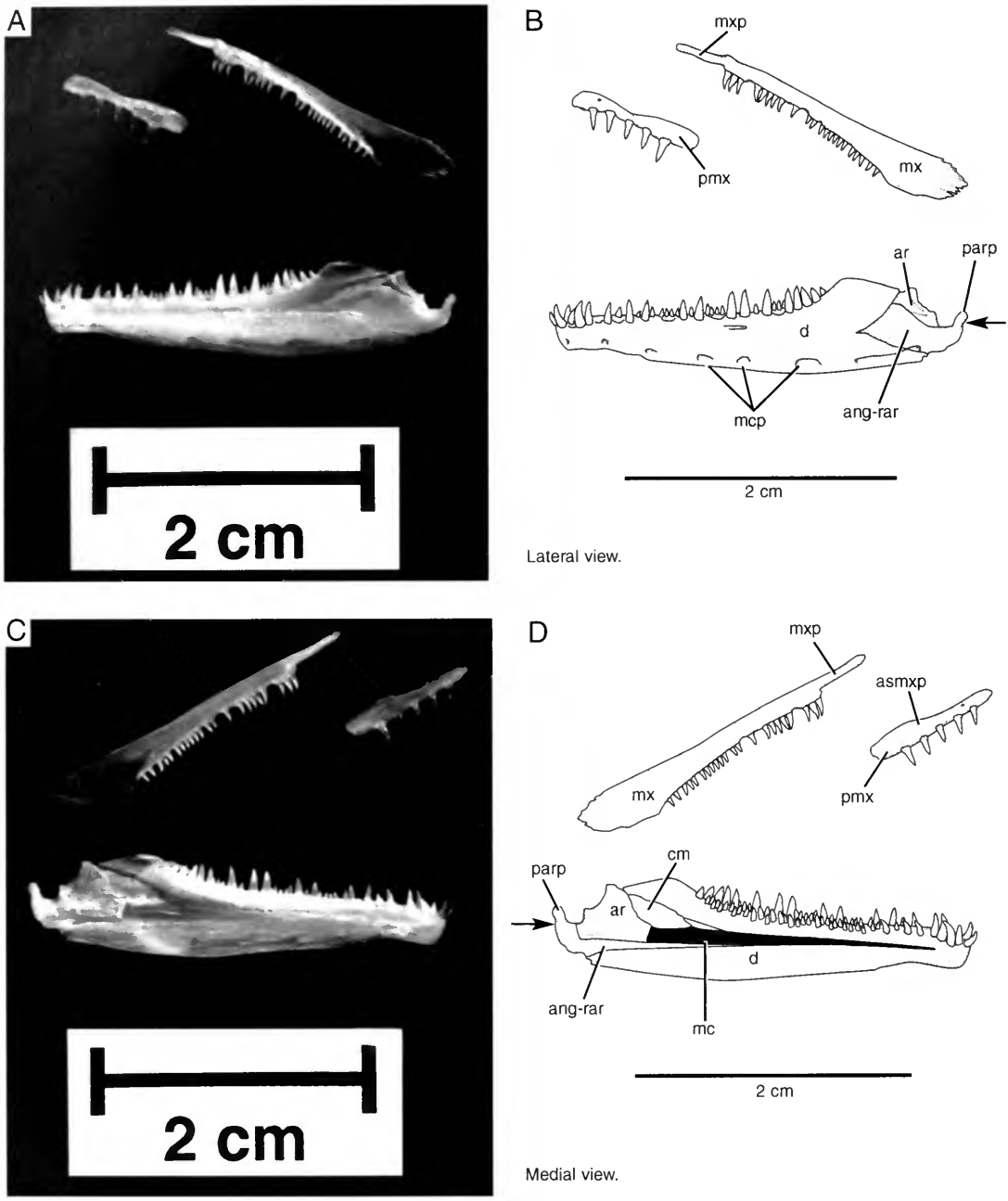

FIG. 38. *Hiodon alosoides*. **A** and **C**, Photographs, and **B** and **D**, line drawings of oral jaws of an adult (UMA F10587, 272 mm SL, male) in lateral (A and B) and medial (C and D) views. Arrow indicates level of posterior mandibular sensory canal pore. Anterior faces left in A and B; anterior faces right in C and D.

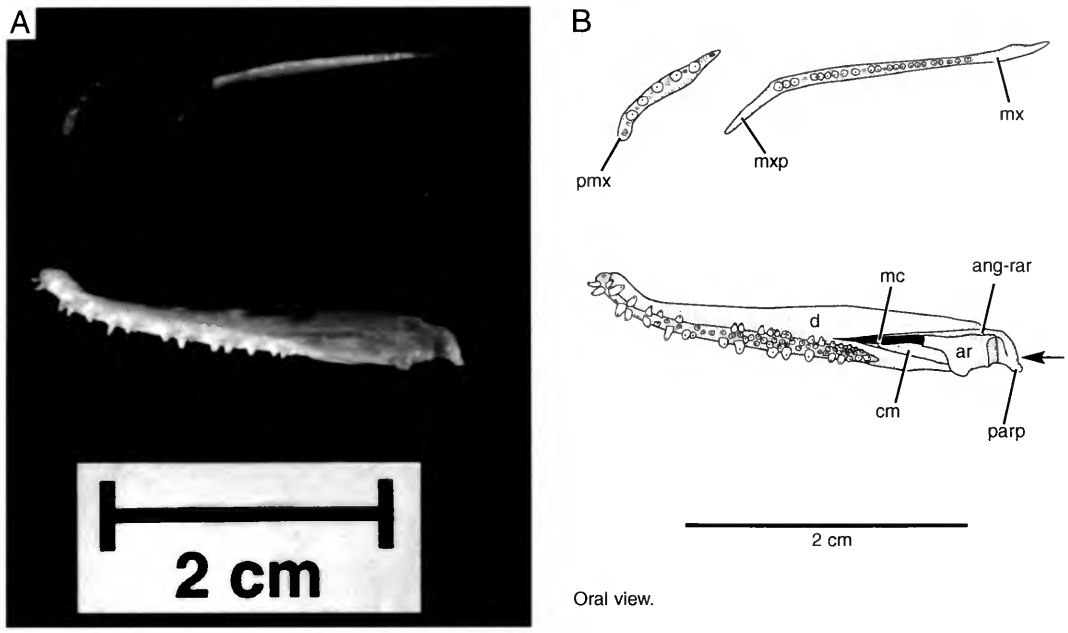

FIG. 39. *Hiodon alosoides*. **A**, Photograph, and **B**, line drawing of oral jaws of an adult (UMA F10587, 272 mm SL, male) in ventral (oral) view. Arrow indicates level of posterior mandibular sensory canal pore. Anterior faces left.

terior edge to this ossification. The articular is the largest of the ossifications within Meckel's cartilage and contributes to the anterior portion of the jaw joint (Fig. 39). The articular is the last bone of the lower jaw to form, and was first found in an approximately 25 mm SL specimen of *H. alosoides* (AUM 5169; Fig. 44; the articular in this specimen, however, is relatively well-developed, suggesting that it begins development earlier). The articular was not found in 21–24 mm SL specimens of *H. tergisus,* suggesting differences in the onset of ossification between the two species. Late development of the articular was also noted by Jollie (1975) for *Esox,* as he first found this bone in a 90 mm specimen, although it was not discovered as a distinct ossification (i.e., it was already fused to the dermal angular).

In *Hiodon,* the angular and retroarticular fuse ontogenetically, forming a compound angulo-retroarticular bone (ang-rar, Figs. 38, 39, 41, and 42). In my smallest specimens (e.g., *H. tergisus,* JFBM 22748, 21 mm SL; JFBM 22747B, 22 mm SL; *H. alosoides,* AUM 5169, approx. 25 mm SL), the chondral retroarticular bone is separate from the dermal angular (Fig. 44). G. J. Nelson (1973a,b) found that the only living teleosts not to have the angular fused to either the articular, retroarticular, or both are the osteoglossomorphs *Arapaima* and *Heterotis.* The genus †*Joffrichthys,* however, has the angular and articular fused to form an angulo-articular (this genus has been aligned to the heterotines by Li & Wilson, 1996b); details of the posterior lower jaw of †*Sinoglossus* Su, 1986, and †*Laeliichthys* da Silva Santos, 1985 (the other members of Heterotinae *sensu* Li & Wilson, 1996a,b), are unknown. Patterson (1977a: 95) suggested that the condition in living teleosts (i.e., presence of either an angulo-articular or angulo-retroarticular) was a case of phylogenetic fusion between the dermal and chondral elements, because all known ontogenies showed this bone developing from a single ossification center (see discussion under Remarks on Phylogenetic Fusion), although, as shown here it is formed through ontogenetic fusion in *Hiodon.* Both the articular and the retroarticular portion of the angulo-retroarticular contribute to the facet for articulation with the quadrate (Fig. 39), a condition that has been considered plesiomorphic for teleosts (G. J. Nelson, 1973a). In *Hiodon,* the angular portion of the angulo-retroarticular possesses a dorsally directed postarticular process (parp, Figs. 38, 39, 41, and 42) on the posterior margin of the bone. This process extends dorsally from the posterior portion

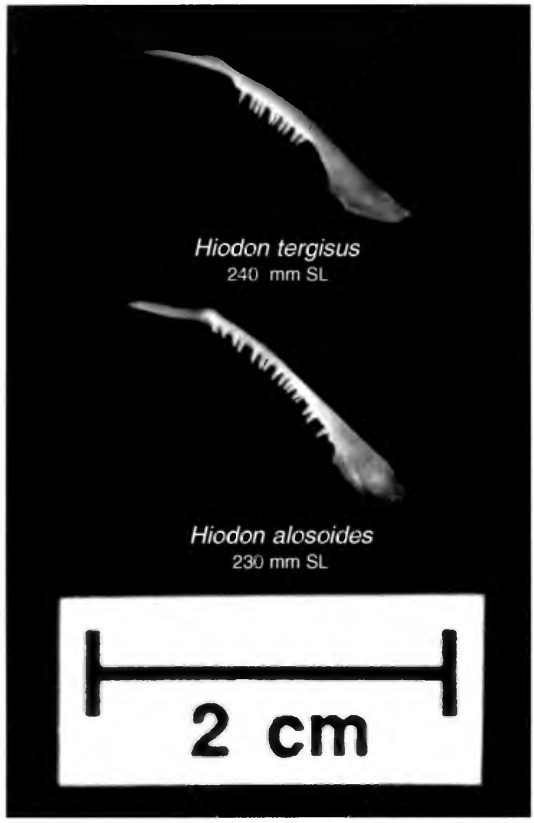

FIG. 40. Left maxillae of *Hiodon tergisus* (UF 31651, 240 mm SL, female) and *H. alosoides* (ANSP 159095, 230 mm SL, female) in lateral view showing difference in dentition. Anterior faces left.

of the quadrate articulation surface. The angulo-retroarticular bone overlaps the medial surface of the dentary for about one-half its entire length. The portion of the angulo-retroarticular exposed in lateral view is marked by a chevron-shaped ridge where it meets the dentary (Fig. 41).

No mentomeckelian is present in *Hiodon*. When present in teleosts, this bone, which is an anterior ossification of Meckel's cartilage, is fused with and surrounded by the dentary (G. J. Nelson, 1973a).

The suspensorium includes the hyosymplectic and palatoquadrate cartilages and their ossifications; these elements are illustrated in Figures 45–49. Portions of the suspensorium were described by Hilton (2001) in reference to the so-called parasphenoid–tongue bite apparatus. No substantial differences were noted between the suspensoria of *H. tergisus* and *H. alosoides*.

The hyomandibula (h, Figs. 45–49) articulates with the neurocranium by two heads. The anterior head sits in a fossa formed by the sphenotic, pterotic, and prootic; the posterior fossa is formed by the pterotic and intercalar (Figs. 18–22). The two heads are bridged dorsally by a thin strut of bone that does not contact any of the neurocranial elements. This strut encloses a large foramen where the anteroventral lateral line nerve exits and runs ventrally along the posterior edge of the hyomandibula (hmf, Figs. 45–49). A shallow, medial shelf of bone ventral to this foramen comes into contact with the prootic wing (Figs. 10C, D, and 47). A third elongate head, the opercular process of the hyomandibula (hp, Figs. 45–49), extends far posteriorly, where it articulates with the opercle. The opercular process bears dorsomedial and ventrolateral bladelike flanges. The ventrolateral flange contacts the medial surface of the vertical arm of the preopercle. In life, the body of the hyomandibula is essentially perpendicular to the neurocranium (Fig. 10) and laterally bears a ridge at the origin of the mandibular adductor

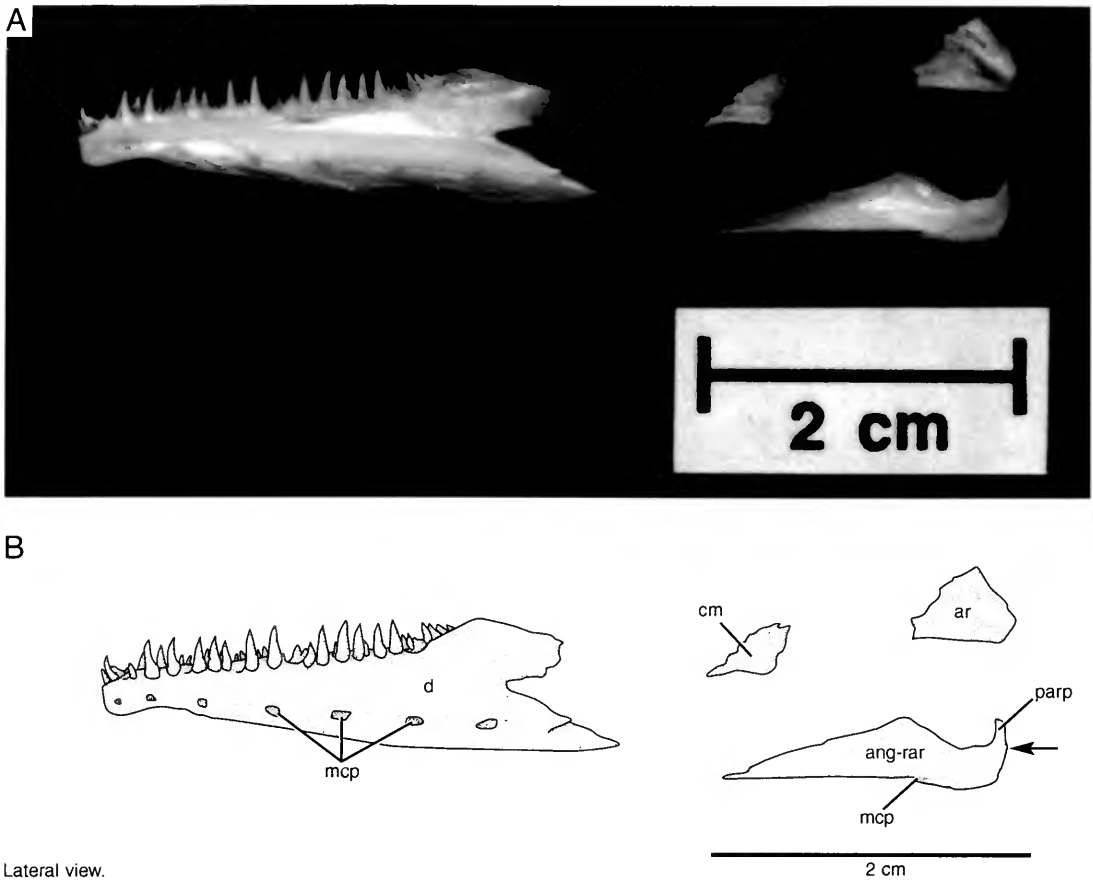

FIG. 41. *Hiodon alosoides*. **A**, Photograph, and **B**, line drawing of disarticulated lower jaw of an adult (UMA F10581, 315 mm SL, female) in lateral view. Arrow indicates level of posterior mandibular sensory canal pore. Anterior faces left.

muscle (Fig. 45). The symplectic (sym, Figs. 45–49) is a small, wedge-shaped bone that articulates medially with a groove on the dorsomedial surface of the preopercular process of the quadrate (Figs. 47 and 48). The symplectic ossifies perichondrally around the ventral portion of the hyosymplectic cartilage.

The quadrate (q, Figs. 45–49) in *Hiodon* is a fan-shaped element that bears an elongate preopercular process (= posteroventral process of the quadrate, Arratia & Schultze, 1991; see below). The quadrate meets the metapterygoid posterodorsally along a smooth, cartilage-filled suture. The quadrate contacts the ectopterygoid and endopterygoid anteriorly, which overlap on its medial surface. A portion of the pars quadrata or pars metapterygoidea extends from the anterior edge of the quadrate and spreads over the lateral surface of the dermal palatoquadrate. This same cartilage is continuous with the anterior margin of the metapterygoid.

Posteriorly, the preopercular process of the quadrate fits into a groove on the dorsal surface of the horizontal arm of the preopercle and extends ventrally, over the dorsolateral surface of the preopercle (Fig. 45). Arratia and Schultze (1991) found that the presence of such a process is a synapomorphy for teleosts (also Arratia, 1999: character 59). This process previously has been interpreted as the quadratojugal of other actinopterygians (Patterson, 1973; see discussions in Gardiner et al., 1996; Grande & Bemis, 1998; and Arratia, 1999). Wiley (1976) described a free dermal bone in the position of the quadrate process in a larva of *Elops saurus* and referred to this bone as the quadratojugal. Other authors (e.g.,

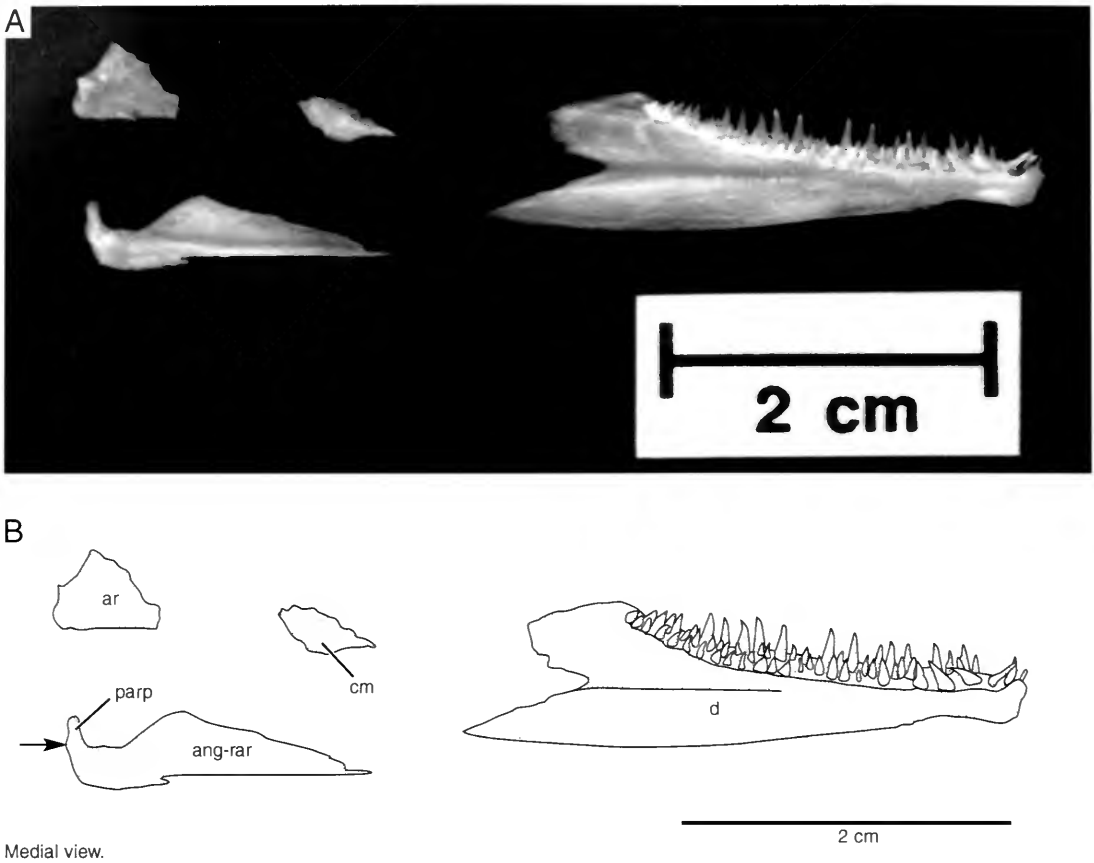

FIG. 42. *Hiodon alosoides*. **A**, Photograph, and **B**, line drawing of disarticulated lower jaw of an adult (UMA F10581, 315 mm SL, female) in medial view. Arrow indicates level of posterior mandibular sensory canal pore. Anterior faces right.

Holmgren & Stensiö, 1936; Jollie, 1975) reported similar autogenous bones in other groups of teleosts (e.g., salmonids and esocids). Jollie (1975, fig. 8) figured and described the jaw joint of an 18 mm (presumably total length) specimen of *Esox lucius*, in which he found a "separate" quadratojugal. However, in Jollie's (1975) figure, a connection between the "quadratojugal" and the quadrate is maintained, drawing into question the nature of this element. Arratia and Schultze (1991) found no ontogenetic evidence that this process is homologous to the quadratojugal. The process was already well-developed in the smallest individuals of *Hiodon* examined here and was never observed to be autogenous. I also examined pre- and postmetamorphic leptocephali of *Megalops atlanticus* (UMA F11250–F11256) and was unable to find a separate quadratojugal. Until such ontogenetic support for the fusion of two bones (i.e., quadrate and quadratojugal) is clearly demonstrated, the teleostean quadrate must be recognized as a single ossification (see Remarks on Phylogenetic Fusion). Grande and Bemis (1998) suggested a possible homology between the preopercular process of teleosts and a cartilaginous splint associated with the quadrate of *Amia*. In *Hiodon*, as in other teleosts, the process develops as a membranous ossification from the quadrate, and is not endochondral in origin (Arratia & Schultze, 1991; pers. obs.). This would suggest that the teleostean quadrate process and the cartilaginous splint of *Amia* are distinct elements that are not homologous (although not conclusively, because elements of different tissue origin can be homologous; e.g., see Hall, 1995).

The metapterygoid (mpt, Figs. 45–49) is a flat, U-shaped bone that is obliquely positioned dorsal to the quadrate and symplectic bones. The dorsal

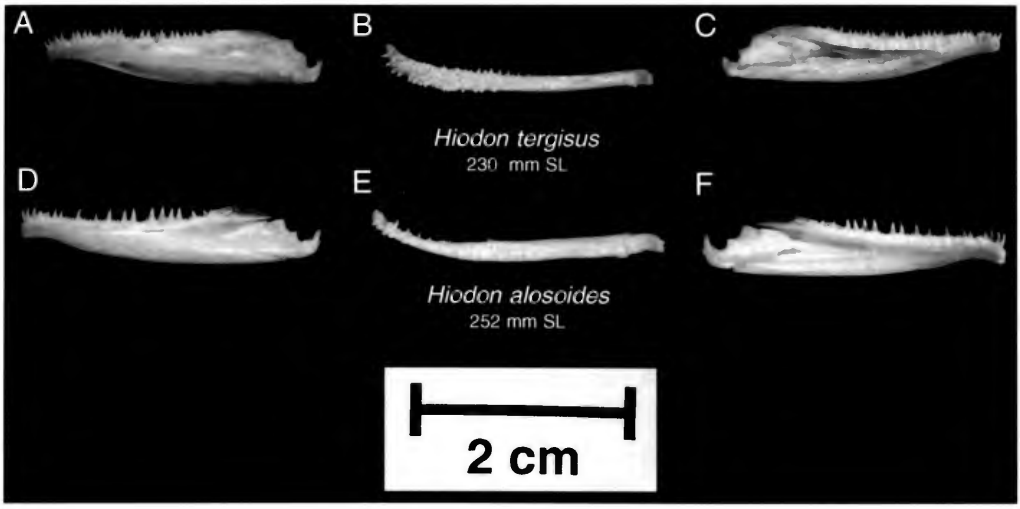

FIG. 43. Lower jaws of *Hiodon tergisus* (**A–C**; UMA F10613, 230 mm SL, female) and *H. alosoides* (**D–F**; UMA F10588, 252 mm SL, male) showing difference in dentition. Specimens in lateral (A and D), dorsal (= oral) (B and E), and medial (C and F) views. Anterior faces left in A, B, D, and E; anterior faces right in C and F.

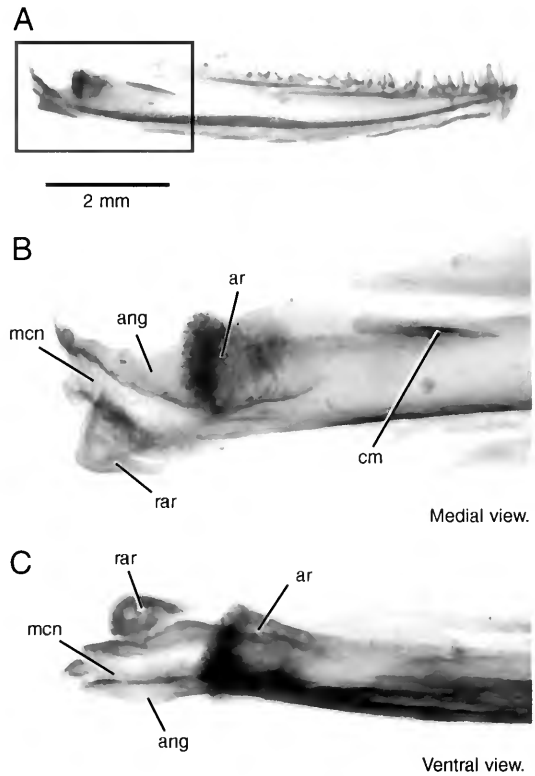

FIG. 44. *Hiodon alosoides,* cleared and stained lower jaw of a small individual (AUM 5169, approx. 25 mm SL) in medial (**A** and **B**) and ventral (**C**) views showing retroarticular as an independent element. Area in box in A is magnified in B and C. Cartilage was not stained in this specimen. Anterior faces right.

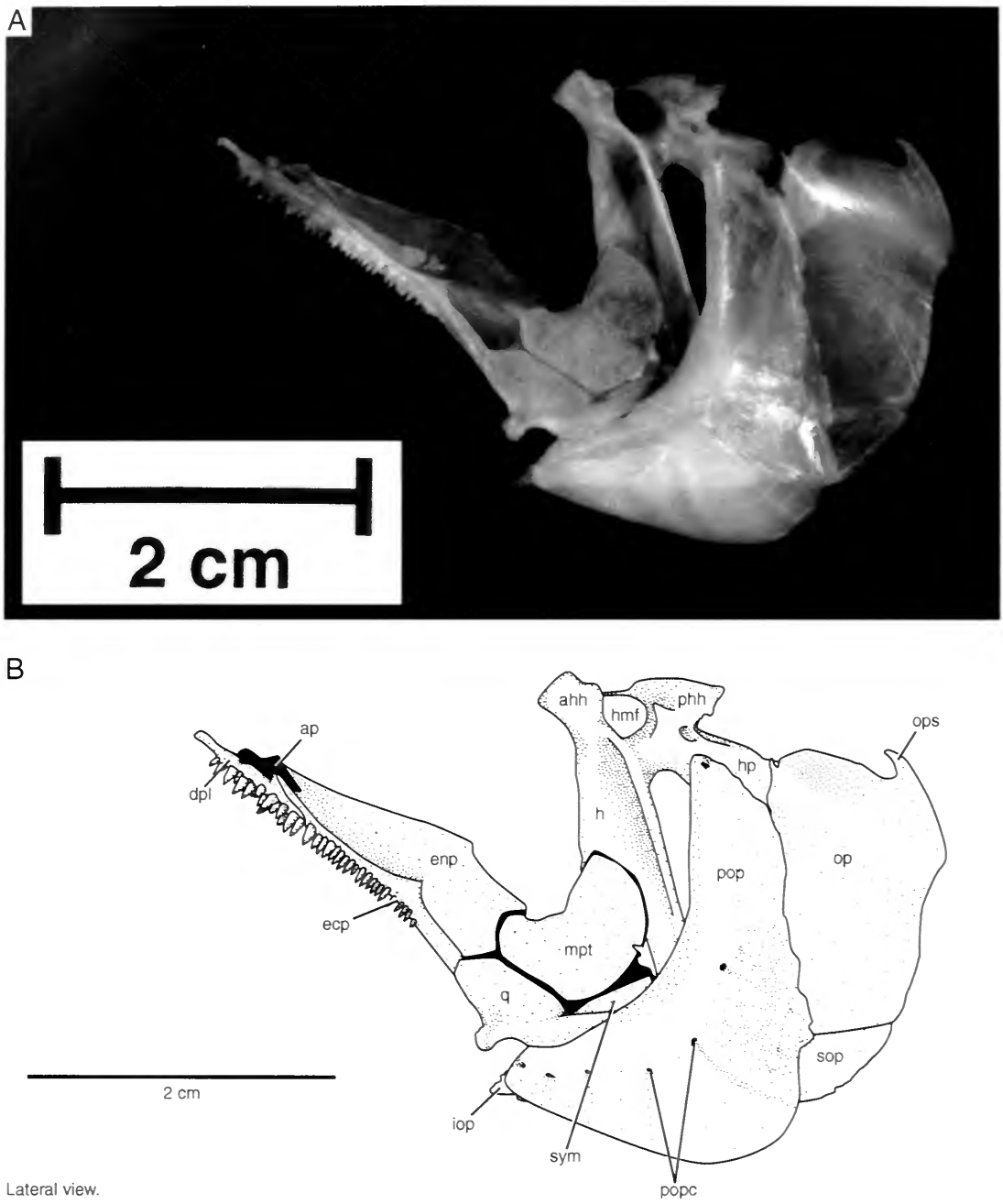

FIG. 45. *Hiodon alosoides*. **A**. Photograph, and **B**. line drawing of suspensorium and opercular elements of an adult (UMA F10177, 267 mm. SL female) in lateral view. Anterior faces left.

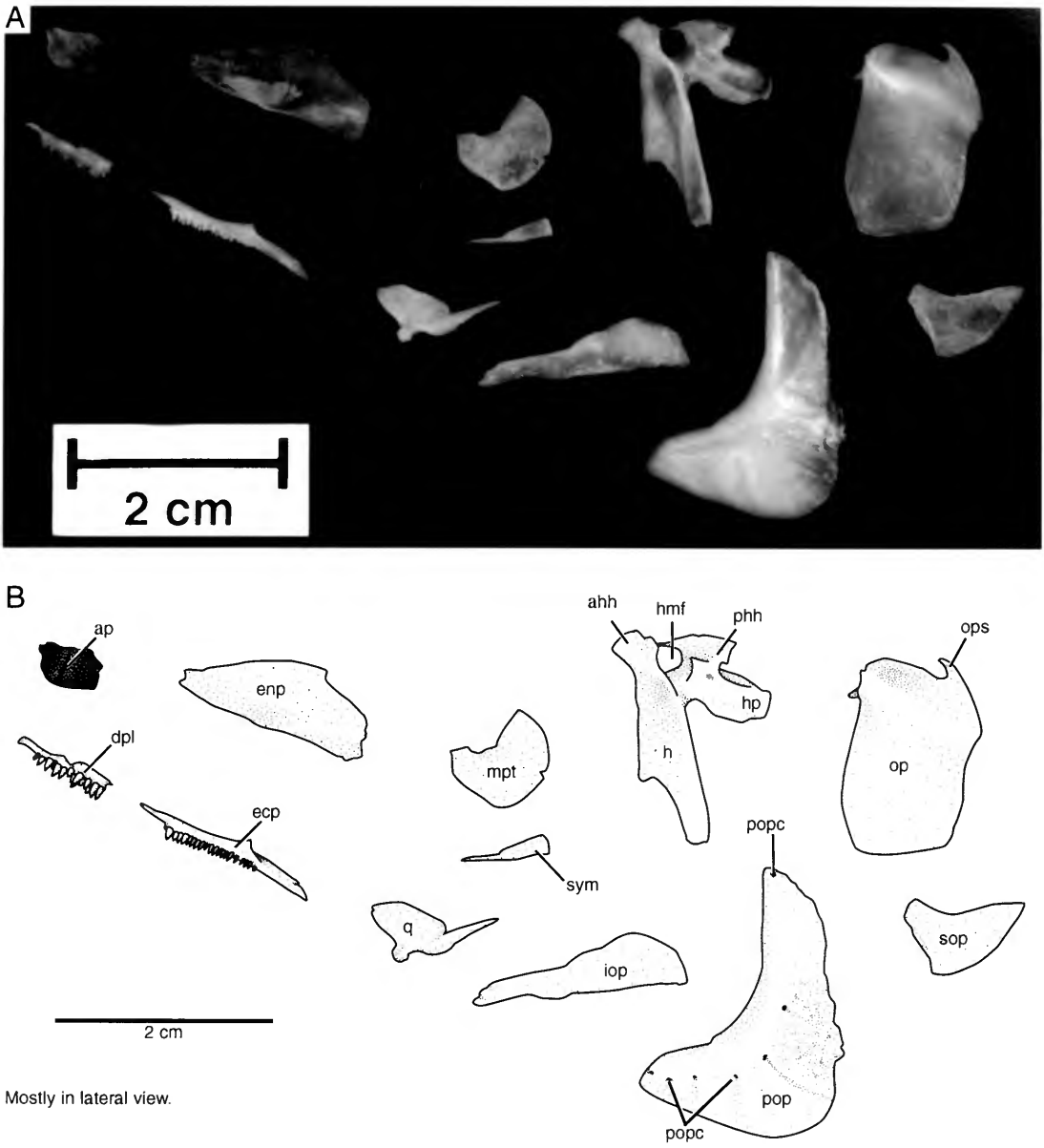

FIG. 46. *Hiodon alosoides*. **A**, Photograph, and **B**, line drawing of disarticulated suspensorium and opercular elements of an adult (UMA F10177, 267 mm SL, female) in lateral view. Cartilaginous pars autopalatina (ap) in dorsal view. Anterior faces left.

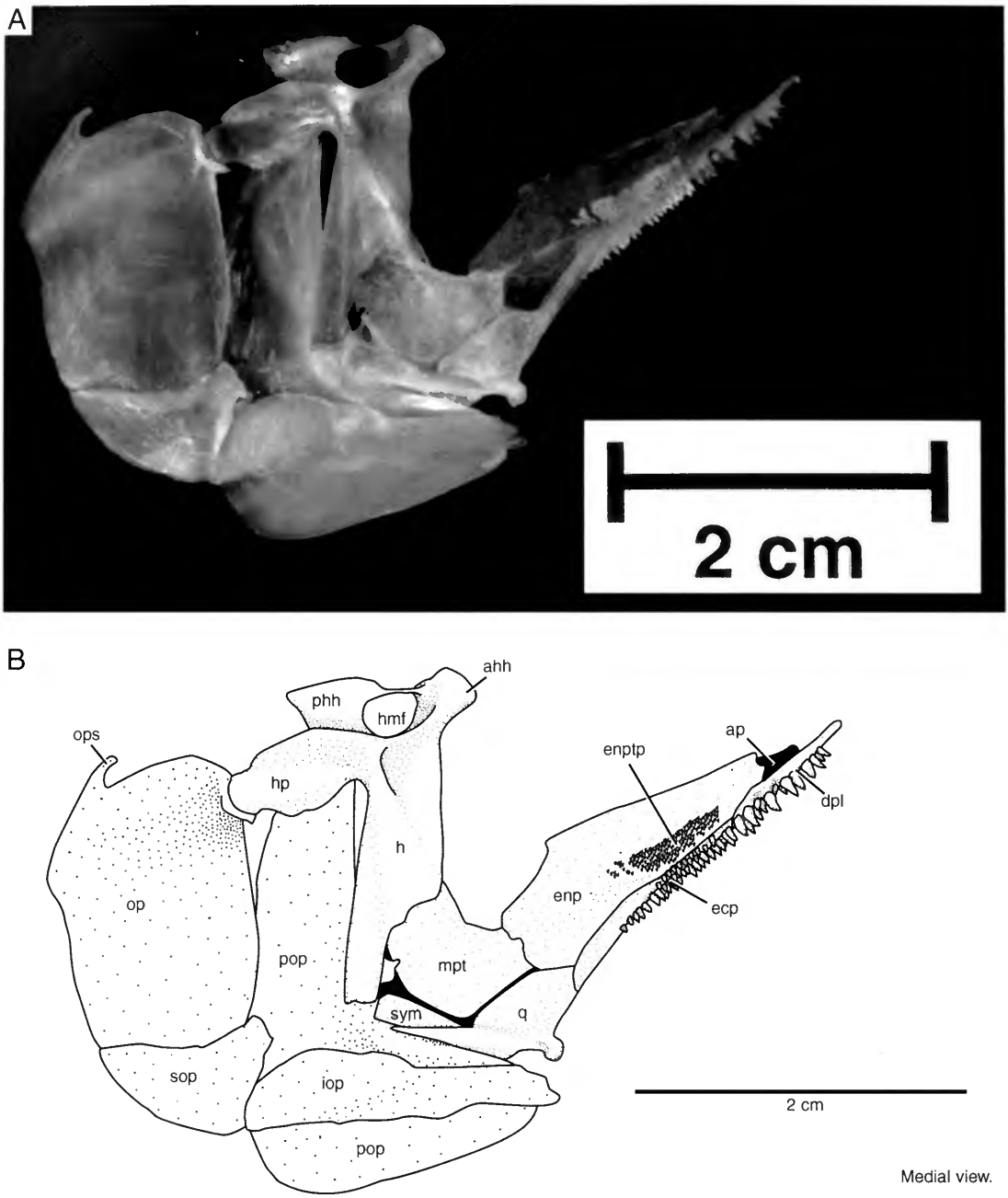

FIG. 47. *Hiodon alosoides*. **A**, Photograph, and **B**, line drawing of suspensorium and opercular elements of an adult (UMA F10177, 267 mm SL, female) in medial view. Anterior faces right.

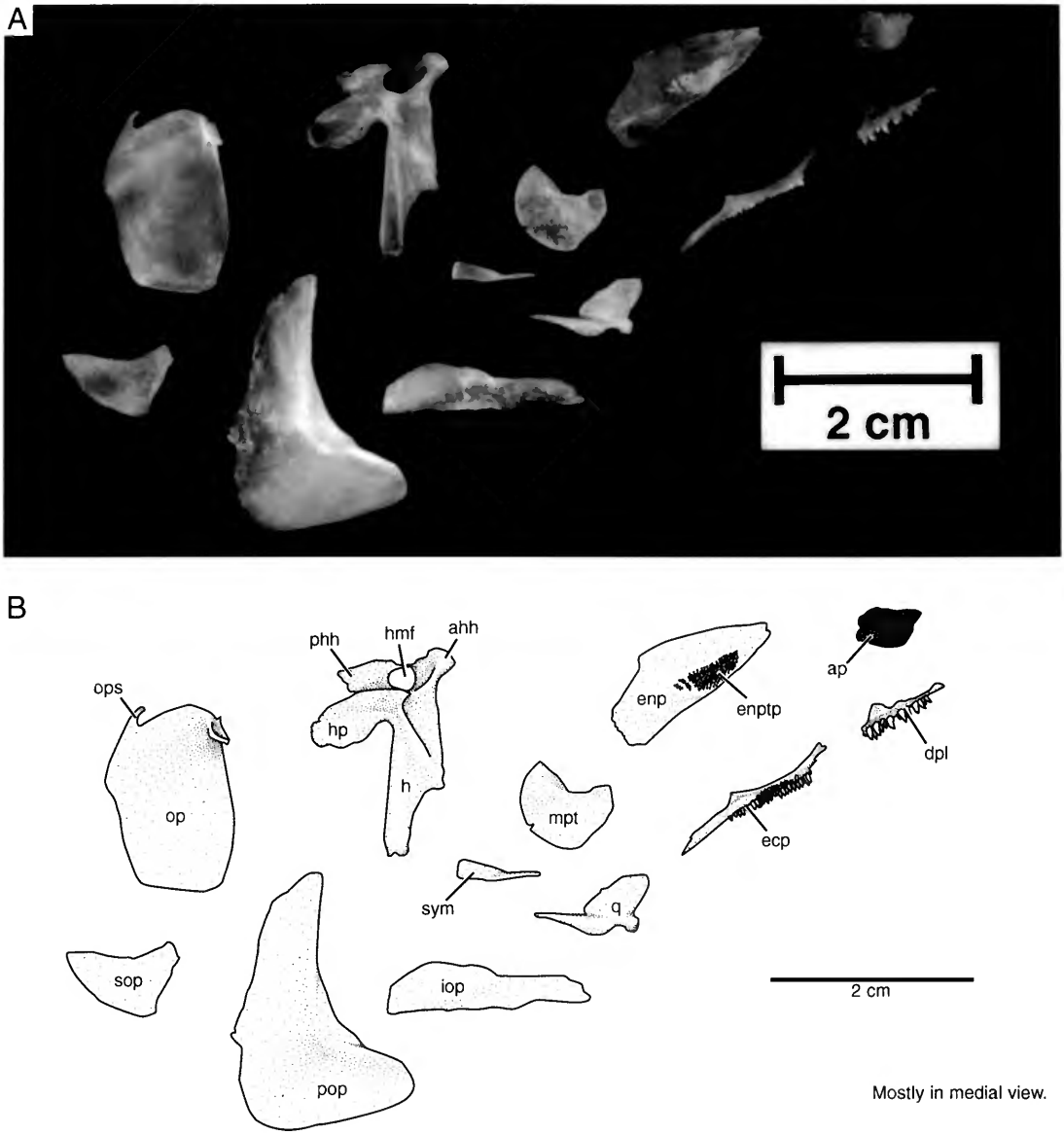

FIG. 48. *Hiodon alosoides*. **A**, Photograph, and **B**, line drawing of disarticulated suspensorium and opercular elements of an adult (UMA F10177, 267 mm SL, female) mostly in lateral view. Cartilaginous pars autopalatina (ap) in ventral view. Anterior faces right.

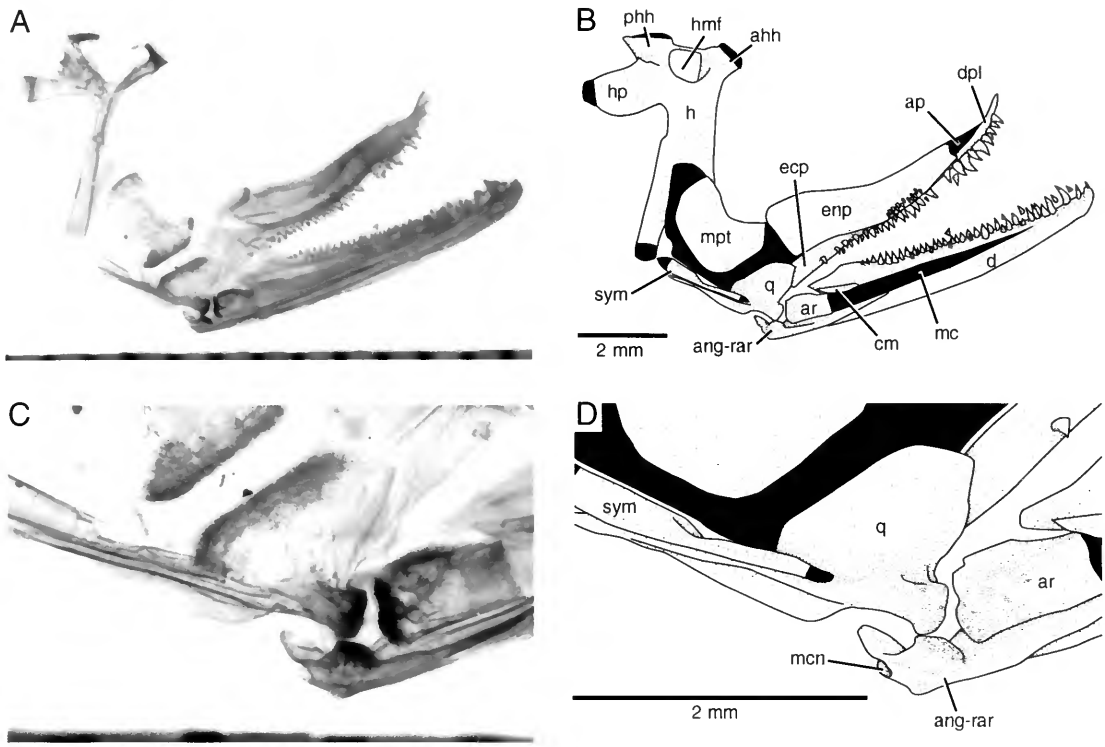

FIG. 49. *Hiodon alosoides*. **A** and **C**, Photographs, and **B** and **D**, line drawings of cleared and stained suspensorium and lower jaw of a juvenile (UMA F10597, 62 mm SL) in medial view. A and B, Suspensorium and lower jaw. C and D, Close-up view of jaw articulation. Anterior faces right.

portion of the metapterygoid contacts the ventrolateral surface of the hyomandibula. Ventrally, the metapterygoid meets the dorsal edge of the quadrate, and in large individuals these elements are very tightly associated. A small notch is present on the posterior border of the metapterygoid. Although the quadrate and metapterygoid bones continue to grow throughout ontogeny, even in the very largest specimens studied a portion of the pars quadrata or pars metapterygoidea cartilage anterior to these elements remains unossified.

A thin cartilage, likely the unossified portion of the pars metapterygoidea, lies along the lateral margin of the suspensorium, dorsal to the ectopterygoid. This cartilage broadens anteriorly into the pars autopalatina (ap, Figs. 45–49), which lies dorsal to the junction of the ectopterygoid, entopterygoid, and dermopalatine. In most teleosts, this cartilage contains an endochondral ossification, the autopalatine. As in most other osteoglossomorphs (Taverne, 1979, 1998) the pars autopalatina remains unossified in *Hiodon*, even in the largest individuals examined. Arratia and Schultze (1991: 33) stated, "In osteoglossomorphs, a bony autopalatine is missing; a fibrocartilaginous *pars autopalatina* was observed in *Pantodon* . . . but not in adult *Hiodon* . . . ." However, an ossified autopalatine is present in *Heterotis niloticus* (e.g., MCZ 50959) and *Scleropages leichardti* (e.g., BMNH 1905.3.20.6; see Taverne, 1998).

The dermal bones of the suspensorium of *Hiodon* include the endopterygoid, ectopterygoid, and dermopalatine. The endopterygoid (enp, Figs. 45–49) is a thin element that forms most of the roof of the mouth. Its dorsal surface is slightly convex and its medial edge contacts the parasphenoid in resting position (i.e., when the suspensorium is not flared). An oblong patch of small conical teeth (entp, Figs. 47 and 48) is present on the ventral surface of the endopterygoid along the edge adjacent to the ectopterygoid.

The ectopterygoid and dermopalatine form the lateral margin of the suspensorium, and both are more robust than the endopterygoid. The ectopterygoid (ecp, Figs. 45–49) meets the anterior portion of the quadrate and bears a row of strong

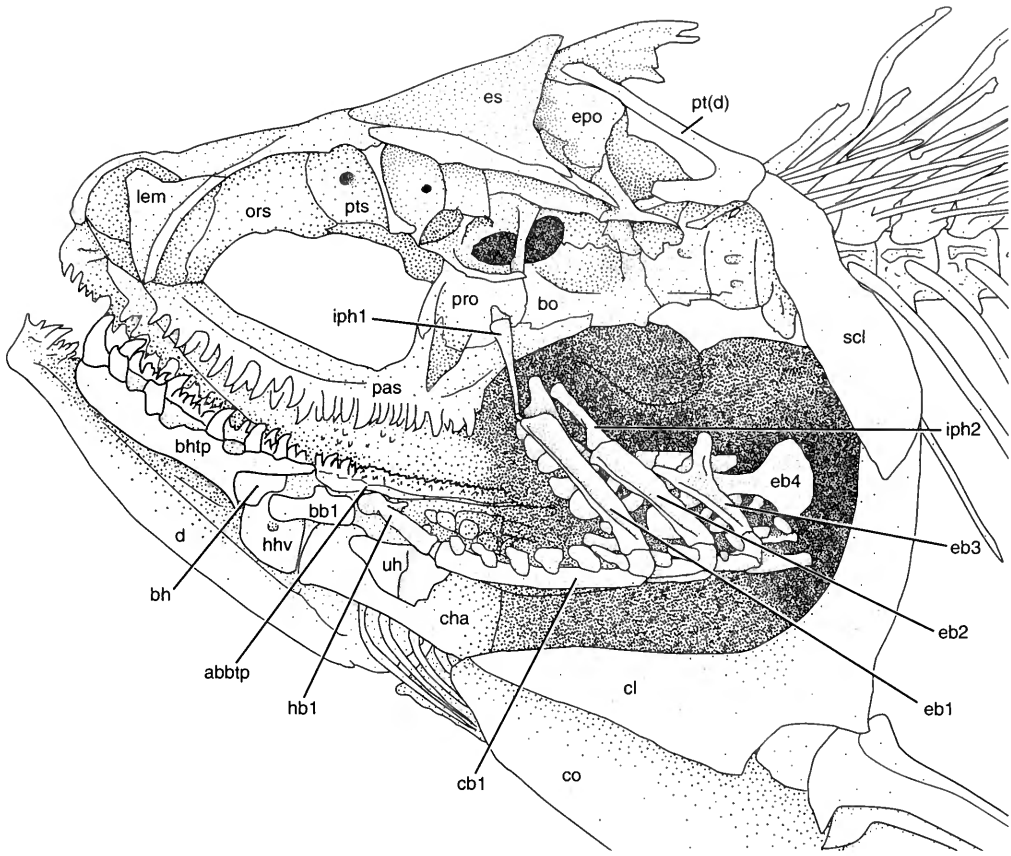

FIG. 50. *Hiodon alosoides,* line drawing of skull and gill arches of an adult (UMA F10150, 293 mm SL, female) in lateral view showing gill arches in situ. Left "cheek" bones removed before preparation by dermestid beetles. (Adapted from Hilton, 2001: fig. 1A.)

conical teeth along its lateral edge for most of its length. Medial to this row, smaller teeth are found scattered over the anterior half of the element.

The dermopalatine (dpl, Figs. 45–49) is the most anterior of the ossifications of the suspensorium, and the posterior portion continues the lateral row of ectopterygoid teeth; there is a single row of the teeth medially. A largely untoothed anterior "finger" of the dermopalatine extends ventral to the ethmoid region of the neurocranium (although the anteriormost region of the dermopalatine is toothed in small specimens, Fig. 32). A posterodorsal wing of the dermopalatine joins the anterodorsal wing of the ectopterygoid along the lateral edge of the suspensorium and forms a shelf for the pars autopalatina (Fig. 45). Arratia and Schultze (1991) suggested that the dermopalatine of osteoglossomorphs is homologous to dermopalatine 2 of *Amia* (= posterior dermopalatine of Grande & Bemis, 1998) because it lies ventral to the pars autopalatina, positionally similar to the posterior dermopalatine in *Amia.* Arratia and Schultze (1991) further suggested that the single dermopalatine of *Elops* is homologous to dermopalatine 1 and 2 (= anterior and posterior dermopalatine of Grande & Bemis, 1998), and that dermopalatine 1 appears to have been lost in most living teleosts. However, direct correlation of the two dermopalatines of *Amia* with the single element in teleosts is difficult.

Opercular Series

The dorsal elements of the opercular series are illustrated with the suspensorium in Figures 45–48, and the ventral elements of the opercular series (i.e., the branchiostegals) are illustrated with

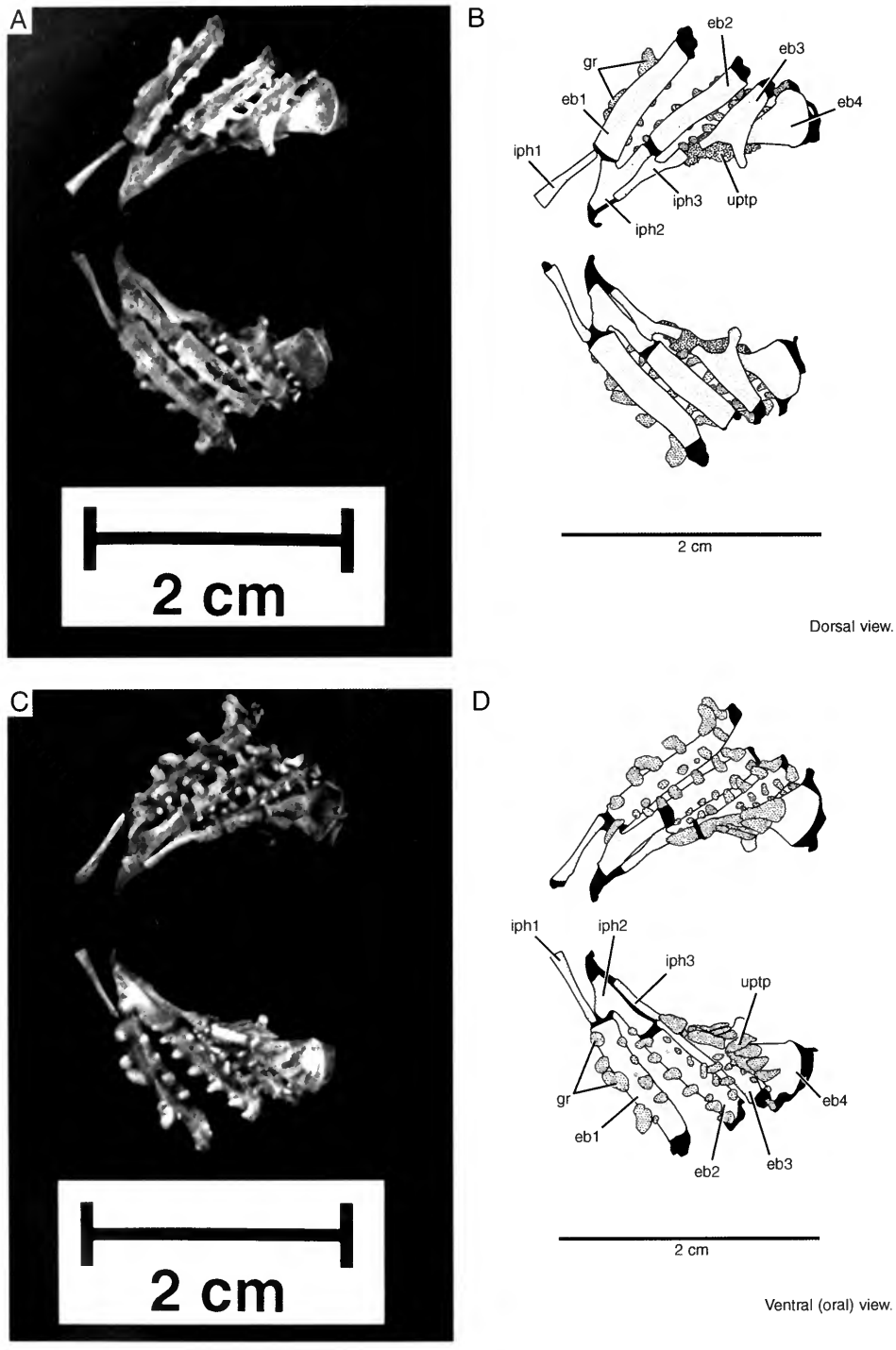

FIG. 51. *Hiodon alosoides*. **A** and **C**, Photographs, and **B** and **D**, line drawings of bones of dorsal portion of gill arches of an adult (UMA F10178, 279 mm SL, female) in dorsal (A and B) and (C and D) ventral (= oral) views. Fourth infrapharyngobranchial is entirely cartilaginous and was not preserved. Anterior faces left.

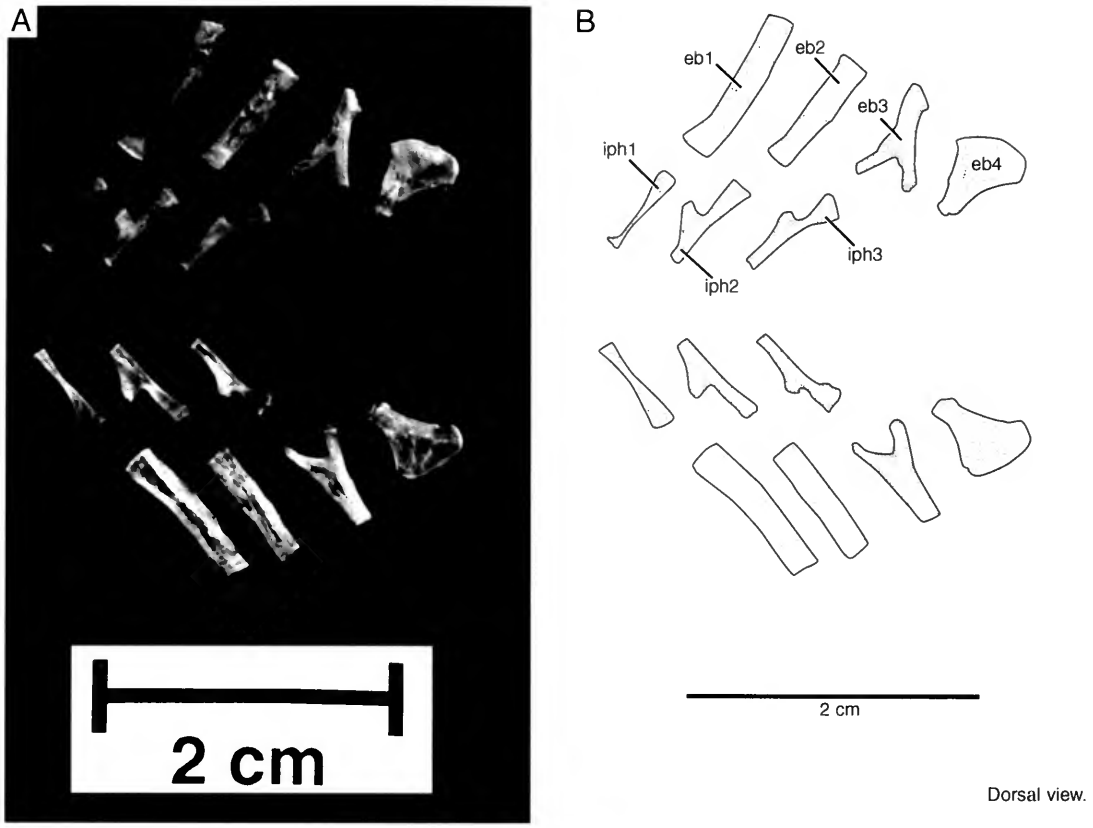

FIG. 52. *Hiodon alosoides*. **A**, Photograph, and **B**, line drawing of disarticulated bones of dorsal gill arches of an adult (UMA F10587, 272 mm SL, female) in dorsal view. Gill rakers and toothplates have been removed. Fourth infrapharyngobranchial is entirely cartilaginous and was not preserved. Anterior faces left.

the gill arches in Figures 53–55. Portions of the opercular series of *Hiodon* were described by McAllister (1968). All elements of the opercular series were present in the smallest specimens examined. The opercle (op, Figs. 45–48) of *Hiodon* is a flat, somewhat rectangular dermal element. Li and Wilson (1994: 161) describe the opercle as possessing a "protruding upper posterior border." I found the extent of this protrusion was individually variable. A similar protrusion was observed in the clupeomorph *Dorosoma cepedianum* (UMA F10279), although this is undoubtedly independently derived. Li and Wilson (1994: character 16) proposed that the prominent posterodorsal spine of the opercle (ops, Figs. 45–48) is diagnostic of *Hiodon*. This spine is continuous with the soft tissue of the dorsal portion of the opercular flap, and its size varies among individuals of similar overall sizes. I did not detect any sexual dimorphism in the size of this spine. A similar spine was also observed in a specimens of †*Eohiodon* (e.g., FMNH PF15167), thus drawing into question this as an unambiguous synapomorphy of the genus *Hiodon*. The dorsal margin of the opercle, between the hyomandibular facet and the posterodorsal spine, is medially deflected; the dorsal surface of this deflection serves as the insertion surface for the levator operculi muscle. The articular facet for the hyomandibula is a cuplike concavity on the medial surface of the opercle (Fig. 48), in line with the anterior margin of the opercle. In one specimen of *H. tergisus* (FMNH 100590), the posterior edges of both left and right opercles are serrated, much like the condition in some notopterids (e.g., *Notopterus*, Taverne 1978: fig. 69), as well as in some nonosteoglossomorph teleostean fishes (e.g., *Esox lucius*, UMA F10273).

The thin and flat subopercle and interopercle lie in series between the opercle and branchiostegals. The somewhat triangular subopercle (sop, Figs.

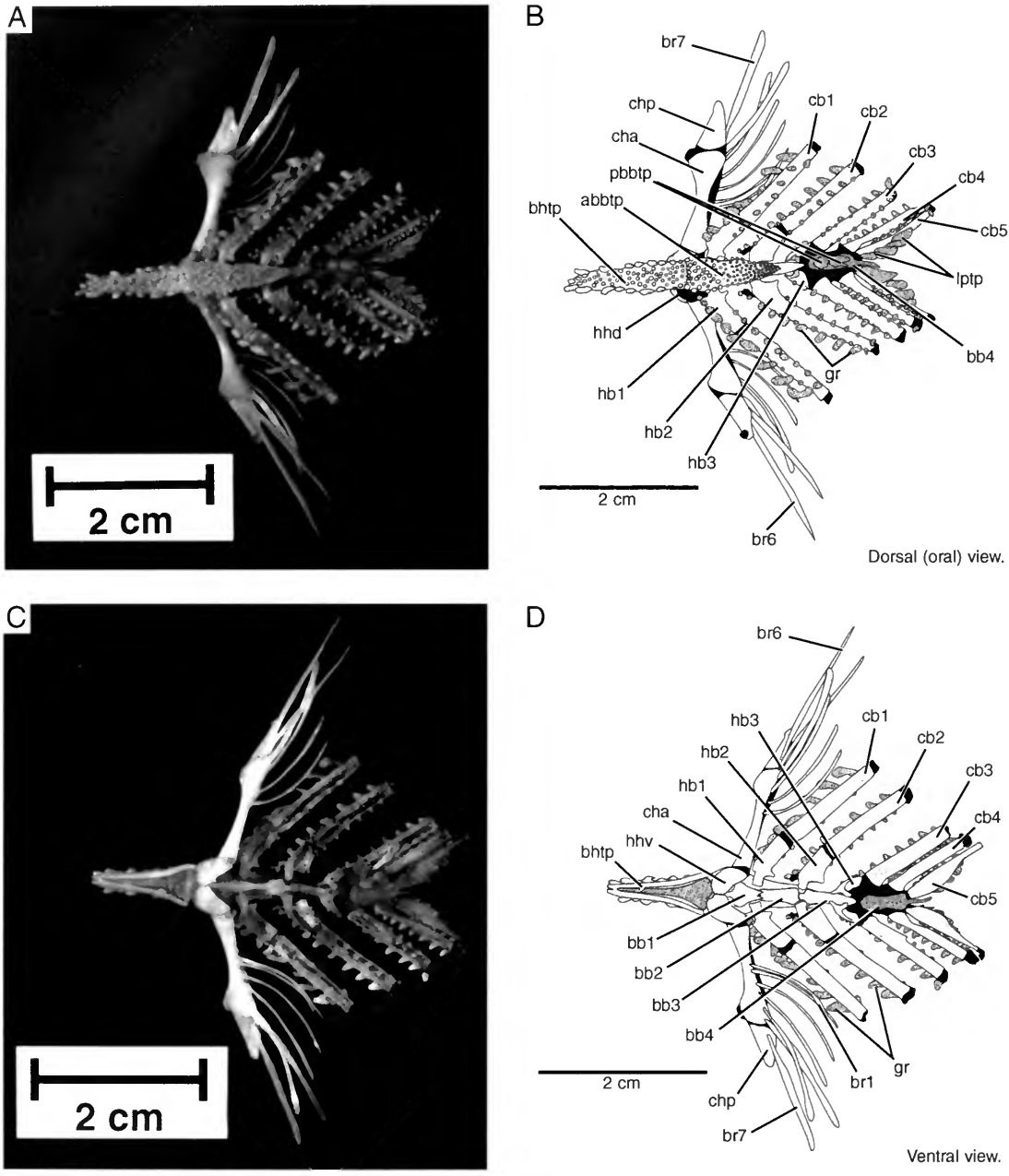

FIG. 53. *Hiodon alosoides*. **A** and **C**, Photographs, and **B** and **D**, line drawings of ventral portion of gill arches of an adult (UMA F10178, 279 mm SL, female) in dorsal (= oral) (A and B) and ventral (C and D) views. Cartilaginous fourth basibranchial (bb4) and cartilage anterior of basihyal (unlabeled) shown in heavy stipple; all other cartilages shown in black. Anterior faces left.

45–48) is closely associated with the ventral margin of the opercle (Fig. 47). The interopercle (iop, Figs. 45–48) lies on the ventromedial portion of the preopercle and contacts the anterior edge of the subopercle. This bone is largely covered in lateral view by the preopercle, although its anterior tip extends past the anterior margin of the preopercle (Figs. 35 and 45).

The preopercle (pop, Figs. 45–48) is a strong, J-shaped bone that dorsally rests against the lateral surface of the opercular process of the hyomandibula (Fig. 45). Ventrally and medially, the preopercle contacts the ventral arm of the hyomandibula, the symplectic, the quadrate, the subopercle, and the interopercle (Fig. 47). The preopercle is intimately associated with the preopercular process of the quadrate by means of a shelf-like fossa along the dorsal edge of its horizontal arm (Fig. 48). The horizontal arm of the preopercle is strongly concave medially, and wraps around the ventral surface of the body (Fig. 35). The preopercular sensory canal opens through a series of pores along the length of the canal (popc, Figs. 45 and 46).

The branchiostegals of *Hiodon* are thin bones that support the gill membrane and are associated with the anterior and posterior ceratohyals. Eight branchiostegals on each side is the modal condition (Tables 6 and 7). McAllister (1968) reported the number of branchiostegals in *Hiodon* to vary from seven to ten (eight or nine in *H. tergisus* and seven to ten in *H. alosoides*). The individual illustrated in Figure 53 (UMA F10178) has seven branchiostegals on the left side and six on the right; this was the only individual observed with six branchiostegals (as this specimen is a dry skeleton, a medial branchiostegal may have been lost during preparation). As noted by McAllister (1968), the lateralmost branchiostegals of *Hiodon* are spathiform (i.e., broad, laminar bones; Figs. 54 and 55), although there is a medial gradation to more a more virgaform shape (i.e., slender rods of bone; McAllister, 1968: 4). There is a substantial curve to the more medial branchiostegals, which may not contact the anterior ceratohyal (Fig. 57).

Ventral Portions of the Hyoid Arch and Gill Arches

The gill arch skeleton of *Hiodon*, and that of osteoglossomorphs in general, was described and illustrated by G. J. Nelson (1968a) and Taverne (1977). Certain elements of the ventral gill arches of *Hiodon* also were described in the context of the "parasphenoid–tongue bite" by Hilton (2001). Elements of the hyoid arch and the branchial arches are shown in situ in Figure 50 and are illustrated independently in Figures 51 to 59.

The interhyals (ih, Fig. 57) never ossify in *Hiodon*, even in large adults. These small cartilages are positioned between the posterior ceratohyal and the preopercle, with which they articulate ventral to the hyomandibula.

Ossifications of the ventral hyoid arch consist of four paired chondral bones (anterior and posterior ceratohyals, dorsal and ventral hypohyals), a median chondral basihyal, and its associated dermal toothplate. The posterior ceratohyals (chp, Figs. 53–55 and 57) are flat, triangular elements that are slightly concave laterally. The lateral branchiostegals contact the ventral edge of the posterior ceratohyal. The anterior ceratohyals (cha, Figs. 53–55 and 57) are flattened, hourglass-shaped bones. The anterior ceratohyal supports most of the branchiostegals, which mostly lie on a ventral cartilaginous ridge (Fig. 57). There is no ceratohyal foramen (G. J. Nelson, 1968c; = beryciform foramen of McAllister, 1968) in the hyoid bones of *Hiodon*.

Two paired hypohyals (dorsal and ventral) are characteristic of teleosts, and possibly some specimens of *Amia calva* (Arratia & Schultze, 1990: fig. 2b), although this was not confirmed by Grande and Bemis (1998: 101). Many teleosts have a single ossified hypohyal secondarily (e.g., the notopterid *Chitala*, UMA F10349). In *Hiodon*, both the dorsal and ventral hypohyals (hhd and hhv, respectively) are irregularly shaped nodules of bone (Figs. 54 and 55) that ossify in a single cartilaginous element (Fig. 57). The ventral hypohyal was ossified in a 22 mm SL specimen of *H. tergisus* (JFBM 22747B) and the smallest available specimen of *H. alosoides* (24 mm SL; TU 113117E), and ossifies before the dorsal hypohyal in both species. The dorsal hypohyal ossifies by 38 mm SL in *H. tergisus* (TU 108166E)[1] and 30 mm SL in *H. alosoides* (TU 108118A). Both the dorsal and ventral hypohyals first form perichondrally along the margins of the cartilaginous element (Fig. 23B), and then grow endochondrally toward one another (Fig. 57) until they meet, as in the adult (Figs. 54 and 55). The foramen for the hyoidean artery is positioned between the dorsal and ventral hypohyals, so that both elements contribute to its formation (Fig. 23B). The hyoidean artery exits the dorsal hypohyal through a foramen on the lateral face of the bone (Figs. 54 and 55); medially, both elements contribute to the

[1] The dorsal hypohyal was not present in a 28 mm SL specimen (JFBM 22747C), and this specimen (TU 108166E) is my next largest. The dorsal hypohyal is well-developed in this specimen; future study will undoubtedly find that this element develops earlier.

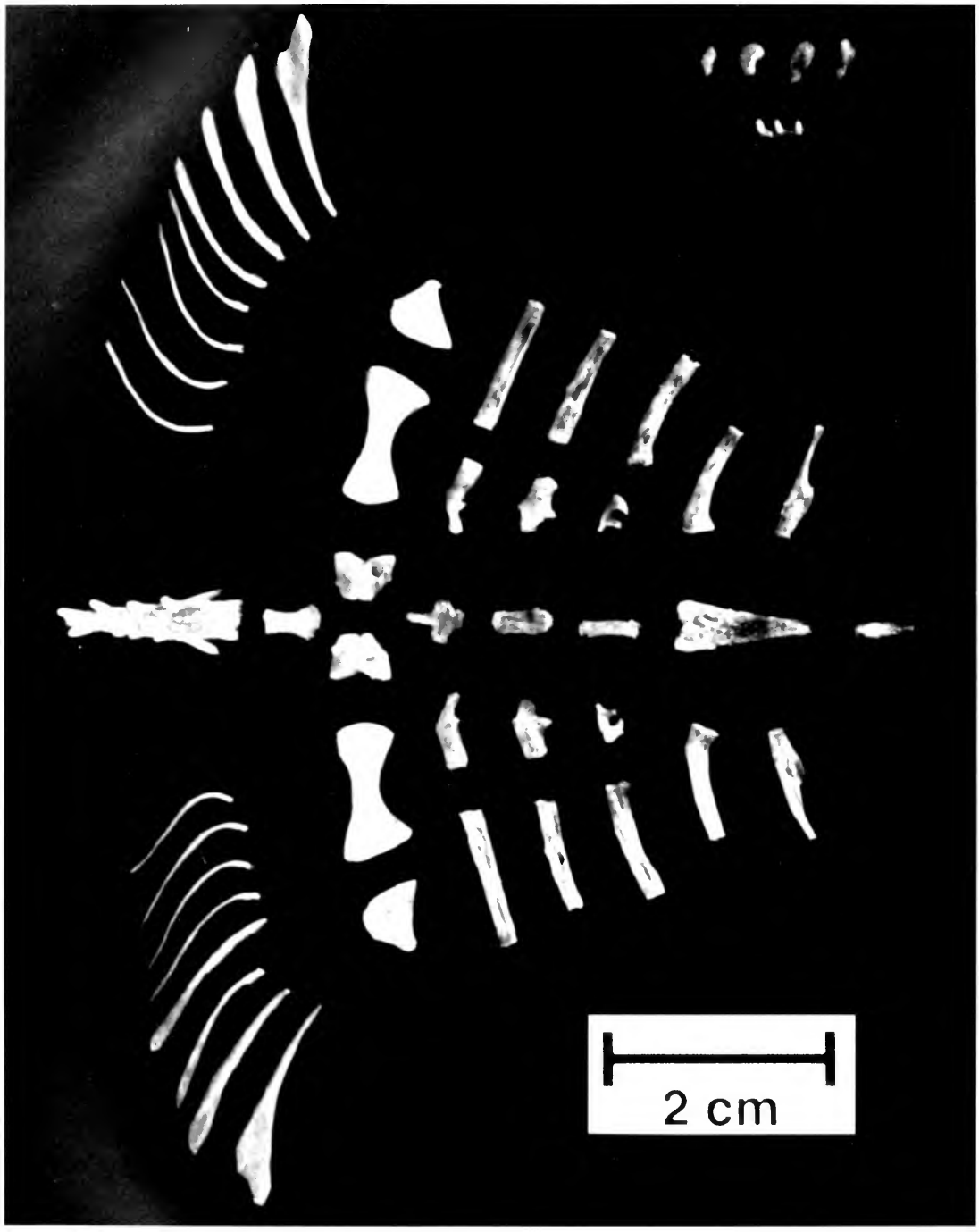

Fig. 54. *Hiodon alosoides*, photograph of disarticulated bones of ventral gill arches of an adult (UMMZ 210587, 272 mm SL, female) in dorsal (= oral) view. Anterior and posterior ceratohyals and dorsal and ventral hypohyals are seen in lateral view. The fourth basibranchial is entirely cartilaginous and was not preserved. Representative isolated gill rakers are from the anterior (top row) and posterior (bottom row) of the gill arch. Anterior faces left.

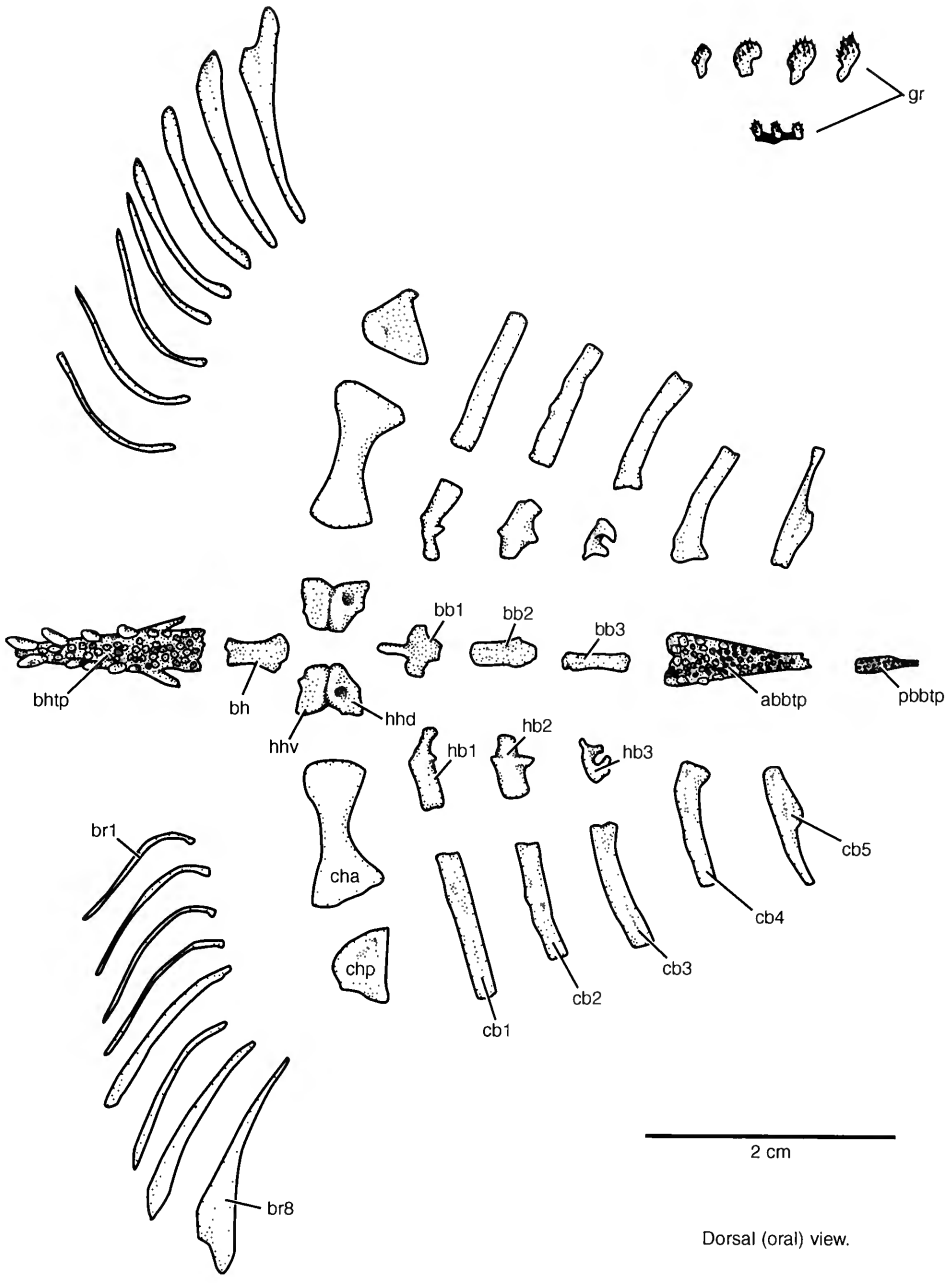

FIG. 55. *Hiodon alosoides*, line drawing of Figure 54.

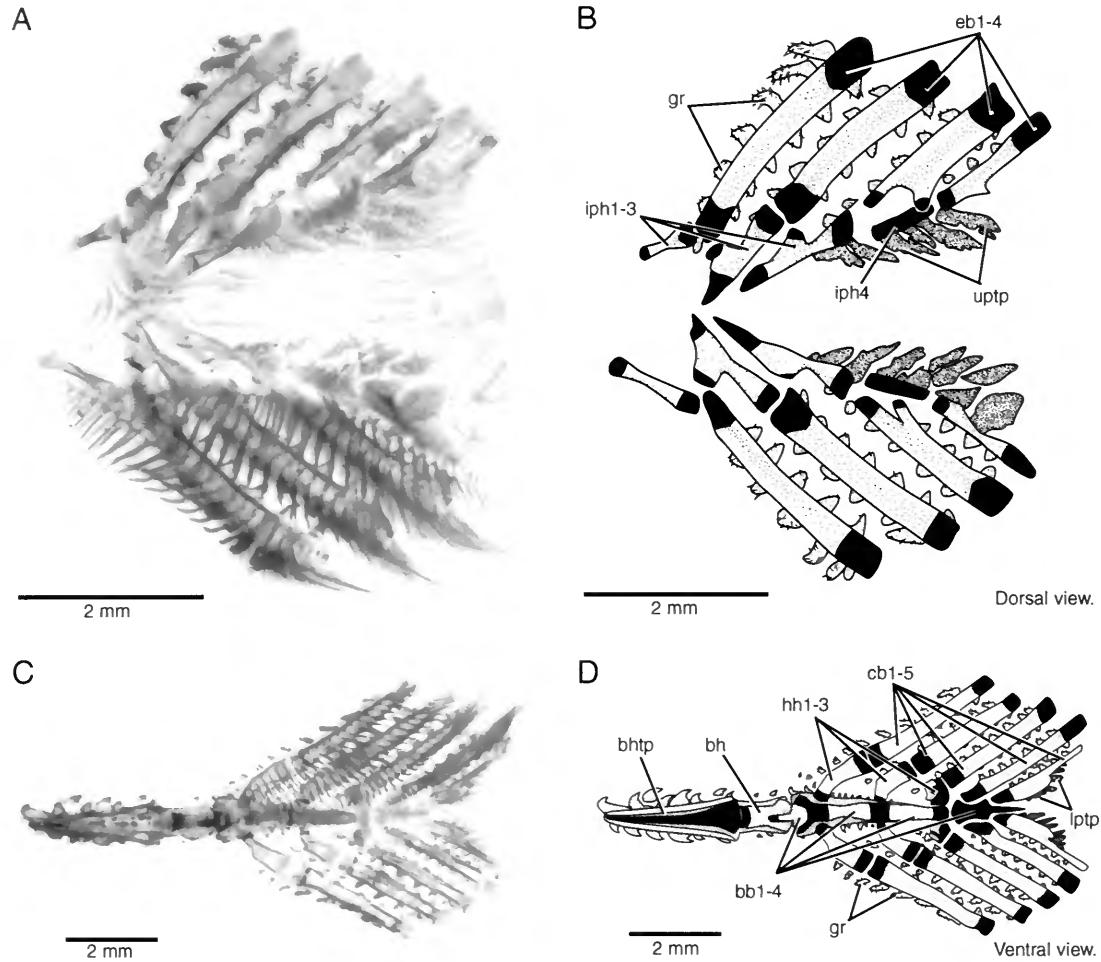

FIG. 56. *Hiodon alosoides*. **A** and **C**, Photographs, and **B** and **D**, line drawings of cleared and stained gill arches of a juvenile (UMA F10597, 62 mm SL). A and B show dorsal portion of gill arches in dorsal view. C and D show ventral portion of gill arches in ventral view. Anterior faces left.

foramen. The trajectory of the hyoidean artery through the hypohyals was discussed by Arratia and Schultze (1990), and the condition in which it pierces both hypohyals, as in *Hiodon*, was considered to be a synapomorphy for extant teleosts by Arratia (1999: character 61). In *Hiodon*, the ventral hypohyals serve as the attachment site for ligaments originating from the urohyal.

The basihyal in *Hiodon* (bh, Figs. 54–56) is a well-developed, hourglass-shaped median element sandwiched between a dermal toothplate dorsally and the hypohyals ventrally. A cartilaginous anterior extension of the basihyal runs to the tip of the basihyal toothplate (Figs. 53 and 56C, D) and is never ossified. The dermal basihyal toothplate (bhtp, Figs. 53–56) is a robust element that bears greatly enlarged, curved caniniform teeth, particularly around the edges of the toothplate (the medial teeth are smaller, although they are still curved and caniniform). The bone of the basihyal toothplate extends far anterior to the ossified portion of the basihyal. This toothplate is uniquely shaped in that it possesses ventrally directed "wings" on the posterolateral corners (= posteroventral processes of G. J. Nelson, 1968a) that wrap around the lateral surfaces of the basihyal. This shape led Nelson (1968a) to comment on the overall similarity of the basihyal toothplate of *Hiodon* to that of the notopterids. Within the genus *Hiodon* there is a great difference in the pro-

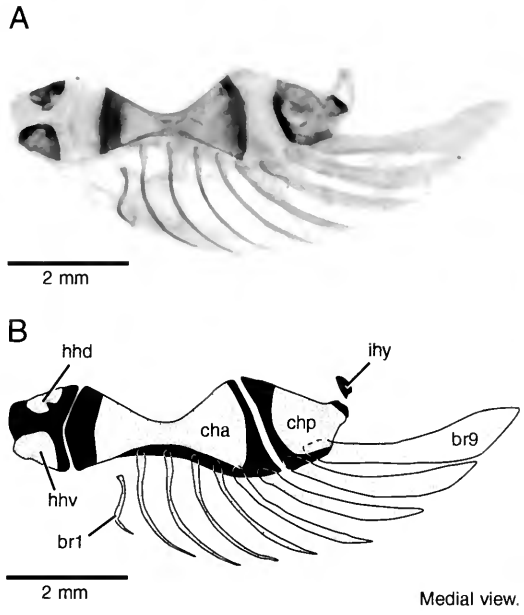

FIG. 57. *Hiodon alosoides*. **A**, Photograph, and **B**, line drawing of cleared and stained right ventral portion of hyoid arch and branchiostegals of a juvenile (UMA F10597, 62 mm SL) in medial view. Anterior faces left.

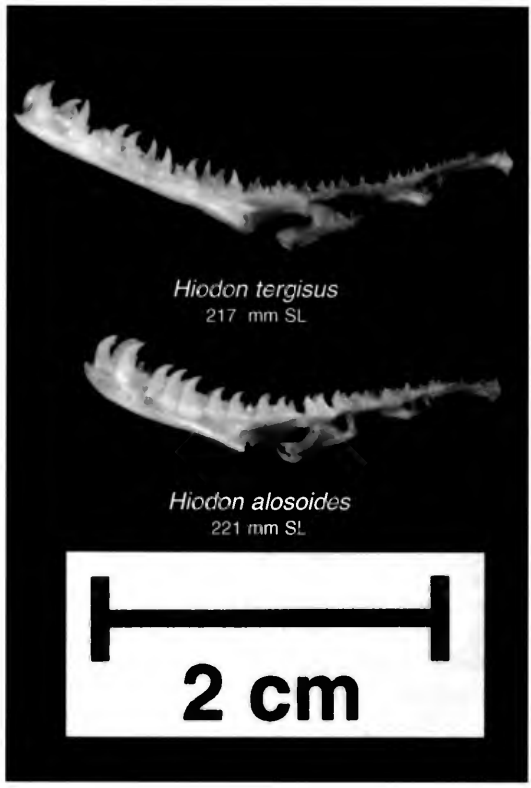

FIG. 58. Basihyal and basibranchial series of *Hiodon tergisus* (UMA F10607, 217 mm SL, male) and *H. alosoides* (UMA F10590, 221 mm SL, male) in lateral view showing variation in the length of the basihyal toothplate. Note that the shorter toothplate is from the slightly longer specimen. Anterior faces left.

portions of the basihyal toothplate (Fig. 58). In adult *H. tergisus,* the basihyal toothplate averages about 70% the length of the lower jaw, whereas that of *H. alosoides* is about 53% the length of the lower jaw in adults (Table 8); this difference is seen in all stages of ontogeny (Tables 6 and 7), but is most striking in adult specimens. In †*H. consteniorum,* the basihyal toothplate is exposed in its entire length only in UALVP 38875, and is approximately 60% the length of the lower jaw. This specimen, despite its small size (61 mm SL), is hypothesized to be an adult, based on the presence of a modified anal fin, as is found in mature males of extant *Hiodon* (Li & Wilson, 1994). In two specimens of †*Eohiodon falcatus* (FMNH PF10637, UMA F10614) in which the basihyal toothplate is exposed, it averages 49% the length of the lower jaw (50% and 48%, respectively). Thus, †*H. consteniorum* shows an intermediate state between *H. alosoides* and *H. tergisus.*

The urohyal (Fig. 59) is a small element that forms in the anterior ligamentous sheath of the sternohyoideus muscle. The left and right portions of this muscle insert on either side of a medial wall of bone on the posterior portion of the urohyal. The anterior part of the urohyal is irregularly shaped and serves as an origin for the ligaments that insert onto the ventral hypohyals. Within teleosts, Arratia and Schultze (1990), following Patterson (1977a), distinguish between the element found in †pholidophorids and all other teleosts. The "†pholidophorid urohyal" appears to be a fusion between a dorsal membrane bone and a ventral dermal denticulate plate. In contrast, the urohyal of all other teleosts is only a membrane-bone element (Patterson, 1977a).

The basibranchial series consists of four elements that form in the midline of the gill arches. The anterior three elements (bb1–3, Figs. 53–56) are simple bony elements that ossify within a single anterior copula (= copula 1–3 of G. J. Nelson, 1969b; Fig. 56C, D). The fourth basibranchial (bb4, Figs. 53 and 56), which is a separate copula (= copula 4–5 of G. J. Nelson, 1969b), remains cartilaginous throughout ontogeny. The first basibranchial (bb1) of *Hiodon* is obliquely posi-

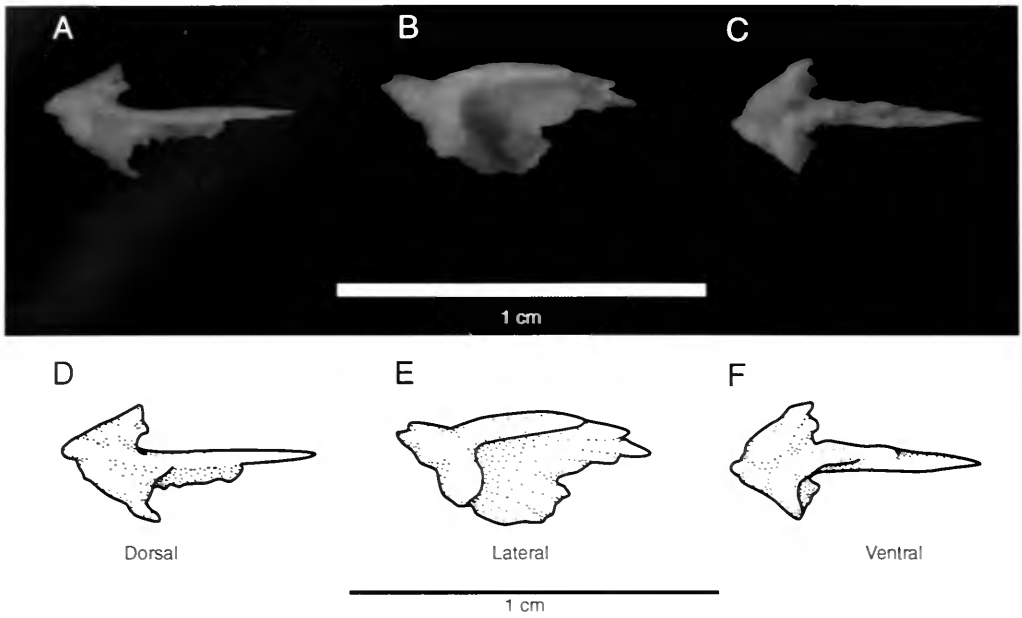

FIG. 59. *Hiodon alosoides*. **A–C**, Photographs, and **D–F**, line drawings of urohyal of an adult (UMA F10591, 280 mm SL, female) in dorsal (A and D), lateral (B and E), and ventral (C and F) views. Anterior faces left.

tioned, such that its anterior end is ventral to the basihyal and is positioned partially between the hypohyals (Fig. 23B). The fourth basibranchial bears an elongate posterior extension, which I also observed in other osteoglossomorphs, including *Chitala* and *Osteoglossum* (see G. J. Nelson, 1968a). All basibranchial elements are associated with dermal toothplates along their dorsal surface. A single anterior basibranchial toothplate covers bb1–3 (abbtp, Figs. 53A, B, 54, and 55), and even in the smallest specimens examined, this toothplate was well-developed and present as a single element. In previous descriptions (e.g., G. J. Nelson, 1968a: Taverne, 1977), this anterior basibranchial toothplate has been labeled as "B1P+B2P+B3P" (e.g., G. J. Nelson, 1968a: fig. 2). Based on the text description ("dermal tooth plate overlying basibranchials 1–3"; G. J. Nelson, 1968a: 263), such terminology reflects a positional description rather than any specific opinion about homology of the toothplate (i.e., a hypothesis of fusion of three individual toothplates). The teeth of the anterior basibranchial toothplate are conical or slightly recurved, and are largest anteriorly where the toothplate abuts the posterior edge of the basihyal toothplate. One or more toothplates are associated with bb4 (pbbtp, Figs. 53A, B, 54, and 55). The number and pattern of the posterior basibranchial toothplates, described by Taverne (1979: 59) as "une série de petites plaquette denticulées formant un dermobasibranchial du quatrième arc," are variable, although they always are separate from the anterior basibranchial toothplate. The posterior basibranchial toothplates bear a shagreen of small conical teeth. Both the anterior and posterior basibranchial toothplates are closely associated with, but never fused to, the underlying basibranchials (see Patterson & Rosen, 1977: 118).

The hypobranchial series is composed of elements in the three anteriormost gill arches (hb1–3, Figs. 53–56). Each of these elements bears a finger of bone on its anterior end which serve as attachment sites for interarcual ligaments; these are most pronounced on the third hypobranchial (hb3, Fig. 55). The distal ends of the hypobranchials support gill lamellae, and their ventral surfaces are concave to receive the afferent and efferent branchial aortae.

The five ceratobranchials (cb1–5, Figs. 53–56) are the longest elements of the ventral gill arch skeleton. Each has a concave ventral surface, and all but the fifth support gill lamellae. The fifth ceratobranchial (cb5, Fig. 55) bears a medial flange.

The dorsal branchial arches of *Hiodon* are il-

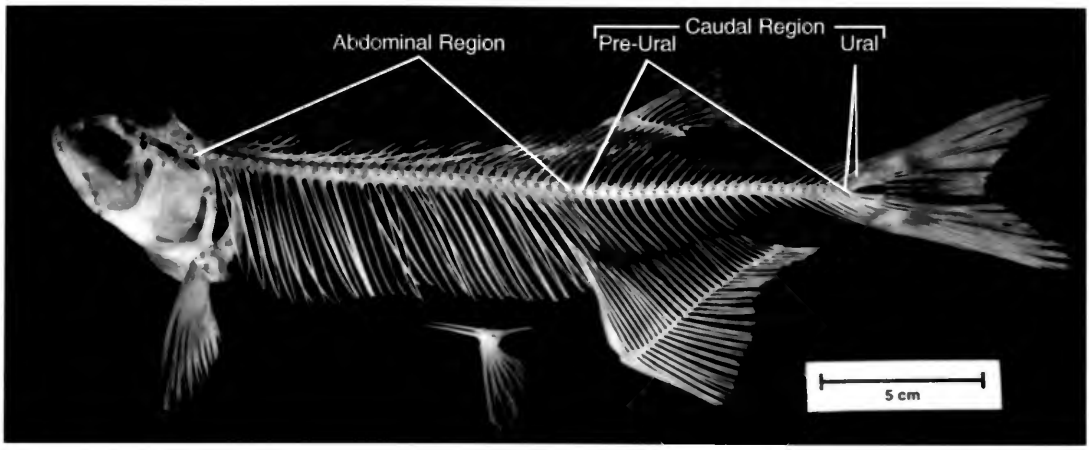

FIG. 60. Complete skeleton of *Hiodon alosoides* (UMA F10150, 293 mm SL, female) showing the different regions of the postcranial skeleton.

lustrated in Figures 51, 52, and 56A and B. This series of elements is composed of four pairs of infrapharyngobranchials and epibranchials; all but the fourth infrapharyngobranchials (iph4, Fig. 56A, B) are ossified. The anterior two epibranchials (eb1–2, Figs. 51 and 52) are relatively simple bars of bone. The third epibranchial (eb3, Figs. 51 and 52) possesses an uncinate process, which lies dorsal to iph4 (Fig. 56A, B). In the adult, the fourth epibranchial (eb4, Figs. 51 and 52) is fan-shaped (not seen in Fig. 56 because of its position) and bears a slight dorsal concavity.

The first infrapharyngobranchial (iph1, Figs. 51 and 52) is a slender rod that distally contacts the anterior corner of epibranchial one and proximally extends farthest dorsally of all the branchial arch bones (Fig. 50). These elements articulate with the neurocranium in a small fossa on the prootic and are the only gill arch to contact the neurocranium. Arratia (1999) noted that in all taxa she examined, iph1 contacts the prootic (as well as the parasphenoid in *Amia* and elopomorphs). Each of the other two ossified infrapharyngobranchials (iph2 and iph3) is in series with the epibranchial of its arch, but also possesses an uncinate process associated with the epibranchial of the next anterior arch (Figs. 51 and 56A, B). The fourth infrapharyngobranchial (iph4, Fig. 56A, B) is a simple cartilaginous bar.

Gill rakers (gr, Figs. 51 and 53–56) line the leading (= anterior) and trailing (= posterior) edges of all branchial arches and are associated with all branchial elements except the first infrapharyngobranchials (Figs. 51 and 56A, B). All gill rakers are covered with small denticles, are similar in form within a series (i.e., leading or trailing edge), and are evenly distributed along the arch. The gill rakers of the leading edges of the gill arch element are larger than those of the posterior edges. The posterior branchial arches support a variable number and pattern of pharyngeal toothplates. The upper pharyngeal toothplates (uptp, Figs. 51 and 56A, B) are supported by iph3, iph4, and eb4 (iph2 supports only gill rakers). The lower pharyngeal toothplates (lptp, Figs. 53 and 56C, D) are supported only by cb5.

Vertebral Column

Following the terminology of Grande and Bemis (1998), a vertebra is composed of a single centrum and all associated elements (e.g., neural arches, pleural ribs, intermuscular bones, and haemal arches). In a more general sense, a vertebra should also be considered to include the ligaments of the myosepta (Baudelot, 1868, cited and discussed by Patterson & Johnson, 1995). However, only those elements that are ossified are described here. Elements of the preural vertebral column are illustrated in Figures 60 to 76 and meristic data are given in Tables 9 through 12. Regions of the postcranial skeleton are illustrated in Figure 60.

The centra (c, Fig. 61) of *Hiodon,* and teleostean fishes in general, are amphicoelous. In adult *Hiodon,* the notochord is strongly constricted, although it persists into the adult stage and is continuous along the length of the body through a

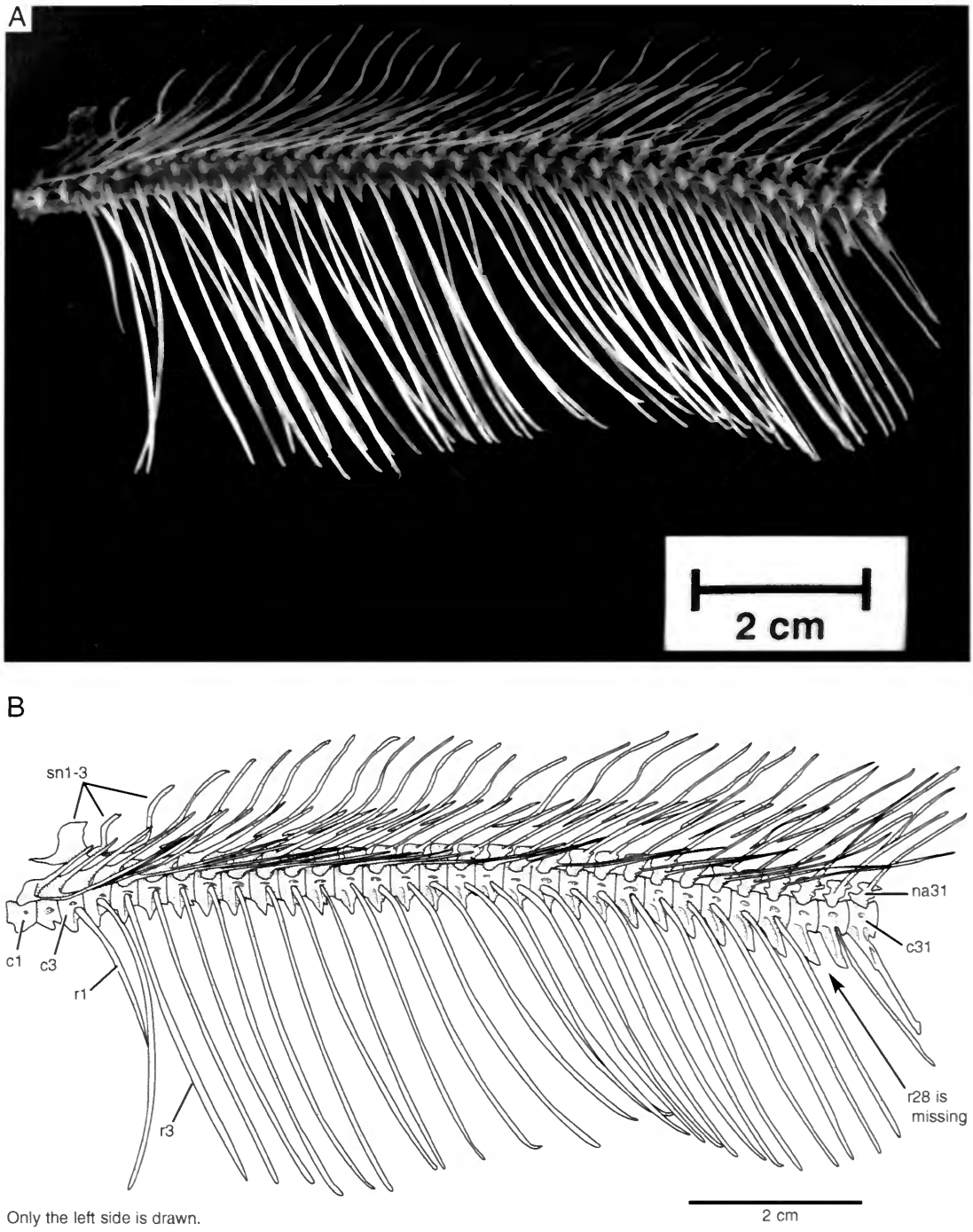

FIG. 61. *Hiodon alosoides*. **A**, Photograph, and **B**, line drawing of abdominal region of the vertebral column of an adult (UMA F10588, 252 mm SL, male) in lateral view. Anterior faces left.

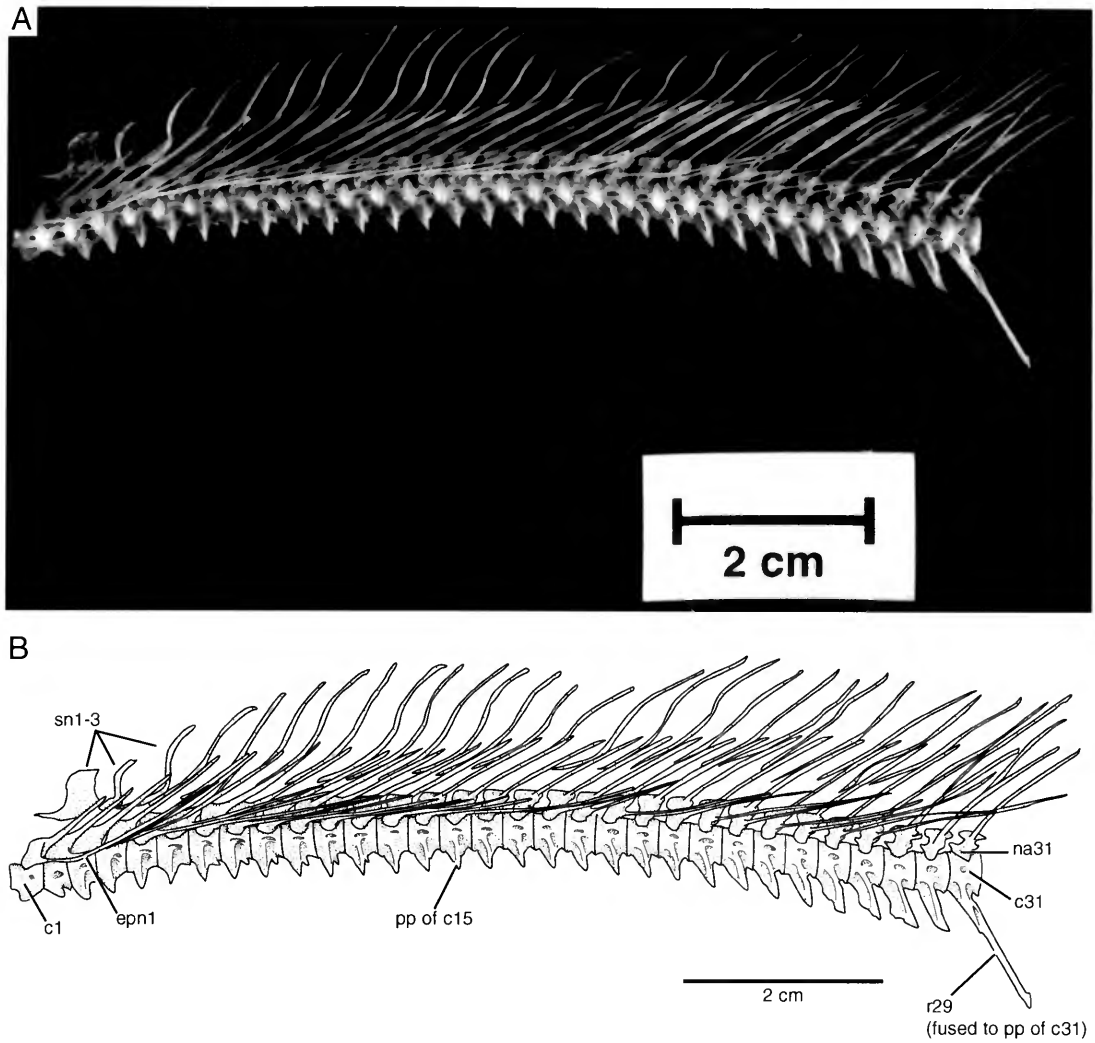

FIG. 62. *Hiodon alosoides*. **A**, Photograph, and **B**, line drawing of abdominal region of the vertebral column of an adult (UMA F10588, 252 mm SL, male) in lateral view; ribs have been removed. Anterior faces left.

notochordal foramen in the center of the centra (ncf, Fig. 64). Early ossification of the centra could not be observed with my material of *H. alosoides,* although in the smallest individuals examined the more posterior centra were more fully developed than the anterior centra. In small individuals of *H. tergisus* (e.g., JFBM 22746, 23 mm SL), the only two centra that have started to form are the most anterior centrum (c1) and the second ural centrum (u2). In specimens larger than 23 mm SL, the anterior centra are very slender rings of bone (the chordacentra), and more posteriorly there are small patches of bone in the ventral midline of the centra. There is no sign of ossification in the dorsal portion of these centra, which suggests that the chordacentrum of each centrum develops in a ventral to dorsal direction, as was also suggested by Schultze and Arratia (1988). In these small stages, separate cartilaginous basidorsal and basiventral elements (= arcualia) are present. The centra of adults are longitudinally oriented cylinders with two or three deep furrows on their lateral surface. The space within these furrows is filled in life with adipose tissue. In *H. alosoides,* there is a prominent longitudinal slit in the ventral surface of the centra (cg, Fig. 63E, F). When present in *H. tergisus,* this slit was well-developed only in the caudal centra.

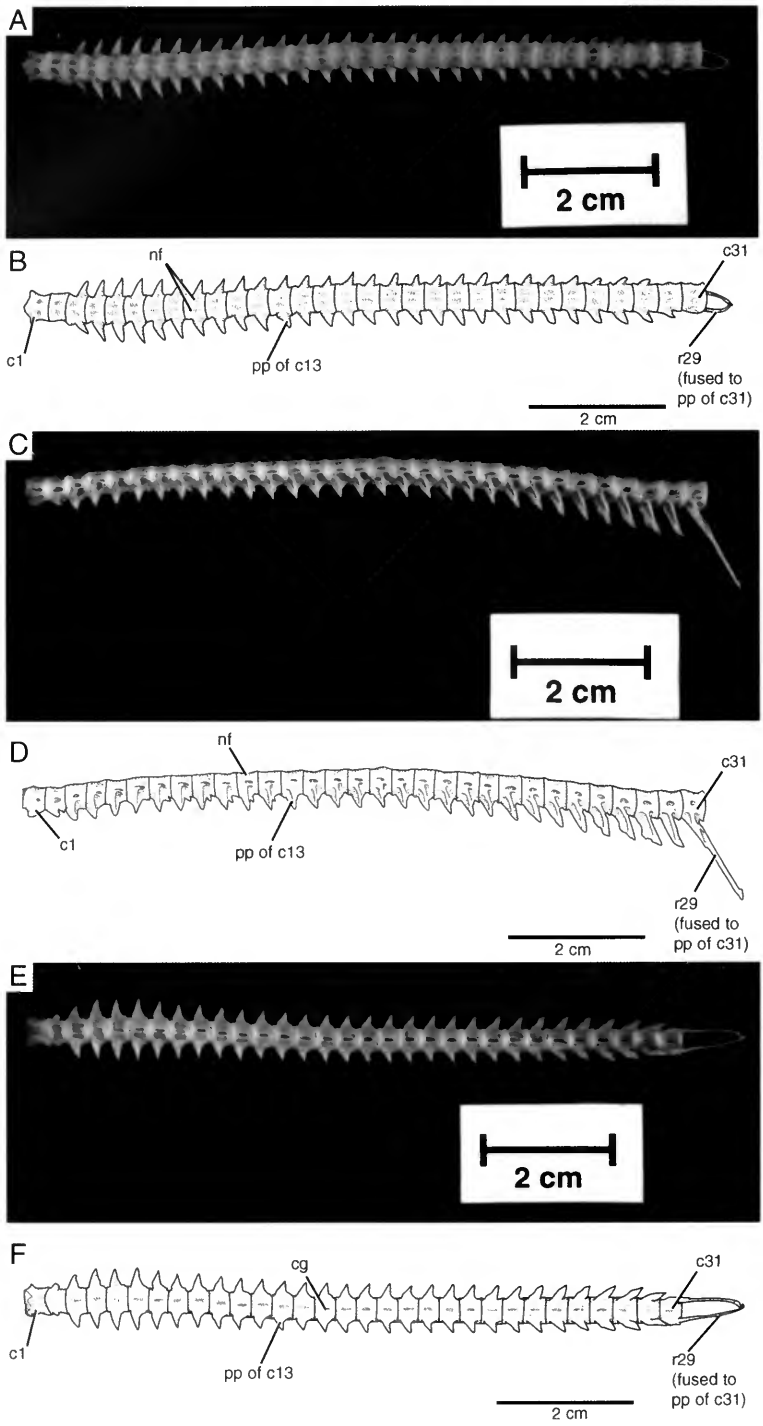

FIG. 63. *Hiodon alosoides*. **A**, **C**, and **E**, photographs, and **B**, **D**, and **F**, line drawings of abdominal vertebral column of an adult (UMA F10588, 252 mm SL, male) in dorsal (A and B), lateral (C and D), and ventral (E and F) views. Ribs, neural arches, and epineural bones have been removed. Anterior faces left.

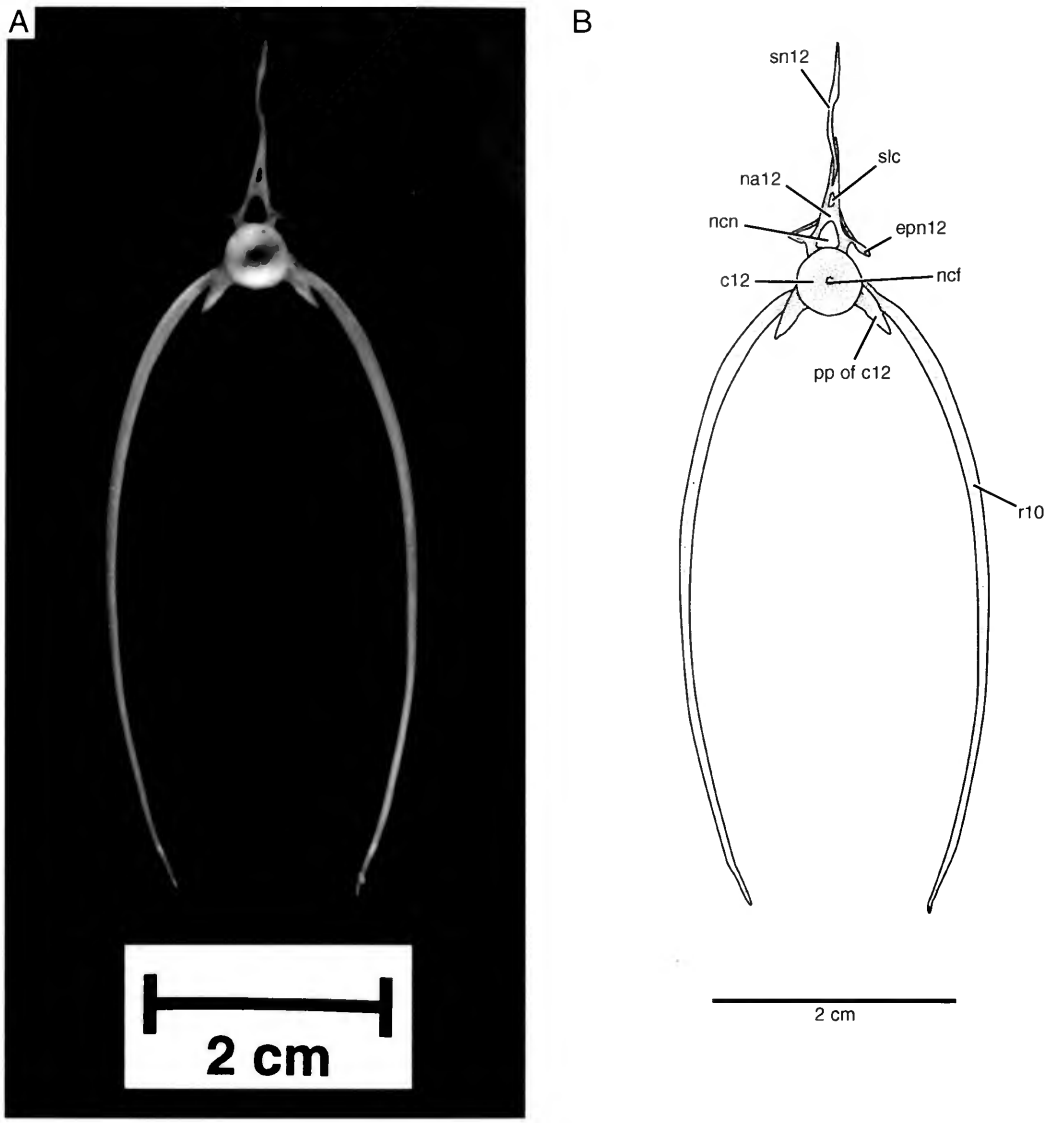

FIG. 64. *Hiodon alosoides*. **A**, Photograph, and **B**, line drawing of isolated abdominal vertebra (vertebra 12) of an adult (UMA F10338, 255 mm SL, female) in anterior view.

The dorsal surfaces of abdominal centra bear paired neural facets (nf, Fig. 63A–D), which mark the point of contact between the basidorsal portion of the neural arches and the centra. Grande and Bemis (1998) defined the neural arch as the elongation of the basidorsal arcualia that meet and possibly fuse along the midline. The distal elongation of the neural arch forms the neural spine. Those neural arches that do fuse in the midline are termed median neural spines (Grande & Bemis, 1998) and in *Hiodon* are almost exclusively limited to the caudal region (a few may be found in the posterior abdominal region). In *Hiodon*, neural arches are associated with the dorsal surfaces of all centra except the second ural centrum. The neural arches of most abdominal vertebrae remain autogenous, whereas those of the preural caudal centra are fused to the centra in the adult.

Among living actinopterygians, ossified intermuscular elements are found only in teleosts, and the condition found in *Hiodon* is considered plesiomorphic for extant teleosts (Patterson & John-

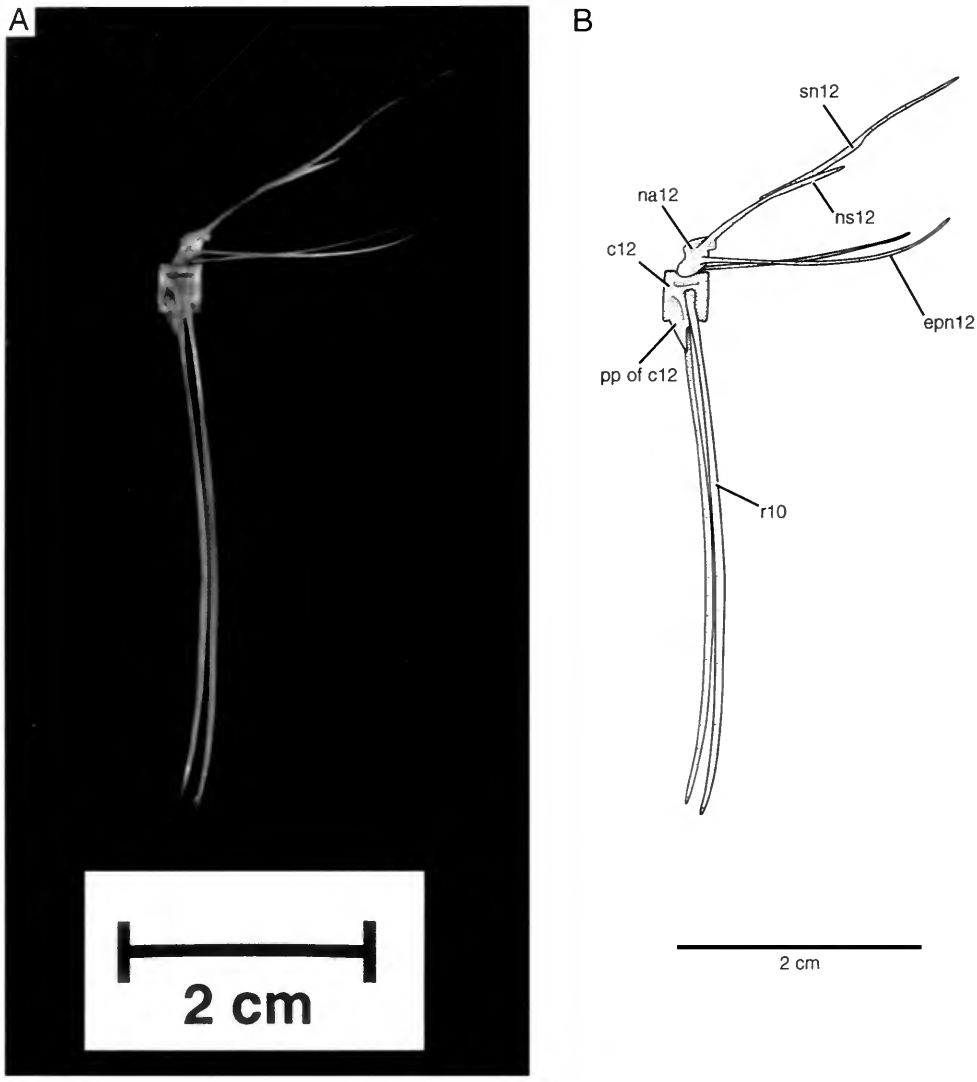

FIG. 65. *Hiodon alosoides*. **A**, Photograph, and **B**, line drawing of isolated abdominal vertebra (vertebra 12) of an adult (UMA F10338, 255 mm SL, female) in lateral view. Anterior faces left.

son, 1995). A series of epineural bones (epn, Figs. 62, 64, and 65) develops in ligaments attached to the bases of the neural arches. In small specimens of *Hiodon*, only the base of each ligament (i.e., where it attaches to the neural arch) is ossified. This suggests a proximal to distal direction of ossification of each epineural bone, but more material should be examined to confirm the pattern of ossification of epineurals. Generally, epineurals are present on the neural arches of the abdominal vertebrae, although considerable variation, including bilateral asymmetry, was observed regarding the number of epineurals (Tables 11 and 12). Patterson and Johnson (1995) discovered that the epineural series of bones in *Hiodon* continues as unossified ligaments into the caudal region. They also noted that epipleural (attached to the ribs) and epicentral (attached to the centra) ligaments are present.

The parapophyses (pp, Figs. 62–65) are defined as the ossifications of the basiventral arcualia in the abdominal region. The anterior parapophyses project transversely from the centra, but gradually shift their orientation to become more vertically

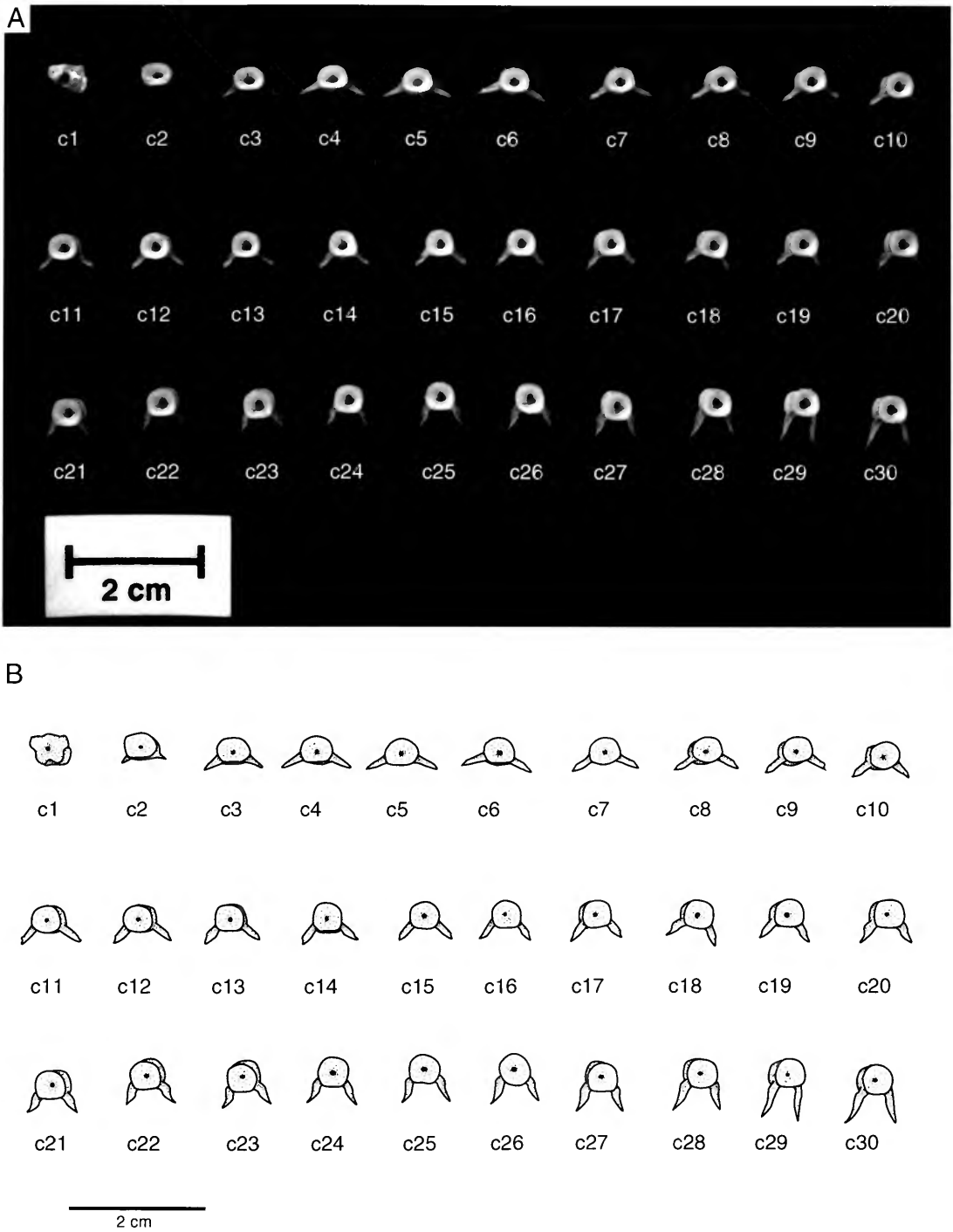

FIG. 66. *Hiodon alosoides*. **A**, Photograph, and **B**, line drawing of isolated abdominal centra of an adult (UMA F10586, 273 mm SL, female) in anterior view.

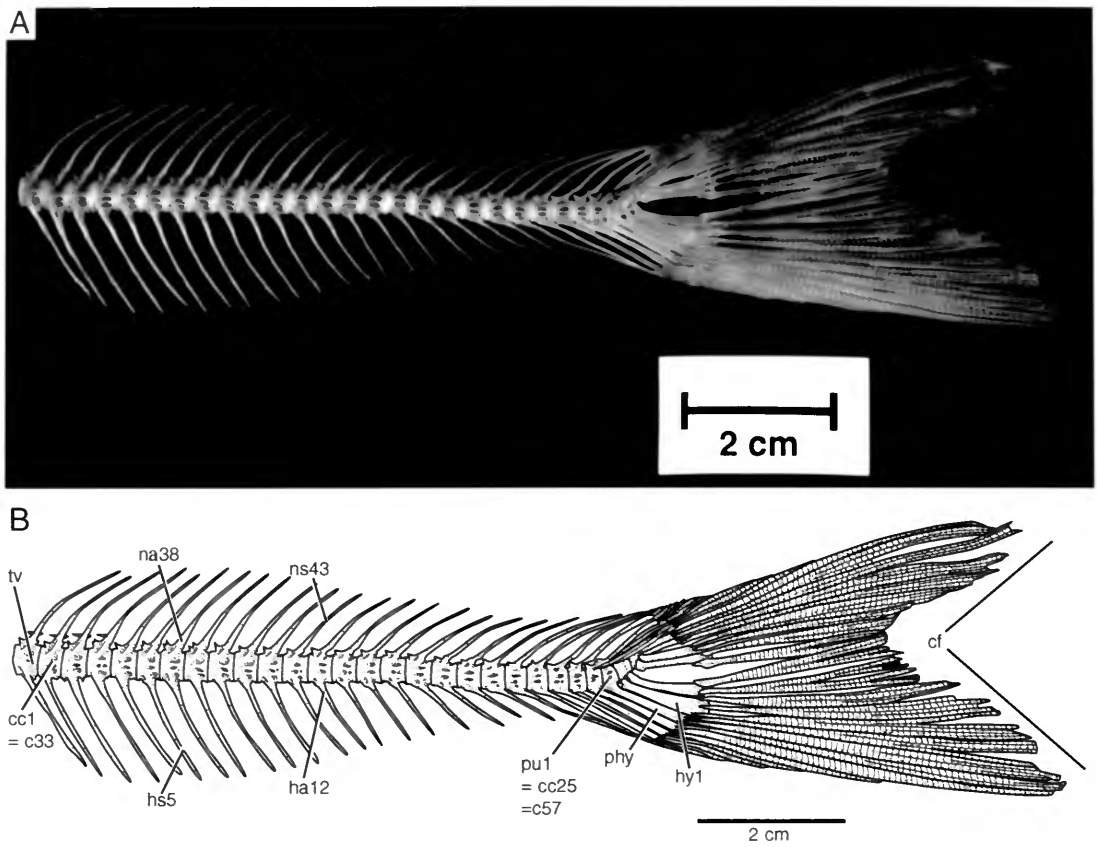

FIG. 67. *Hiodon alosoides*. **A**, Photograph, and **B**, line drawing of caudal vertebral column and fin of an adult (UMA F10588, 252 mm SL, male) in lateral view. The first preural vertebral centrum (= c57 in this specimen) and parhypural are highlighted in blue. Anterior faces left.

oriented toward the posterior portion of the abdominal region (Fig. 66). The parapophyses and pleural ribs may fuse in posterior abdominal vertebrae. In such vertebrae it is difficult to delimit the parapophysis and rib (i.e., the vertebrae could be interpreted as possessing elongated parapophyses rather than parapophyses that are fused to ribs). Vertebrae that display such a condition are here termed transitional vertebrae (tv, Fig. 67) and are individually variable in number (Tables 9 and 10). Because the caudal region is defined as starting at the anteriormost centrum that bears a complete haemal arch, all transitional vertebrae are by definition abdominal vertebrae. In *Hiodon*, all haemal arches (ha, Figs. 67–69) are completely fused with the centra and bear elongations that are fused distally to form haemal spines (hs, Figs. 67–69).

Each vertebral segment anterior to the insertion of the dorsal fin bears a chondral supraneural (sn, Figs. 61 and 62). In some specimens (e.g., UMA F10613) the supraneural series extends posteriorly to end among the proximal radials of the dorsal fin (Fig. 70). The first supraneural lies anterior to the first neural arch, and the succeeding supraneurals are positioned alternately between two neural arches. For the most part, the supraneurals are slight, rodlike ossifications that form in cartilage in the median vertical septum. Most supraneurals possess a slight dorsal deflection or bend in the bone. A notable exception is the first supraneural (sn1, Figs. 61 and 62), which is bladelike and S-shaped. Although there is individual shape variation within this element, it never resembles the more posterior supraneurals. Li and Wilson (1999: character 67) described the anterior supraneurals of †*Tongxinichthys*, †*Jiuquangichthys*, and †*Kuyangichthys* as being dorsally broad and leaflike, and those of †*Kuntulunia* and †*Huashia* as being dorsally broad and platelike.

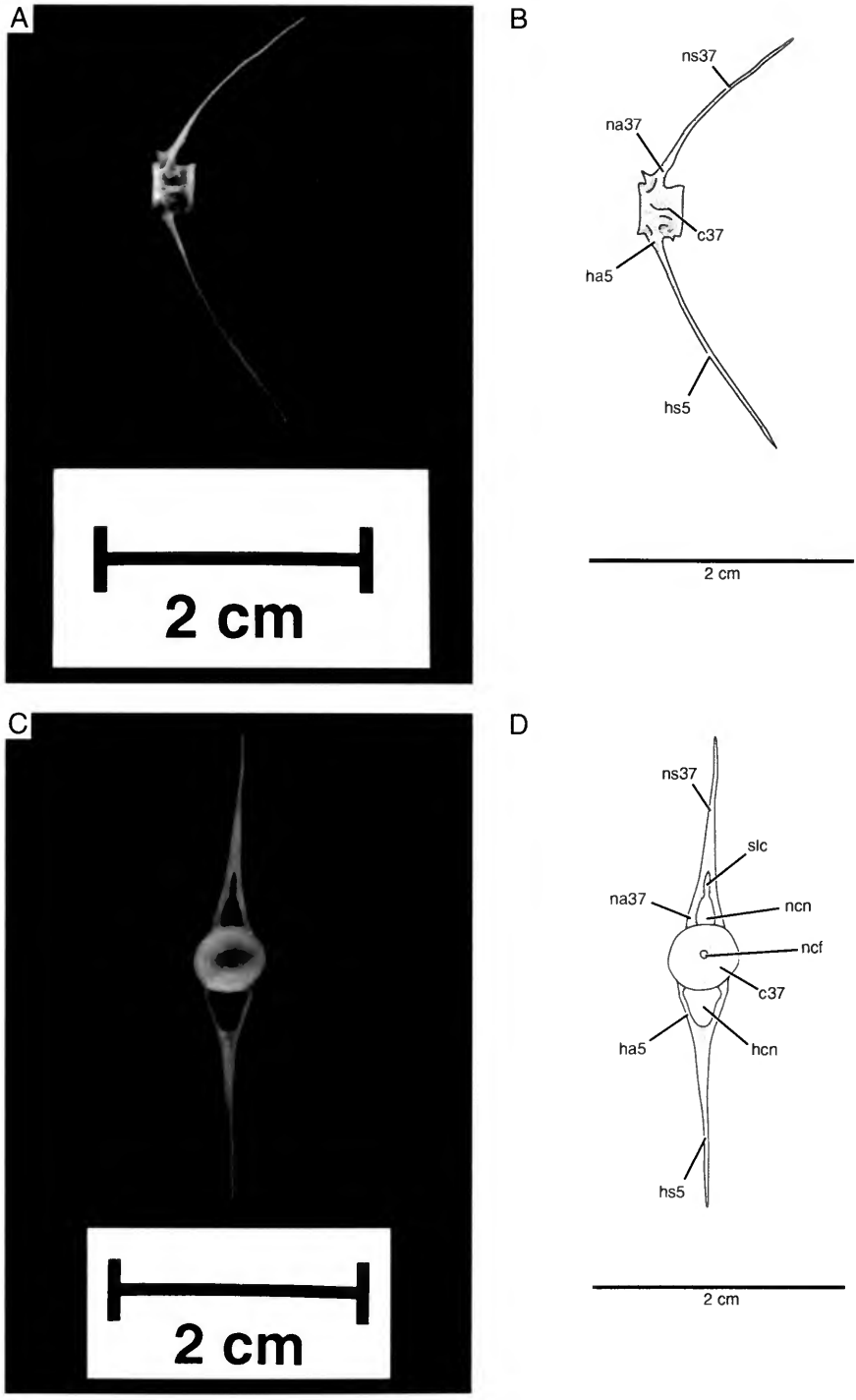

FIG. 68. *Hiodon alosoides*. **A** and **C**, Photographs, and **B** and **D**, line drawings of isolated caudal vertebra (vertebra 37) of an adult (UMA F10338, 255 mm SL, female) in lateral (A and B) and anterior (C and D) views. In A and B, anterior faces left.

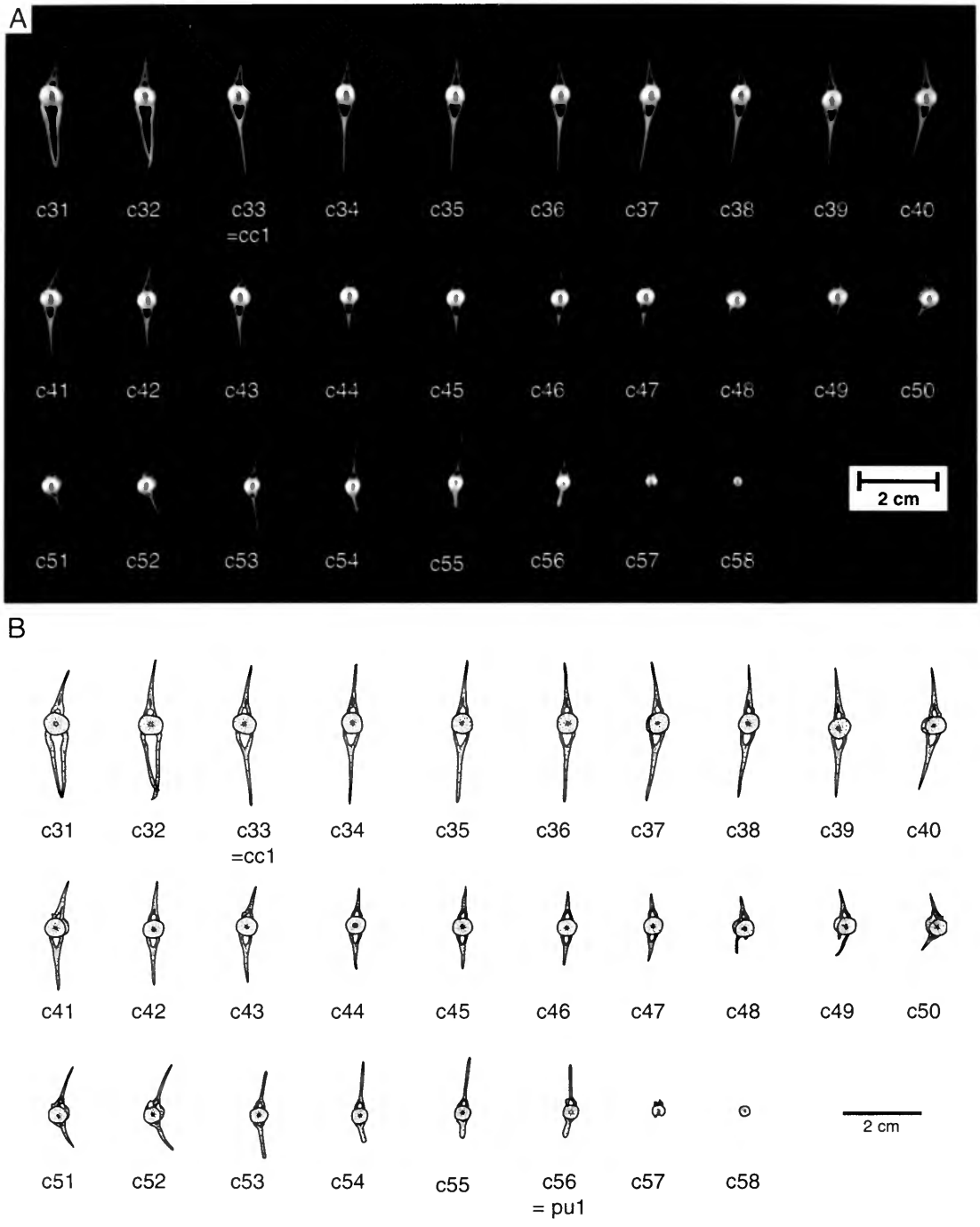

FIG. 69. *Hiodon alosoides*. **A**, Photograph, and **B**, line drawing of isolated caudal vertebrae of an adult (UMA F10586, 273 mm SL, female) in anterior view. Some centra (e.g., c49, c50, c51, c52) appear slightly laterally displaced because of the parallax of the camera lens; most centra were mounted at an angle to compensate for this effect. The first preural vertebral centrum (= c56 in this specimen) and parhypural are highlighted in blue.

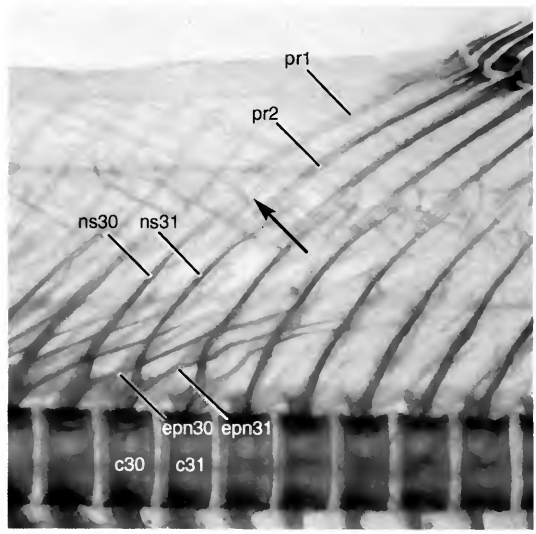

FIG. 70. *Hiodon tergisus*, photograph of cleared and stained juvenile (TU 113117B, 38 mm SL) in lateral view, showing the posteriormost supraneural (arrow) that lies between the anterior pterygiophores of the dorsal fin. Anterior faces left.

However, Li and Wilson (1999: 376) described *Hiodon* (among other taxa) as having anterior supraneurals that are "not different from the posterior ones in shape"; other taxa that have modified anterior supraneurals (e.g., *Elops*; UMA F10255; Forey, 1973) were similarly scored. While the anterior supraneurals in these taxa may not be similar to one another in shape, they are also not similar in shape to the more posterior supraneurals, so the definition or scoring of this character by Li and Wilson (1999) is in need of revision.

The slightly flattened proximal ends of the ribs (r, Fig. 61) loosely articulate with the centra in a deep socket just dorsal to the parapophyses (Fig. 65). All ribs are approximately the same length except for the anteriormost one, which is approximately half the length of the others (Fig. 61). The first rib articulates with the third vertebral centrum, a condition that is "remarkably constant in lower teleosts" (Patterson & Johnson, 1995: 19). The last pair of pleural ribs is variably fused to the parapophyses (e.g., Figs. 61–63), and this fusion was in some cases found to be bilaterally asymmetrical. The ribs are preformed in cartilage and appear to ossify proximally to distally along their length, although a cartilaginous distal tip persists into the adult.

Caudal Fin and Supports

The caudal skeleton of *Hiodon* has previously been illustrated by Gosline (1960: fig. 4), Patterson (1968: fig. 11), Monod (1968: fig. 108*bis.* and *ter.*), Greenwood (1970: fig. 8), Taverne (1977: figs. 26 and 27), Li and Wilson (1994: figs. 3 and 4), and Li, Wilson, and Grande (1997: fig. 5-2). The development and morphology of the caudal skeleton of *Hiodon* were described in detail by Schultze and Arratia (1988: figs. 1–13; see also Schultze & Arratia, 1989). The caudal fin and supporting skeleton are illustrated in Figures 71 to 76; meristic data and measurements for this region are presented in Tables 13 to 16. Portions of the caudal fin and skeleton (e.g., hypurals) have begun to ossify in the smallest individuals examined in the present study (e.g., Fig. 74A, B). Caudal fin rays are supported by all hypural elements, as well as the epural and the neural and haemal arches of the first five preural caudal vertebrae (Fig. 71). Eighteen principal caudal fin rays was considered by Patterson and Rosen (1977) to be a synapomorphy of Osteoglossomorpha (this corresponds to 16 branched plus two unbranched principal caudal fin rays, Fig. 71). In one of his specimens of *H. tergisus*, Monod (1968) found only 15 branched caudal fin rays (eight in the dorsal lobe and seven in the ventral lobe). The ventral

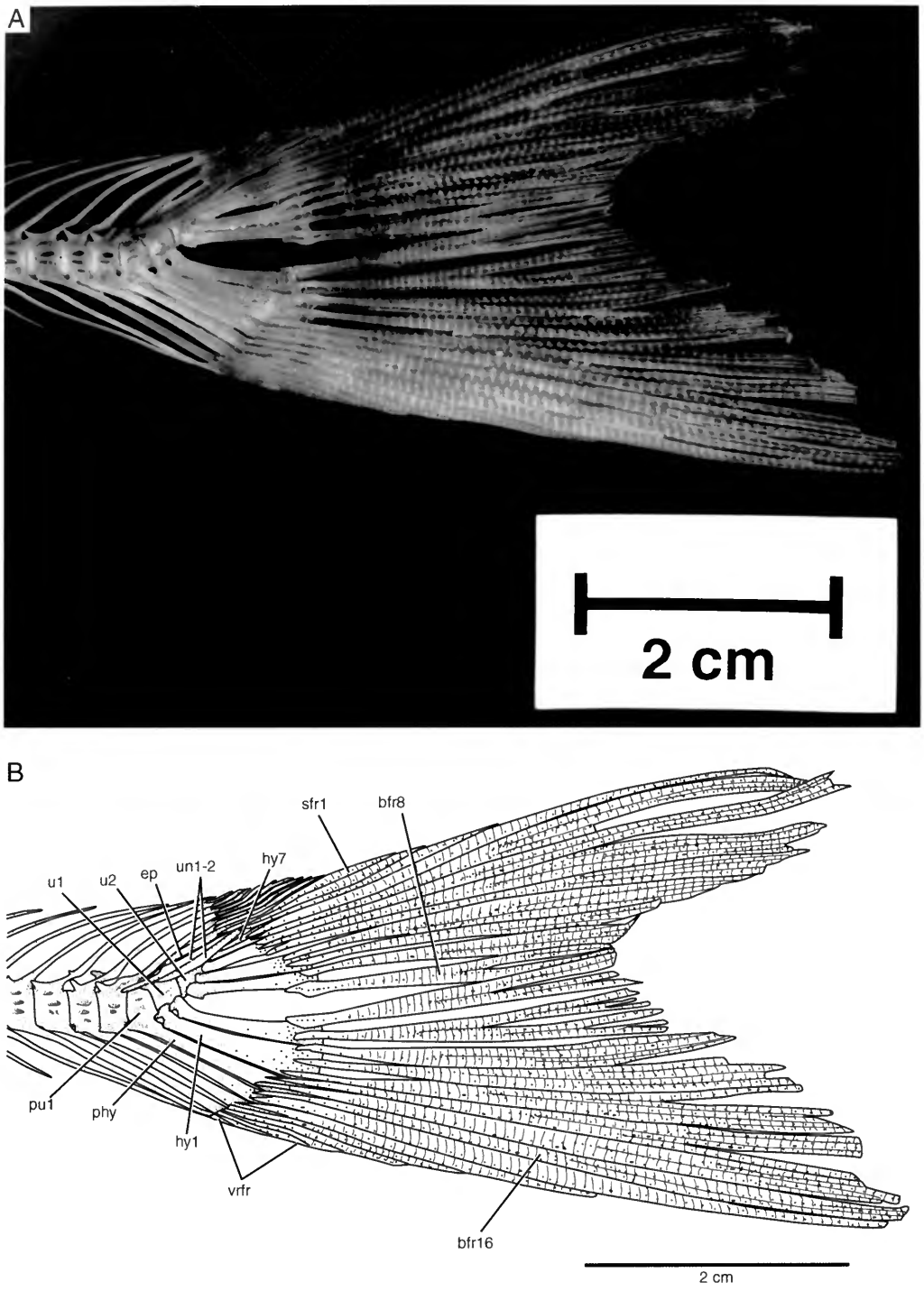

FIG. 71. *Hiodon alosoides*. **A**, Photograph, and **B**, line drawing of posterior caudal region of vertebral column and caudal fin of an adult (UMA F10588, 252 mm SL, male) in lateral view. The first preural vertebral centrum (= c57 in this specimen) and parhypural are highlighted in blue. Anterior faces left.

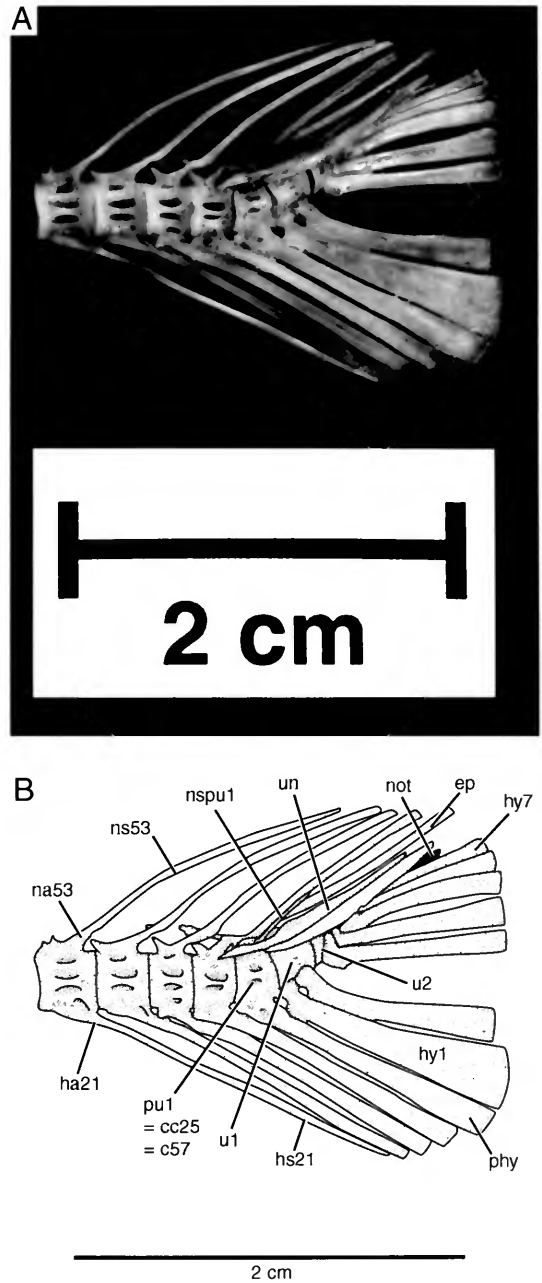

FIG. 72. *Hiodon alosoides.* **A**, Photograph, and **B**, line drawing of posterior caudal region of an adult (UMA F10588, 252 mm SL, male) in lateral view. The first preural vertebral centrum (= c57 in this specimen) and parhypural are highlighted in blue. Anterior faces left.

lobe of the caudal fin is supported by elements anterior to and including hypural 2. The ventral lobe of the caudal fin is generally longer than the dorsal lobe (Tables 13 and 14).

In *Hiodon,* two centra support hypural elements and are defined as ural centra (u1, u2; Figs. 71 and 72). Schultze and Arratia (1988) suggested that the more anterior of these represents two ontogenetically fused centra and the more posterior represents three ontogenetically fused centra (in

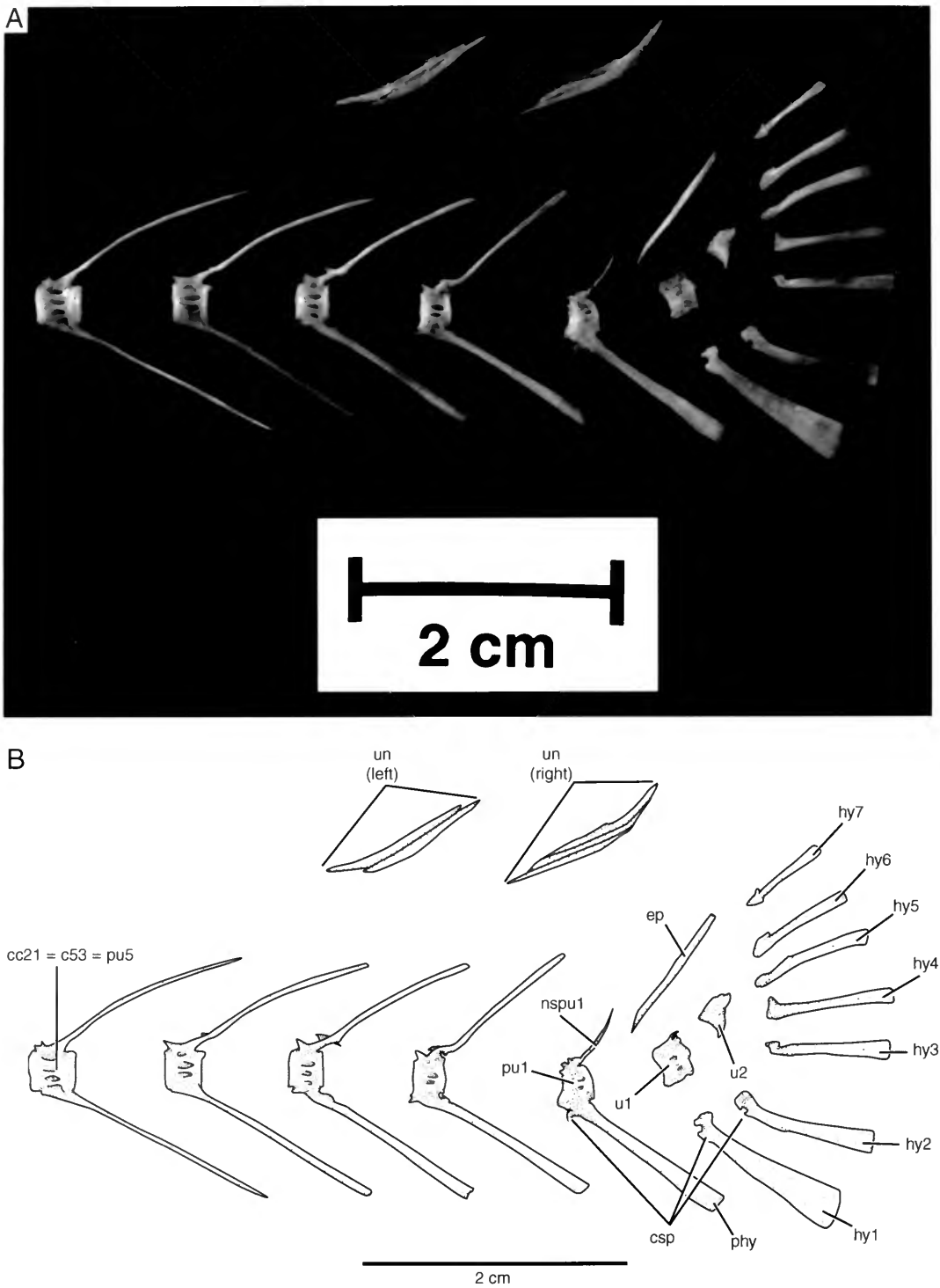

FIG. 73. *Hiodon alosoides*. **A**, Photograph, and **B**, line drawing of disarticulated posterior caudal region of an adult (UMA F10588, 252 mm SL, male) in lateral view. The first preural vertebral centrum (= c57 in this specimen), its associated neural spine, and parhypural are highlighted in blue. Anterior faces left.

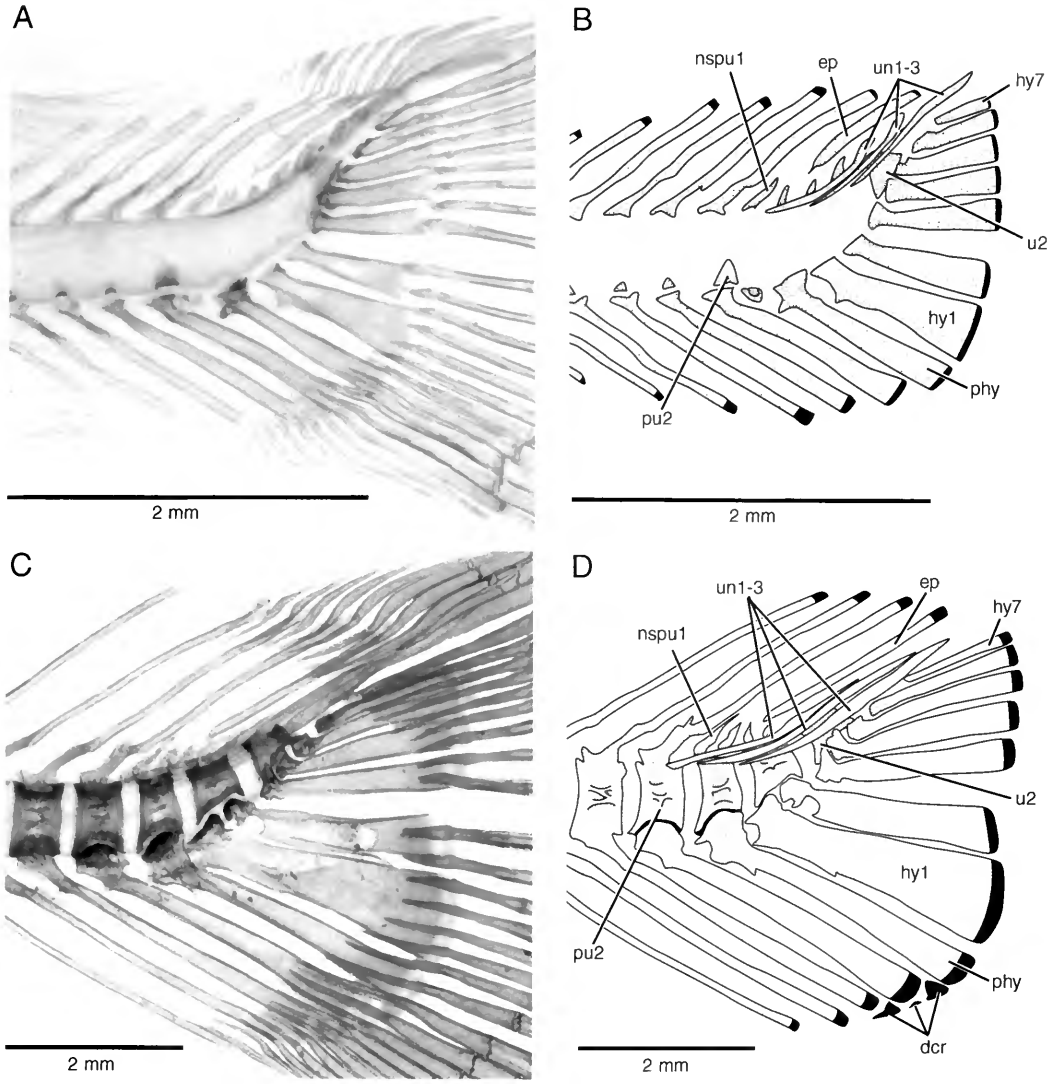

FIG. 74. *Hiodon tergisus*. **A** and **C**, Photographs, and **B** and **D**, line drawings of cleared and stained caudal skeletons of juveniles in lateral view. A and B: JFBM 22747A, 23 mm SL. C and D: TU 108166A, 52 mm SL. Fin rays omitted from line drawings. Centrum of pu1 has not yet formed in specimen shown in A and B, but the neural spine and haemal arch and spine (= parhypural) that it will bear are highlighted in blue; all elements of pu1 are highlighted in D. Haemal spine of pu4 and hypural 2 of specimen in C and D were damaged during preparation. Distal caudal radials (dcr) are likely present in the specimen in A and B, but did not stain with alcian blue, and therefore were omitted from the drawing. There is an anomalous ossification immediately posterior to the base of the haemal spine of pu2 in the specimen in A and B. Anterior faces left.

their terminology, u1+2, and u3+4+5, respectively; Schultze & Arratia, 1988: figs. 4 and 7). In contrast, I found no ontogenetic evidence of this or any other pattern of fusion (e.g., Fig. 74A, B). However, the u1 is often associated with two neural arches (see below), which may be hypothesized to each be "ancestrally" associated with independent ural centra (see Remarks on Phylogenetic Fusion). Therefore, I refer to the ural centra as "u1" and "u2" without implying specific homologies to the ural centra of other fishes.

In *Hiodon*, the number of neural arches associated with the ural region is quite variable, with between one and three pairs of neural arches as-

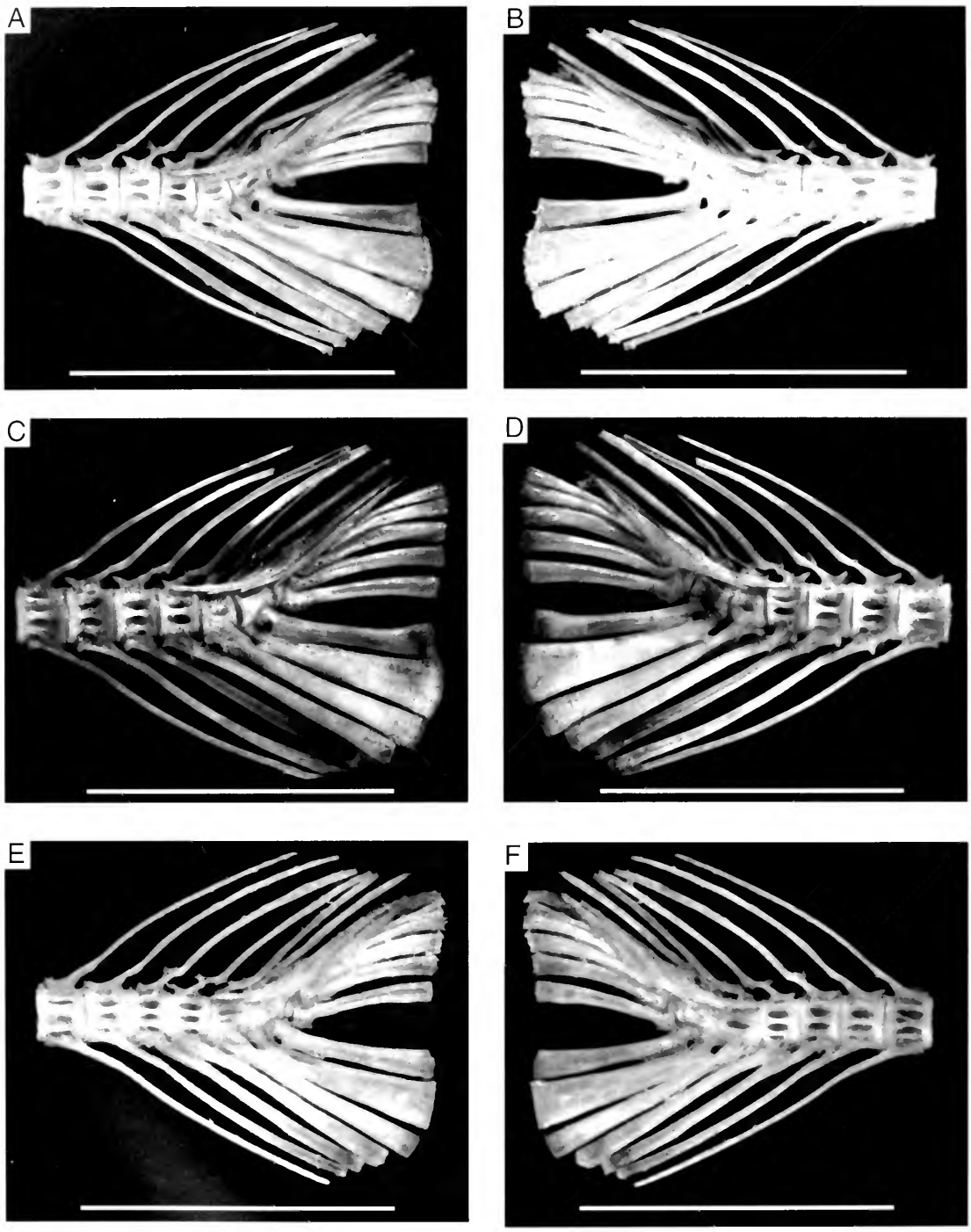

FIG. 75. *Hiodon alosoides*, photographs of posterior caudal skeleton of three adults (**A** and **B**: UMA F10593, 254 mm SL, male; **C** and **D**: UMA F10592, 292 mm SL, female; **E** and **F**: UMA F10594, 270 mm SL, female) in lateral view showing individual variation of the caudal skeleton. Left-hand column shows left side of specimen; anterior faces left. Right-hand column shows right side of specimen; anterior faces right. The "typical" condition for nspu1 is shown in **A** and **B**. Scale bars = 2 cm.

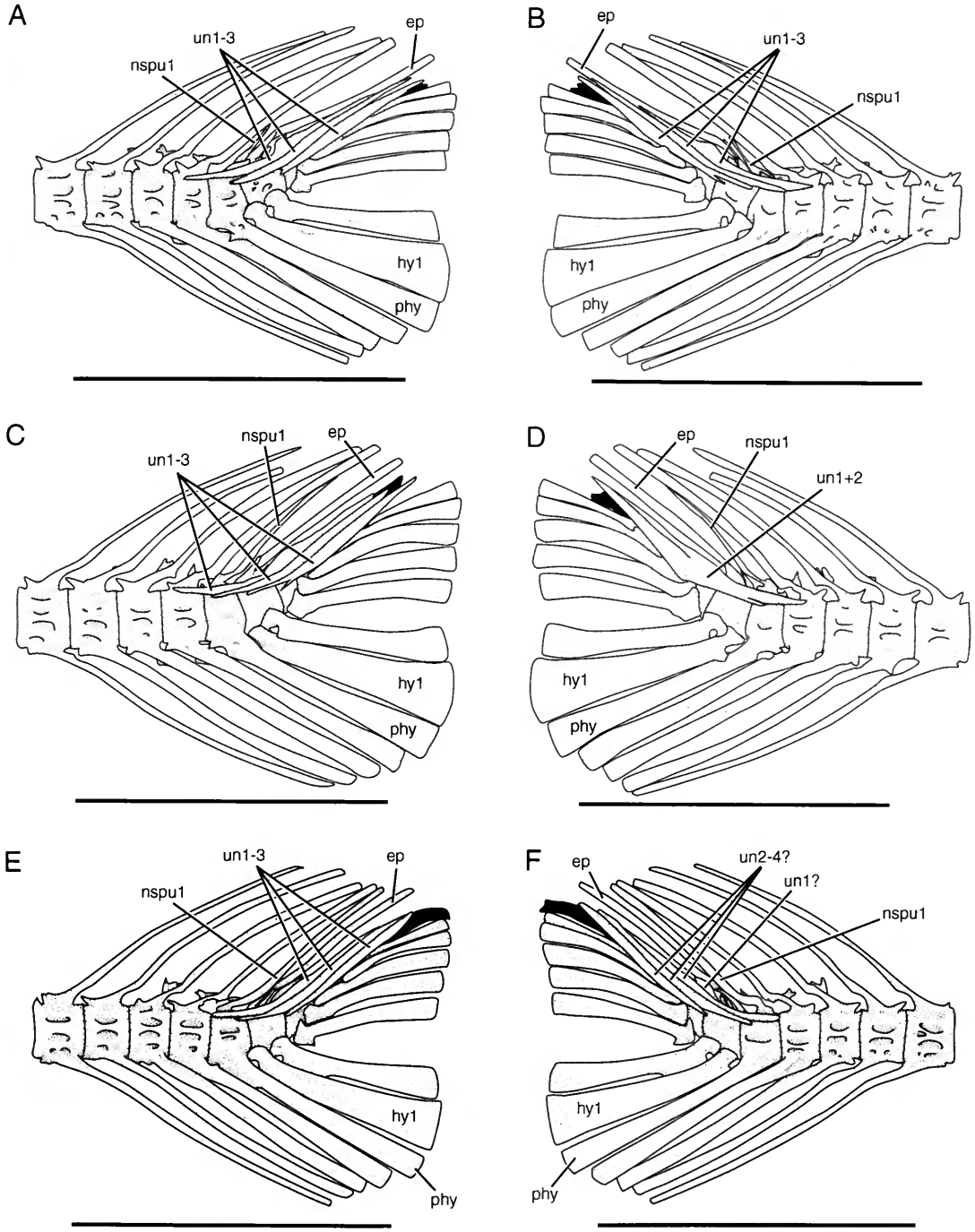

FIG. 76. *Hiodon alosoides,* line drawings of specimens in Figure 75. In each specimen, the first preural vertebral centrum, its associated neural spine, and parhypural are highlighted in blue. The "typical" condition for nspu1 is shown in **A** and **B**. Scale bars = 2 cm.

sociated with u1 (Tables 15 and 16). These arches are much reduced, and often do not form complete arches (e.g., UMA F10606 and UMA F10634). The anteriormost of the ural neural arches may lie in the intercentral space between pu1 and u1 (e.g., TU 108166E, UMA F10613).

A short, sticklike epural (ep, Figs. 71–76) ossifies around a cartilaginous rod in the dorsal midline of the ural region. In small specimens, the proximal end of the epural appears pinched (e.g., Fig. 74A, B). I observed variation in the position of the epural. In some specimens of *H. alosoides,* the epural is in series with the second neural arch of u1 (e.g., UMA F10600, UMA F10601, TU 113117E, UAMZ 4041B), whereas in others, it lines up with the anterior neural arch on u1 (e.g., TU 108118A). This does not seem to be related to ontogeny, as the specimen in which the epural is associated with the first neural arch is nested (sizewise) within those that exhibit the other condition (Table 16).

In *Hiodon,* the number and disposition of uroneurals vary between individuals, as well as bilaterally within an individual (un, Figs. 75 and 76, Tables 15 and 16); this sort of variation is well documented in the literature (e.g., Gosline, 1960; Patterson, 1968; Monod, 1968; Taverne, 1977; Schultze & Arratia, 1988: fig. 11). For example, Monod (1968: fig. 108*bis.* and *ter.*) found three uroneurals in his specimens of *H. tergisus,* although there was considerable shape variation in the morphology of the uroneurals between the two specimens. I found that the number of uroneurals ranged between two and four discrete bones (although in many specimens there is evidence of fusion between adjacent uroneurals), and that the number of uroneurals was not correlated with the size of the specimen. Schultze and Arratia (1988) concluded that the base number of uroneurals in *Hiodon* is four (the most of any extant teleost; Patterson & Rosen, 1977) and that these elements were derived from the neural arches of ural centra 4 through 7.

The hypural bones (hy, Figs. 71–76) are the serial homologues in the ural region of the more anterior haemal spines. These flattened bones decrease in size from anterior to posterior. All hypurals have started to ossify in the smallest specimens available to me, although their posterior portions may still be cartilaginous (e.g., TU 113117E). There is a small process (csp, Fig. 73) on the anteroventral extent of hypurals, as well as some of the posterior haemal arches. On hypural 2, this process contributes to the margin of the hypural foramen (Monod, 1968). Schultze and Arratia (1988: 279) reported six to eight hypurals in *Hiodon,* and noted that eight hypurals ("without exception") are present in small (22–38 mm SL) specimens; the eighth (posteriormost) being resorbed during ontogeny. I found only seven hypurals in all of my specimens of both species, even in small specimens (e.g., 21 mm SL; Tables 15 and 16) in which the cartilage is well-stained. There is a distinct diastema between the second and third hypurals (Monod, 1968) that marks the boundary between the dorsal and ventral lobes of the caudal fin (i.e., the dorsal lobe fin rays are associated with elements dorsal to the diastema and the ventral lobe fin rays are associated with elements ventral to the diastema); this diastema has been considered a synapomorphy of teleosts (de Pinna, 1996: character 3).

There are distal caudal radials (dcr, Fig. 74C, D) in the caudal skeleton of *Hiodon* that are completely surrounded by the fin rays (see Schultze & Arratia, 1989, for a discussion of these and other elements of the teleostean caudal skeleton). These irregularly shaped elements, which Fujita (1989) termed "inter-haemal spine cartilages" and "post-hypural cartilages," lie distal to the posteriormost haemal spines and the first hypural, and were never found to be ossified.

The neural spine of preural centrum 1 (nspu1, Fig. 73) is often rudimentary in *Hiodon* (Figs. 73, 75, and 76; Tables 15 and 16). Patterson and Rosen (1977) used the presence of a full neural spine on pu1 as a synapomorphy of Osteoglossomorpha. Schultze and Arratia (1988), however, found this condition in only 6% of their specimens of *Hiodon* (my data suggest that it is even less common, e.g., Tables 15 and 16). In one of my specimens of *H. tergisus* (TU 108166E), the neural spine of pu2 is also rudimentary, and in another (TU 108166D), there are two neural arches on pu1. Li and Wilson (1994) used the reduced or absent condition of the neural arch on pu1 as a diagnostic feature of the genus *Hiodon.* I never observed the absent condition in my sample of *H. tergisus* and *H. alosoides.* Given the clear variation of this character (Figs. 75 and 76), I caution against its use as a diagnostic character for the genus.

Included in the diagnosis of *Hiodon* given by Li and Wilson (1994: 155) is the character "two neural spines usually developed on the second preural" (described as "often" present by Li & Wilson, 1994: 163). This character follows from the observation that some specimens of both *H. tergisus* and *H. alosoides* have two neural arches

on pu2 (e.g., Monod, 1968: fig. 108*bis.*; Arratia & Schultze, 1988: fig. 11; Li & Wilson, 1994: fig. 4); one of the specimens of †*H. consteniorum* also shows this condition. This condition is not present in any of my specimens of *H. tergisus* and *H. alosoides* (e.g., Figs. 75 and 76), and I consider it an uncommon individual variation (although further research is needed to determine its frequency). Therefore, I also caution against using the presence of this character, or even its "potential" presence (Li & Wilson, 1999: character 60), as a diagnostic character for *Hiodon*.

Dorsal and Anal Fins and Pterygiophores

The skeletal supports of the fin rays of both the dorsal and anal fins of *Hiodon* consist of a series of elongate proximal radials (pr, Fig. 77) and a series of small, irregularly shaped distal radials (dr, Fig. 78). All radial elements are preformed in cartilage. The distal ends of the proximal radials are enlarged and distinctly bent, and look like fused proximal and middle radials (e.g., Fig. 78). A series of autogenous middle radials, however, was not found in even small specimens, although in some small specimens of *H. alosoides* (e.g., TU 113117E, 24 mm SL; TU 113117C, 28 mm SL) I did observe a constriction in the cartilage of the proximal radials, suggesting a series of cartilaginous medial radials fused to the cartilage of the proximal radials (the proximal radials of my small specimens of *H. tergisus* did not stain very well). Additionally, in slightly larger specimens, the shaft of the proximal radial is ossified and the distal tip is a cartilaginous plug, which may represent elements of the middle radial series. The dorsal and anal fin of other osteoglossomorphs have various patterns of presence and absence of pterygiophore elements. For instance, the anal fins of notopterids are supported only by a series of proximal ossifications (e.g., Taverne, 1978: figs. 75, 108, 110, and 129; pers. obs.), whereas the dorsal fin is supported by a series of ossified proximal radials and cartilaginous distal radials (e.g., *Chitala* sp., UMA F10341, pers. obs.). In the mormyrid *Petrocephalus simus* (MCZ 50113, pers. obs.), the posterior portion of both the dorsal and anal fin are supported by three separate elements (proximal, middle, and distal radials), whereas the anterior portion of the fins have only two elements (proximal and distal radials); see Taverne (1977, 1978) for the condition of other osteoglossomorphs. In salmonids, the proximal and middle radials of the median fins ossify within the same cartilaginous element, and in the dorsal fin the "first two to three middle pterygiophores [= middle radials] do not ossify and cannot be distinguished as separate elements" (Sanford, 2000: 166). A study of specimens of earlier stages than available for the present study may help to determine if a series of middle radials (fused to the proximal radials) is present in the dorsal and anal fins of *Hiodon*.

The dorsal fin and pterygiophores of *H. alosoides* are illustrated in Figures 77 and 78A, B. The predorsal fin length in *H. tergisus* is relatively shorter than in *H. alosoides* (Fig. 79A; cf. Tables 2 and 3; Trautman, 1957; Scott & Crossman, 1977; Page & Burr, 1986). Structurally, the dorsal fins of *H. tergisus* and *H. alosoides* are virtually identical, although they differ in the number of fin rays (13–16 versus 9–10, respectively) and proximal radials (13–15 versus 11–13, respectively; Tables 17 and 18). A prominent ridge projects from the lateral surface of each of the proximal radials and serves as the origin for fin elevator and depressor muscles. There is roughly a one-to-one correlation between the number of proximal radials and number of segmented fin rays, although this pattern breaks down anteriorly because the supernumerary fin rays (Patterson, 1992; these include both the unsegmented rudimentary fin rays and the anterior unbranched segmented fin rays recorded here) become crowded together (Fig. 77). The series of distal radials (dr, Fig. 78A, B) are largely covered by the proximal ends of the fin rays.

Meristic data concerning the anal fin are recorded in Tables 17 and 18. The relative pre-anal fin length is virtually indistinguishable between the two species (Fig. 79B; Tables 2 and 3). As for the dorsal fin, the number of anal fin rays and pterygiophores differs between *H. tergisus* and *H. alosoides* (cf. Tables 17 and 18). The shape of the anal fin is sexually dimorphic in mature specimens of *Hiodon* (e.g., see Scott & Crossman, 1973; Roberts, 1989). The overall shape of the fin in the female is triangular, whereas in the male the anterior portion of the fin is rounded, and the anterior rays are thinner in males than in females (Figs. 80 and 81). Sexual dimorphism in the external shape of the anal fin has also been reported in †*Eohiodon* (Wilson, 1978; Grande, 1979; Li & Wilson, 1994; Li, Wilson, & Grande, 1997). The proximal radials (pr, Figs. 78C, D, 80, and 81) of the anal fin also are sexually dimorphic in form in *Hiodon*. In both sexes there is a lateral ridge

on the anterior elements. In the males only, however, these ridges are enlarged distally to form a wing that nearly overlaps the next posterior proximal radial (cf. Figs. 80 and 81).

Sexual dimorphism of anal fin morphology has been reported in many actinopterygians (e.g., polypterids, Britz & Bartsch, 1998). This dimorphism is often associated with spawning, during which the "male's anal and caudal fins wrap around the female's genital opening, forming a spoon-like chamber into which released eggs fall and are fertilised by the male" (Britz & Bartsch, 1998: 328). Within nonhiodontiform osteoglossomorphs, Brown, Benveniste, and Moller (1996) discovered internal and external sexual dimorphism in the structure of the anal fin of two species of the mormyrid genus *Brienomyrus*. In male specimens, the hypertrophied bases of the fin rays cause an indentation in the dorsal margin of the anal fin. Similar external sexual dimorphism is known in other species of mormyrids. For example, Okedi (1969: 40) noted differences in the shape of the fin between the two sexes and the presence of a notched dorsal margin of the anal fin in males ("ventral flank of the body curved inwards") for members of three genera (*Gnathonemus, Marcusenius,* and *Petrocephalus*) from Uganda, and suggested that this is a permanent dimorphism in mature males. Iles (1960), however, found that in *Mormyrus kannume* this dimorphism is only seasonal, and that the shape of the anal fin in males returned to the "female" shape when the testes were resorbed after spawning. The observed sexual dimorphism of the anal fin (internal and external) is present in specimens of *Hiodon* collected throughout the year.

Pectoral Girdle, Fin, and Supports

The pectoral girdle and fin of *Hiodon* are illustrated in Figures 82 to 88 and meristic data associated with the pectoral fin are presented in Tables 19 and 20. Each side of the pectoral girdle is comprised of four dermal and three chondral ossifications. The two dorsalmost dermal bones, the posttemporal (pt) and supracleithrum (scl, Figs. 82–86) form in conjunction with the lateral sensory canal (e.g., Fig. 14). The ventral arm of the posttemporal is forked so that the posttemporal is triradiate (i.e., there are three arms present: a dorsal arm, a ventromedial arm, and a ventrolateral arm). The dorsal arm (pt(d), Figs. 82–86) is more than twice as long as the ventrolateral arm (pt(l), Figs. 82, 83, 85, and 86), a condition regarded as diagnostic of Hiodontiformes (Li & Wilson, 1996a). The dorsal arm of the posttemporal is firmly connected to the epioccipital by a stout ligament, which attaches to the posterior peak of the epioccipital (Fig. 24). The ventromedial arm (pt(m), Figs. 84–86) is associated with a ligament that attaches to the lateral surface of the intercalar (not shown in Fig. 24 because it was not preserved in this specimen). The ventrolateral arm of the posttemporal carries the lateral sensory canal, posterior to where it enters the pterotic and the cephalic sensory canal system. Ventral to the posttemporal is the supracleithrum, which is a flat element with a slight anterior curve. Like the posttemporal, it carries a sensory canal (Figs. 82 and 83). Dorsally the supracleithrum overlaps the posttemporal, and ventrally it overlaps the cleithrum and postcleithrum.

There is a single postcleithrum (pcl, Figs. 83–85) in *Hiodon*. This bone is a small, diamond-shaped element that is completely covered in lateral view by the supracleithrum and cleithrum. It is positioned posterior to the large medial ridge on the vertical arm of the cleithrum.

The large dermal cleithrum (cl, Figs. 82–87) forms much of the ventrolateral pectoral girdle in *Hiodon* and has distinct horizontal and vertical arms. The cleithrum is a thin bone, except for the thickened ridge that forms along the length of its medial edge. Ventromedially, the cleithrum contacts the coracoid, with which it forms a large, oblong fenestra (cl-cofn, Figs. 84 and 87), the medial edge of which serves as the origin of a division of the pectoral fin adductor musculature. This muscle passes posteriorly through a canal formed by coracoid, mesocoracoid, and cleithrum (not visible in the figures), to insert on the dorsal surface of the pectoral fin rays. Another portion of this muscle originates dorsally on the medial surface of the mesocoracoid and the chondral component of the coracoid. There is a small foramen of unknown function on the lateral surface of the cleithrum where the horizontal and vertical arms meet (clf, visible only in Fig. 88A, B).

Three chondral elements form much of the ventral portion of the pectoral girdle. The coracoid (co, Figs. 82–87) begins ossification as a chondral element posteriorly, where it contacts the other chondral elements of the pectoral girdle and supports the medial two radial elements. Most of the coracoid is an anterior membranous ossification that soon follows in development (Fig. 14A, B). The left and right coracoids meet at the midline

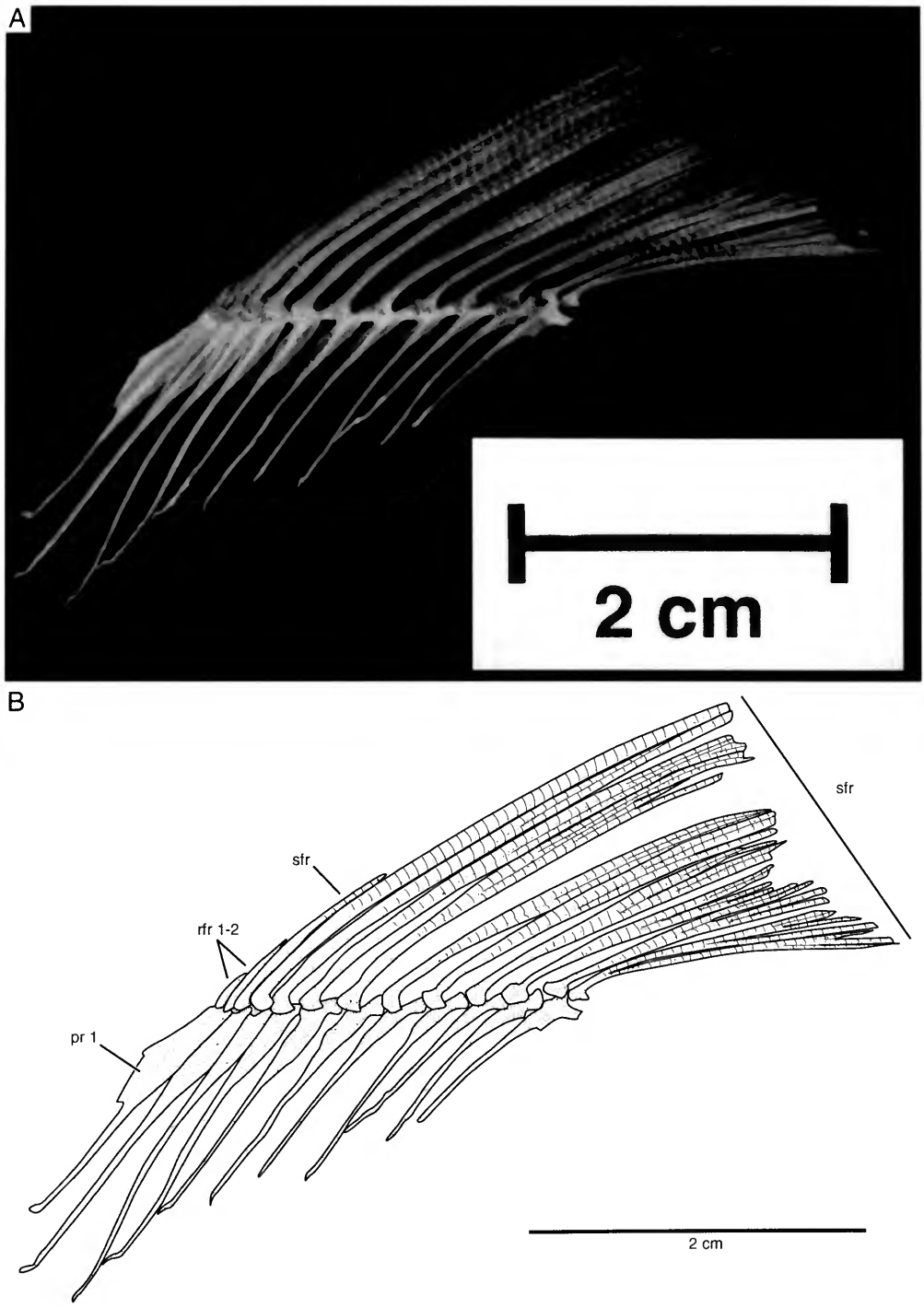

FIG. 77. *Hiodon alosoides*. **A**, Photograph, and **B**, line drawing of dorsal fin and pterygiophores of an adult (UMA F10592, 292 mm SL, female) in lateral view. Anterior faces left.

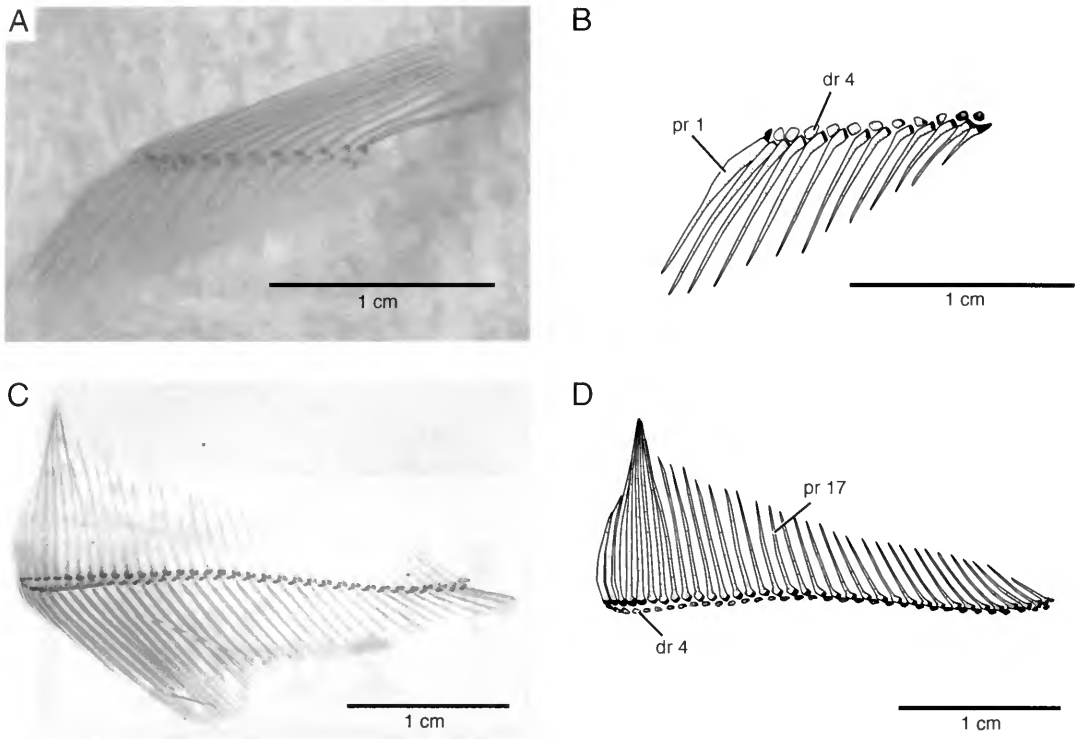

FIG. 78. *Hiodon alosoides*. **A** and **C**, Photographs, and **B** and **D**, line drawings of cleared and stained dorsal (A and B) and anal (C and D) fins and supports of a juvenile (UMA 10615, 102 mm SL) in lateral view. Fin rays were omitted from the drawing. Anterior faces left.

of the body and form a large keel, which serves as the origin for much of the ventral pectoral abductor musculature. Of living osteoglossomorphs, *Hiodon* is unique in that it lacks an enlarged fenestra within the coracoid (Cavin & Forey, 2001: fig. 12), although there is a small foramen (cof, Figs. 84, 85, and 88A, B) for a blood vessel in a position similar to the position of the fenestra of other osteoglossomorphs.

Two small chondral bones, the scapula and mesocoracoid, form dorsal to the coracoid, medial to the cleithrum. The scapula (sc, Figs. 83–85 and 87) supports the lateral two pectoral fin radials (Fig. 88A, B). A dorsal winglike projection meets the ventromedial face of the cleithrum. A thin column of bone from the lateral corner of the scapula extends dorsally to meet the mesocoracoid. The scapular foramen (scf, Figs. 83 and 85–87) is completely enclosed by the scapula. The hooked mesocoracoid bone (mco, Figs. 83–85) forms a bridge with the coracoid and the cleithrum that encloses the canal through which the pectoral fin adductor musculature passes. Some of the pectoral fin adductor musculature also originates along the posterior surface of the mesocoracoid.

The pectoral fin rays of *Hiodon* are supported by four ossified proximal radials (ra, Figs. 83–88) and generally five distal radials (dr, Fig. 88; although more were found in one specimen; ?, Fig. 88C, D), some of which were found to be ossified in an adult specimen of *H. tergisus* (Fig. 88A, B). Among osteoglossomorphs, ossified distal radials of the pectoral fin have also been recorded in notopterids (e.g., Taverne, 1978: figs. 72 and 107) and osteoglossids (e.g., Taverne, 1977: figs. 57 and 86). I also observed irregularly shaped ossified distal radials in *Albula vulpes* (e.g., AMNH 88678SD, est. 300 mm SL; AMNH 55998SD, est. 470 mm SL), and up to nine ossified elements in large specimens of *Megalops atlanticus* (e.g., UMA F11023, 1741 mm SL; AMNH 90905SD, est. 1400 mm SL; although they were unossified in a smaller specimen, UMA F10251, est. 500 mm SL). Ossified distal radials are also found in clupeo-

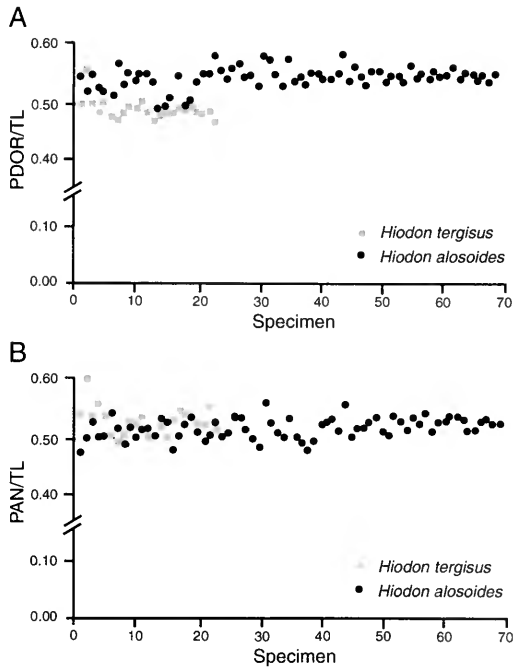

FIG. 79. Ratio of pre-dorsal fin length (**A**) and pre-anal fin length (**B**) to total length for a sample of *H. tergisus* and *H. alosoides*. The difference between the pre-dorsal fin length of the two species is greater than the difference between the pre-anal fin length.

morphs (Grande, 1985; Arratia, 1997). The proximal pectoral radials of *Hiodon* are ossified in both species by 24 mm SL (Tables 19 and 20). The lateralmost proximal radial (ra1) is a small, irregularly shaped block of bone, and the remaining proximal radials (ra2, ra3, ra4) are progressively longer. In *H. tergisus,* ra2–ra4 bear elongated uncinate processes that articulate with the ventral surface of the adjacent radial (Fig. 88D); in *H. alosoides,* only the middle two radials (ra2 and ra3) bear a well-developed uncinate process (Figs. 83 and 85). These processes are well-developed in *H. alosoides* by 39 mm SL. The medialmost proximal radial (ra4) is the longest of the series and in *H. alosoides* is essentially a bar of bone, although there is some variation in its overall shape (a slight medial enlargement may represent an uncinate process, e.g., in the specimen illustrated in Figs. 83 and 85, but this was never as well-developed as that of *H. tergisus,* e.g., Fig. 88D).

In *Hiodon* there is a thin, scalelike bony element (pap, Fig. 88E) positioned on the lateral surface of the pectoral girdle just dorsal to the leading fin ray. Arratia (1997), who termed this structure a pectoral axillary process, distinguished between true and false processes. True pectoral axillary processes are defined as those that consist of an "elongated structure formed by one or more bones, scales, or a combination of both, and is firmly attached to a skin fold just above the articular condyle of the upper most fin ray," and are found in †*Varasichthys, Elops, Chirocentrus, Ethmidium, Lycengraulis, Dorosoma* and *Engraulis* (Arratia, 1997: 133). False axillary processes, on the other hand, are "formed by a row of slightly elongated scales, each of which is independently attached or inserted in the skin" and were reported in *Sardinops* and *Clupea* (Arratia, 1997: 134). By these definitions, the elements in *Hiodon* are true axillary processes.

Hiodon tergisus has 12–14 pectoral fin rays, whereas there are 11–12 in *H. alosoides* (Tables 19 and 20); some left-right asymmetry was noted in *H. alosoides* (Table 20). The leading fin ray of the pectoral fin is unbranched, articulates with the ventrolateral corner of the scapula, and has an enlarged base. The formation of this enlarged base is a fusion between the dermal fin ray and the chondral propterygium (Fig. 88F–H), and even in

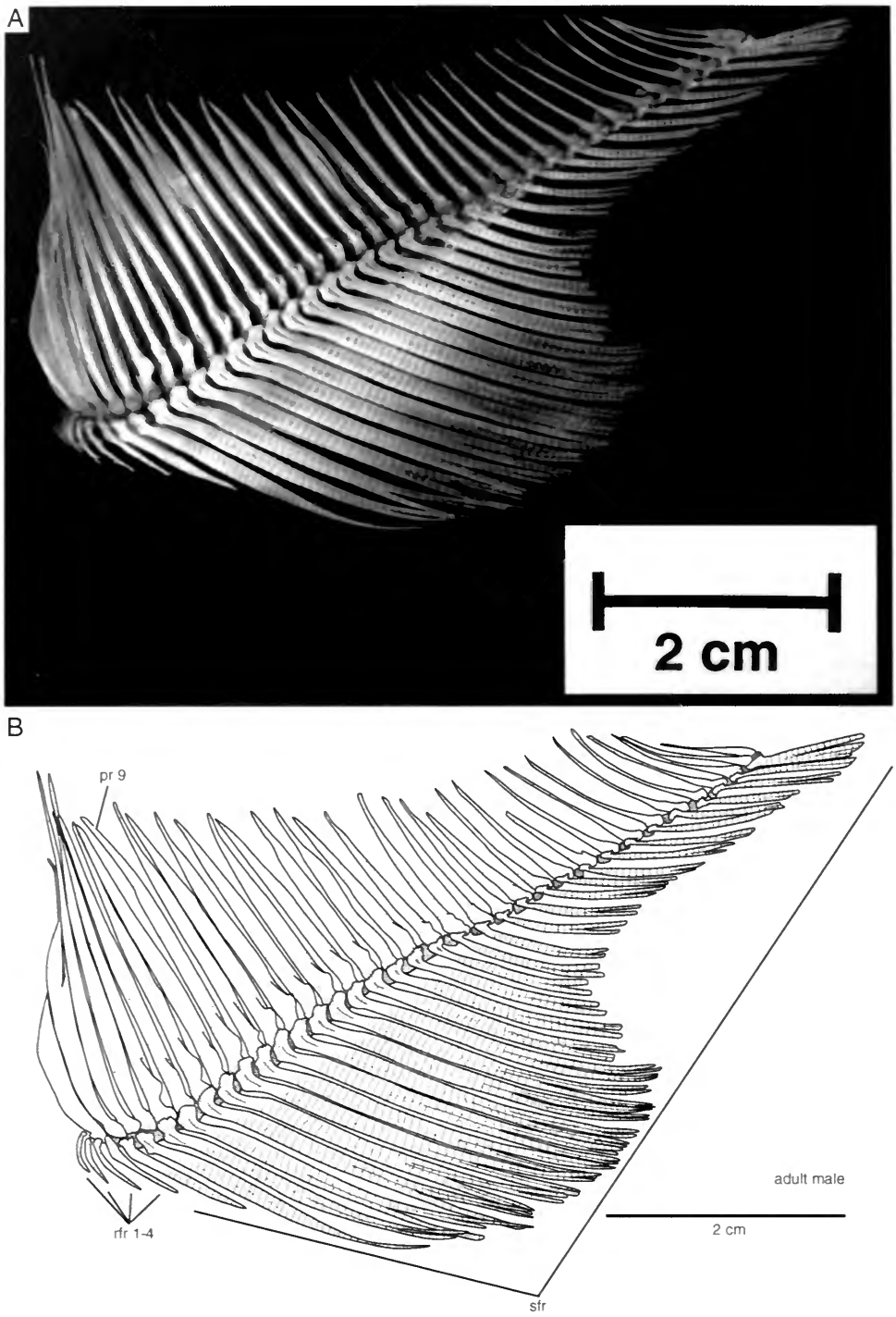

FIG. 80. *Hiodon alosoides*. **A**, Photograph, and **B**, line drawing of anal fin and pterygiophores of an adult (UMA F10588, 252 mm SL, male) in lateral view. Anterior faces left.

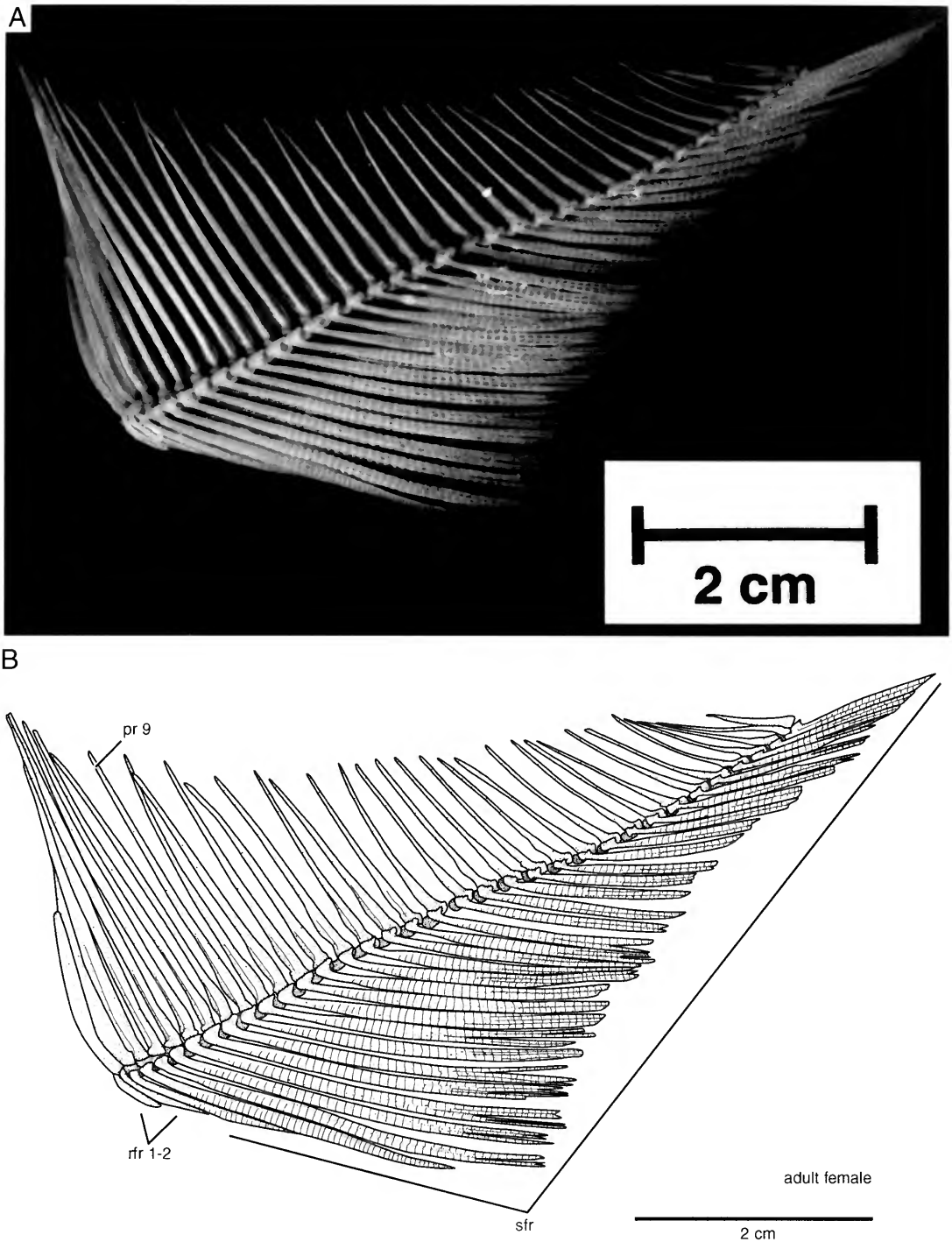

FIG. 81. *Hiodon alosoides*. **A**, Photograph, and **B**, line drawing of anal fin and pterygiophores of an adult (UMA F1078, 279 mm SL, female) in lateral view. Anterior faces left.

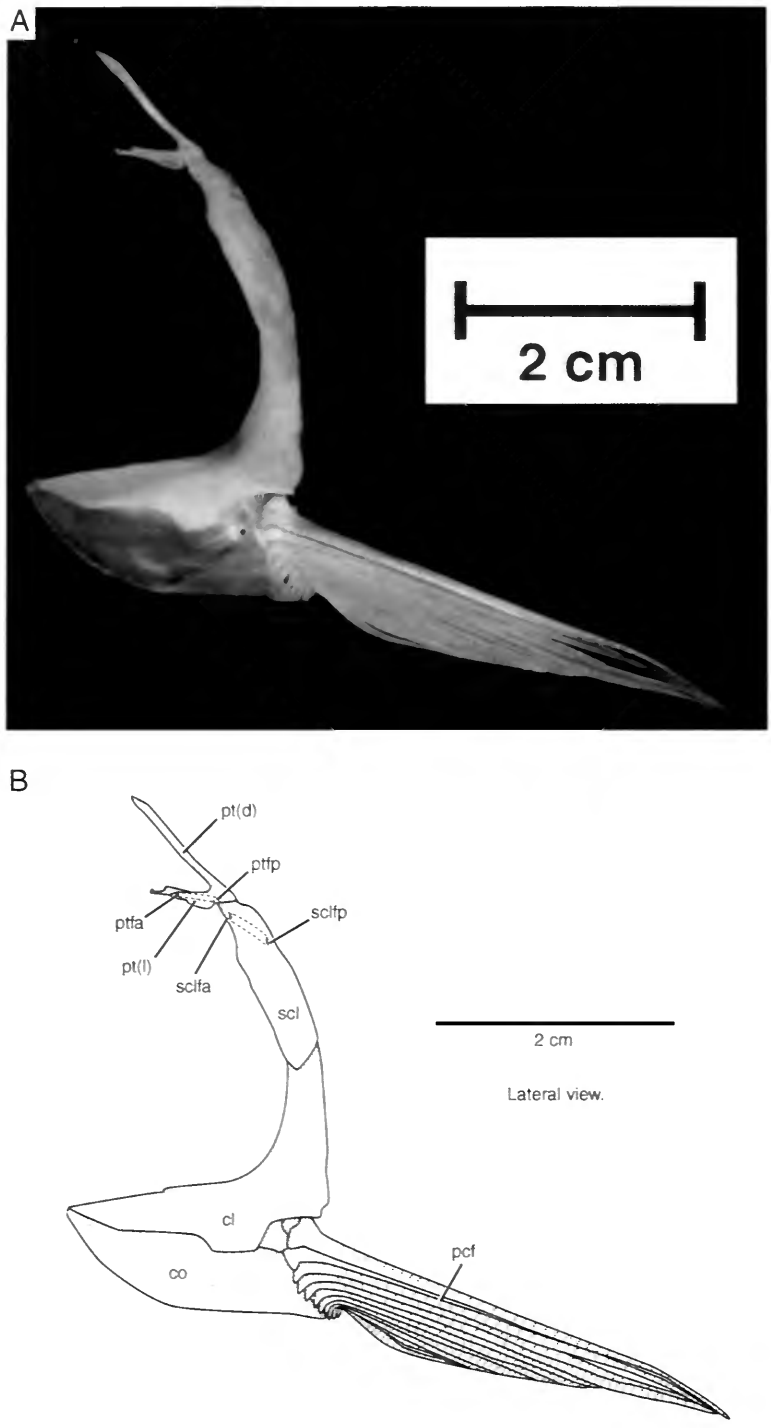

FIG. 82. *Hiodon alosoides*. **A**. Photograph, and **B**. line drawing of left pectoral girdle and fin of an adult (UMA F10588, 252 mm SL, male) in lateral view. Dashed lines indicate position of sensory canal enclosed in bone. Anterior faces left.

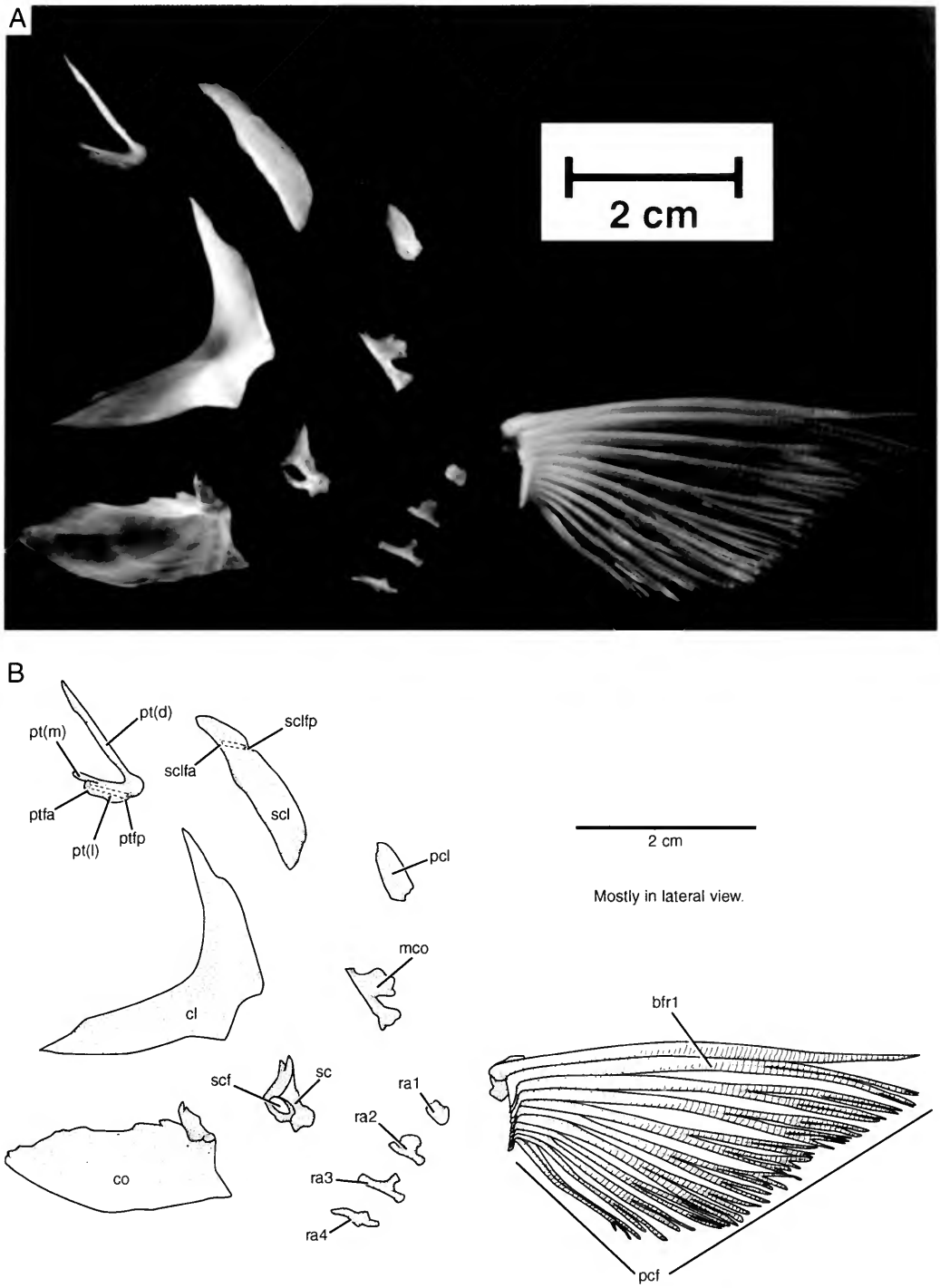

FIG. 83. *Hiodon alosoides*. **A**, Photograph, and **B**, line drawing of disarticulated left pectoral girdle and fin of an adult (UMA F10589, 275 mm SL, female) in lateral view; radials (ra) in dorsal view. Dashed lines indicate position of the sensory canal enclosed in bone. Anterior faces left.

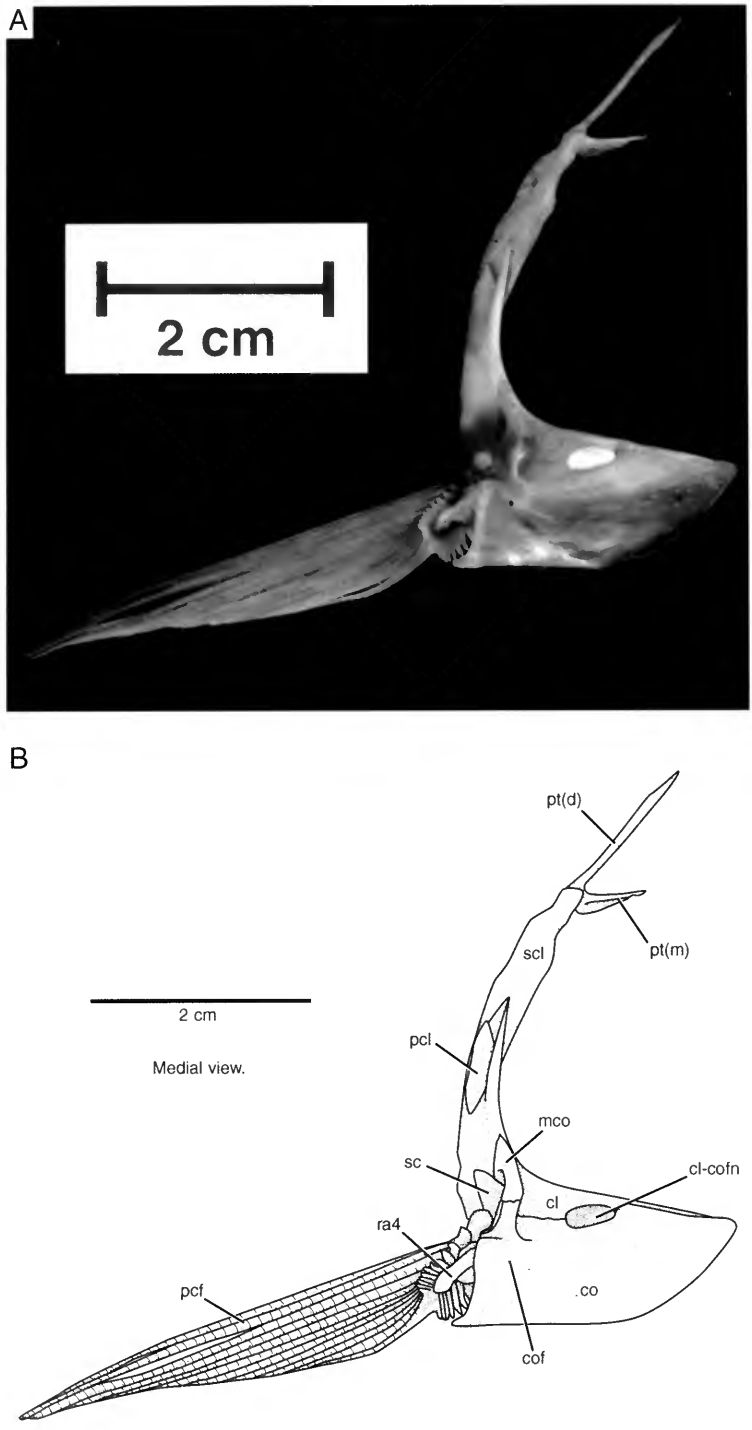

FIG. 84. *Hiodon alosoides*. **A**, Photograph, and **B**, line drawing of left pectoral girdle and fin of an adult (UMA F10588, 252 mm SL, male) in medial view. Anterior faces right.

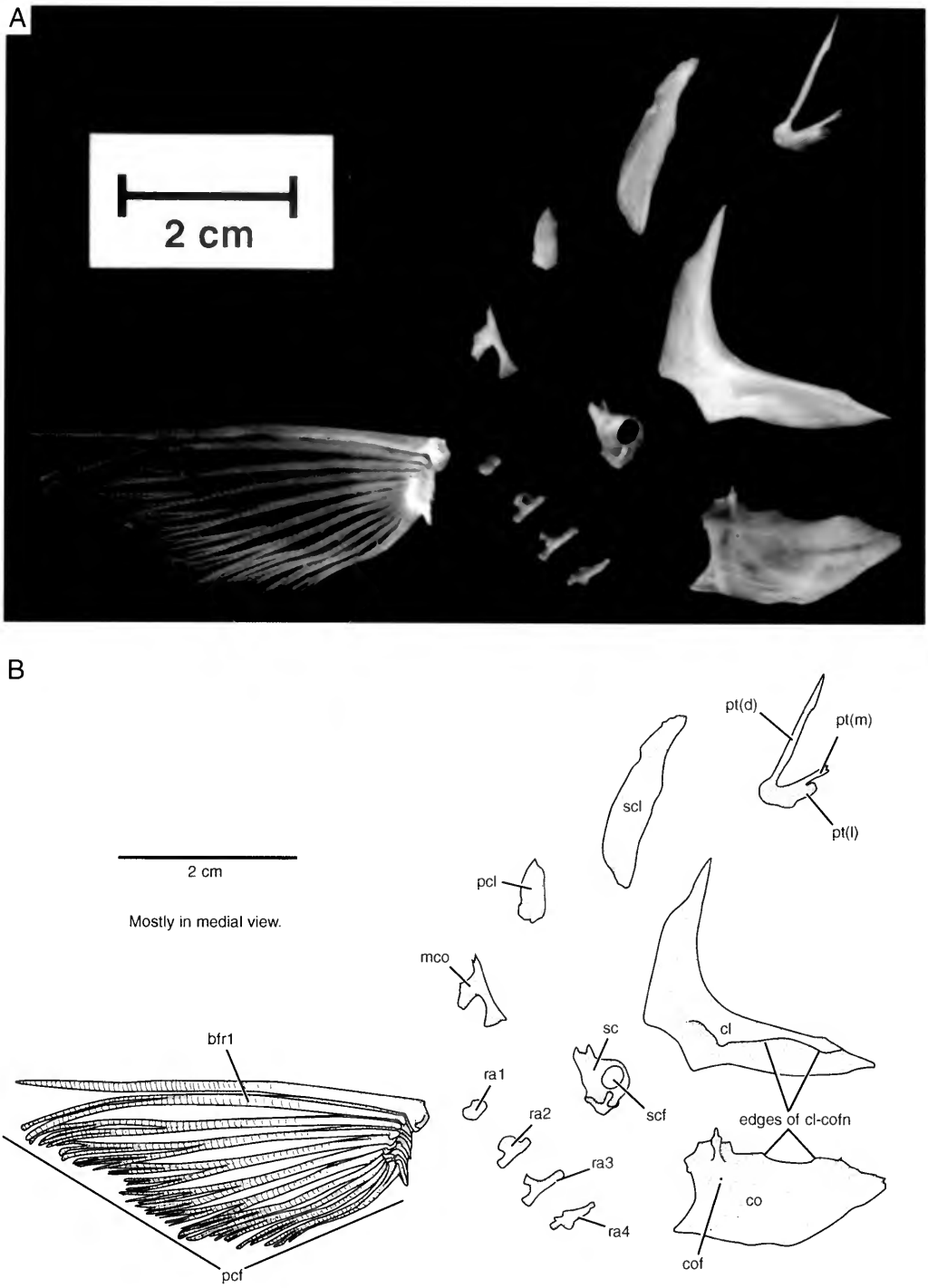

FIG. 85. *Hiodon alosoides*. **A**, Photograph, and **B**, line drawing of disarticulated left pectoral girdle and fin of an adult (UMA F10589, 275 mm SL, female) in medial view; radials (ra) in ventral view. Anterior faces right.

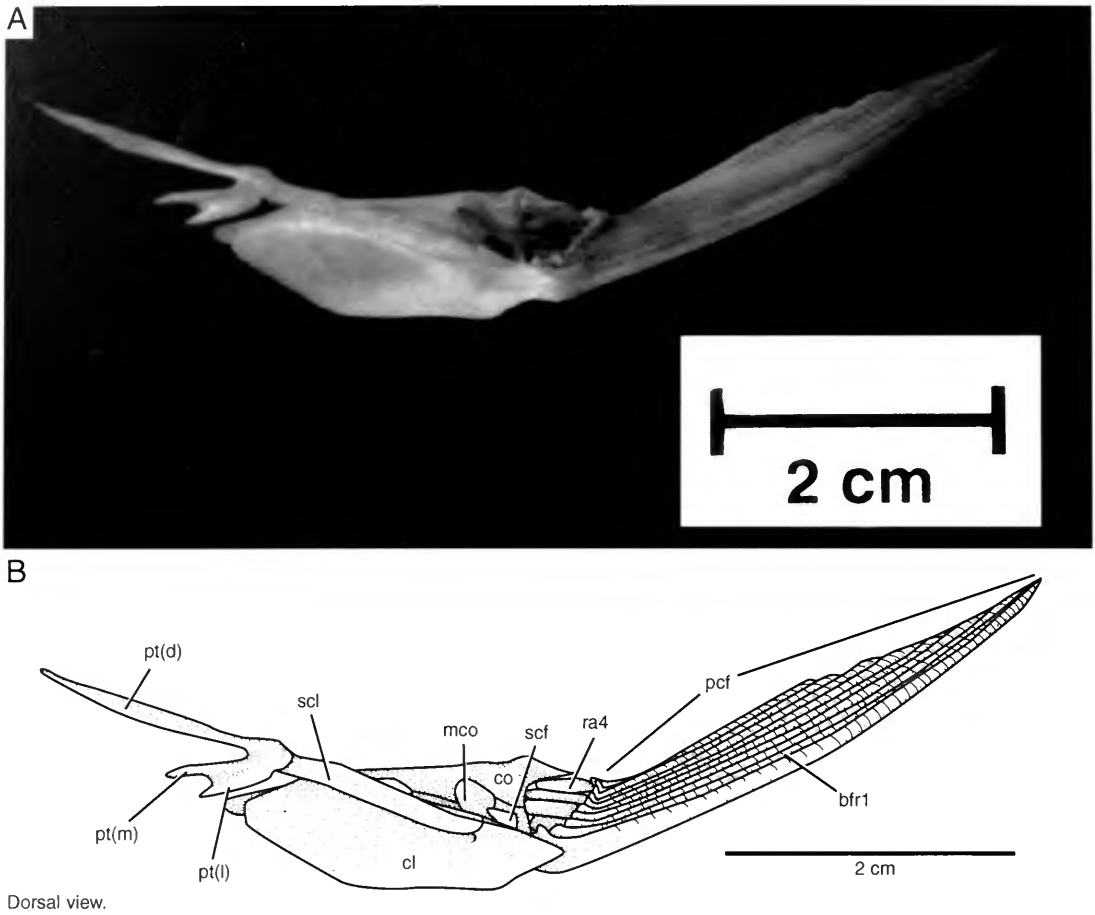

FIG. 86. *Hiodon alosoides*. **A**, Photograph, and **B**, line drawing of left pectoral girdle and fin of an adult (UMA F10588, 252 mm SL, male) in dorsal view. Anterior faces left.

the smallest individuals examined the elements have started to fuse together; further study of the development of this association is needed. The fusion between the leading fin ray and a chondral element was considered a synapomorphy of teleosts by Patterson (1977b; see also Arratia, 1999) and is widespread in teleosts. For example, in the gobiid genus *Schindleria*, Johnson and Brothers (1993) found that it is the medial half of the leading fin ray that fuses with the chondral element; in *Hiodon* the propterygium fuses to the lateral half of the leading fin ray. There is an obvious foramen in the proximalmost extent of the lateral half of the first dorsal fin ray (Fig. 88H), which corresponds to the opening Jessen (1972: pl. 2, figs. 1 and 2) labeled as "vorder Öffnung des Kanals durchs Propterygium" in *Elops saurus*.

Pelvic Girdle, Fin, and Supports

The pelvic girdle and fin of *Hiodon* are illustrated in Figures 89 to 91; meristic data associated with the pelvic fin are presented in Tables 19 and 20. The pelvic girdle consists entirely of endochondral elements. A pair of elongated pelvic bones (pb, Figs. 89–91), the only ossifications of the basipterygium (Sewertzoff, 1934), form most of the girdle and are tightly sutured to each other posteriorly along the midline; their anterior tips never meet. There is a large protuberance on the ventral surface of each pelvic bone (vppb, Fig. 90C, D). Taverne (1977: fig. 19) figured a single radial element in a 58 mm SL individual of *H. alosoides*. I observed up to three cartilaginous radial elements supporting the fin rays in small ju-

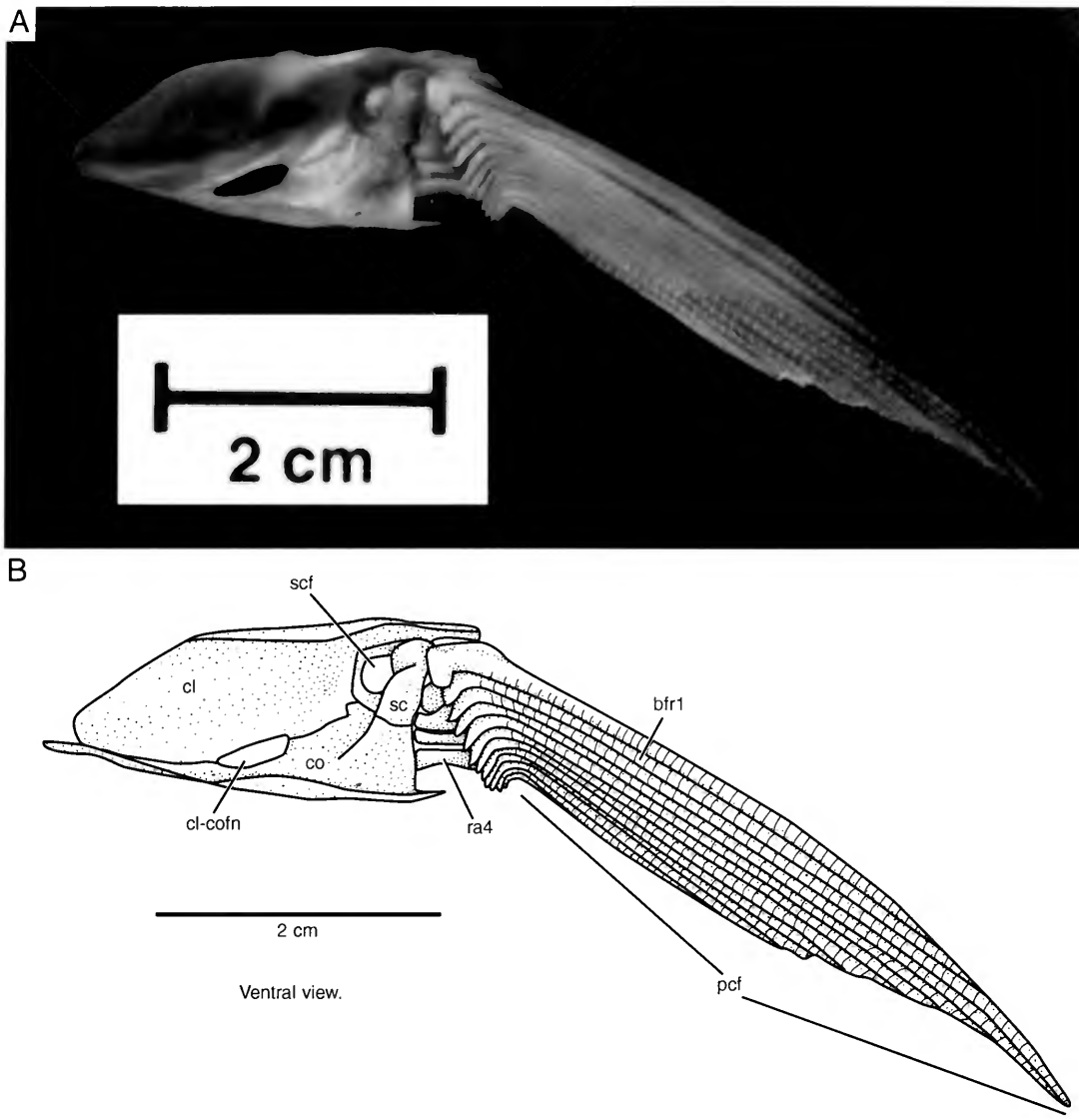

FIG. 87. *Hiodon alosoides*. **A**, Photograph, and **B**, line drawing of left pectoral girdle and fin of an adult (UMA F10588, 252 mm SL, male) in ventral view. Anterior faces left.

venile specimens (e.g., Fig. 91). The lateralmost of these was always the first to ossify, although in large individuals there may be an additional, more medial small ossification as well.

A single median postpelvic bone (ppb, Figs. 89–91) articulates with the pelvic bones in a slight concavity formed by the rounded posterior edges of these elements. The thin postpelvic bone is oriented in the dorsoventral plane and is bladelike. This element is unique to the genus *Hiodon* among all teleosts known to the author. The conditions of †*H. consteniorum* and members of †*Eohiodon* are unknown, owing to typically poor preservation of the pelvic girdle and fin.

Curving dorsally along the anterior portion of the pelvic fin is a short, thin bone (ps, Fig. 89E, F) termed a pelvic splint by Gosline (1961). Gosline (1961: 18–19) noted that "there is probably no great systematic significance to be attached to the loss of this splint" and that "it represents, when present, the holdover of a primitive teleostean" condition. This element is present in *Amia*

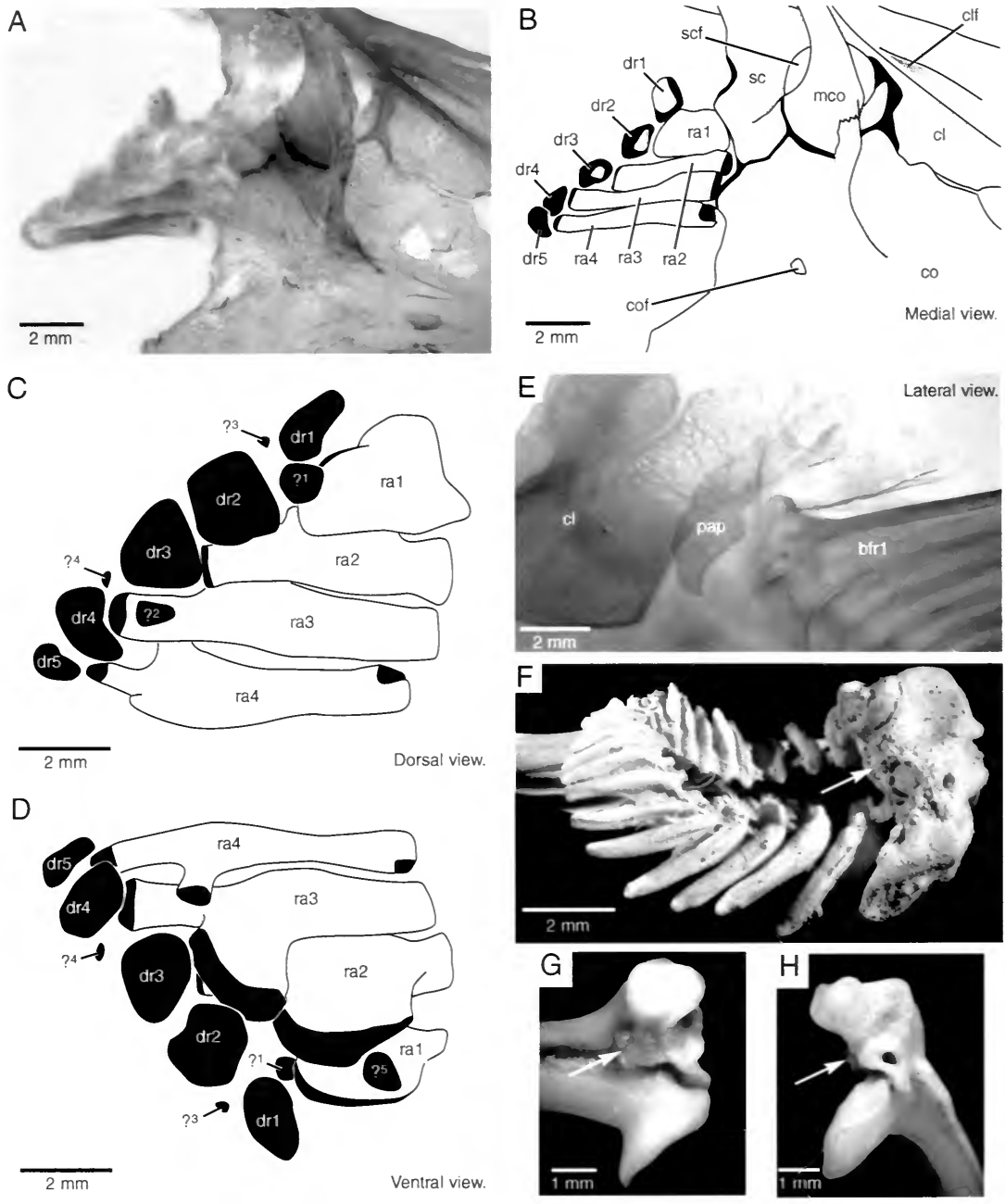

FIG. 88. *Hiodon tergisus*. **A**, Photograph, and **B**, line drawing of left pectoral girdle of a cleared and stained adult (JFBM 27508, 270 mm SL, female) in dorsomedial view; pectoral fin rays have been dissected away. **C** and **D**, line drawings of pectoral radials of a cleared and stained adult (UMA F10640, 184 mm SL, male) showing unknown cartilages (?) in dorsal (C) and ventral (D) view. **E**, Photograph of left pectoral girdle of a cleared and stained adult (UMA F10610, 183 mm SL, male) in lateral view showing pectoral axillary process (pap). **F**, Photograph of the proximal portion of the left pectoral fin rays of an adult (UMA F10589, 275 mm SL, female) in medial view; propterygium fused to first fin ray (arrow). Specimen was dusted lightly with ammonium chloride. **G** and **H**, Photographs of first pectoral fin ray in an adult (UMA F11259, 270 mm SL, female) in medial (G) and anterior (H) views showing fused propterygium (arrow). Also note opening of pectoral canal in H (unlabeled). In line drawings, cartilage shown in black. In A–D and F–H, anterior faces right; in E, anterior faces left.

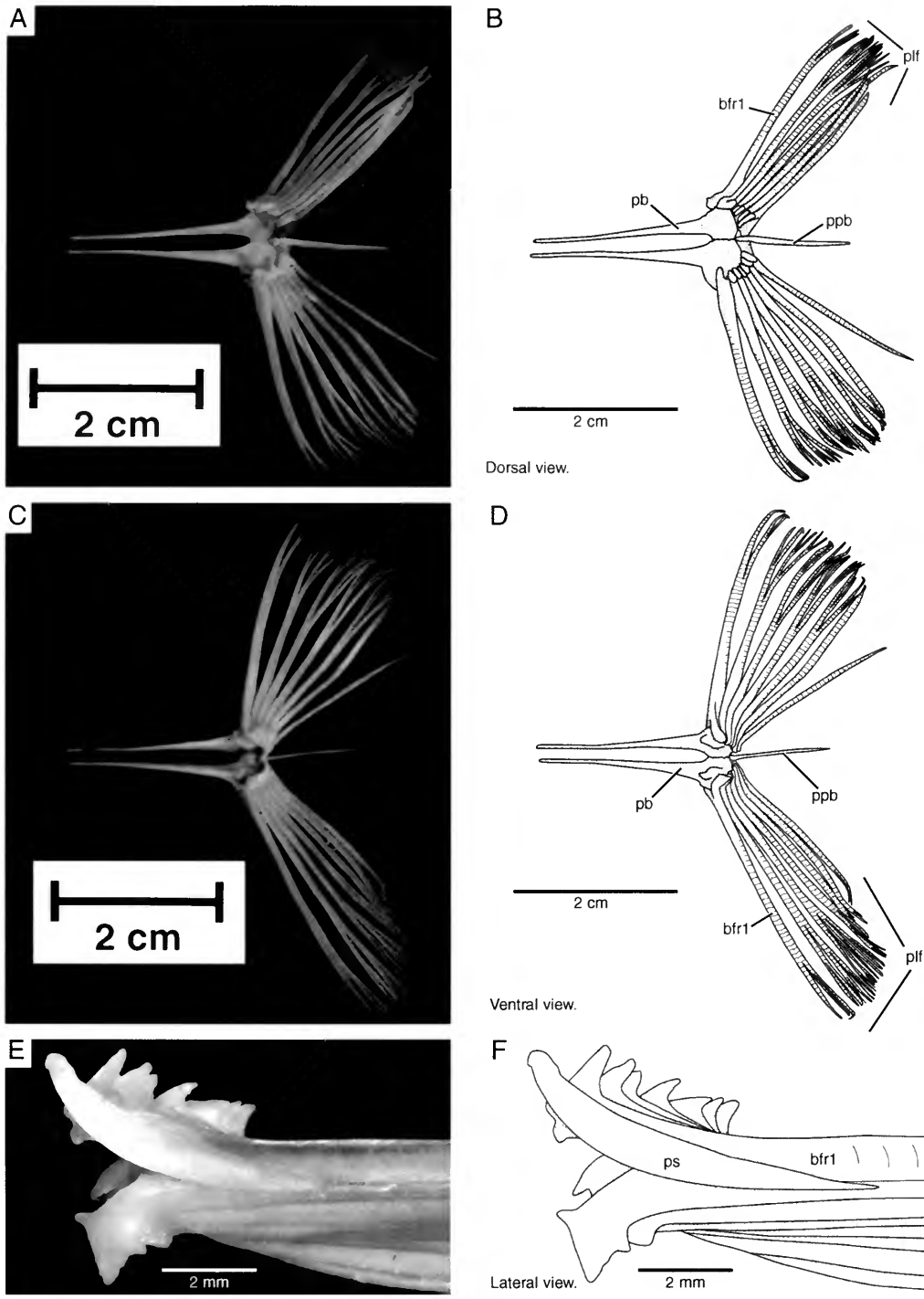

FIG. 89. *Hiodon alosoides*. **A** and **C**, Photographs, and **B** and **D**, line drawings of pelvic girdle and fin of an adult (UMA F10589, 275 mm SL, female) in dorsal (A and B) and ventral (C and D) view. **E**, Photograph, and **F**, line drawing of pelvic fin rays of an adult (UMA F11259, 270 mm SL, female) dissected away from girdle in lateral view, showing pelvic splint (ps). Anterior faces left.

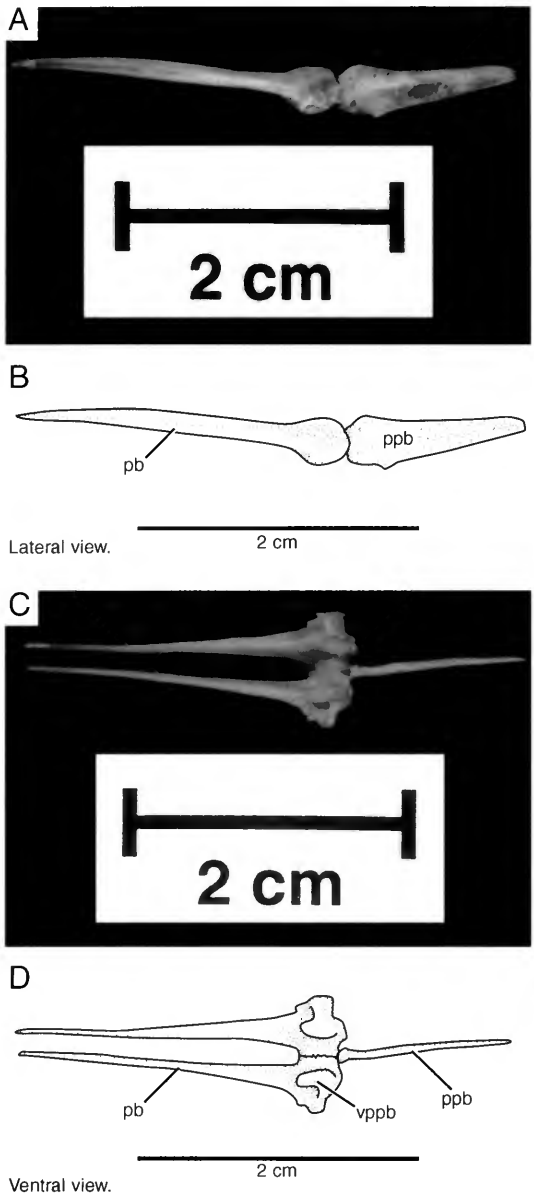

FIG. 90. *Hiodon alosoides*. **A** and **C**, Photographs, and **B** and **D**, line drawings of pelvic girdle of an adult (UMA F10589, 275 mm SL, female) in lateral (A and B) and ventral (C and D) views. Anterior faces left.

(Gosline, 1961; Grande & Bemis, 1998: fig. 91) and possibly in *Lepisosteus* (Gosline, 1961; pers. obs.), and therefore is possibly plesiomorphic at the level of Neopterygii (the presence of this element in *Lepisosteus* remains debatable because of the gradation between irregular body scales immediately surrounding the pelvic fin and the fulcra that line the leading edge of the pelvic fin; pers. obs.).

The pelvic fin of *Hiodon* normally has seven fin rays. The presence of a seven-rayed pelvic fin was found to be a synapomorphy of Hiodontidae by Li and Wilson (1994). In my sample, some individuals have only six pelvic fin rays, although this condition appears to be aberrant, typically occurring only on a single side of the specimen (although see Table 19). An elongate axillary scale is present on the lateral edge of the pelvic fin (as, Fig. 94C; see below).

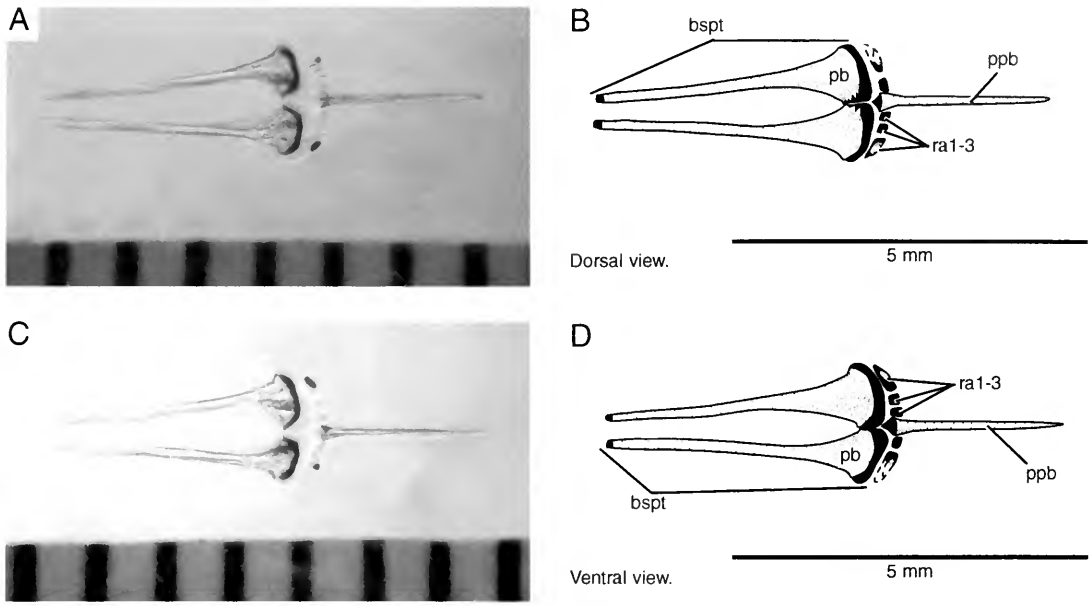

FIG. 91. *Hiodon alosoides*. **A** and **C**, Photographs, and **B** and **D**, line drawings of pelvic girdle of a cleared and stained juvenile (TU 108118E, 57 mm SL) in ventral (A and B) and dorsal (C and D) views. Scale bars in A and B in millimeters. Anterior faces left.

Scales

The scales of *Hiodon*, and of teleosts generally (although not universally), are thin and flexible and of cycloid elasmoid type (Lagler, 1947; Schultze, 1996; Grande & Bemis, 1998). There is much regional variation in the shape of the scales (Fig. 92). The scales of *Hiodon* possess slight ridges (ri, Fig. 93) that completely circumscribe the focus (= circuli). Arratia (1997) observed that of all osteoglossomorphs, only †*Lycoptera davidi* and the species of *Hiodon* lack deep furrows over the entire scale. The scales have radial furrows (rad, Fig. 93; = radii) which form grooves from the focus through both the anterior and posterior fields (afd, pfd, Fig. 93; see also Arratia, 1997, fig. 97B), although those of the anterior field are more numerous and closely arranged than those of the posterior field. An unossified (unmineralized) extension to the posterior field of each scale (uos, Fig. 93) is continuous with the bony portion of the scale and overlaps the next posterior scale. The histology of actinopterygian scales has recently been reviewed by Schultze (1996; see also references therein).

In my smallest specimen with scales (*H. alosoides*; AUM 5169; 25 mm SL), the lateral line scale row is almost completely developed, and consists of 52 scales. The caudal peduncle of this specimen is naked. The scale row immediately ventral to the lateral line has also started to form but is not as complete as the lateral line. The complete anterior portion of these two scale rows suggests that development of the scales occurs in an anterior-to-posterior progression (a few isolated scales in the first row dorsal to the lateral line row are present at about the level of the dorsal fin insertion). The anterior-to-posterior direction of scale development is also found in *Amia* (Grande & Bemis, 1998); other taxa, however, show a posterior-to-anterior pattern of scale development (e.g., *Lepisosteus*, W. E. Bemis, pers. comm.). In slightly larger specimens of *Hiodon*, a few more rows have developed on the anterior portion of the body, although none of these is complete, including the lateral line row. The single median dorsal scale row is the last scale row to form, and by approximately 40 mm SL, squamation is complete.

The two extant species of *Hiodon* are comparable in their scale meristics, although *H. tergisus* tends to have fewer scales along its lateral line (cf. Tables 21 and 22; see also Page & Burr, 1991). *Hiodon tergisus* also differs from *H. alosoides* in the arrangement of the scales just dorsal to the anal fin. In *H. alosoides*, the rows of scales

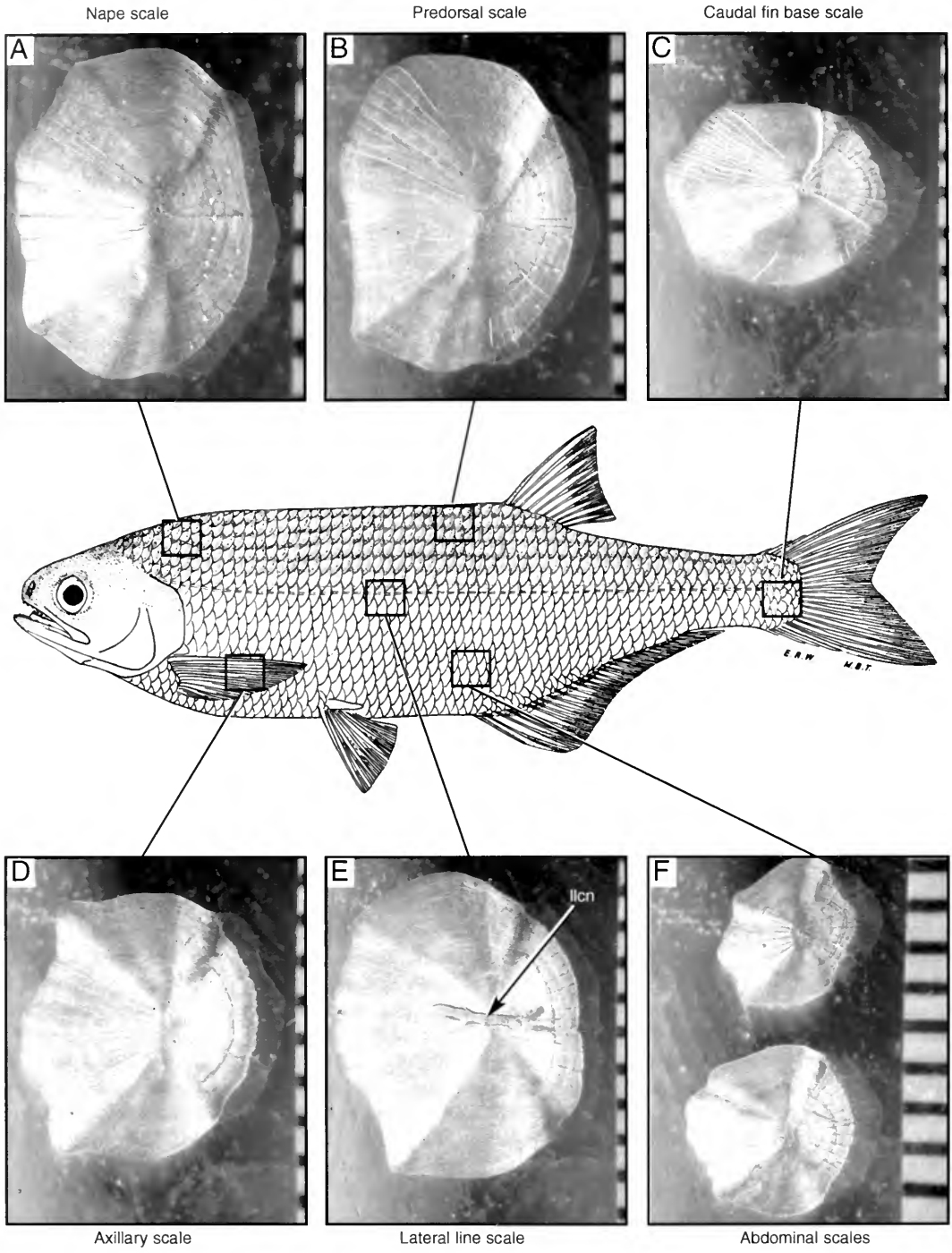

FIG. 92. *Hiodon alosoides*, photographs of scales of a juvenile (UMA F10598, 100 mm SL) in lateral view. **A**, Nape scale; **B**, predorsal scale; **C**, caudal fin base scale; **D**, axillary, or anterior abdominal, scale; **E**, mid-body lateral line scale; and **F**, posterior abdominal scales. Scale bars in millimeters. Anterior faces left. (Drawing of *H. alosoides* modified from Trautman, 1957.)

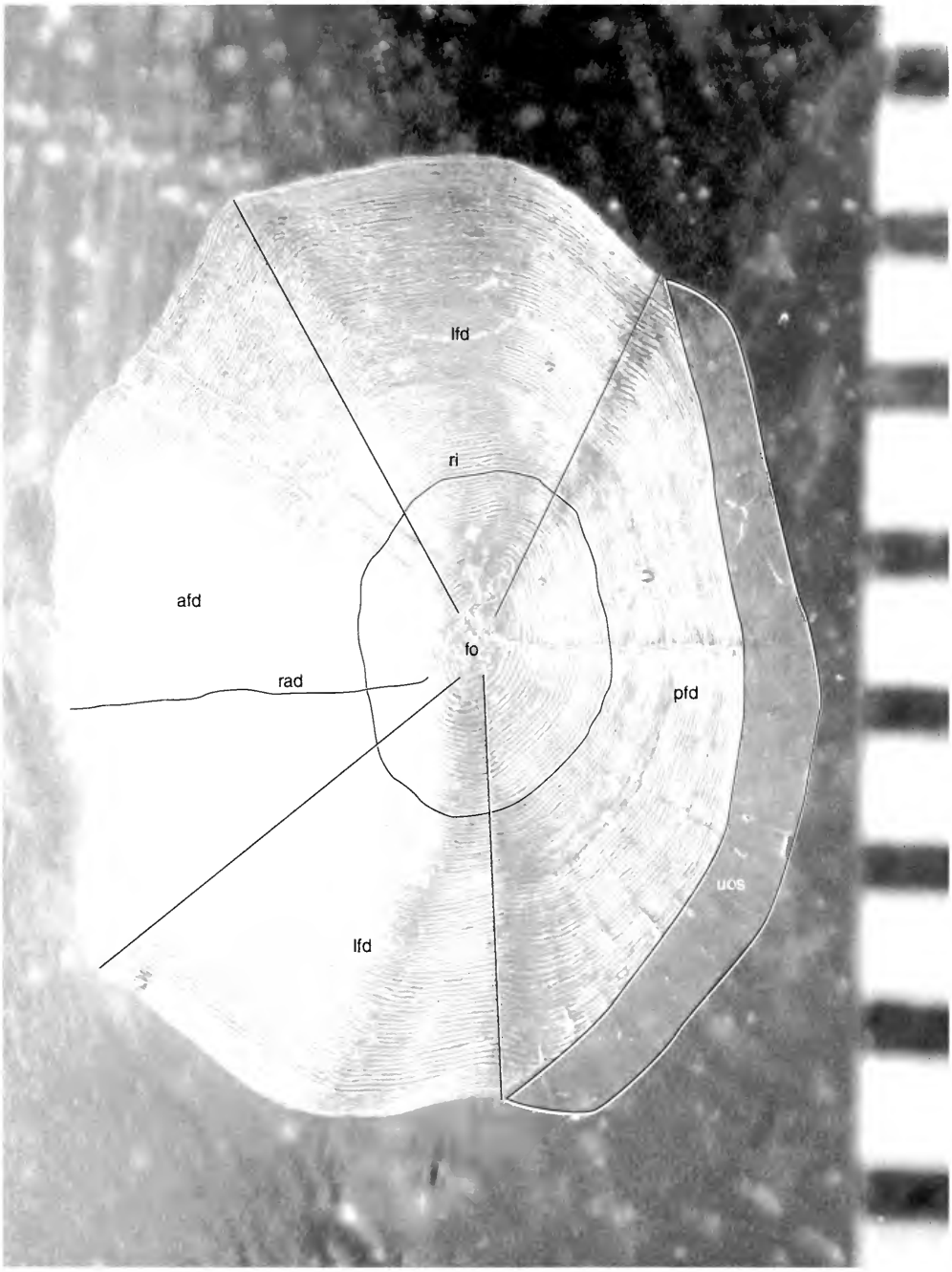

FIG. 93. *Hiodon alosoides*, photograph showing detail of a nape scale of a juvenile (UMA F10598, 100 mm SL) in lateral view. Same scale as in Figure 92A. Scale bar in millimeters. Anterior faces left.

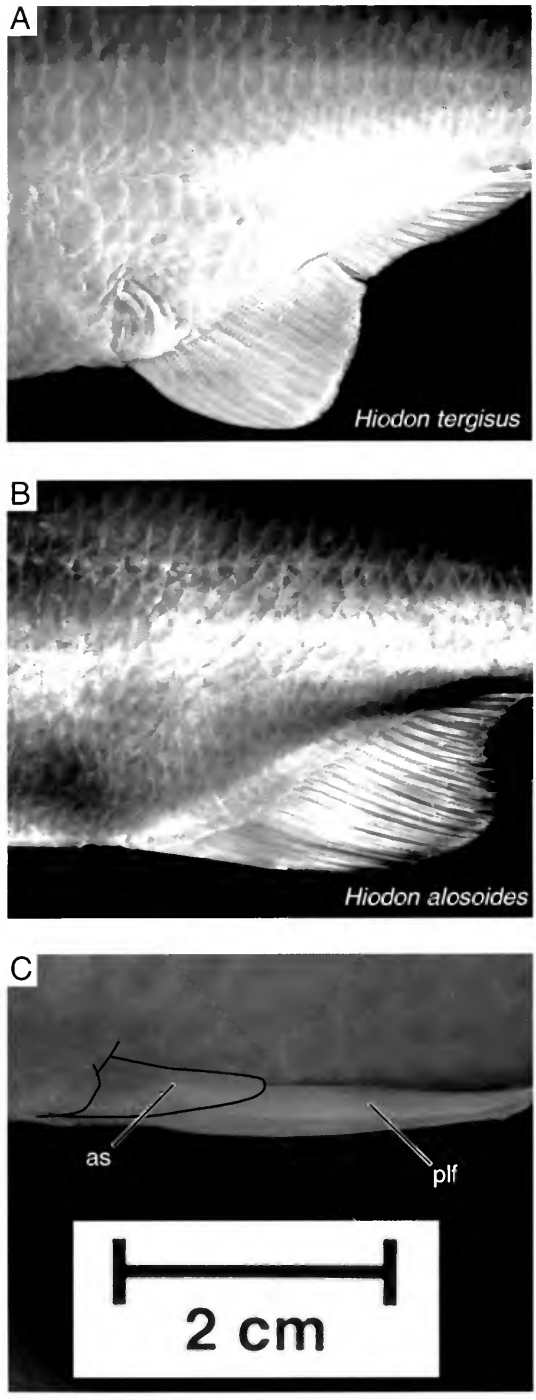

FIG. 94. Scale rows above the anal fin in **A**, *Hiodon tergisus* (UMA F10599, 235 mm SL, male) and **B**, *H. alosoides* (UMA F10380, 285 mm SL, male) showing the irregular scale rows present in *H. tergisus* above the anal fin insertion. **C**, Close-up view of the pelvic axillary scale (as) in an adult *H. tergisus* (UMA F10599, 235 mm SL, male). Specimens are shown in lateral view. Anterior faces left.

in this area are continuous with those of the rest of the body, whereas in *H. tergisus* these rows are irregular (Fig. 94A, B; Trautman, 1957).

Cockerell (1910: 4) offered a brief description of the scales of *Hiodon* and commented, "A remarkable thing about the scales of *Hiodon* is their close resemblance to those of certain old world Cyprinidae .... The Hiodontidae cannot be directly related to the Cyprinidae, but I believe that they may stand close to the ancestors of the Characinidae." In a later paper, Cockerell (1914: 92) wrote, "If *Hiodon* ... has any relationship with the Characinids, it must be with the Curimatines, although the Serrasalmonine scale is not without resemblances ...." While it is highly unlikely that these taxa share a close common ancestor, the scales of *Hiodon* and characiformes are very similar in shape and form (Cockerell, 1914: pl. XXV).

An elongated axillary scale is present on the lateral (leading) edge of the pelvic fin (as, Fig. 94). Arratia (1997, 1999: character 98) termed this structure a "pelvic axillary process" and identified four states, depending on its composition (e.g., bone and/or modified scale). She found that an axillary process composed solely of small bones was a synapomorphy of †Varasichthyidae and that a process composed of a combination of bone and elongated scales evolved independently in (*Elops* + *Megalops*) and (*Thymallus* + *Oncorhynchus*). An axillary process formed only by a modified scale was found independently derived in (*Opsariichthys* + (†*Gordichthys* + *Chanos*)) and *Hiodon* (Arratia, 1999). These axillary scales are distinct from the pelvic splints of Gosline (1961: fig. 5; see Fig. 89E, F), which are thin bones that lie lateral to the outermost fin ray.

Conclusions

Although fishes are mostly hidden by the element in which they live, so that the knife of the anatomist generally first reveals new facts connected with their life, we have sufficient evidence to show that the phenomena of life are more varied in their different groups than in any of the higher Vertebrata, and that their study will form a solid basis for the solution to those general biological questions which, perhaps rather prematurely, agitate the minds of many zoologists.

—Albert Günther (1870: x)

After having attempted to confine our discourse to facts it is a pleasure to relax into the more genial atmosphere of opinion and hypothesis.

—Henry Fairfield Osborn (1912: 276)

Future Study of Hiodontid Osteology

I have described and illustrated the osteology of the genus *Hiodon* in more detail than has been done in the past, yet many aspects of its skeletal anatomy remain incompletely known. I observed differences in timing of ossification between the two species. However, given the material that I have assembled, it is impossible to say whether these differences represent actual ontogenetic differences between the species or are the result of some preservational, preparational, or ecological artifact particular to the available material. A large size gap exists in my specimens of *H. tergisus,* between 24 mm SL and 38 mm SL, and my smallest specimen of *H. alosoides* was only 24 mm SL. Comparisons of my 24 mm SL *H. tergisus* and 24 mm SL *H. alosoides* showed that *H. alosoides* was much further along in its development than *H. tergisus* (e.g., all vertebral centra were complete rings and the articular bone was present in *H. alosoides,* but not in *H. tergisus*). All specimens used in this study were wild-caught specimens and came from different parts of their respective ranges. Therefore, it is possible, if not likely, that the differences in development discovered here were induced by environmental or other extrinsic influences. Most bones of the skull already had mineralized in the smallest available specimens of both species. As well as standardizing the development of the skeleton in *Hiodon* by using specimens reared in controlled environments (i.e., laboratory conditions), future studies must investigate the very earliest ossifications in still smaller specimens than were available for my study. Individuals of *Hiodon* are notoriously fragile and die easily in captivity (G. V. Lauder, pers. comm.), so this poses challenges for future collection of developmental series.

The inner ear and its relationship to the cranial diverticula of the swimbladder of *Hiodon* has been of great interest, both from a morphological standpoint and as a source for systematic characters (e.g., Ridewood, 1904; Greenwood, 1963, 1973), although as Greenwood (1973: 321) stated, "Taking into account the complexity of these interconnections, and the modifications to the associated skull bones, the otophysic connection in *Hiodon* can only be considered a derived condition." The description of the membranous labyrinth and its association

with the swimbladder presented herein is admittedly brief and should, in the future, be based on reconstruction from serial sections of specimens. Other remaining questions (e.g., What are the intra- and extracranial spaces of the occipital region shown in Figure 25?) might further be addressed by preparation and study of additional sectioned material. An important study could also be made of the soft tissue systems (e.g., the brain, cranial nerves, and circulatory system) of *Hiodon* in comparison to other teleostean fishes. I identified foramina based on gross dissection and confirmation through study of serial sections (e.g., the foramen for the anterior cephalic vein was confirmed to carry a blood vessel, but the vessel itself was not completely traced; facv, Fig. 20, also Taverne, 1977), although some of these identifications may be corrected with future work. While the morphological interpretations of this study are defensible, further study and reconstruction of even more detailed anatomy of *Hiodon* can be expected to provide further insight into the anatomy of teleostean fishes in general. Such studies are basic to understanding systematic interrelationships, which in turn allow the formulation of hypotheses concerning the evolution of the unique morphology that characterizes *Hiodon*.

Ontogeny and the Establishment of Primary Homology

Homology . . . exists only in the human mind. . . .

—Colin Patterson (1982: 59)

Comparative developmental osteology can greatly influence the way in which scientists detect topographic correspondence (Rieppel, 1988: = primary homology of de Pinna, 1991; and topographic identity + character state identity of Brower & Schawaroch, 1996), and thereby influence the way in which we discover homology (Rieppel, 1988: = synapomorphy of Patterson, 1982, secondary homology of de Pinna, 1991, and corroborated homology of Brower & Schawaroch, 1996).[2]

The vomer in nonteleostean neopterygians (e.g., *Amia*, *Lepisosteus*, †pachycormids, †caturids, †parasemionotids, †saurichthyids; Patterson, 1975) consists of a paired element. In †pholidophorids, †leptolepids, and most extant teleosts (Patterson, 1975), a single vomer has been hypothesized to represent a fusion of the paired elements of other neopterygian fishes. A character with two character states can then be conceptualized and described as "vomer: paired [0]; single [1]." Implicit in this definition—or, in fact, in any character scored for phylogenetic analysis—is a hypothesis that the conditions of the character (i.e., the character states) represent "the same but different" thing (Hawkins, Hughes, and Scotland, 1997: 275; see the discussion under the heading "What is a character?" in Rieppel & Zaher, 2000: 508–511). As observed by Hawkins et al. (1997), this amounts to a transformational approach (e.g., Patterson, 1982; Rieppel, 1988; de Pinna, 1991) to primary homology assessment. In other words, a hypothesis of phylogenetic fusion (or division, depending on character distribution and polarity resulting from an analysis; both are processes of character transformation) is implicit in the above example of the teleostean vomer (see next section, Remarks on Phylogenetic Fusion). By equating the two conditions as alternative conditions of the same structure, there is necessarily a hypothesis of change in morphology, albeit unstated.

If assessment of homology follows a two-step sequence of events (called "generation and legitimation" by de Pinna, 1991: 372; but see also Brower & Schawaroch, 1996), a distinction can be made between taxic and transformational approaches to both the "generation" and the "legitimation" step. The above example is transformational in its approach only in terms of character state identity, i.e., "generation" of the homology statement (e.g., the one bone in one set of taxa corresponds to the two bones in another set of taxa), and does not concern the approach toward the analysis of that correspondence (i.e., "legitimation"), which also can follow either transformational (e.g., ordered and/or weighted characters) or taxic (e.g., unordered and unweighted characters) approaches. I see the "generation" stage (i.e., the identification of different states of a character) of homology assessments as necessarily transformational in nature, following the "same but different" idea of Hawkins et al. (1997).

Even if the topographical correspondence criterion for this primary homology statement between the two forms of the vomer, for example,

[2] The amount of literature invested in discussion of "primary" versus "secondary" homology and the number of names given to its various concepts (only a few are cited here) are indications of the importance of these concepts to the context of comparative biology; see also papers in Hall (1994), Wagner (2001), and Rieppel and Kiemey (2002).

is accepted (e.g., dermal ossification(s) on the ventral surface of the ethmoid region, anterior and ventral to the anterior process of the parasphenoid), this character is much more complex. In *Hiodon*, I found that the single median vomer typical of the adult begins its development as two distinct ossifications that ontogenetically fuse to form a single median element. To incorporate these new observations into an analysis, there are now two ways to characterize the vomer of teleostean fishes. The first is to define a single multistate character, in which the vomer is described as "paired throughout ontogeny [0]; paired in early development and fused later in development [1]; median throughout development [2]." If the character is ordered [0] → [1] → [2], then this is a transformational approach not only to character identification and primary homology estimation but also to character analysis (if [0] is plesiomorphic), in that state [1] is recognized as an ontogenetic terminal addition of state [0] and state [2] is recognized as an ontogenetic nonterminal deletion of state [1]. As an unordered character, however, it only invokes the hypothesis of same but different (again, fundamentally transformational in nature) but does not add a priori conjectures of character evolution. The latter (unordered) is, therefore, a taxic approach to character analysis.

A second taxic approach would be to define a second character (beyond the original "adult condition" character described above) that describes the ontogeny of those taxa that possess a median vomer in the adult (e.g., "median vomer develops: paired to paired [0]; paired to median [1]; always median [2]"). Its advantage is that there is no a priori hypothesis of relationship among the various character states (e.g., terminal addition or nonterminal deletion in reference to an "ancestral" ontogeny). Ultimately, how to code such characters comes down to choice or, perhaps more accurately and importantly, justification of the coding strategy employed for dealing with multistate characters in phylogenetic analyses, as recently reviewed by Forey and Kitching (2000).

There is an unfortunate lack of comparable data for most taxa that bear on problems similar to the above example of conceptualization and analysis of the neopterygian vomer character. While this is potentially (in theory, if not in practice) a "problem" of all characters put into an analysis, it is particularly prevalent to studies that incorporate ontogenetic data. For example, information on the early ontogeny of the vomer in fossil taxa is unlikely to be forthcoming from even the most completely and abundantly preserved taxa, and even for most relevant extant taxa the development of the skeleton remains incompletely known. Further morphological studies on basal teleostean fishes should therefore include not only descriptions of adult morphology but also evaluation of ontogenetic changes in morphology as complete as possible given available materials.

Remarks on Phylogenetic Fusion

> *Whatever the details of the phylogenetic process, which are not demonstrable, the overall result is called fusion here, for want of a better word.*
>
> —Gareth J. Nelson (1969a: 9)

In many instances, identification of topographical correspondence draws links between parts of the skeleton that are separate elements in one set of taxa (plesiomorphic state) with a single element present at all ontogenetic stages in a second set of taxa (apomorphic state). Just as the study of ontogeny can greatly influence our assessment of putatively homologous characters, hypotheses of so-called "phylogenetic fusion" also may have a great impact on assessment of primary homology[3] (e.g., see Westoll, 1962, and Ørvig, 1962, for differing views of primary homology statements concerning some skull bones of placoderms). For example, Jarvik (1948: 68–74), in a discussion of the skull roof of species of *Acipenser,* listed several variations pertaining to the "lateral extrascapular" bones. Jarvik (1948) named compound bones that incorporated (= fused to) the lateral extrascapular (e.g., he labeled an "extrascapulosupratemporo-intertemporal" bone; Jarvik, 1948: fig. 19D), so that each specimen he examined had a unique complement of skull roofing bones. For cases in which extreme individual variability of ossifications is well-known, such as in *Acipenser,* naming of compound elements is hard to justify (Hilton & Bemis, 1999). Such individual variations in *Acipenser* are most likely the product of unique patterns of ontogenetic fusion, although the ontogenetic history of such variations is rare-

[3] Patterson and Johnson (1995: 38) discussed a situation they considered analogous to phylogenetic fusion "with the added dimension or complication of serial homology" in sorting the homologies of epineural and epicentral intermuscular bones of acanthomorph teleostean fishes.

ly, if ever, discernible in adults. An analogous problem of structural identification arises when fusion ("for want of a better word;" G. J. Nelson, 1969a: 9) is argued to have occurred during phylogeny.

De Beer (1937: 502–512) discussed at length the difficulty of tracing the homology of bones, and cited four potential causes for observed differences in patterns of bones: (1) the bones compared are not homologous; (2) two or more bones are fused into a single bone; (3) a single bone was subdivided into two or more bones; and (4) of two or more bones, one has been lost and the other(s) filled its space. Each of these categories was followed by one or more examples (de Beer discussed elements of the skull, but this may be applicable to other regions of the skeleton as well). As an example of fused elements, de Beer (1937: 505, 508–509) discussed and compared the dermal bones of the snout of *Polypterus* and *Amia*. In *Polypterus*, there are three bones that de Beer identified as the "terminale," "adnasal," and "nasal" bones. In *Amia*, each nasal bone develops as three ossification centers that fuse into a single element (although this was not described by Grande & Bemis, 1998: 49, fig. 11). Therefore, de Beer concluded that the nasal bone of *Amia* is the fused terminale, adnasal, and nasal of *Polypterus* (this represents ontogenetic fusion, an "observable" process, rather than phylogenetic fusion). If this hypothesis is true, and if, as is generally accepted, the nasal bones in *Amia* correspond to those of teleosts, then it logically follows (although not explicitly stated by de Beer) that the nasals of teleosts, which arise as a single ossification, also correspond to the terminale, adnasal, and nasal of *Polypterus* ("true" phylogenetic fusion). This example was also discussed by Moy-Thomas (1938: 313), who wrote, "The nasals of *Amia* develop from three rudiments round three sense organs, those of *Polypterus* each from a single organ. Are those of *Amia*, therefore, the product of fusion or are the bones of *Polypterus* the results of fragmentation? . . . Unfortunately the trouble does not end with the acceptance or rejection of one of these possibilities." Acceptance or rejection can only follow from an hypothesis of phylogeny and subsequent character polarization. Hypotheses of phylogenetic fusion, often much more subtle than the above example, are common in the definition of characters for phylogenetic analysis and in effect enter additional assumptions of character evolution into an analysis a priori.

Phylogenetic fusion is a hypothesis about evolutionary process (i.e., a transformational homology statement) and may be rejected because it constructs a priori causal relationships between character states. Additionally, phylogenetic fusion cannot be distinguished from phylogenetic loss, except in four specific circumstances discussed by Patterson (1977a): (1) the primitive condition has separate elements; (2) the elements fuse in late ontogeny in "primitive" members of a group; (3) the elements fuse in early ontogeny in some members; and (4) there is a reversal in derived taxa. An important component to this line of reasoning is that it is based on phylogenies that are generated independently of this data. For example, in nonteleostean neopterygians the posterior portion of the lower jaw typically has three postdentary bones (the dermal angular bone and the chondral articular and retroarticular bones). In most teleosts, two or more of these bones appear to have fused and actually develop from a single ossification center (G. J. Nelson, 1973a; Patterson, 1977a). Patterson and Rosen (1977) demonstrated the first two "lines of evidence" of phylogenetic fusion (i.e., plesiomorphic state with separate elements, and elements fusing in late ontogeny in basal members of a group) in their study of †leptolepids and †Ichthyodectiformes. Here, I provide evidence for the third (i.e., early ontogenetic fusion in some members) during the course of development of *Hiodon* (Fig. 44). The fourth (i.e., a reversal) is satisfied by the presence of separate elements in the lower jaw of *Heterotis* and *Arapaima* (G. J. Nelson, 1973a; Taverne, 1977; pers. obs.). Therefore, a "justified" hypothesis of phylogenetic fusion can be made for taxa that have only a single ossification center for a compound (= dermal + chondral) postdentary bone (e.g., in the lower jaw of most teleosts).

A distinction can be made between hypotheses of phylogenetic fusion between two (or more) dermal or two (or more) chondral bones, and phylogenetic fusion between dermal and chondral bones. Similar "rules," as outlined by Patterson (1977a), cannot be applied to cases of phylogenetic fusion between dermal bones or between chondral bones because there is no initial morphological reason for hypothesizing fusion over loss. Coalescence of ossification centers between elements of similar histogenesis does offer a mechanism through which phylogenetic fusion may occur ("at least, I can imagine no other way in which the process might come about"; Patterson, 1977a: 93), but again, such a hypothesis is dependent on phylogeny. Patterson (1977a: 92–

93) remarked on the difficulty of studying and "documenting" phylogenetic fusion of two or more dermal or chondral bones, but offered single median bones (e.g., the single median vomer of teleosts) as a possible example. The infraorbitals of *Hiodon* and other osteoglossomorph fishes can be regarded as another (G. J. Nelson, 1969a; Li & Wilson, 1996a). Most "basal" teleosts have six bones (exclusive of the dermosphenotic) in the infraorbital series, and osteoglossomorphs have only five (with the exception of *Pantodon*; Taverne, 1978; pers. obs.). A hypothesis of fusion between two of the elements has generally been preferred over the hypothesis of loss of one of the elements, but the actual process by which the reduction occurred is irrelevant to the phylogenetic pattern observed (G. J. Nelson, 1969a). However, the correlation of specific infraorbital elements with number of neuromast organs offers an interesting mechanism of element identification between taxa. Through such correlation, Nelson (1969a) argued that it was io3 and io4 that had "fused" in most osteoglossomorphs. Li and Wilson (1996), on the other hand, argued that it is io4 and io5 that are present as a fused single element, based on the position of the osteoglossomorph infraorbital bones compared with those of other basal teleosts (e.g., Elopiformes). Without such independent lines of evidence (e.g., neuromast correlation, as suggested by Nelson, 1969a), however, phylogenetic fusion between elements of similar histogenesis in which there is a single ossification center is an untestable hypothesis ("a meaningless concept": Patterson, 1977a: 93; 1975). Establishing a relationship between bones and other structures offers great potential for establishing statements of primary homology in instances where there is no direct (e.g., ontogenetic) evidence for correspondence. It seems to me that defining the infraorbital character of osteoglossomorph fishes, for example, as a reduction, rather than specifying which elements have become fused or which element has been lost, both of which are ultimately theory-laden, is more methodologically sound.[4] The process by which this reduction took place can then be hypothesized based on taxonomic relationships, character distribution, and polarity.

[4] This discussion is written with the full realization that not every case is clear-cut. It should be emphasized, however, that clear justification of homology statements (including discussion or recognition of a priori theories of character transformation) is of the utmost importance in rigorous analyses of morphological evolution.

Beyond hypothesizing phylogenetic fusion a priori, a second way of approaching such characters is to define two (or more) binary characters describing the presence or absence of each of the conditions that would be defined as character states if a single character were defined. This also avoids a priori judgments of character identity between the two conditions (e.g., paired and single bones), so that analysis of these conditions can be treated in a taxic manner. If, for example, a single element was found to be a synapomorphy of a group nested within a larger group defined by the presence of paired elements, a reasonable hypothesis of the evolutionary process that resulted in that morphology (i.e., phylogenetic fusion) then could be made (O. C. Rieppel, pers. comm.). Still, following this approach of analysis, there first must be some morphological criteria (e.g., relation to other structures) that is met in order to logically connect the two characters as *different* conditions of the *same* element. For example, Grande and Bemis (1998) found that the presence of a median parietal was a synapomorphy of †Sinamiidae. This bone (Grande & Bemis, 1998: fig. 397D) occupies the space of the paired parietals found in other halecomorph fishes. Because †Sinamiidae is nested deeply within a group characterized by paired parietals (all other halecomorphs [except anomalous specimens of *Amia calva*; e.g., Grande & Bemis, 1998: figs. 12F and 13F], lepisosteids, and primitive teleosts), it is reasonable to hypothesize that the single parietal of †sinamiids is a fusion of paired parietals (specimens studied by Grande & Bemis [1998] represented a range of sizes, so it is believed that this is indeed an ontogenetically fixed character; W. E. Bemis, pers. comm.). While Grande and Bemis (1998) did not split this character into two characters (i.e., a character describing each of the conditions), the theoretical interpretation is, at least, similar (i.e., the median parietal is a phylogenetic fusion of paired parietals).

While an intuitively believable phenomenon, phylogenetic fusion strictly depends on a particular phylogenetic context, because it never can be directly observed and can be used only to hypothesize "cause" of morphology subsequent to an analysis of relationships that is independent of the theory of process (i.e., hypotheses of phylogenetic fusion—a process—must follow from hypotheses of phylogeny—a pattern; Rieppel & Grande, 1994). The discussion above has been one of ideal situations, and it is acknowledged that most often character conceptualization is not

this straightforward. However, the question ultimately becomes whether characters that are defined based on unobserved processes, even if they do show hierarchical patterns of taxonomic variation (i.e., "process" characters that are phylogenetically informative), can be used in analyses of morphological evolution? If an hypothesis of phylogenetic fusion (or other process) is invoked as part of the definition of a character state, without ontogenetic, corroborative or correlative supporting evidence (in many cases, I do not regard positional correspondence as being sufficient), then the subsequent use of this character to infer anything concerning the evolution of structure based on a phylogenetic analysis is logically circular.

Remarks on the Study of Individual Variation

> *These individual differences are of the highest importance for us, for they afford materials for natural selection to act upon and accumulate. . . . I am convinced that the most experienced naturalist would be surprised at the number of the cases of variability, even in important parts of structure. . . .*
>
> —Charles Darwin (1859: 45)

Individuals of a single taxon always vary in structure. In a broad sense, this simple truth is what allows us to recognize the physical differences, for example, between strangers and acquaintances (Patterson, 1978: 5). However, even characters of seemingly great systematic "importance" are known to vary from individual to individual within a taxon. The recognition and description of individual variation in the vertebrate skeleton has become an increasingly important component to modern systematic and morphological studies, yet is still underappreciated by many morphologists and systematists.

Morphological variation can result from one of four sources (or any combination thereof): phylogenetic, ontogenetic, sexual dimorphic, or individual (e.g., Grande & Bemis, 1998). Individual variation is defined as "variation between individuals of the same species at similar stages of development" (Hilton & Bemis, 1999: 69). Much of the individual variation documented in the literature is variation in meristic or morphometric data (e.g., Hubbs & Hubbs, 1945; Bailey & Gosline, 1955; Hubbs & Miller, 1965) and is often correlated with ecological or geographic "morphs" of a taxon (e.g., Cutwa & Turingan, 2000; although see Reimchen & Nelson, 1987). These are the so-called "trophic polymorphisms" of Hanken & Hall (1993). Discrete or "natural" variation (i.e., variation in shape, form, or presence of particular elements) has received relatively little attention, and those studies that have been done concern only one or a few portions of the skeleton (e.g., cranial roofing bones of †*Chierolepis canadensis,* Arratia & Cloutier, 1996; dermal and endochondral skull bones and scutes of *Acipenser brevirostrum,* Hilton & Bemis, 1999). Examination of large series of specimens in terms of numbers, sexes, and ontogenetic stages is essential to the detection of such variation.

Various forms of individual variation are distinguishable.[5] The primary dichotomy that I recognize is between "correlated" and "uncorrelated" individual variation (Table 23). Correlated individual variations are the most commonly studied and documented types of individual variation, probably because they are readily observable and contingent upon factors intrinsic (e.g., a physiological response to environmental conditions) or extrinsic (i.e., geographic range) to the organism. Sexual dimorphism legitimately could be viewed as a subset of this category because it is found between individuals of the same taxon at the same ontogenetic stage (Hilton & Bemis, 1999) and is correlated with the sex of the individual. However, in sexually reproducing organisms there necessarily will be some variation (e.g., morphological and physiological) between individuals of different sexes. Sexual dimorphism, therefore, is better thought of as a type of variation in and of itself (L. Grande, pers. comm.).

Uncorrelated individual variations, on the other hand, include teratological and natural variations, and have been much less well studied. In particular, the level of natural variation in the morphology of even phylogenetically "important" taxa is relatively unknown. The sources and coding of such polymorphisms are at the center of much debate in systematic methodology (e.g., Nixon & Davis, 1991; Campbell & Frost, 1993; Wiens, 1999, 2000), and, as with other "problematic data" (Grande & Bemis, 1998: 568–569), individually polymorphic characters are treated by computer algorithms essentially as missing data.

[5] I have presented these terms for use in systematic morphological studies, but a similar approach is surely applicable to other research programs, such as behavioral or functional morphological studies.

TABLE 23. Types and sources of individual variation.

Type	Source	Definition and example
Correlated individual variation	Temporal individual variation	Morphological variation due to a physiological response to the environment or other factors dependent on time at any scale; e.g., day, year, etc. (the dentition of male Atlantic stingrays, *Dasyatis sabina,* becomes pointed during the mating season and returns to a platelike dentition during the rest of the year; Kajiura & Tricas, 1996)
	Ecomorphological individual variation	Morphological variation in response to a particular ecological niche filled by a particular population or subset of a taxon (papilliform and molariform pharyngeal teeth of *Cichlasoma minckleyi,* associated with herbivorous and carnivorous forms, respectively; Kornfield et al., 1982)
	Geographic individual variation*	Morphological variation between individuals from different portions of a taxon's geographic range (color pattern in the milk snake *Lampropeltis triangulum*; Williams, 1978)
Uncorrelated individual variation	Teratological individual variation	Morphological variation that is drastically atypical, including that caused by disease, injury or is otherwise pathological (two-headed and two-bodied snakes; Cunningham, 1937)
	Natural individual variation	Morphological variation that has no apparent direct or correlative cause (skull roofing bones of *Acipenser brevirostrum*; Hilton & Bemis, 1999)

* The distinction between geographic morphological variation and phylogenetic variation may be blurred in some instances. If geographic "morphs" or "races" are distinct (i.e., there is no overlap in frequency of a trait), then this logically can be interpreted to be the result of phylogenetic variation. True geographic individual variation must be represented by a continuous gradation of phenotypes across the range of a taxon.

However, it is useful to understand the source of the "problem" so that this information can be incorporated into character analysis once a phylogeny has been recovered (e.g., Platnick, Griswold, & Coddington, 1991; Grande & Bemis, 1998).

Natural individual variation may differ substantially among various components of the skeleton. For example, characters of the caudal skeleton of teleostean fishes are often included in broad analyses of teleost relationships (e.g., Patterson & Rosen, 1977; Arratia, 1991, 1997, 1999), despite the well-documented individual variation typical of this part of the skeleton (e.g., Arratia, 1983; Davis & Martill, 1999). For example, I found that the number of uroneurals present in *Hiodon* is highly variable, with each specimen seemingly displaying a unique number and pattern of ontogenetic fusion among the uroneural series, including left and right asymmetry (Tables 15 and 16, Figs. 75 and 76; see also the discussion and references under Caudal Fin and Supports). The condition of the neural spine on preural centrum one (nspu1, Figs. 75 and 76) also varies in *Hiodon.* Patterson and Rosen (1977) found the presence of a full neural spine on pu1 to be a synapomorphy of Osteoglossomorpha. Schultze and Arratia (1988), however, found this character in only 6% of their specimens of *Hiodon,* and my study shows that it is likely even less common (Tables 15 and 16). The "typical" condition of *Hiodon* clearly is to have a rudimentary neural spine on pu1. The extreme variation of the caudal skeleton of the species of *Hiodon* is in contrast to the extreme stability in the pattern of their infraorbitals. In my sample, less than 1% had a pattern of infraorbitals other than the "typical" condition. However, the high prevalence of individual variation in even some regions of the skeleton underscores the need for rigorous morphological character analysis, both during construction of a data matrix and after analysis of that matrix (Patterson & Johnson, 1997a,b).

Comparative morphology remains a keystone for hypotheses about interrelationships among living and fossil taxa. Clear conceptualization of characters is impossible without rigorous knowledge of morphological variation, whether it is within a species or at some higher taxonomic level. As modern computer-aided phylogenetic analyses become more powerful and approaches to analyses of data become more sophisticated, it is critical not to disregard the clear and explicit ar-

ticulation of the primary data (i.e., the morphology), for if spurious morphology serves as the basis of analysis, no amount of sophistication can bring to it any significant meaning.

Acknowledgments

This study formed a portion of dissertation research conducted primarily at the University of Massachusetts Amherst (UMA) under the guidance of W. E. Bemis, whose enthusiasm for comparative morphology of fishes served as a stimulus for this study and the growth of my interest in comparative osteology. I am extremely grateful for the comments, suggestions, and encouragement of my entire dissertation committee: W. E. Bemis, E. L. Brainerd, P. L. Forey, L. Grande, and B. Kynard. All have served as great inspiration, and I will be forever in their debt for all they have taught me. I especially thank L. Grande for sponsoring my wonderful and productive fellowship at the Field Museum and for the kindness he has shown throughout my time as a student. For reading and commenting on portions of the manuscript, I thank O. C. Rieppel, and for critically reading the entire manuscript, I thank my committee members, G. D. Johnson and M. V. H. Wilson. This work and the ideas it is based on benefited greatly from discussion, comments, suggestions, and encouragement of G. Arratia, R. Britz, C. Brochu, B. Chernoff, A. Filleul, P. Z. Goldstein, T. Grande, S. Huber, G. D. Johnson, M. Kearney, N. J. Kley, G. V. Lauder, K. F. Liem, J. S. Nelson, A. M. Richmond, O. C. Rieppel, C. P. Sanford, A. M. Simons, A. Ward, P. Willink, M. V. H. Wilson, and R. Zaragueta, as well as numerous persons I have inadvertently left from this list; mistakes, inconsistencies, and misinterpretations are, of course, my own. W. B. Sillin gave much helpful advice on the production of the illustrations.

For loan of specimens, permission to prepare specimens in their care, or help during museum visits, without which this work would have been impossible, I thank W. E. Bemis (UMA), J. S. Nelson and W. Roberts (UAMZ), D. Didier-Dagit and W. Saul (ANSP, retired), S. Jewett and J. Williams (USNM), S. Laframboise and D. Balkwill (NMC), K. E. Hartel and A. Everly (formerly MCZ—Fishes), C. Schaff (MCZ—Vertebrate Paleontology), G. Burgess and R. Robins (FL), A. M. Simons (JFBM), H. Bart and M. Taylor (TU), G. J. Nelson (retired) and B. Brown (AMNH), B. Chernoff and M. A. Rogers (FMNH—Department of Zoology), L. Grande (FMNH—Department of Geology), J. Armbruster and J. Evans (AUM), D. Goujet, P. Janvier, and H. Lelièvre (MHNH—Paleontology), G. Duhamel, P. Pruvost, and X. Gregorio (MHNH—Ichthyology), and P. L. Forey (BMNH—Paleontology). For gifts of specimens, I am grateful to R. L. Mayden (formerly), B. R. Khajda, and D. A. Neely (UAIC), J. C. Hendrickson (North Dakota Game and Fish Department), J. La Rose (Trent University), and P. Cieslewicz (Missouri Department of Conservation).

This work was financially supported by a National Science Foundation (NSF) Doctoral Dissertation Improvement Grant (DEB-0073066, to W. E. Bemis for E. J. Hilton), NSF DEB-0075460 (to W. E. Bemis and L. Grande), NSF DEB-9707705 (to L. Grande and W. E. Bemis), the Jane H. Bemis Fund for Research in Natural History, the Lester Armour and William A. and Stella Rowley Graduate Fellowships (FMNH), a Visiting Scientist Scholarship (FMNH), a Sigma Xi Grant-in-Aid-of Research, the Graduate School at the University of Massachusetts Amherst (UMA), the Woods Hole Scholarship Fund (UMA), the Department of Biology (UMA), and the Graduate Program in Organismic and Evolutionary Biology (UMA). Costs associated with the publication of this work were defrayed in part by a grant from the David J. Klingener Memorial Fund and the Jane H. Bemis Fund for Research in Natural History.

Note Added in Proof

Article 75.2 of the International Code of Zoological Nomenclature (ICZN, 1999: 84) states, "A neotype is not to be designated as an end in itself, or as a matter of curatorial routine, and any such designation is invalid." Although there is no recent history of confusion concerning the validity of the two extant species of *Hiodon*, the ranges of these two species overlap, and my efforts to track down the type specimens were unsuccessful (also see Eschmeyer, 1998, vol. 1: 76; vol. 2: 1664). Therefore, the neotypes designated in this monograph serve to preserve current usage of the species names by providing specimens to refer to in my comparisons of morphometric measurements and meristic counts for the two species, thereby clarifying the taxonomic status of both species (in accordance with Article 75.3.1). Furthermore, it is imperative that type specimens of

the extant species be available for ongoing and future studies of fossil hiodontid taxa. Information regarding other qualifying conditions for neotype designations (Articles 75.3.2–7) is provided in the section titled Systematic Description of *Hiodon*. I thank Ralf Britz for pointing out this section of the Code and its potential effect on my designations of these neotypes, and Bill Eschmeyer for his advice on this matter.

Literature Cited

ALLIS, E. P. 1919. The myodome and trigemino-facialis chamber of fishes and the corresponding cavities in higher vertebrates. Journal of Morphology, **32:** 207–322.

ARRATIA, G. 1983. The caudal skeleton of ostariophysan fishes (Teleostei): Intraspecific variation in Trichomycteridae (Siluriformes). Journal of Morphology, **177:** 213–229.

———. 1991. The caudal skeleton of Jurassic teleosts: A phylogenetic analysis, pp. 249–340. *In* Chang, M.-M., Y. H. Liu, and G. R. Zhang, eds., Early Vertebrates and Related Problems in Evolutionary Biology. Science Press, Beijing.

———. 1997. Basal teleosts and teleostean phylogeny. Paleoichthyologica, **7:** 1–168.

———. 1999. The monophyly of Teleostei and stem-group teleosts, consensus and disagreements, pp. 265–354. *In* Arratia, G., and H.-P. Schultze, eds., Mesozoic Fishes. 2. Systematics and Fossil Record. Verlag Pfeil, Munich.

ARRATIA, G., AND R. CLOUTIER. 1996. Reassessment of the morphology of *Cheirolepis canadensis* (Actinopterygii), pp. 165–197. *In* Schultze, H.-P., and R. Cloutier, eds., Devonian Fishes and Plants of Miguasha, Quebec, Canada. Verlag Pfeil, Munich.

ARRATIA, G., AND H.-P. SCHULTZE. 1990. The urohyal: Development and homology within osteichthyans. Journal of Morphology, **203:** 247–282.

———. 1991. Palatoquadrate and its ossifications: Development and homology within osteichthyans. Journal of Morphology, **208:** 1–81.

BAILEY, R. M., AND W. A. GOSLINE. 1955. Variation and systematic significance of vertebral counts in the American fishes of the family Percidae. Miscellaneous Publications, Museum of Zoology, University of Michigan, **93:** 1–44.

BAMFORD, T. W. 1948. Cranial development of *Galeichthys felis*. Proceedings of the Zoological Society of London, **118:** 364–391.

BATTLE, H. I., AND W. M. SPRULES. 1960. A description of the semi-buoyant eggs and early developmental stages of the goldeye, *Hiodon alosoides* (Rafinesque). Journal of the Fish Research Board of Canada, **17:** 245–266.

BAUDELOT, É. 1868. Considérations relatives à la pièce scapulaire des silures. Bulletin de la Société des Sciences Naturelles de Strasbourg, **12:** 83–84.

BEMIS, W. E., AND P. L. FOREY. 2001. Occipital structure and the posterior limit of the skull in actinopterygians, pp. 359–378. *In* Ahlberg, P., ed., Major Events in Early Vertebrate Evolution: Palaeontology, Phylogeny, and Development. Systematics Association. Taylor and Francis, London.

BENNETT, D. K. 1979. Three Late Cenezoic fish faunas from Nebraska. Transactions of the Kansas Academy of Science, **82:** 146–177.

BEST, A. C. G., AND J. A. C. NICOL. 1979. On the eye of the goldeye *Hiodon alosoides* (Teleostei: Hiodontidae). Journal of Zoology, London, **188:** 309–322.

BOESEL, M. W. 1938. The food of nine species of fish from the western end of Lake Erie. Transactions of the American Fisheries Society, **67:** 215–223.

BOULENGER, G. A. 1922. Systematic account of Teleostei, pp. 541–727. *In* Harmer, S. F., and A. E. Shipley, eds., Cambridge Natural History, vol. 7. MacMillan and Co., London.

BRAEKEVELT, C. R. 1982a. Fine structure of the retinal epithelium and retinal tapetum lucidum of the goldeye (*Hiodon alosoides*). Anatomy and Embryology, **165:** 177–192.

———. 1982b. Photoreceptor fine structure in the goldeye (*Hiodon alosoides*) teleost. Anatomy and Embryology, **165:** 177–192.

———. 1985. Further observation on the presence of wandering phagocytes within the teleostean retina. Anatomische Anzeiger, **160:** 45–54.

BRIDGE, T. W. 1899. The air-bladder and its connection with the auditory organ in *Notopterus borneensis*. Journal of the Linnean Society of London (Zoology), **27:** 503–540.

BRITZ, R., AND P. BARTSCH. 1998. On the reproduction and early development of *Erpetoichthys calabaricus*, *Polypterus senegalus*, and *Polypterus ornatipinnis* (Actinopterygii: Polypteridae). Ichthyological Explorations of Freshwaters, **9:** 325–334.

BROWN, B., L. M. BENVENISTE, AND P. MOLLER. 1996. Basal expansion of anal-fin rays: A new osteological character in weakly discharging electric fish (Mormyridae). Journal of Fish Biology, **49:** 1216–1225.

BROWER, A. V. Z., AND V. SCHAWAROCH. 1996. Three steps to homology assessment. Cladistics, **12:** 265–272.

BURR, B. M., AND R. L. MAYDEN. 1992. Phylogenetics and North American freshwater fishes, pp. 18–75. *In* Mayden, R. L., ed., Systematics, Historical Ecology, and North American Freshwater Fishes. Stanford University Press, Stanford, California.

CAMPBELL, J. A., AND D. R. FROST. 1993. Anguid lizards of the genus *Abronia*: Revisionary notes, descriptions of four new species, a phylogenetic analysis, and key. Bulletin of the American Museum of Natural History, **216:** 1–121.

CAVENDER, T. 1966a. Systematic position of the North American Eocene fish, "*Leuciscus*" *rosei* Hussakof. Copeia, **1968:** 311–320.

———. 1966b. The caudal skeleton of the Cretaceous teleosts *Xiphactinus*, *Ichthyodectes*, and *Gillicus*, and its bearing on their relationship with *Chirocentrus*. Occasional Papers of the Museum of Zoology, **650:** 1–14.

———. 1986. Review of the fossil history of North American freshwater fishes, pp. 699–724. *In* Hocutt, C. H., and E. O. Wiley, eds., The Zoogeography of North American Freshwater Fishes. John Wiley and Sons, New York.

Cavin, L., and P. L. Forey. 2001. Osteology and systematic affinities of *Palaeonotopterus greenwoodi* Forey 1997 (Teleostei: Osteoglossomorpha). Zoological Journal of the Linnean Society, **133:** 25–52.

Chang, M.-M. 1999. "Mid"-Cretaceous fish faunas from northeast China, pp. 469–480. *In* Arratia, G., and H.-P. Schultze, eds., Mesozoic Fishes. 2. Systematics and Fossil Record. Verlag Pfeil, Munich.

Chang, M.-M., and C. Chou. 1976. [The discovery of *Plesiolycoptera* from Song Liao Basin, with notes on the origin of osteoglossomorph fishes]. Vertebrata PalAsiatica, **14:** 146–153. In Chinese.

Cloutier, R. 1997. Morphologie et variations du toit cranien du dipneuste *Scaumenacia curta* (Whiteaves) (Sarcopterygii) du Devonien superieur du Quebec. Geodiversitas, **19:** 61–105.

Cockerell, T. D. A. 1910. The scales of the mormyrid fishes with remarks on *Albula* and *Elops*. Smithsonian Miscellaneous Collections, **56:** 1–4.

———. 1914. The scales of the South American characinid fishes. Annals of the Carnegie Museum, **9:** 92–113.

———. 1925. The affinities of the fish *Lycoptera middendorfi*. Bulletin of the American Museum of Natural History, **51:** 313–317.

Cooper, E. L. 1983. Fishes of Pennsylvania and the Northeastern United States. Pennsylvania State University Press, University Park.

Cunningham, B. 1937. Axial Bifurcation in Serpents: An Historical Survey of Serpent Monsters Having Part of the Axial Skeleton Duplicated. Duke University Press, Durham, North Carolina.

Cutwa, M. M., and R. G. Turingan. 2000. Intralocality variation in feeding biomechanics and prey use in *Archosargus probatocephalus* (Teleostei, Sparidae), with implications for the ecomorphology of fishes. Environmental Biology of Fishes, **59:** 191–198.

Cuvier, G., and A. Valenciennes. 1846. Histoire Naturelle Des Poissons, vol. 19. Société Géologique de France, Strasbourg [1969 facsimile reprint; A. Asher and Company, Amsterdam].

Daget, J. 1964. Le crane des téléostéens. Mémoires du Muséum National d'Histoire Naturelle Série A. Zoologie, **31:** 1–341.

Daget, J., and d'Aubenton. 1957. Développement et morpologie du crane d'*Heterotis nilotious* Ehr. Bulletin de l'Institut Français d'Afrique Noire, série A, **19:** 881–936.

Darwin, C. 1859. On the Origin of Species by Means of Natural Selection, or the Preservation of Favoured Races in the Struggle for Life. John Murray, London.

da Silva Santos, R. 1985. *Laelichthys ancestralis*, novo genero e especie de Osteoglossiformes do Aptianoda Formac ao Areado, estado de Minas Gerais, Brasil. Coletânea de Trabalhos Paleontologiâ, Ser. Geol 27, sec. Paleontol. e Estratigr., **2:** 161–167.

Davis, S. P., and D. M. Martill. 1999. The gonorhynchiform fish *Dastilbe* from the Lower Cretaceous of Brazil. Palaeontology, **42:** 715–740.

de Beer, G. R. 1937. The Development of the Vertebrate Skull. Oxford University Press, Oxford, England.

de Pinna, M. C. C. 1991. Concepts and tests of homology in the cladistic paradigm. Cladistics, **7:** 367–394.

———. 1996. Teleostean monophyly, pp. 147–162. *In* Stiassny, M. L. J., L. R. Parenti, and G. D. Johnson, eds., Interrelationships of Fishes. Academic Press, San Diego, California.

Dingerkus, G., and L. D. Uhler. 1977. Enzyme clearing of alcian blue stained whole small vertebrates for demonstration of cartilage. Journal of Stain Technology, **52:** 229–232.

Donald, D. B. 1997. Relationship between year-class strength for goldeyes and selected environmental variables during the first year of life. Transactions of the American Fisheries Society, **126:** 361–368.

Donald, D. B., and A. H. Kooyman. 1977a. Food, feeding habits and growth of goldeye, *Hiodon alosoides* (Rafinesque), in waters of the Peace–Athabasca Delta. Canadian Journal of Zoology, **55:** 1038–1047.

———. 1977b. Migration and populational dynamics of the Peace–Athabasca Delta goldeye population. Occasional Papers of the Canadian Wildlife Service, **31:** 1–19.

Doyle, A. C. 1887. A Study in Scarlet. Beeton's Christmas Annual.

Eldredge, N., and S. M. Stanley. 1984. Living fossils: Introduction to the casebook, pp. 1–3. *In* Eldredge, N., and S. M. Stanley, eds., Living Fossils. Springer-Verlag, New York.

Eschmeyer, W. N., Ed. 1998. Catalog of Fishes, Vols. 1–3. California Academy of Science, San Francisco.

Etnier, D. A., and W. C. Starnes. 1993. The Fishes of Tennessee. University of Tennessee Press, Knoxville.

Fink, W. L. 1981. Ontogeny and phylogeny of tooth attachment modes in actinopterygian fishes. Journal of Morphology, **167:** 167–184.

Forey, P. L. 1973. A revision of the elopiform fishes, fossil and recent. Bulletin of the British Museum (Natural History) Geology, Supplement, **10:** 1–222.

———. 1998. History of the Coelacanth Fishes. Chapman and Hall, London.

Forey, P. L., and I. J. Kitching. 2000. Experiments in coding multistate characters, pp. 54–80. *In* Scotland, R., and R. T. Pennington, eds., Homology and Systematics: Coding Characters for Phylogenetic Analysis. Systematics Association, Special Volume 58. Taylor and Francis, London.

Fujita, K. 1989. Nomenclature of cartilaginous elements in the caudal skeleton of teleostean fishes. Japanese Journal of Ichthyology, **36:** 22–29.

Gardiner, B. G., J. G. Maisey, and D. T. J. Littlewood. 1996. Interrelationships of basal neopterygians, pp. 117–146. *In* Stiassny, M. L. J., L. R. Parenti, and G. D. Johnson, eds., Interrelationships of Fishes. Academic Press, San Diego, California.

Gaudant, J. 1968. Recherches sur l'anatomie et la position systématique du genre *Lycoptera* (Poisson Téléostéen). Mémoires de la Société Géologique de France (Nouvelle Série), **109:** 1–40.

GLENN, C. L. 1975. Seasonal diets of mooneye, *Hiodon tergisus,* in the Assiniboine River. Canadian Journal of Zoology, **53:** 232–237.

GLENN, C. L., AND R. R. G. WILLIAMS. 1976. Fecundity of mooneye, *Hiodon tergisus,* in the Assiniboine River. Canadian Journal of Zoology, **54:** 156–161.

GOSLINE, W. A. 1960. Contributions toward a classification of modern isospondylous fishes. Bulletin of the British Museum (Natural History), Zoology, **6:** 327–365.

———. 1961. Some osteological features of modern lower teleostean fishes. Smithsonian Miscellaneous Collections, **142:** 1–42.

GOODE, G. B. 1884. Natural History of Useful Aquatic Animals. U.S. Commission of Fish and Fisheries. The Fisheries and Fishery Industries of the U.S., sect. I. Washington, D.C.

GRANDE, L. 1979. *Eohiodon falcatus,* a new species of hiodontid (Pisces) from the Late Early Eocene Green River Formation of Wyoming. Journal of Paleontolology, **53:** 103–111.

———. 1985. Recent and fossil clupeomorph fishes with materials for revision of the subgroups of clupeoids. Bulletin of the American Museum of Natural History, **181:** 231–372.

GRANDE, L., AND W. E. BEMIS. 1991. Osteology and phylogenetic relationships of fossil and Recent paddlefishes (Polydontidae) with comments on the interrelationships of Acipenseriformes. Journal of Vertebrate Paleontology, Memoir 1, **11:** 1–121.

———. 1998. A comprehensive phylogenetic study of amiid fishes (Amiidae) based on comparative skeletal anatomy: An empirical search for interconnected patterns of natural history. Journal of Vertebrate Paleontology, Memoir 4, **18:** 1–690.

GRANDE, L., AND T. M. CAVENDER. 1991. Description and phylogenetic reassessment of the monotypic Ostariostomidae (Teleostei). Journal of Vertebrate Paleontology, **11:** 405–416.

GREENWOOD, P. H. 1963. The swimbladder in African Notopteridae (Pisces) and its bearing on the taxonomy of the family. Bulletin of the British Museum (Natural History), Zoology, **11:** 377–412.

———. 1970. On the genus *Lycoptera* and its relationship with the family Hiodontidae (Pisces, Osteoglossomorpha). Bulletin of the British Museum (Natural History), Zoology, **19:** 257–285.

———. 1971. Hyoid and ventral gill arch musculature in osteoglossomorph fishes. Bulletin of the British Museum (Natural History), Zoology, **22:** 1–55.

———. 1973. Interrelationships of osteoglossomorphs, pp. 307–332. *In* Greenwood, P. H., R. S. Miles, and C. Patterson, eds., Interrelationships of Fishes. Academic Press, London.

GREENWOOD, P. H., R. S. MILES, AND C. PATTERSON, EDS. 1973. Interrelationships of Fishes. Academic Press, London.

GREENWOOD, P. H., AND C. PATTERSON. 1967. A fossil osteoglossoid fish from Tanzania (E. Africa). Journal of the Linnean Society (Zoology), **47:** 211–223.

GREENWOOD, P. H., D. E. ROSEN, S. H. WEITZMAN, AND G. S. MYERS. 1966. Phyletic studies of teleostean fishes, with a provisional classification of living forms. Bulletin of the American Museum of Natural History, **131:** 341–455.

GREENWOOD, P. H., D. E. ROSEN, S. H. WEITZMAN, AND G. S. MYERS. 1967. Named main divisions of teleostean fishes. Proceedings of the Biological Society of Washington, **80:** 227–228.

GREGORY, W. K. 1933. Fish skulls: A study of the evolution of natural mechanisms. Transactions of the American Philosophical Society, **23:** 75–481.

GÜNTHER, A. 1868. Catalogue of the Physostomi, containing the families Heteroptygii, Cyprinidae, Gonorhynchidae, Hyodontidae, Osteoglossidae, Clupeidae, Chirocentridae, Alepocephalidae, Notopteridae, Halosauridae, in the Collection of the British Museum. British Museum Trustees, London.

———. 1870. Catalogue of the Physostomi, containing the families Gymnotidae, Symbranchidae, Muraenidae, Pegasidae and the Lophobranchii, Plectognathi, Dipnoi, Ganoidei, Chondropterygii, Cyclostomata, Leptocardii in the British Museum. British Museum Trustees, London.

HAEDRICH, R. L., J. WINTERBERG, AND G. J. NELSON. 1973. A septum in the eye of osteoglossoid fishes. Copeia, **1973:** 594–595.

HALL, B. K., ED. 1994. Homology: The Hierarchical Basis of Comparative Biology. Academic Press, San Diego, California.

———. 1995. Homology and development. Evolutionary Biology, **28:** 1–37.

HANKEN, J., AND B. K. HALL. 1993. Mechanisms of skull diversity and evolution, pp. 1–36. *In* Hanken, J., and B. K. Hall, eds., The Skull. Vol. 3. Functional and Evolutionary Mechanisms. University of Chicago Press, Chicago.

HANKEN, J., AND R. WASSERSUG. 1981. The visible skeleton. Functional Photography, **1981** (July/August): 22–26, 44.

HAWKINS, J. A., C. E. HUGHES, AND R. W. SCOTLAND. 1997. Primary homology assessment, characters and character states. Cladistics, **13:** 275–283.

HECKEL, J. J. 1842. Ichthyologie, pp. 990–1099. *In* von Russegger, J., ed., Reisen in Europa, Asien und Africa, mit besonderer Rücksicht auf die naturwissenschaftlichen Verhältnisse der betreffenden Länder unternommen in den Jahren 1835 bis 1841, vol. 1. Stuttgart, Germany.

HENDRICKSON, J. C., AND G. J. POWER. 1999. Changes in fish species abundance in a Missouri River mainstem reservoir during its first 45 years. Journal of Freshwater Ecology, **4:** 407–416.

HENNIG, W. 1966. Phylogenetic Systematics. University of Illinois Press, Urbana.

HILDEBRAND, M. 1968. Anatomical Preparations. University of California Press, Berkeley.

HILTON, E. J. 2001. The tongue bite apparatus of osteoglossomorph fishes: Variation of a character complex. Copeia, **2001:** 372–382.

HILTON, E. J., AND W. E. BEMIS. 1999. Skeletal variation in shortnose sturgeon (*Acipenser brevirostrum*) from the Connecticut River: Implications for the comparative osteological studies of fossil and living fishes, pp.

69–94. *In* Arratia, G., and H.-P. Schultze, eds., Mesozoic Fishes. 2. Systematics and Fossil Record. Verlag Pfeil, Munich.

Hocutt, C. H., and E. O. Wiley, Eds. 1986. The Zoogeography of North American Freshwater Fishes. John Wiley and Sons, New York.

Holmgren, N., and E. A. Stensiö. 1936. Kranium und Visceralskelet der Akranier, Cyclostomen und Fische. pp. 203–500. *In* Bolk, L., E. Göppert, E. Kallius, and H. Lubosch, eds., Handbuch der Vergleichenden Anatomie. Urban and Schwarzenberg, Berlin.

Hubbs, C. L., and L. C. Hubbs. 1945. Bilateral asymmetry and bilateral variation in fishes. Papers of the Michigan Academy of Science, Arts and Letters, **30:** 229–310.

Hubbs, C. L., and K. F. Lagler. 1958. Fishes of the Great Lakes Region. Bulletin of the Cranbrook Institute of Science, **26:** 1–213.

Hubbs, C. L., and R. R. Miller. 1965. Studies of cyprinodont fishes: XXII. Variation in *Lucania parva*, its establishment in western United States, and description of a new species from an interior basin in Coahuila, México. Miscellaneous Publications, Museum of Zoology, University of Michigan, **127:** 1–104.

Humason, G. L. 1979. Animal Tissue Techniques, 4th ed. W.H. Freeman and Co., San Francisco.

Hussakoff, L. 1916. A new cyprinid fish *Leuciscus rosei* from the Miocene of British Columbia. American Journal of Science, **42:** 18–20.

Iles, R. B. 1960. External sexual differences and their significance in *Mormyrus kannume* Forskål. 1975. Nature, **188:** 516.

International Commission on Zoological Nomenclature. 1999. International Code of Zoological Nomenclature, 4th ed. International Trust for Zoological Nomenclature, London.

Jaeger, E. C. 1978. A Source Book for Biological Names and Terms. Charles C Thomas, Springfield, Illinois.

Janvier, P. 1998. Bowfins and the revenge of comparative biology. Science, **281:** 1150.

Jarvik, E. 1948. On the morphology and taxonomy of the Middle Devonian osteolepid fishes of Scotland. Kungligar Svenska Vetenskapsakademiens Handligar, **25:** 1–301.

Jessen, H. 1972. Schultergürtel und Pectoralflosse bei Actinopterygiern. Fossils and Strata, **1:** 1–101.

Jin, F. 1991. [A new genus and species of Hiodontidae from Xintai, Shandong]. Vertebrata PalAsiatica, **29:** 46–54. In Chinese with an English summary.

Jin, F., J. Zhang, and Z. Zhou. 1995. [Late Mesozoic fish fauna from western Liaoning, China]. Vertebrata PalAsiatica, **33:** 169–193. In Chinese with an English summary.

Johnson, G. D., and E. B. Brothers. 1993. Schindleria: A paedomorphic goby (Teleostei: Gobiuidei). Bulletin of Marine Science, **52:** 441–471.

Johnson, G. D., and C. Patterson. 1996. Interrelationships of lower euteleostean fishes, pp. 251–332. *In* Stiassny, M. L. J., L. R. Parenti, and G. D. Johnson, eds., Interrelationships of Fishes. Academic Press, San Diego, California.

Johnson, G. H. 1951. An investigation of the mooneye (*Hiodon tergisus*). Abstracts of the 5th Technical Session of the Research Council, Ontario, **1951:** 16.

Jollie, M. 1962. Chordate Morphology. Reinhold Publishing Corp., New York.

———. 1975. Development of the head skeleton and pectoral girdle in *Esox*. Journal of Morphology, **147:** 61–88.

Jordan, D. S. 1923. A classification of fishes including families and genera as far as known. Stanford University Publication, University Series, Biological Sciences, **3:** 77–243.

Jordan, D. S., and T. Bean. 1877. Hyodontidae. *In* Jordan, D. S., Contributions to North American ichthyology based primarily on the collections of the United States National Museum. No. 2. A.—Notes on Cottidae, Etheostomatidae, Percidae, Centrarchidae, Aphododeridae, Umbridae, Esocidae, Dorysomatidae, Cyprinidae, Catastomidae, and Hyodontidae, with revisions of the genera and descriptions of new or little known species. Bulletin of the United States National Museum, **10:** 67–68.

Jordan, D. S., and C. H. Gilbert. 1883. Synopsis of the fishes of North America. Bulletin of the United States National Museum, **16:** 1–1018.

Jordan, D. S., and B. W. Evermann. 1896. The fishes of North and Middle America. Part 1. Bulletin of the United States National Museum, **47:** 1–1240.

Jordan, D. S., and W. F. Thompson. 1910. Note on the gold-eye, *Amphiodon alosoides* Rafinesque, or *Elattonistius chrysopsis* (Richardson). Proceedings of the National Museum, **38:** 353–357.

Kajiura, S. M., and T. C. Tricas. 1996. Seasonal dynamics of dental sexual dimorphism in the Atlantic stingray *Dasyatis sabina*. Journal of Experimental Biology, **199:** 2297–2306.

Kennedy, W. A., and W. M. Sprules. 1967. Goldeye in Canada. Bulletin of the Fisheries Research Board of Canada, **161:** 1–45.

Kitching, I. J., P. L. Forey, C. J. Humpheries, and D. M. Williams. 1998. Cladistics: The Theory and Practice of Parsimony Analysis, 2nd ed. Oxford University Press, Oxford, England.

Kindred, J. E. 1919. The skull of *Amiurus*. Illinois Biological Monographs, **5:** 1–120.

Kirtland, J. P. 1847. Descriptions of the fishes of Lake Erie, the Ohio River, and their tributaries (continued from page 276). Boston Journal of Natural History, **5:** 330–344.

Kocher, T. D., and C. A. Stepien, Eds. 1997. Molecular Systematics of Fishes. Academic Press, San Diego, California.

Kornfield, I. L., D. C. Smith, P. S. Gagnon, and J. N. Taylor. 1982. The cichlid fish of Cuatro Cienegas, Mexico: Direct evidence of conspecificity among distinct morphs. Evolution, **36:** 658–664.

Lagler, K. F. 1947. Lepidological studies: 1. Scale characters of the families of Great Lakes fishes. Transactions of the American Microscopical Society, **66:** 149–171.

LAUDER, G. V., AND K. F. LIEM. 1983. The evolution and interrelationships of the actinopterygian fishes. Bulletin of the Museum of Comparative Zoology, **150:** 1–197.

LEE, D. S., C. R. GILBERT, C. H. HOCUTT, R. E. JENKINS, D. E. MCALLISTER, AND J. R. STAUFFER, JR. 1980. Atlas of North American Freshwater Fishes. North Carolina Biological Survey, Raleigh.

LEKANDER, B. 1949. The sensory line system and the canal bones of the head of some Ostariophysi. Acta Zoologica, Stockholm, **30:** 1–131.

LESUEUR, C. A. 1818. Descriptions of several new species of North American fishes. Journal of the Academy of Natural Sciences of Philadelphia, **1:** 359–368.

LI, G.-Q. 1987. [A new genus of Hiodontidae from Luozigou Basin, East Jilin]. Vertebrata PalAsiatica, **25:** 91–107. In Chinese with an English summary.

———. 1994. New osteoglossomorphs (Teleostei) from the Upper Cretaceous and Lower Tertiary of North America and their phylogenetic significance. Ph.D. diss., University of Alberta, Edmonton, Canada.

LI, G.-Q., AND M. V. H. WILSON. 1994. An Eocene species of *Hiodon* from Montana, its phylogenetic relationships, and the evolution of the postcranial skeleton in the Hiodontidae (Teleostei). Journal of Vertebrate Paleontology, **14:** 153–167.

———. 1996a. Phylogeny of Osteoglossomorpha, pp. 163–174. *In* Stiassny, M. L. J., L. R. Parenti, and G. D. Johnson, eds., Interrelationships of Fishes. Academic Press, San Diego, California.

———. 1996b. The discovery of Heterotidinae (Teleostei: Osteoglossidae) from the Paleocene Paskapoo Formation of Alberta, Canada. Journal of Vertebrate Paleontology, **16:** 198–209.

———. 1999. Early divergence of Hiodontiformes *sensu stricto* in East Asia and phylogeny of some Late Mesozoic teleosts from China, pp. 369–384. *In* Arratia, G., and H.-P. Schultze, eds., Mesozoic Fishes. 2. Systematics and Fossil Record. Verlag Pfeil, Munich.

LI, G.-Q., M. V. H. WILSON, AND L. GRANDE. 1997. Review of *Eohiodon* (Teleostei: Osteoglossomorpha) from western North America, with a phylogenetic reassessment of Hiodontidae. Journal of Paleontology, **71:** 1109–1124.

LIEM, K. F., W. E. BEMIS, W. F. WALKER, AND L. GRANDE. 2001. Functional Anatomy of the Vertebrates: An Evolutionary Perspective, 3rd ed. Harcourt College Publishers, Philadelphia.

MA, F. 1980. [A new genus of Lycopteridae from Ningxia, China.] Vertebrata PalAsiatica, **18:** 286–295.

———. 1987. Review of *Lycoptera davidi*. Vertebrata PalAsiatica, **25:** 8–19.

MABEE, P. M., E. ALDRIDGE, E. WARREN, AND K. HELENURM. 1998. Effect of clearing and staining on fish length. Copeia, **1998:** 346–353.

MAISEY, J. G. 1999. The supraotic bone in neopterygian fishes (Osteichthyes, Actinopterygii). American Museum Novitates, **3267:** 1–52.

MCALLISTER, D. E. 1968. The evolution of branchiostegals and associated opercular, gular, and hyoid bones and the classification of teleostome fishes, living and fossil. Bulletin of the National Museum of Canada, **221:** 1–239.

METTEE, M. F., P. E. O'NEIL, AND J. M. PIERSON. 1996. Fishes of Alabama and the Mobile Basin. Oxmoor House, Birmingham, Alabama.

MONOD, T. 1968. Le complex urophore des poissons téléostéens. Mémoires de l'Institut Fondamental d'Afrique Noire, **81:** 1–705.

MOON, D. N., S. J. FISHER, AND S. C. KRENTZ. 1998. Assessment of larval fish consumption by goldeye (*Hiodon alosoides*) in two Missouri River backwaters. Journal of Freshwater Ecology, **13:** 317–321.

MOORE, G. A. 1944. The retinae of two North American teleosts, with special reference to their tapeta lucida. Journal of Comparative Neurology, **80:** 369–379.

MOORE, G. A., AND R. C. MCDOUGAL. 1949. Similarity in the retinae of *Amphiodon alosoides* and *Hiodon tergisus*. Copeia, **1949:** 298.

MOY-THOMAS, J. A. 1938. The problem of the evolution of the dermal bones in fishes, pp. 305–319. *In* de Beer, G. R., ed., Evolution: Essays on Aspects of Evolutionary Biology Presented to Professor E. S. Goodrich on His Seventieth Birthday. Oxford University Press, Oxford, England.

MÜLLER, J. 1844. Über den Bau und die Grenzen der Ganoiden und über das natürliche System der Fische. Bericht über die zur Bekanntmachung geeigneten Verhandlungen der Akademie der Wissenschaften, Berlin, **1844:** 117–216.

———. 1846. On the structure and characters of the Ganoidei, and on the natural classification of fish. Scientific Memoirs, **4:** 499–558 [a published English translation of Müller, 1844].

———. 1847. Fossile Fische. *In* von Middendorff, A. T., ed., Reise in den aussersten norder und osten Sibiriens während der Jahre 1843 und 1844 (Erster Band). Buchdrukerei der Kaiserlichen Akademie der Wissenschaften, St. Petersburg, Russia.

NELSON, G. J. 1968a. Gill arches of teleostean fishes of the division Osteoglossomorpha. Journal of the Linnean Society (Zoology), **47:** 261–277.

———. 1968b. Gill-arch structure in *Acanthodes*, pp. 129–144. *In* Ørvig, T., ed., Current Problems of Lower Vertebrate Phylogeny. John Wiley and Sons, New York.

———. 1968c. Review of "Evolution of branchiostegals and classification of teleostome fishes." Copeia, **1968:** 888–889.

———. 1969a. Infraorbital bones and their bearing on the phylogeny and geography of osteoglossomorph fishes. American Museum Novitates, **2394:** 1–37.

———. 1969b. Gill arches and the phylogeny of fishes, with notes on the classification of vertebrates. Bulletin of the American Museum of Natural History, **141:** 475–552.

———. 1972a. Observations on the gut of the Osteoglossomorpha. Copeia, **1972:** 325–329.

———. 1972b. Cephalic sensory canals, pitlines, and the classification of esocoid fishes, with notes on galaxiids and other teleosts. American Museum Novitates, **2492:** 1–49.

———. 1973a. Relationships of clupeomorphs, with remarks on the structure of the lower jaw in fishes, pp. 333–350. *In* Greenwood, P. H., R. S. Miles, and C.

Patterson, eds., Interrelationships of Fishes. Academic Press, London.

———. 1973b. Notes on the structure and relationships of certain Cretaceous and Eocene teleostean fishes. American Museum Novitates, **2524:** 1–31.

Nelson, J. S. 1976. Fishes of the World. John Wiley and Sons, New York.

———. 1984. Fishes of the World, 2nd ed. John Wiley and Sons, New York.

———. 1994. Fishes of the World, 3rd ed. John Wiley and Sons, New York.

Nelson, J. S., and M. J. Paetz. 1992. The Fishes of Alberta, 2nd ed. University of Alberta Press, Edmonton.

Nixon, K. C., and J. I. Davis. 1991. Polymorphic taxa, missing values and cladistic analysis. Cladistics, **7:** 233–241.

Nolf, D. 1985. Otolithi Piscium, pp. 1–145. *In* Schultze, H.-P., ed., Handbook of Paleoichthyology. Vol. 10. Gustav Fischer Verlag, Stuttgart, Germany.

Northcutt, R. G. 1989. The phylogenetic distribution and innervation of craniate mechanoreceptive lateral lines, pp. 17–78. *In* Coombs, S., P. Görner, and H. Münz, eds., The Mechanoreceptive Lateral Line: Neurobiology and Evolution. Springer-Verlag, New York.

Northcutt, R. G., and W. E. Bemis. 1993. Cranial nerves of the coelacanth *Latimeria chalumnae* [Osteichthyes: Sarcopterygii: Actinistia] and comparisons with other Craniata. Brain, Behavior and Evolution, **42** (suppl. 1): x + 1–76.

Okedi, J. 1969. Observations on the breeding and growth of certain mormyroid fishes of the Lake Victoria Basin. Revue de Zoologie et de Botanique Africaines, **79:** 34–64.

Ørvig, T. 1962. Y a-t-il une relation directe entre les arthrodires ptyctodontides et les holocéphales? Colloques Internationaux du Centre National de la Recherche Scientifique, **104:** 49–60.

Osborn, H. F. 1912. The continuous origin of certain unit characters as observed by a palaeontologist: II. Evidences for continuity. American Naturalist, **46:** 249–278.

Page, L. M., and B. M. Burr. 1991. A Field Guide to Freshwater Fishes of North America North of Mexico. Houghton-Mifflin Co., Boston.

Pankhurst, N. W. 1985. Final maturation and ovulation of oocytes of the goldeye, *Hiodon alosoides* (Rafinesque), *in vitro*. Canadian Journal of Zoology, **63:** 1003–1009.

Pankhurst, N. W., N. E. Stacey, and G. Van Der Kraak. 1986. Reproductive development and plasma levels of reproductive hormones of goldeye, *Hiodon alosoides* (Rafinesque), taken from the North Saskatchewan River during the open water season. Canadian Journal of Zoology, **64:** 2843–2849.

Paterson, C. G. 1966. Life history notes on the goldeye, *Hiodon alosoides* (Rafinesque), in the North Saskatchewan River in Alberta. Canadian Field Naturalist, **80:** 250–251.

Patterson, C. 1968. The caudal skeleton in Lower Liassic pholidophorid fishes. Bulletin of the British Museum (Natural History), Geology, **16:** 201–239.

———. 1973. Interrelationships of holosteans, pp. 233–305. *In* Greenwood, P. H., R. S. Miles, and C. Patterson, eds., Interrelationships of Fishes. Academic Press, London.

———. 1975. The braincase of pholidophorid and leptolepid fishes, with a review of the actinopterygian braincase. Philosophical Transactions of the Royal Society of London, **269:** 275–597.

———. 1977a. Cartilage bones, dermal bones, and membrane bones, or the exoskeleton versus the endoskeleton, pp. 77–121. *In* Andrews, S. M., R. S. Miles, and A. D. Walker, eds., Problems in Vertebrate Evolution. Academic Press, London.

———. 1977b. The contribution of paleontology to teleostean phylogeny, pp. 579–643. *In* Hecht, M. K., P. C. Goody, and B. M. Hecht, eds., Major Patterns in Vertebrate Evolution. Plenum Publishing Corp., New York.

———. 1978. Evolution. British Museum (Natural History), London.

———. 1981a. Significance of fossils in determining evolutionary relationships. Annual Review of Ecology and Systematics, **12:** 195–223.

———. 1981b. The development of the North American fish fauna: A problem of historical biogeography, pp. 265–281. *In* Forey, P. L., ed., The Evolving Biosphere. Cambridge University Press, Cambridge, England.

———. 1982. Morphological characters and homology, pp. 21–74. *In* Joysey, K. A., and A. E. Friday, eds., Problems of Phylogenetic Reconstruction. Academic Press, London.

———. 1984. Family Chanidae and other teleostean fishes as living fossils, pp. 132–139. *In* Eldredge, N., and S. M. Stanley, eds., Living Fossils. Springer-Verlag, New York.

———. 1992. Supernumerary median fin-rays in teleostean fishes. Zoological Journal of the Linnean Society, **106:** 147–161.

Patterson, C., and G. D. Johnson. 1995. The intermuscular bones and ligaments of teleostean fishes. Smithsonian Contributions to Zoology, **559:** 1–85.

———. 1997a. The data, the matrix, and the message: Comments on Begle's "Relationships of the osmeroid fishes." Systematic Biology, **46:** 358–365.

———. 1997b. Comments on Begle's "Monophyly and relationships of argentinoid fishes." Copeia, **1997:** 401–409.

Patterson, C., and D. E. Rosen. 1977. Review of the ichthyodectiform and other Mesozoic fishes and the theory and practice of classifying fossils. Bulletin of the American Museum of Natural History, **158:** 81–172.

Pflieger, W. L. 1997. The Fishes of Missouri, rev. ed. Missouri Department of Conservation, Jefferson City.

Platnick, N., C. E. Griswold, and J. A. Coddington. 1991. On missing entries in cladistic analysis. Cladistics, **7:** 337–343.

Popper, A. N., and S. Coombs. 1982. The morphology and evolution of the ear in actinopterygians fishes. American Zoologist, **22:** 311–328.

Poyato-Ariza, F. J. 1999. The elopiform fish †*Anaethalion angustus* restored, with comments on individ-

ual variation, pp. 361–368. *In* Arratia, G., and H.-P. Schultze, eds., Mesozoic Fishes. 2. Systematics and Fossil Record. Verlag Pfeil, Munich.

RAFINESQUE, C. S. 1818. Discoveries in natural history, made during a journey through the western region of the United States. American Monthly Magazine and Critical Review, **2:** 354–356.

———. 1819. Prodrome de 70 nouveaux genres d'animaux découvert dans l'intérieur des Etats-Unis d'Amérique durant l'année 1818. Journal de Physique, Paris, **88:** 417–429.

———. 1820. Ichthyologica Ohioensis, or Natural History of the Fishes Inhabiting the River Ohio and its Tributary Streams, Preceded by a Physical Description of the Ohio and its Branches. W. G. Hunt, Lexington, Kentucky [1970 facsimile reprint, Arno Press, New York].

REIMCHEN, J. S., AND J. S. NELSON. 1987. Habitat and morphological correlates to vertebral number as shown in a teleost, *Gasterosteus aculeatus*. Copeia, **1987:** 868–874.

RICHARDSON, J. 1823. Notice of the fishes, pp. 705–728. *In* Appendix 6. Appendix to narrative of a journey to the shores of the Polar Sea in the years 1819, 1820, 1821 and 1822. J. Franklin. John Murray, London.

———. 1836. The Fish, pp. 1–327. *In* Fauna Boreali-Americana; or the zoology of the northern parts of British America: Containing descriptions of the objects of natural history collected on the late northern land expeditions, under the command of Sir John Franklin, R. N., Part 3. J. Murray, London.

RIDEWOOD, W. G. 1904. On the cranial osteology of the fishes of the families Mormyridae, Notopteridae, and Hyodontidae. Journal of the Linnean Society of London (Zoology), **29:** 188–217.

———. 1905. On the cranial osteology of the fishes of the families Osteoglossidae, Pantodontidae, and Phractolaemidae. Journal of the Linnean Society of London (Zoology), **29:** 252–282.

RIEPPEL, O. C. 1988. Fundamentals of Comparative Biology. Birkhäuser, Basel, Switzerland.

RIEPPEL, O. C., AND L. GRANDE. 1994. Summary and comments on systematic pattern and evolutionary process, pp. 227–255. *In* Grande, L., and O. Rieppel, eds., Interpreting the Hierarchy of Nature. Academic Press, San Diego, California.

RIEPPEL, O., AND M. KEARNEY. 2002. Similarity. Biological Journal of the Linnean Society, **75:** 59–82.

RIEPPEL, O. C., AND H. ZAHER. 2000. The braincase of mosasaurs and *Varanus*, and the relationships of snakes. Zoological Journal of the Linnean Society, **129:** 489–514.

ROBERTS, W. 1989. The mooneye in Alberta. Alberta Naturalist, **19:** 134–140.

ROBINSON, H. W., AND T. M. BUCHANAN. 1988. Fishes of Arkansas. University of Arkansas Press, Fayetteville.

ROHDE, F. C., R. G. ARNDT, D. G. LINDQUIST, AND J. F. PARNELL. 1994. Freshwater Fishes of the Carolinas, Virginia, Maryland, and Delaware. University of North Carolina Press, Chapel Hill.

ROHDE, F. C., M. L. MOSER, AND R. G. ARNDT. 1998. Distribution and status of selected fishes in North Carolina, with a new state record. Brimleyana, **25:** 43–68.

ROSEN, D. E., AND P. H. GREENWOOD. 1970. Origin of the Weberian apparatus and the relationships of the ostariophysan and gonorhynchiform fishes. American Museum Novitates, **2428:** 1–25.

SANFORD, C. P. J. 2000. Salmonid fish osteology and phylogeny (Teleostei: Salmonoidei). Theses Zoologicae, **33:** 1–264.

SCHAEFFER, B. 1949. A teleost from the Livingston Formation of Montana. American Museum Novitates, **1427:** 1–16.

SCHULTZE, H.-P. 1996. The scales of Mesozoic actinopterygians, pp. 83–93. *In* Arratia, G., and G. Viohl, eds., Mesozoic Fishes: Systematics and Paleoecology. Verlag Pfeil, Munich.

SCHULTZE, H.-P., AND G. ARRATIA. 1988. Reevaluation of the caudal skeleton of some actinopterygian fishes: II. *Hiodon, Elops,* and *Albula*. Journal of Morphology, **195:** 257–303.

———. 1989. The composition of the caudal skeleton of teleosts (Actinopterygii: Osteichthyes). Zoological Journal of the Linnean Society, **97:** 189–231.

SCOTT, W. B., AND E. J. CROSSMAN. 1973. Freshwater Fishes of Canada. Bulletin of the Fisheries Research Board of Canada, **184:** 1–966.

SEWERTZOFF, A. N. 1925. The place of the cartilaginous ganoids in the system and evolution of the Osteichthyes. Journal of Morphology, **38:** 105–145.

———. 1934. Evolution der Bauchflossen der Fische. Zoologische Jahrbücher, Abteilung für Anatomie und Ontogenie der Tiere, **58:** 415–500.

SHEN, M. 1989. [*Eohiodon* from China and the distribution of Osteoglossomorphs]. Vertebrata PalAsiatica, **10:** 237–247. In Chinese with an English summary.

———. 1996. Fossil "osteoglossomorphs" from East Asia and their implications for teleostean phylogeny, pp. 261–272. *In* Arratia, G., and G. Viohl, eds., Mesozoic Fishes: Systematics and Paleoecology. Verlag Pfeil, Munich.

SMITH, C. L. 1985. The Inland Fishes of New York State. New York State Department of Environmental Conservation, Albany.

SMITH, G. R. 1981. Late Cenozoic freshwater fishes of North America. Annual Review of Ecology and Systematics, **12:** 163–193.

SMITH, G. R., AND J. G. LUNDBERG. 1972. The Sand Draw fauna. Bulletin of the American Museum of Natural History, **148:** 40–54.

SMITH, M. M., AND B. K. HALL. 1990. Development and evolutionary origins of vertebrate skeletongenetic and odontogenetic tissues. Biological Review, **65:** 277–373

———. 1993. A developmental model for evolution of the vertebrate exoskeleton and teeth, pp. 387–448. *In* Hecht, M. K., R. J. Macintyre, and M. T. Clegg, eds., Evolutionary Biology, vol. 27. Plenum Press, New York.

SNYDER, D. E., AND S. C. DOUGLAS. 1978. Description and identification of mooneye, *Hiodon tergisus,* protolarvae. Transactions of the American Fisheries Society, **107:** 590–594.

STARKS, E. C. 1926. Bones of the ethmoid region of the fish skull. Stanford University Publications, University Series, Biological Science, **4:** 139–338.

STEWART, J. D. 1999. A new genus of Saurodontidae (Teleostei: †Ichthyodectiformes) from Upper Cretaceous rocks of the western interior of North America, pp. 335–360. *In* Arratia, G., and H.-P. Schultze, eds., Mesozoic Fishes. 2. Systematics and Fossil Record. Dr. Friedrich Pfeil, Munich.

STIASSNY, M. L. J., L. R. PARENTI, AND G. D. JOHNSON, EDS. 1996. Interrelationships of Fishes. Academic Press, San Diego, California.

STORER, D. H. 1846. A synopsis of the fishes of North America. Memoirs of the American Academy, **7:** 1–298.

SU, D.-Z. 1986. [The discovery of a fossil osteoglossid fish in China]. Vertebrata PalAsiatica, **24:** 10–19. In Chinese with an English summary.

———. 1991. [A new fossil hiodontid fish from Fuxin Group of western Liaoning, China]. Vertebrata PalAsiatica, **29:** 38–45. In Chinese with an English summary.

TAVERNE, L. 1977. Ostéologie, phylogénèse et systématique des Téléostéens fossiles et actuels du super-ordre des ostéoglossomorphes. Première partie. Ostéologie des genres *Hiodon, Eohiodon, Lycoptera, Osteoglossum, Scleropages, Heterotis* et *Arapaima.* Mémoires de la Classe des Sciences, Académie Royale de Belgique, **42:** 1–235.

———. 1978. Ostéologie, phylogénèse, et systématique des Téléostéens fossiles et actuels du super-ordre des ostéoglossomorphes. Deuxième partie. Ostéologie des genres *Phareodus, Phareoides, Brychaetus, Musperia, Pantodon, Singida, Notopterus, Xenomystus* et *Papyrocranus.* Mémoires de la Classe des Sciences, Académie Royale de Belgique, **42:** 1–212.

———. 1979. Ostéologie, phylogénèse et systématique des Téléostéens fossiles et actuels du supre-ordre des osteoglossomorphes. Troisième partie. Evolution des structures ostéologiques et conclusions générales relatives à la phylogénèse et à la systématique du super-ordre. Mémoires de la Classe des Sciences, Académie Royale de Belgique, **43:** 1–168.

———. 1998. Les ostéoglossomorphes marins de l'Éocène du Monte Bolca (Italie): *Monopteros* Volta, 1796, *Thrissopterus* Heckel, 1856 et *Foreyichthys* Taverne, 1979. Considérations sur la phylogénie des téléostéens ostéoglossomorphes. Studi e Ricerche sui Giacimenti Terziari di Bolca, **7:** 67–158.

THOMAS, K. 1983. A nitrocellulose embedding technique for vertebrate morphologists. Herpetological Review, **14:** 80–81.

TRAUTMAN, M. B. 1957. The Fishes of Ohio. Ohio State University Press, Columbus.

WAGNER, G. P., ED. 2001. The Character Concept in Evolutionary Biology. Academic Press, San Diego, California.

WAGNER, H.-J., AND M. A. ALI. 1978. Retinal organization in goldeye and mooneye (Teleostei: Hiodontidae). Revue of Canadian Biology, **37:** 65–85.

WALLUS, R. 1986. Larval development of *Hiodon tergisus* Lesueur with comparisons to *Hiodon alosoides* (Rafinesque). Journal of the Tennessee Academy of Science, **61:** 77–80.

———. 1990. Family Hiodontidae, pp. 153–166. *In* Wallus, R., T. P. Simon, and B. L. Yeager, eds., Reproductive Biology and Early Life History of Fishes in the Ohio River Drainage. Vol. 1. Acipenseridae Through Esocidae. Tennessee Valley Authority, Chattanooga.

WALLUS, R., AND J. P. BUCHANAN. 1989. Contributions to the reproductive biology and early life ecology of mooneye in the Tennessee and Cumberland Rivers. American Midland Naturalist, **122:** 204–207.

WASSERSUG, R. J. 1976. A procedure for differential staining of cartilage and bone in whole formalin fixed vertebrates. Journal of Stain Technology, **51:** 131–134.

WEITZMAN, S. H. 1962. The osteology of *Brycon meeki,* a generalized characid fish, with an osteological definition of the family. Stanford Ichthyological Bulletin, **8:** 1–77.

WESTOLL, T. S. 1962. Ptyctodontid fishes and the ancestry of Holocephali. Nature, **194:** 949–952.

WIENS, J. J. 1999. Polymorphism in systematics and comparative biology. Annual Review of Ecology and Systematics, **30:** 327–362.

———. 2000. Coding morphological variation within species and higher taxa for phylogenetic analysis, pp. 115–145. *In* Wiens, J. J., ed., Phylogenetic Analysis of Morphological Data. Smithsonian Institution Press, Washington, D.C.

WILEY, E. O. 1976. The phylogeny and biogeography of fossil and Recent gars (Actinopterygii: Lepisosetidae). Miscellaneous Publications of the University of Kansas Museum of Natural History, **64:** 1–111.

———. 1981. Phylogenetics: The Theory and Practice of Phylogenetic Systematics. John Wiley and Sons, New York.

WILLIAMS, K. 1978. Systematics and natural history of the American milk snake *Lampropeltis triangulum.* Publications in Biology and Geology, Milwaukee Public Museum, **2:** 1–258.

WILSON, M. V. H. 1977. Middle Eocene freshwater fishes from British Columbia. Life Sciences Contributions Royal Ontario Museum, **113:** 1–61.

———. 1978. *Eohiodon woodruffi* n. sp. (Teleostei, Hiodontidae) from the middle Eocene Klondike Mountain Formation near Republic, Washington. Canadian Journal of Earth Sciences, **15:** 679–686.

———. 1980. Oldest known *Esox* (Pisces: Esocidae), part of a new Paleocene teleost fauna from western Canada. Canadian Journal of Earth Sciences, **17:** 307–312.

WILSON, M. V. H., AND R. R. WILLIAMS. 1992. Phylogenetic, biogeographic and ecological significance of early fossil records of North American freshwater teleostean fishes, pp. 224–244. *In* Mayden, R., ed., Systematics, Historical Ecology, and North American Freshwater Fishes. Stanford University Press, Stanford, California.

WINTERBOTTOM, R. 1974. A descriptive synonymy of the striated muscles of the Teleostei. Proceedings of the Academy of Natural Sciences of Philadelphia, **125:** 225–317.

ZYZNAR, E. S., F. B. CROSS, AND J. A. C. NICOL. 1978. Uric acid in the tapetum lucidum of mooneyes *Hiodon* (Hiodontidae, Teleostei). Proceedings of the Royal Society of London, Series B, **201:** 1–6.

Field Museum of Natural History
1400 South Lake Shore Drive
Chicago, Illinois 60605-2496
Telephone: (312) 665-7055